THE UNIVERSITY
of EDINBURGH

Balancing the Variability of Flow in Carbon Dioxide Transport and Storage Networks: Low-Carbon Electricity Systems in Great Britain

Thomas Martin Spitz

Doctor of Philosophy

School of Engineering

THE UNIVERSITY OF EDINBURGH

2019

The beginning of knowledge is the discovery of something we do not understand.

- Frank Herbert

Lay Summary

Carbon Capture and Storage (CCS) is expected to play a significant role in the urgently required decarbonisation of economies around the world. In the power sector CCS allows to decarbonise fossil power stations enabling them to deliver power and stabilise electricity systems at reasonable cost. The strong uptake of intermittent renewable power supply is likely to lead to significant amounts of flexible operation demanded of CCS equipped fossil power stations in future power networks.

This study examines the operating profiles of CCS power stations in future low carbon electricity systems scenarios. A range of UK power system scenarios are developed and analysed. The scenarios differ in the emission intensity ambitions and in the power generation portfolio (e.g. level of wind deployment). The study finds that particularly in low carbon emission intensity scenarios CCS power stations are required to operate in a highly flexible manner.

The study continues by reviewing the ability of the individual components along the CCS process chain (i.e. CO_2 capture, transportation, injection and storage) to support the required levels of flexible operation. It is found that particularly CO_2 injection wells can have difficulties handling frequent and large feed flow fluctuations. Several operational and design options are reviewed to enable injection wells to operate more flexibly. Significant risks, however, were found to be specifically associated with the reliability of many of these options.

To circumvent these risks, alternative options are explored that consist of reducing the flow variability injection wells need to handle. A range of options were found to be available at the power plant level as well as on the transportation system level. Two options were quantitatively examined in detail: line-packing and solvent storage. Line-packing consists of manipulating the pressure in the pipeline and by exploiting the compressibility the fluid (i.e. carbon dioxide) using the pipeline as a temporary buffer store. Similarly, solvent storage at post-combustion amine based CO_2 capture power plants allows to balance flows by smoothing out CO_2 flow profiles feeding into the downstream T&S (incl. injection) systems. Particularly line-packing into oversized CO_2 transportation pipelines can help avoiding many if not most of the critical low flow periods at the injection well level even in the worst case energy system scenarios considered within this work.

Overall, this work shows that whilst there are no clear showstoppers to flexible operation of CCS process chains several issues need to be considered at the CO_2 injection well level. A range of options, nevertheless, exist to mitigate these issues. Which option, if any, will be deployed in future systems will ultimately be a matter of cost-effectiveness. Generally, however, it can be concluded that whilst the issues associated with variable operation need to be considered they seem manageable.

Abstract

The variability of flows can cause challenges to the long term integrity of the carbon dioxide (CO_2) transport and storage infrastructure. In particular, repeated cycling and periods of low flow in injection wells can lead to a range of deleterious effects that impair the integrity of injection wells and reduce their lifetimes. How flow variability will be managed cost-effectively across clusters of CO_2 sources or CO_2 sinks is still unclear. At the time of writing, CCS deployment has indeed focused on single source-to-sink projects operating continuously, and, in most cases, supplying CO_2 continuously for the purpose of enhanced oil recovery.

Using a combination of economic dispatch models of power stations, including wind, solar, nuclear and combined cycle gas turbines with CO_2 capture, with hydraulic models of dense phase CO_2 pipelines, a method to characterise the magnitude and frequency of the variability of flow changes in CO_2 transport networks and at injection wells is presented for the first time.

A case study of the electricity system of Great Britain shows that CO_2 flow variability and repeated periods of low flow are prevalent at high levels of deployment of wind power and at carbon intensity of electricity generation of approximately 60g/kWh, and very likely beyond. The effects on flow variability of the deployment of large levels of solar capacity are, however, limited.

It is possible to reduce the number of occurrences of periods of low flow at injection by increasing the diameter of dense phase CO_2 pipelines, and by extension their linepacking capabilities. For an offshore pipeline of 100 km and 24 inch (36 inch) diameter, this number is reduced from 202 to 32 per year (7) in the reference electricity system scenario of this study.

The use of solvent storage in combined cycle gas turbines with post-combustion CO_2 capture can balance flow variability, within the boundaries of CCS power plants, reducing further the need for injection wells to operate flexibly. A rigorous state-of-the-art process model determines operating limits for an 804MW power plant in terms of output of electricity and CO_2, and the extent and duration to which electricity and CO_2 production can be decoupled. An additional solvent inventory of 6200m^3 (7.8 m^3/MW_e) allows decoupling electricity and CO_2 production for up to 3hrs, with a fixed pressure operating strategy for steam extraction from the combined cycle.

Smoothing of flows with solvent storage, sized to deliver at least 10% of nominal pipeline flow, further reduces the number of occurrences of low flow periods to 2 per year (2) representing an overall 99% reduction for the reference electricity system scenario.

Acknowledgements

This thesis would not have been possible without the continuous and invaluable support and guidance of my supervisors Dr. Mathieu Lucquiaud, Dr. Hannah Chalmers, and Dr. Francisco Ascui. I would like to thank my friends and colleagues at the School of Enginnering for many inspiring lunch as well as coffee times, and after work conversations. In particular I would like to thank Laura Herraiz, Vitali Avagyan, Bill Buschle, Erika Palfi and Charlotte Mitchell for making our office a wonderful place to work in, for giving me technical advice whenever needed, and for making me understand the world a bit better.

I would also like to thank all my friends that I had the absolute pleasure of sharing my time with in Edinburgh.

Finally, I would like to thank my family and especially my parents who are always there to support me and who encourge me to follow my passions and dreams.

Financial support of the EPSRC and the University of Edinburgh is also very gratefully acknowlegded.

Declaration

I declare that the work presented in this thesis is my own except where specific reference is made to other sources. The work has been conducted under the guidance of Dr. Mathieu Lucquiaud, Dr. Hannah Chalmers, and Dr. Francisco Ascui. It has not been submitted for any other degree or professional qualification.

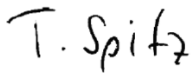

_____

Thomas Martin Spitz

List of Publications

Journal Publications:

Spitz, T., Avagyan, V., Ascui, F., Bruce, A.R.W., Chalmers, H., Lucquiaud, M., 2018. On the variability of CO_2 feed flows into CCS transportation and storage networks. *International Journal of Greenhouse Gas Control* 74, 296-311. DOI: 10.1016/j.ijggc.2018.04.008.

Spitz, T., Gonzáles Díaz, A., Chalmers, H., Lucquiaud, M., 2019. Operating Flexibility of Natural Gas Combined Cycle Power plant integrated with Post-Combustion Capture. *International Journal of Greenhouse Gas Control* - Submitted.

Conference Publications:

Spitz, T., Chalmers, H., Ascui, F., Lucquiaud, L., 2017. Operating Flexibility of CO_2 Injection Wells in Future Low Carbon Energy System. *Energy Procedia* 114, 4797–4810. DOI: 10.1016/j.egypro.2017.03.1619.

Oral presentations:

Spitz, T., Palfi, E., Mitchell, C., Reiner, D., Wilkinson, M., Lucquiaud, M., 2018. Learnings from the world's first Massice Open Online Course on CCS. *14th International Conference on Greenhouse Gas Control Technologies,* Melbourne, Australia: 21-26 October.

Spitz, T., Ascui, F., Chalmers, H., Lucquiaud, M., 2017. Operating flexibility of CCS systems. *All Energy Conference 2018*, Glasgow, UK: 2-3 May.

Spitz, T., Ascui, F., Chalmers, H., Lucquiaud, M., 2017. The role of CCS power stations in future low carbon energy systems & their interaction with the downstream CO_2 transportation and storage infrastructure. *Energy Technology Partnership Annual Conference 2017*, Edinburgh, UK: 10th October.

Spitz, T., Ascui, F., Chalmers, H., Lucquiaud, M., 2017. Operating flexibility in future low carbon energy systems. *UKCCSRC biannual meeting*, Sheffield, UK: 11-12 September.

Spitz, T., Ascui, F., Chalmers, H., Lucquiaud, M., 2017. The role of CCS power stations in future low carbon energy systems & their interaction with the downstream CO_2 transportation and storage infrastructure. 9th *Trondheim Carbon Capture and Storage Conference,* Trondheim, Norway: 12-14 June.

Spitz, T., Ascui, F., Chalmers, H., Lucquiaud, M., 2016. Cycling Flexibility of CO_2 injection wells. *Carbon Capture Utilization and Storage Conference 2016,* Tysons Corner, Virginia, USA: 14-16 June.

Poster presentations:

Spitz, T., Avagyan, V.,Mitchell, C., Chalmers, H., Lucquiaud, M., 2018. Right-Sizing CO_2 Transportation and Storage Infrastructure. *Accelerating CCUS: A Global Conference to Progress CCUS*, Edinburgh, United Kingdom: 28-29th November.

Spitz, T., Ascui, F., Chalmers, H., Lucquiaud, M., 2018. Interim Storage Potential of Dense Phase CO_2 Pipelines. *14th International Conference on Greenhouse Gas Control Technologies*, Melbourne, Australia: 21-26 October.

Spitz, T., Gonzáles Díaz, A., Chalmers, H., Lucquiaud, M., 2018. Flexible Operation of NGCC-PCC power stations at the interface of CO_2 transport and electricity transmission networks. *14th International Conference on Greenhouse Gas Control Technologies*, Melbourne, Australia: 21-26 October.

Spitz, T., Ascui, F., Chalmers, H., Lucquiaud, M., 2016. Operating Flexibility of CO_2 injection wells. *13th International Conference on Greenhouse Gas Control Technologies*, Lausanne, Switzerland: 14-18 November.

Spitz, T., Ascui, F., Chalmers, H., Lucquiaud, M., 2016. Operating Flexibility of CO_2 injection wells. *UKCCSRC biannual meeting*, Edinburgh, UK: 14-15 September.

Spitz, T., Ascui, F., Chalmers, H., Lucquiaud, M., 2016. CCS power stations at the interface of CO_2 transport and electricity transmission networks: How to deal with the dual set of requirements?. *UKCCSRC biannual meeting*, Manchester, UK: 13-14 April.

Spitz, T., Ascui, F., Chalmers, H., Lucquiaud, M., 2016. CCS power stations at the interface of CO_2 transport and electricity transmission networks: How to deal with the dual set of requirements?. *Early Career Researcher Winter School 2016*, Sheffield, UK: 15-18 February.

Spitz, T., Ascui, F., Chalmers, H., Lucquiaud, M., 2015. CCS power stations at the interface of CO_2 transport and electricity transmission networks: How to deal with the dual set of requirements?. *8th Trondheim Carbon Capture and Storage Conference*, Trondheim, Norway: 16-18 June.

Table of Contents

Table of Figures

Table of Tables

Nomenclature

Acronyms

ADM	Archer Daniels Midland Company
ANN	Artificial Neural Network
Ar	Argon
ASU	Air Separation Unit
BECCS	Bio-Energy with Carbon Capture and Storage
BEIS	Department for Business, Energy and Industrial Strategy
CCC	Committee on Climate Change
CCGT	Combined Cycle Gas Turbine
CCS	Carbon Capture and Storage
CCU	Carbon Capture and Utilisation
CCUS	Carbon Capture Utilisation and Storage
CO_2	Carbon dioxide
COS	Carbonyl sulfide
CU	Capacity Utilisation
DAC	Direct Air Capture
DECC	Department for Energy and Climate Change
DOGR	Depleted Oil and Gas Reservoir
DP	Dynamic Programming
DSR	Demand Side Response
ED	Economic Dispatch
EFR	Enhanced Frequency Response
EGR	Enhanced Gas Recovery
EI	Emission Intensity
EIA	US Energy Information Administration
EON	E.ON UK Energy Company
EOP	Electricity Output Penalty
EOR	Enhanced Oil Recovery
ERCOT	Electric Reliability Council of Texas

ERP	Energy Research Partnership
ETI	Energy Technology Partnership
FDC	Flow Duration Curve
FEED	Front End Engineering and Design
GB	Great Britain
GCCSI	Global Carbon Capture and Storage Institute
GEP	Generation Expansion Planning
GHG	Greenhouse Gases
GT	Gas Turbine
H_2	Hydrogen
H_2S	Hydrogen sulfide
HRSG	Heat Recovery Steam Generator
ICV	Inflow Control Valve
IEA	International Energy Agency
IEAGHG	IEA Greenhouse Gas R&D Programme
IEC	International Electrotechnical Commission
IGCC	Integrated Gasification Combined Cycle
IPCC	Intergovernmental Panel on Climate Change
JT	Joule Thomson
LACE	Levelised Avoided Cost of Electricity
LCICG	Low Carbon Innovation Coordination Group
LCOE	Levelised Cost of Electricity
LFP	Low Flow Period
LHV	Lower Heating Value
LNG	Liquified Natural Gas
LOEE	Loss of Energy Expectation
LOLE	Loss of Load Expectation
LOLP	Loss of Load Probability
LOx	Liquid Oxygen Storage
LP	Linear Programming
MAOP	Maximum Operating Pressure

MEA	Monoethanolamine
MEG	Monoethyleneglycol
MILP	Mixed Integer Linear Programming
MTPA	Million Tonnes per Annum
N_2	Nitrogen
NETL	National Energy Technology Lab
NG	National Grid
NGC	National Grid Carbon Ltd.
NGCC	Natural Gas Combined Cycle power plant
NLP	Non Linear Programming
NO_2	Nitrogen dioxide
NO_x	Nitrogen oxide
NPV	Net Present Value
O_2	Oxygen
OD	Outer Diameter
OPF	Optimal Power Flow
PCC	Post-combustions CO_2 Capture
PV	Photovoltaic
RoCoF	Rate of Change of Frequency
SAFT	Statistical Associated Fluid Theory
SDSN	Sustainable Development Solution Network
SMYS	Specified Minimum Yield Stress
SO	System Operator
SO_2	Sulfur dioxide
SO_3	Sulfur trioxide
SRMC	Short Run Marginal Costs
ST	Steam Turbine
SV	System Value
T&S	Transportation and Storage
TSC	Total System Cost
UC	Unit Commitment

UCC	Unit Construction and Commitment
UCED	Unit Commitment and Economic Dispatch
UCL	University College London
UK	United Kingdom
UKERC	UK Energy Research Centre
UNFCC	United Nations Framework Convention on Climate Change
USC-PC	Ultra-Supercritical Pulverised Coal Power Plant
VRE	Variable Renewable Energy
VSD	Variable Speed Drive
VSR	Variable Solvent Regeneration
ZEP	Zero Emission Platform

Symbols

a	Pipeline design factor
A	Flow rate change amplitude
$\bar{A}$	Average flow rate change amplitude
d	Delta
$	US dollar
D	Electricity demand
D_i	Pipeline inner diameter
D_o	Pipeline outer diameter
D_{net}	Net demand
e	Weld factor
€	Euro
f	Darcy friction factor
F	Flow rate
h	Enthalpy
p	Pressure
£	British pound stirling
q_w	Heat flux
ρ	Density
σ_h	Maximum tolerable hoop stress
σ_{SMYS}	Specified Minimum Yield Stress
S	Solar power
u	Local velocity
wt	Wall thickness
W	Wind power
x	Local coordinate along pipeline

1. Introduction

1.1. Background

1.1.1. Carbon capture and storage in the context of climate change

Greenhouse gas emissions need to be reduced substantially over the next decades to mitigate the risks and dangerous effects associated with climate change. Since the entry into force of the Paris Agreement in November 2016 (UNFCC 2018), nearly all countries world-wide have agreed to drastically reduce greenhouse gas emissions in order to limit the rise in average global temperature to well below 2 degrees Celsius compared to pre-industrial levels. An even more ambitious target has been set of pursuing efforts to limit the global temperature increase to 1.5 degrees Celsius.

Due to the relatively proportional relationship between anthropogenic greenhouse gas emissions and global average temperature rise, the term carbon budget has been coined (Allen 2016, Matthews et al. 2009, IPCC 2014). Limiting the average global temperature rise to 2 degrees Celsius, a scenario that is henceforth referred to as the '2 degree scenario', corresponds to the disposal of around 1000Gt of carbon (CO_2 equivalents) into the atmosphere (World Resources Institute 2018). The carbon contained in global resources of fossil fuels in contrast is estimated to be 11 fold this amount (Jakob and Hilaire 2015). At the current rate of emissions (~36.8GTCO_2/year in 2017; Global Carbon Project 2017) it would leave the world community around 20 years, before the 2 degree scenario becomes unachievable without large scale negative emissions (i.e. by creating additional carbon sinks – for example via Direct Air Capture, Bio-Energy with CCS; Trillionthtonne 2018, Allen et al. 2009). Strong efforts are, hence, needed to achieve drastic cuts in greenhouse gas emissions over the next few decades.

There are different ways of achieving these cuts. Many countries are focusing their efforts in reducing their GHG contributions on supporting renewable and nuclear power as low carbon power generation technologies. Operating an energy system entirely based on renewable and nuclear power in the near future will, however, be challenging. On one hand, national and global energy infrastructure is slow to change. Many assets of the energy system from the energy transmission and distribution networks, over the power generation facilities have lifetimes spanning up to 30-50 years (IEC 2015). Updating this infrastructure and enabling it to satisfy the large energy demands of modern societies in a low carbon fashion will be a costly as well as a time-consuming task. On the other hand fossil fuel power plants are in many cases needed as a cost effective way of stabilising the electricity grid by providing firm and flexible back-up power during periods of low or variable renewable energy resource availability (e.g. times of low wind and/or solar insolation) as well as inertia.

Adding to the challenge, the decarbonisation of the energy system alone does not bring the required reductions in emissions that are necessary to reach climate goals. Whilst the power generation sector alone is responsible for around 42% of global anthropogenic CO_2

emissions, the global transport sector and industry are accountable for roughly 23% and 19% of emissions, respectively (IEA 2015, 2016). A deep decarbonisation of the world economy therefore requires a comprehensive approach addressing all of these emission sources.

Last but not least the growth of populations and energy consuming economies around the world add to the strain of driving down emissions to a sustainable level (IPCC 2014).

Despite the commonly acknowledged necessity of reducing the consumption of fossil fuels, these are some of the main reasons why the dependency on fossil fuels is expected to remain substantial or even increase over the next decades (Abdilahi et al. 2018, IEA 2016b).

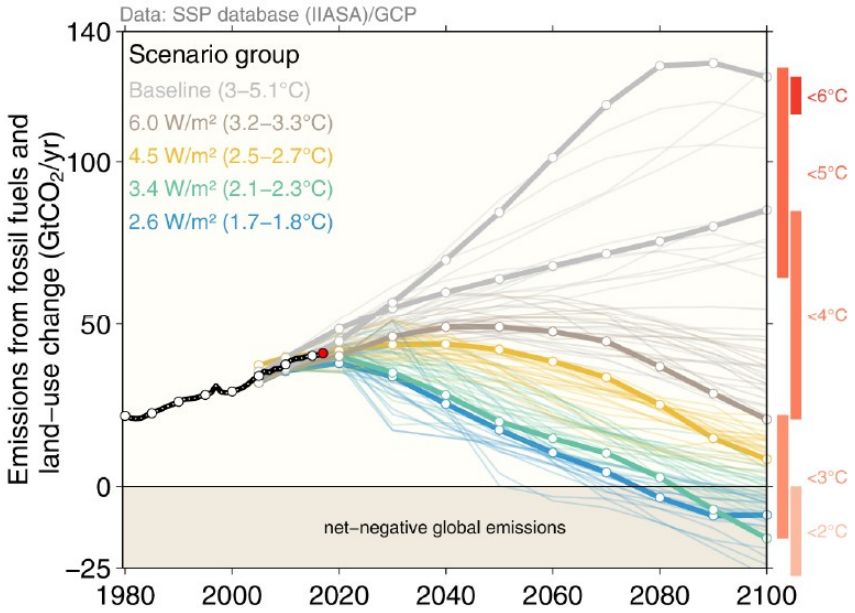

Figure 1.1: Different global net emission pathway scenarios leading to a range of global average temperature rises by the end of the century (Global Carbon Project 2017).

The dependency is in fact predicted to be so strong that the Intergovernmental Panel for Climate Change estimates that large amounts of net negative emissions are necessary towards the end of the century (see Figure 1.1, approx. from 2070) to reach the '2 degree' climate target (IPCC 2014).

This puts Carbon Capture and Storage (CCS) in a very unique situation for several reasons:

1) CCS is the only technology that can deliver significant amounts of negative emissions at large scale and already in the near future (see Bio-Energy with CCS in section 1.1.3).
2) In contrast to renewables and (arguably) nuclear power, fossil fuel power stations can provide firm yet flexible power to balance electricity systems at relatively low

(e.g. capital) cost. However, only fossil power stations used in conjunction with CCS technology have carbon intensities sufficiently low to be consistent with the set climate targets.

3) CCS has the capability to decarbonise large parts of the industry, without requiring it to switch to alternative energy vectors (energy vectors are used to 'carry' or transfer energy across the economy to the end user). CCS is further the only currently available technology that can decarbonise industrial processes that inherently produce large quantities of CO_2 (e.g. refining of certain fuels or cement production – the latter alone was responsible for around 4% of world-wide CO_2 emissions in 2016 equivalent to around 1.45GtCO_2; Andrew 2018).
4) By allowing the retrofitting of CCS technology to large point polluters, the technology offers to keep much of the current infrastructure by avoiding turning existing power stations or industrial plants into stranded assets. It also avoids a radical re-building of infrastructure in order to supply industrial plants with alternative low carbon energy vectors (e.g. electricity or hydrogen).

As such CCS offers to be a unique solution to tackle and mitigate the risks and dangerous effects associated with climate change. The value of CCS in the context of climate change is acknowledged by a wide range of scientific studies (IPCC 2014, IEAGHG 2017, LCICG 2012, CCC 2015, ETI 2015). It is further demonstrated by the fact that 8 of 10 of the climate models deployed by the IPCC are not able to reach the '2 degree' climate target without the deployment of CCS in the capacity mix (IPCC 2014). In the remaining two models, excluding CCS from the capacity mix increases the cost of reaching the climate targets by 138% by the end of the century (IPCC 2014) – a vast number given the scale of the required changes to the global energy supplying infrastructure.

1.1.2. Carbon capture and storage (CCS) versus carbon capture and utilisation (CCU)

CCS is a family of technologies with a wide range of applications. The common feature is the separation and isolation of carbon dioxide (CO_2), as the main contributor to global GHG emissions, and its permanent geological storage in underground formations (e.g. depleted oil and gas fields, saline formations, etc.) where it cannot act as a greenhouse gas fuelling climate change.

CO_2 in varying purity forms can, however, also be used as a raw material for a range of products. As such CO_2 can be used in the food and drink industry (e.g. fizzy drinks), for fire suppression, as an inerting agent, as dry ice, or in agriculture for desalination. Alternatively, it can be converted into urea and used as fertilisers or into fuels such as methanol and methane. Potentially the biggest uses of CO_2 in terms of scale could be made through mineralising it and using it as building materials, or by using it for Enhanced Oil Recovery (EOR) and Enhanced Gas Recovery (EGR). EOR or EGR refers to injection of CO_2 into oil and

gas fields, respectively, to increase or sustain production rates. For a more extensive review of the usages of CO_2 the reader is referred to Al-Mamoori et al. (2017), GCCSI (2011), and European Commission (2018).

For referring to this form of recycling of CO_2 the term Carbon Capture and Utilisation (CCU) is usually used. The positive climate effect of CCU is, however, varied and depends on the application. Frequently the captured and recycled CO_2 is released into the atmosphere ultimately via detours (e.g. food and drink industry, urea) and with time-delays of days, months, or several years, with no significant positive long term effect for the climate. Although carbonate mineralisation is a naturally occurring process and traps CO_2 permanently, it happens at an exceptionally slow rate (Mac Dowell et al. 2017). Speeding up this process would require vast amounts of decarbonised energy that most likely could be used more beneficial for society for example for electrification of heating or charging of electric vehicles (Mac Dowell et al. 2017). Conversion of CO_2 into fuels is similarly problematic from an energetic perspective, as it would require vast amounts of decarbonised energy if it is to be achieved in a carbon neutral way. This leaves EOR and EOG as the CCU technologies that are commonly estimated to have the largest long term climate mitigation (GCCSI 2011, Mac Dowell et al. 2017).

Nevertheless, when comparing scales it shows that the volumes of CO_2 over the next decades are likely to exceed the amounts that can be reused and recycled by one magnitude or two. For example, Mac Dowell et al. (2017) estimates that the chemical conversion of CO_2 is unlikely to contribute to more than 1% of the mitigation challenge, and even an optimistic scale up of the EOR industry is unlikely to be able to achieve sequestration of more than 4-8% of the CO_2 that needs to be retained from the atmosphere if the 2 degrees scenario is to be met. Even when making more optimistic assumptions about the mineralisation potential of CO_2 the global CCS Institute (GCCSI) concludes that the reuse potential of CO_2 is too small to make a material contribution to global CO_2 abatement (GCCSI 2011). As such, CCU is commonly seen as a way of unlocking additional revenue streams to CO_2 capture, a useful proposition in the absence of strong carbon prices or in emerging economies. Nevertheless, this economic driver delivering additional revenue streams might be undermined and weakened substantially with increasingly stringent emission targets and vast volumes of CO_2 flooding the market in the future (GCCSI 2011).

When speaking about carbon capture as a climate mitigation strategy the term CCS is, hence, generally used within this thesis. Summarising both applications it shall be noted that the term Carbon Capture Utilisation and Storage (CCUS) is also sometimes used.

1.1.3. Classification of CCS technologies

To understand the wide range of CCS technologies that exist or are conceivable it is helpful to classify them. Common ways of classifying them are (i) by application or capture source, (ii) by capture strategy, (iii) by capture method, and (iii) by the net climate effect.

CO_2 can be captured from all kinds of carbon dioxide containing gases. It can be captured from the air (Direct Air Capture – DAC) or from combustion flue gases of cars, ships, and other stacks. Due to the relatively high spatial footprint of the CO_2 capture facility and a higher energy intensity when separating out CO_2 from diluted sources it is generally considered most economical to capture CO_2 from large point emitters with relatively high concentrations of carbon dioxide. Amongst the largest point emitters are fossil fuel power stations, and industrial facilities such as refineries, and cement and steel plants (IPCC 2005). Collectively these sectors account for nearly 60% of global GHG emissions (IEA 2016a, Worldsteel Association 2017). The climate potential of decarbonising some or all of these plants is therefore substantial.

The available capture strategies can be broadly distinguished into pre-combustion, post-combustion and oxy-fuel combustions. Pre-combustion and post-combustion capture refer to the place at which the process of separation and isolation of CO_2 from the combustion gases takes place. Oxy-fuel combustion refers to a strategy mainly aimed at the power generation sector, in which fuel is burned in an environment of pure oxygen creating a combustion flue gas consisting of predominantly CO_2 and water. The CO_2 subsequently only needs purification, drying and compression before it is ready for transportation and permanent storage (IPCC 2005). For more information on the individual capture strategies the reader is referred to (IPCC 2005).

The most common capture method is capture via scrubbing of the flue gas stream using chemical solvent composed of aqueous amines, such as MEA (monoethanolamine). It has been deployed in the chemical and oil industry for many decades for the removal of hydrogen sulphide and CO_2 from natural gas and is as such extensively tested, cost-competitive and reliable (Gupta et al. 2003, GCCSI 2017). Other promising technologies that are heavily researched are capture via membranes, solid sorbents, and chemical looping. For more details on these, the reader is referred to reviews by Wang et al. (2017) and Lockwood (2017).

Finally, carbon capture and storage facilities can also be categorised based on their net effect on climate change. Broadly speaking, CCS facilities can be classified into carbon positive, near carbon neutral and carbon negative facilities, based on how much residual emissions they release into the atmosphere (Scott et al. 2013). Carbon positive facilities capture substantial amounts of CO_2 (e.g. capture rates of 0-80%) that has been produced for example by the combustion of fossil fuels, however, still release significant amounts into the atmosphere. Near carbon neutral CCS facilities retain most of the GHGs generated (e.g. 80-99%) by the combustion of fossil fuels from the atmosphere. Carbon negative facilities in contrast have a net positive effect on the atmosphere. Overall, these facilities extract more CO_2 from the atmosphere (either directly via e.g. DAC or indirectly via e.g. combustion of biomass) than they emit to it. They achieve this, for example, by extracting energy from biomass that over its lifetime has naturally absorbed large quantities CO_2 from the atmosphere. The combustion process of biomass can contribute to the production of power and/or heat, whilst the captured and permanently sequestered CO_2 previously accrued in

the biomass (and before that contained in the atmosphere) can have a net positive effect on mitigating climate change. This process is commonly referred to as BECCS (Bio-Energy with Carbon Capture and Storage). It is a key component in the battle against climate change, in particular if negative emissions become necessary – a case predicted in most of the modelled scenarios by the IPCC if the current climate targeted are to be reached. It is worth noting, however, that there is an ongoing controversy surrounding the extent to which BECCS can deliver the levels of negative emissions required at the scale of global mitigation in a resource sustainable way (Fajardy and Mac Dowell 2018, Fridahl and Lehtveer 2018).

1.1.4. Status of CCS and examples

Given the large infrastructure developments, the long lead times, and the urgently desired cost reductions of the technology, a continuous stream of CCS projects is important for benefitting from ongoing improvements of the technology (i.e. learning-by-doing), as well as to reach the required CCS capacities by the middle and end of the century consistent with set climate targets. Figure 1.2 provided by the Global CCS Institute (GCCSI) presents an overview of the start date of large scale CCS projects around the globe.

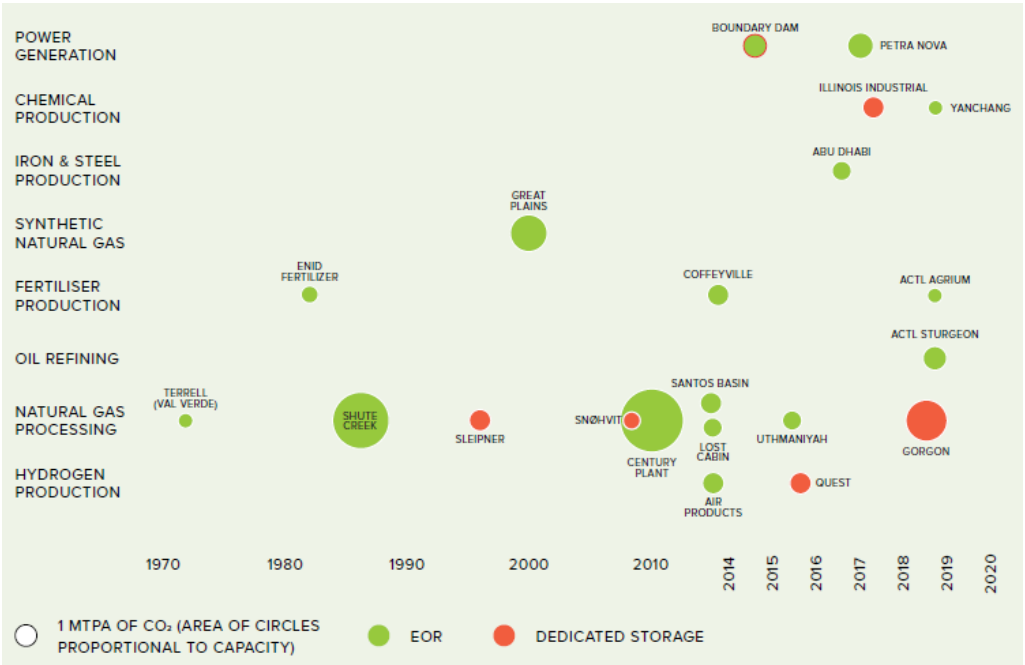

Figure 1.2: CCS large-scale facilities in operation and construction by industry and operations start date (GCCSI 2017).

The figure illustrates that large scale CCS projects have been developed since the 1970s, predominantly for the processing of natural gas and in the fertiliser production industry. The first full chain and full scale CCS project in the power generation sector has taken up

operation at Boundary Dam in Canada in 2014 (SaskPower 2018). The figure also shows that up to the point of writing most CCS projects have been set up for with Enhanced Oil Recovery as the main economic driver. By 2018 only five projects have been dedicated to long term geological storage of CO_2 (Sleipner, Snøvit, QUEST, Illinois Industrial and Gorgon). With stronger climate mitigation incentives and more stringent emission limits this is, however, expected to change in the future.

The ongoing development of CCS projects is also reflected by the strong uptake of cumulative installed CCS capacity and volumes of CO_2 stored, as depicted in Figure 1.3. In 2017, a record of 220 cumulative million tonnes of CO_2 has been injected into deep underground geologic formations (GCCSI 2017). By 2018, the installed CCS capacity is expected to reach a new peak with the capture capability of 37MTPA (Million Tonnes Per Annum) of CO_2 (GCCSI 2017). Yet, this represents only a small fraction of the CCS capacity able to capture the 3800MTPA of CO_2 as required by 2040 to stay consistent with the 2 degree global warming scenario, according to the International Energy Agency (IEA 2017).

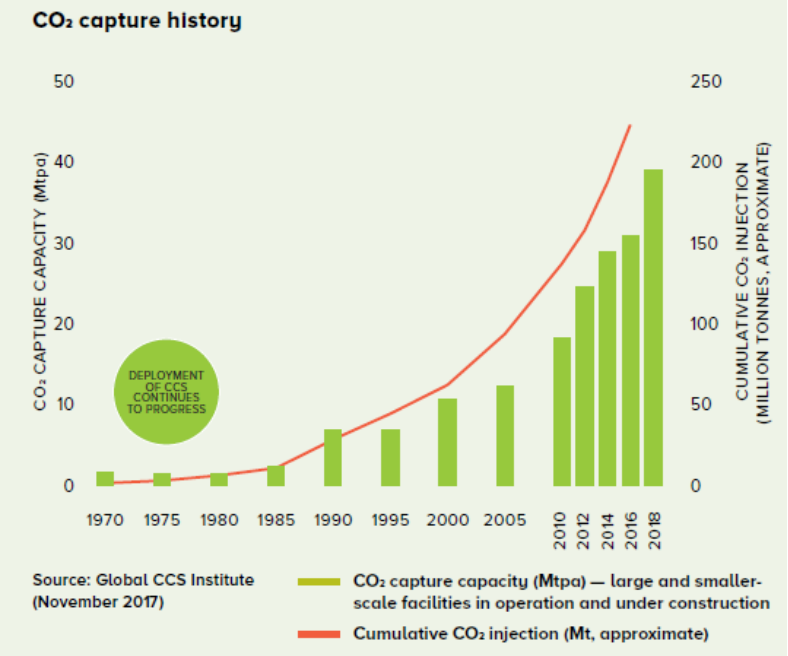

Figure 1.3: Historical CO_2 capture volumes over time (GCCSI 2017).

Figure 1.4 illustrates the geographical distribution of large scale CCS projects in operation or under construction at the time of writing. It shows that CCS evolved into a global technology with projects being planned or operated world-wide. When it comes to projects operational at the time of writing North America features the majority as well as some of the most modern and largest CCS facilities, such as Century plant (ZeroCO2 2018; 8.4MTPA), Boundary Dam (SaskPower 2018; 1MTPA), Petra Nova (NRG Energy 2018; 1MTPA), and Illinois Industrial CCS facility (ADM 2017; 1MTPA).

Figure 1.4: Global CCS facilities in operation and under construction (gCCSI 2017). For colour coding see legend.

In Europe, the flagship projects Sleipner and Snøvit projects have been operating since 1996 and 2008 with storage volumes of 1MTPA and 0.7MTPA, respectively (Equinor 2018, gCCSI 2017). In the Middle East two large-scale projects are running at the time of writing in Abu Dhabi gCCSI 2017; 0.8MTPA) and Uthmaniyah (gCCSI 2017; 0.8MTPA). Injection has started at the time of writing at the Tomakomai demonstration project in Japan (JapanCCS 2018; up to 0.3MTPA capacity). For more information about the projects, in particular about the ones under construction and in planning, the reader is referred to gCCSI (2017).

1.1.5. Research on flexible operation of integrated CCS process chains

A key engineering challenge in CCS is the scope of the application. It stretches from the CO_2 capture process in power, industrial, or chemical plants, over the transportation of CO_2, its injection, and its permanent safe storage in underground geological formations for thousands of years.

For the system to work efficiently, the individual parts of the process chain need to be carefully integrated at full load and design conditions as well as at any other load point the system might need to operate at. Whilst this might be reasonably straight forward to achieve at industrial plants that run predominantly base-load, it becomes a particular challenge when CCS is applied to fossil fuel power stations operating in future low carbon energy systems. Traditionally, fossil fuel power stations have had the role of providing large amounts of base load and mid-merit power in an energy system they dominated. This leads to relatively constant operating profiles of all individual conventional power plants, governed predominantly by recurring electricity demand profiles throughout the day.

The large changes in the energy sectors expected over the coming years and decades (e.g. roll-out of renewables electrification of transport, smart grids, energy storage, electric vehicles) make it difficult to predict the exact role of CCS enabled fossil fuel power stations in low carbon energy systems. Nevertheless, there is a growing consensus, particularly amongst energy system modellers, that the primary role of fossil power stations (with or without CCS capability) will shift away from providing mere base-load power to supporting the high levels of intermittent renewable penetration by balancing the power system through provision of firm and flexibly dispatchable power (IEAGHG 2017) as well as inertia.

This flexible, time variable operation expected of a conventional fossil power generator in the future will also impact any CCS infrastructure connected to it. In particular, this will affect CO_2 capture facilities that will consequently need to operate in a time-variable fashion capturing CO_2 from the varying amounts of fossil fuel that is burned throughout the day. Equally, CO_2 transportation and storage (CO_2 T&S) networks will need to be able to handle time-variable feed flows.

The ability of the integrated CCS infrastructure to regularly operate in a flexible manner is to date, however, still to be understood. Significant concerns have, for example, been raised relating to the injection wells' ability to accommodate frequent and large feed flow fluctuations (Lund et al. 2015, Roy et al. 2016, Aursand et al. 2017). Only few studies exist in the literature that explore the operating flexibility constraints of other components of the CCS process chain such as the transportation or storage system (Jensen et al. 2014, Edlmann et al. 2019, ZEP 2017). Identifying this gap in the literature, ZEP (2017) recently stresses that "*flexibility is a key requirement for the transport and storage elements of the CCS chain*" (p. 4), and that future research urgently needs to "*investigate the impact of intermittent flow on the well system*". Given strong concerns related to injection wells abilities to operate flexibly, a key question ZEP (2017) raises is "*where to build capacity and redundancy into a system, which copes with volatility in supply and demand for CO_2*" (p. 91), and "*where … [this] capacity for flexibility is to be build most cost-effectively*" (p. 100).

Despite this identified and urgent need, no comprehensive study could be identified in the literature that investigates the expected requirements for flexible operation of the integrated CCS infrastructure and puts it into perspective to its ability to support this flexible operation. It is only when the requirement for operating flexibility is better understood, that the implications and the potentially additional costs associated with managing the operational issues that flexible operation imply can be minimised.

This thesis, therefore, advances the body of knowledge by taking a whole chain perspective. The study contributes to the literature by identifying (i) the requirements for flexible operation of CCS infrastructure when accommodating CO_2 flows from the electricity sector; (ii) the constraints to flexible operation along the entire CCS process chain, predominantly related to the injection well and storage sites; and (iii) possible options to overcome these constraints, which can be accomplished, for example, by balancing flow rates upstream in the system, in order to ensure the safe and efficient operation of integrated CCS process chains.

1.2. Research aims and objectives

The main research objectives of this thesis in this context are:

- Examining the requirements for flexible operation of CCS power stations in future low carbon electricity systems. A case study of GB low carbon electricity system scenarios is used.
- Understanding the consequences this has in terms of time variable CO_2 flows that need to be accommodated by downstream transportation and storage networks.
- Identifying relevant bottlenecks to flexible operation along the CCS process chain consisting of CO_2 capture, compression, transportation, injection, and geological storage.
- Identifying and qualitatively comparing available options for mitigating issues associated with variable CO_2 flow rates and low flow events along the T&S system.
- Quantitatively assessing the effectiveness of two options available for mitigating the issues associated with variable CO_2 flows, and in particular low flow events, at the injection level: Line-packing of dense phase CO_2 transportation pipelines and solvent storage at PCC.
- Informing the discussion about the strategic development of infrastructure to avoid potential future operating problems as a consequence of the changing requirements and operating regimes of CCS power stations in the transition towards low carbon electricity systems.

1.3. Novelty and contributions

The following results can be considered an original contribution to advancing the body of knowledge in the field of flexible operation of CCS infrastructure:

- For the first time in the literature a detailed characterisation of CO_2 flow profiles is provided for timeframes of up to 1 year, generated by CCS power stations operating in GB low carbon electricity system scenarios. This can serve CCS infrastructure designers as a benchmark for developing the system according to the expected need for flexible operation. It is only when the requirements for flexible operation are understood that the system can be designed most cost-effectively.
- Identification and compilation of potential constraints to flexible operation of all major components along the CCS process chain via a rigorous literature review complemented by the consultation of several industry leading experts.
- Identification and compilation of an extensive summary of options that allow mitigating the issues associated with CO_2 flow variability, and that can be implemented at different parts of the CCS process chain - via a literature review.

- Quantitative technical assessment of two options that allow reducing CO_2 flow rate variability by balancing flows, and, hence, mitigating potential issues associated with variable flows: Line-packing of dense phase CO_2 transportation pipelines and solvent storage at PCC power stations – via process modelling.
- Simulation and analysis of line-packing times for a large range of dense phase CO_2 pipelines designs frequently considered for the long distance transportation of CO_2 – via process modelling.
- Quantitative analysis of the extent to which critical low flow periods in CO_2 injection wells can be avoided in different GB electricity system and CO_2 T&S network scenarios by exploiting the line-packing potential of dense phase CO_2 pipelines.
- Assessment of the performance of two alternative operating strategies of gas fired CCS power stations under solvent storage and regeneration operation at full load and at part-load – via process modelling.
- Deployment of CO_2 compressor model that is able to predict operation at part-load in more detail than previous literature, delivering novel insights into compressor behaviour under solvent storage operation – via process modelling.
- The well-founded conclusion that it is reasonable to believe that the issues associated with variable CO_2 flows can be overcome, even though it is to this date unclear at which cost.

1.4. Thesis overview

The thesis is composed of eight Chapters. Their contents are summarised below.

- Chapter 2 describes the issues associated with flexible operation and the constraints to flexible operation of the individual components along the CCS process chain. It provides the background for the research conducted in the following chapters of this thesis.
- Chapter 3 demonstrates the requirements for flexible operation of the CCS infrastructure imposed by the needs of the investigated low carbon GB electricity systems scenarios. The strong contrast to the findings of the previous chapter constitutes the rationale behind this thesis.
- Chapter 4 explores the options that exist for accommodating the requirements for flexible operation of CCS power stations, whilst simultaneously mitigating the integrity risks this implies to the overall system.
- Chapter 5 explores the option of line-packing at dense phase CO_2 pipelines and demonstrates how it can be used as a way to avoid critical periods of low flow at the injection well level by balancing variable CO_2 flow rates within the transportation system, mitigating potential downstream integrity risks.

- Chapter 6 quantifies the extent to which extreme periods of low flow can be avoided at the injection well level by utilising the option for line-packing in several selected GB electricity system and transportation network scenarios.
- Chapter 7 investigates the behaviour of a NGCC-CCS power station with interim solvent storage under delayed solvent regeneration operation, as an option to balance CO_2 flow rates and mitigate integrity risks associated with variable operation of the downstream T&S network. A particular focus is placed on the energetic performance of the power station at the different required load points.
- Chapter 8 summarises and concludes. It further discusses the relevancy and urgency of further research to be conducted on the topic of operating flexibility of CCS networks, and on ways of overcoming the main constraints to flexible operation. Several core areas are identified as particularly relevant for future research.

2. Issues associated with variability

Providing the basis for all subsequent chapters of this thesis, the present chapter discusses and reviews the ability and the constraints of all main components of the CCS process chain to regularly operate in a flexible and load following manner. Conceptually the CCS process chain can be divided into 4 subsystems: CO_2 capture (including purification and compression), transportation, injection and storage. All of these parts of the system will be reviewed, respectively, in subsections 2.2.1-2.2.4 in more detail. Section 2.1 starts off with a description of commonly expected configurations of CCS process chains in order to provide a foundation for the following discussions.

2.1. CCS process chain description

The common feature of CCS networks is that they integrate locations of CO_2 production and capture (can be individual CO_2 source or combination of sources referred to as 'CO_2 clusters') with a practical and cost-effective way for transporting the CO_2 frequently of varying purity levels and compositions to storage sites (can be a single storage site or multiple sites, also referred to as 'CO_2 storage clusters') that are able to permanently lock it away from the atmosphere. A regular CCS process chain as such includes CO_2 capture facilities, a transportation system, injection wells, and long term geological storage sites.

Although the fundamental parts of the network do not differ, CCS networks are highly flexible systems in terms of their design. The many possible permutations of all involved components add to the challenge of designing and integrating a CCS system efficiently, and proofing it against the range of operating requirements and extensions that it might face over the expected operating timescales of usually several decades. Equally, the definition of a 'standard' or 'common' CCS system for subsequent analysis is difficult.

For example, CO_2 is expected to be captured from fossil power stations (coal or natural gas fired) in the future. An extensive decarbonisation of the economy, however, makes it necessary to capture CO_2 equally from cement and steel factories, from waste-to-energy plants, and from industrial facilities such as chemical processing plants. At each of these facilities, several alternative CO_2 capture technologies are available for use (see also discussion in section 1.1.3). Both capture source and capture technology, however, affect the purity of the produced CO_2 and its composition (i.e. impurities). This in turn can significantly affect the required design of the downstream system and the measures that need to be taken for its safe operation (e.g. materials that need to be used and safe operating envelopes/conditions). As the elimination of all impurities from the CO_2 is cost-ineffective and impractical it is widely acknowledged that CO_2 purity standards or specifications will need to be put in place. These, however, can be tailored to the needs of the individual systems (Porter et al. 2015).

Once captured, the CO_2 still needs to be compressed and dried in order to make it ready for transportation (Vermeulen 2011). Whilst compression usually occurs via several compression steps in an axial inline or an integrally geared centrifugal compressor there are different strategies for efficiently compressing the fluid to pressures of around 110-150bar. The strategies can be broadly classified into: (i) Compression to subcritical conditions, liquefaction and pumping; (ii) Compression to supercritical conditions and pumping; and (iii) Compression to supercritical conditions and to final delivery pressure (Vermeulen 2011, González-Díaz et al. 2017). Investigating strategy (i) and (ii) Vermeulen (2011) concludes that the reduction in power consumption by reducing the required amount of compression via using an external refrigeration cycle for liquefaction is not significant. Due to the density of the fluid becoming very high at high pressures pumping becomes gradually more efficient beyond the critical pressure. Vermeulen (2011) and González-Díaz et al. (2017) therefore suggest that option (ii) is specifically interesting for reaching high delivery pressures (e.g. 150bar or higher). For delivery pressures of around 110bar the considered compression strategy in literature varies predominantly between strategy (ii) and (iii) (EBTF 2011, Sanchez Fernandez et al. 2016b, González-Díaz et al. 2017). Finally, drying of the CO_2 is usually performed alongside the stepwise compression process with intercooling and liquid knock-out drums. Dependent on the required water content this process is followed by a dedicated dehydration unit (Vermeulen 2011).

There are several ways for transporting the CO_2 to suitable storage sites that can be either onshore or offshore: by pipeline, by truck, or by ship (IPCC 2005, Mohitpour et al. 2012, IEAGHG 2012, Onyebuchi et al. 2018). Transportation by pipeline is, in general, characterised by high capital costs and low operational costs, whilst the opposite is valid for transportation via truck or ship. It is, hence, widely established that for large volumes of CO_2 pipeline transport is preferred, as long as distances are not excessive (GCCSI 2011b Knoope et al. 2015, Roussanaly et al. 2014, Hussein 2017). ZEP (2011) estimates for an example large scale CCS network with CO_2 volumes of 20MTPA (Figure 2.1) that ship transportation only gets competitive with pipeline transport at distances of 1500km or higher. However, this number is sensitive to the underlying cost data. Roussanaly et al. (2014) determines for CCS networks with CO_2 flow volumes of 20MTPA and 10MTPA, respectively, that ship transport only gets competitive with pipeline transportation at distances over around 600km and 400km. At small CO_2 volumes of 1-4MTPA this threshold can fall to 150-300km (GCCSI 2011b, Roussanaly et al. 2014). It should be noted that generally CO_2 is predicted to be most cost effectively transported in supercritical or dense form (regardless of whether ship or pipeline transport is considered) due to the significantly higher densities. However, particularly during the early stages of injection of CO_2 into low pressure and depleted oil and gas reservoirs (DOGR) transportation and injection of the fluid in the gas phase has also been proposed to avoid significant pressure reductions and Joule Thomson (JT) induced temperature drops over the wellhead (EON 2011, GCCSI 2013).

Spine Distance km	180	500	750	1500
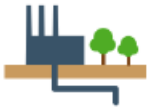 Onshore pipeline	1.5	3.7	5.3	n. a.
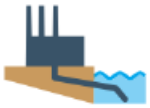 Offshore pipeline	3.4	6.0	8.2	16.3
 Ship (including liquefaction)	11.1	12.2	13.2	16.1

Figure 2.1: Cost estimate for large scale CO_2 transportation networks of 20Mtpa (ZEP 2011).

A significant cost factor when transporting CO_2 via ship is not only the fuel and the energy associated with liquefaction and cooling of CO_2, but also the on- and offloading that requires large scale terminals, frequently with additional temporary buffer storage facilities (see Figure 2.2). Although direct offloading from ships into offshore buoys or to floating injection facilities is generally considered feasible, it comes with uncertainties and risks associated with the technology that is to date not commercially available (Norwegian Ministry of Petroleum and Energy 2016, ZEP 2017). Alternatively, offloading onto an offshore platform can be used (Kler et al. 2016). Another option proposed by Norwegian state company Gassnova (with support from Equinor formerly known as Statoil) for a planned large scale CCS project in Norway is to utilise a hybrid system consisting of either short distance onshore pipeline transport or transport via tanker trucks from the CO_2 capture facilities (e.g. around Oslo) to a harbour, long distance transportation via ship (approx. 600km) to an onshore offloading point in the proximity of the offshore injection site, with subsequent offshore pipeline transportation for the remaining distance to the storage site at Smeaheia (approx. 50km) (Norwegian Ministry of Petroleum and Energy 2016, Gassnova 2017). This represents another layer of complexity and integration, and illustrates the wide range of conceivable future CCS process chain configurations.

Adding to the complexity it is generally acknowledged that transportation networks can benefit from substantial cost-reductions when exploiting economies of scale (in particularly pipeline networks; Energy Technologies Institute 2014a, Summit Power 2017). Effectively, this implies large cost advantages when centrally collecting relatively large volumes of CO_2 in so called CO_2 clusters from a number of CO_2 sources, and transporting it via a few trunklines to a storage hub, also referred to as CO_2 storage cluster, where it is distributed and injected via a number of wells into the geological storage reservoirs.

The long distance transportation via pipeline leads to pressure drops that can require pressure boosting stations to be installed along the way, ensuring that the fluid stays within the allowable pressure operating envelope, as well as to achieve required injection

pressures. The strategic placement of booster stations in CO_2 pipeline transportation networks represents a further challenge to consider.

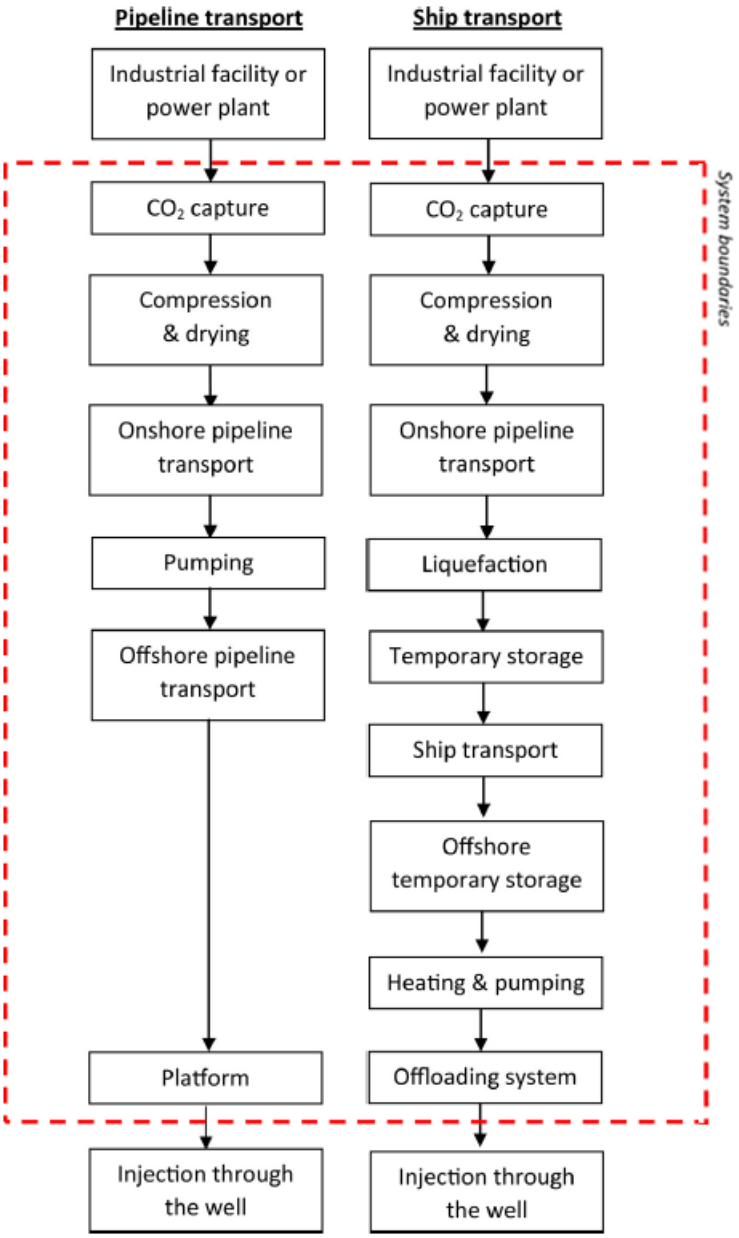

Figure 2.2: Schematic overview of the transportation process chain when achieved exclusively via pipeline (left), and when utilising ship transport (right). Adopted from Knoope et al. (2015).

It becomes clear that CCS networks - although being made up of similar components - are highly complex and individual systems that it can be difficult to compare. To reduce the number of permutations that need to be considered, and to account for the fact that relatively high volumes of CO_2 will need to be captured and transported if significant contributions to climate mitigation are to be achieved, that for cost reason would be transported only for the shortest necessary distances, transportation via pipeline is

considered the baseline within this study. This is considered to be reasonable especially in the GB context with expected volume flows of 60-180MTPA by 2050 (UK CCUS Cost Challenge Taskforce 2018, Summit Power 2017) and an abundance of storage sites in the Southern and Northern North Sea usually in the range of 100-200km from large scale emission sources (Summit Power 2017). However, even if transportation via pipeline is assumed to be the baseline method in this study many of the discussed issues associated with variable CO_2 flow rates are equally or even more relevant when transportation is carried out via ships (or trucks).

With geological storage formations being situated usually 800-2500m under the surface (L.E.K.Consulting 2009), injection wells are necessary to bridge the last vertical kilometres of transportation of the CO_2. Although injection well technology has advanced significantly over the last decades (Bruno et al. 2011, Fombad 2016) and may offer solutions to some of the problems associated particularly with the injection of CO_2 into DOGR (e.g. low reservoir pressure that can lead to two-phase flow in well) these are not commonly discussed in the CCS literature. As the general strategy to bridge the last vertical kilometres of transport via creating a flow path is similar between all of these options, a more detailed comparison is considered dispensable in the present section. A more detailed summary of the relevant options is, however, provided in Chapter 4 (section 4.1).

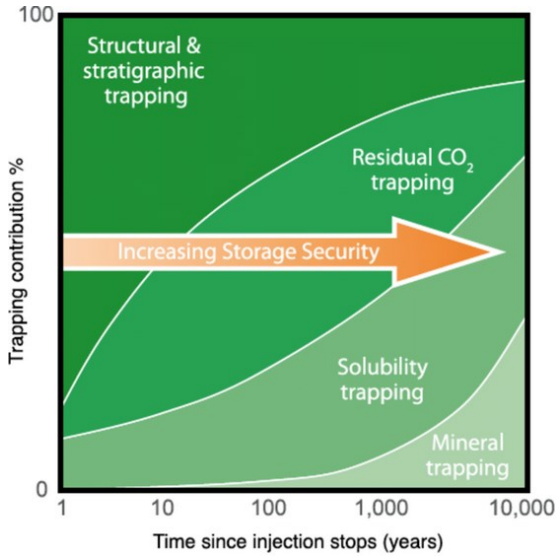

Figure 2.3: Trapping mechanisms and contributions depend on a range on physical and geochemical processes and change over time influencing the storage security (IPCC 2005).

Finally, the main types of geological formations usually considered for long term storage of CO_2 are saline aquifers and depleted oil and gas reservoirs (DOGR). Saline aquifers are formations of porous rock that are filled with brine (i.e. salty water). By injection of CO_2 the brine can be either replaced or compressed unlocking large storage volumes. It is estimated that world-wide saline aquifers offer the largest potential volumes for long term storage of CO_2 (NETL 2017). Saline aquifers can be 'closed' or 'open' aquifers, which refers to their hydraulic connection with adjacent rock formations (ETI 2014). Alternatively, DOGR are

frequently seen as ideal CO_2 storage sites having previously demonstrated their storage integrity by containing pressurised hydrocarbons for millions of years (NETL 2017). Due to previous oil and gas production these fields are usually very well characterised reducing the uncertainties and risks associated with the injection of large volumes of CO_2 (Sanchez Fernandez et al. 2016). Further, utilisation of DOGRs for the storage of CO_2 can benefit from the reuse of infrastructure that has previously been installed for the exploitation of the oil and gas fields (e.g. platforms and pipelines; Pale Blue Dot Energy 2016).

Once in the storage reservoir it is fundamental for the success of any CCS project that the CO_2 stays locked up in the store over time frames of 1,000s to 10,000s of years. The trapping mechanisms to serve this purpose can be classified into 'structural & stratigraphic trapping', 'residual CO_2 trapping', 'solubility trapping', and 'mineral trapping' (see Figure 2.3; IPCC 2005, Bellona 2007). Initially, CO_2 is predominantly physically trapped below geological seals such as very low permeability caprocks or shale or salt beds. Subsequently, residual hydrodynamic trapping can occur in systems such as saline formations without predefined closed traps (e.g. such as domes), but where the CO_2 can migrate driven by its buoyancy at very slows speed over long distances in a separate phase in a layer just below the sealing formation until it gets trapped in local structures or stratigraphic traps. Solubility trapping refers to CO_2 dissolving in water with the benefit of creating a single phase and eliminating the buoyance of the single phase CO_2. Finally, as the most secure and long term mechanism CO_2 can undergo a sequence of geochemical interactions with the rock and formation water that lead to conversion of the CO_2 to stable carbonate minerals. Although this geochemical process of mineral trapping is slow and believed to take a thousand years or longer, it is highly desirable due to the stability and permanence of the resulting storage mechanism. For further information on the geological trapping and storage mechanism the reader is referred to (IPCC 2005, Bellona 2007).

2.2. Issues associated with flexible operation of CCS infrastructure

The previous chapter and sections have outlined the likely requirement for flexible operation as well as typical CCS process chain configurations expected in the future. The remainder of the present chapter reviews and discusses the ability of all main subsystems of a typical CCS process chain consisting of CO_2 capture, transportation, injection and storage, to operate in a flexible manner.

As previously explained, the literature on the flexible operating capabilities of CCS components is relatively scarce, and a large part of it has only developed over the recent years in parallel to the research conducted in this study. Nevertheless, this chapter is primarily based on a thorough literature review. Many of the findings and constraints to flexible operation raised by the literature have, nevertheless, been independently identified and confirmed with leading industrialists in the field of CCS. This has been achieved partly via a secondment to the National Grid Carbon (NGC) FEED study team of the White Rose

CCS Demonstration project in the UK, responsible for the initial design and feasibility study for the CO_2 transportation and storage systems. Additionally, other leading industrialists (i.e. from the Shell Peterhead CCS demonstration in the UK, as well as the American Electric Power Mountaineer Plant Product Validation Facility) have been consulted on a series of conferences to further improve the credibility of the findings. As part of the secondment and the knowledge transfer program of the White Rose CCS project a summary of learnings report has been produced (Spitz 2016) and approved by National Grid Carbon Ltd.. The key constraints to flexible operation of the CO_2 T&S system identified throughout the secondment have been compiled in Figure 2.4 which will guide subsequent discussion.

Transportation Pipeline - Pressure envelope to maintain single phase and to respect max. limit - Max. speed (erosional velocity) - (Ramp rates: 'Hammer effects')	**Booster Station** - Ramp rates - Maximum and minimum flow
Injection well - Hydrate formation (JT-cooling) - Cracking of cement and wellbore materials (JT-cooling) - Reduced lifetime due to cyclic thermal stresses (JT-cooling) - Hydrogen induced embrittlement of well material (Phase change) - Oscillations and vibrations (exaggerated by phase change) - (Ramp rates: 'Hammer effects')	**Reservoir** - Maximum pressure levels - Halite build up (saline aquifers) - (Temperature variations to limit thermal stresses on rock)

Figure 2.4: Summary table of constraints to flexible operation in CO_2 transportation and storage networks; based on secondment to FEED study team of National Grid Carbon Ltd. for White Rose project in the UK (Spitz 2016).

2.2.1. Capture

The need for operational flexibility of the holistic CCS process chain is governed by the requirements and capabilities of the first stage of the system - i.e. CO_2 capture - to operate flexibly. Very little information in the literature exists surrounding the flexibility requirements of CO_2 capture units on industrial applications such as cement plants, steel plants or chemical plants. Driven by the more obvious need for flexible operation of power stations in future energy systems dominated by variable renewable power sources a moderate body of literature has formed in recent years discussing the operating flexibility

of CO_2 capture plants at fossil power stations. Both CCS applications will be discussed in the following.

2.2.1.1. Power plants

When the need for CO_2 capture on fossil fuel power stations became more widely acknowledged a common concern in the power generation industry was whether this would further constrain the operational flexibility of the affected power stations. Noticing the very limited information in the public domain literature the IEAGHG (2012b) commissioned an extensive study for assessing the effect CO_2 capture has on the common flexibility aspects of coal and natural gas fired power stations. The report forms the basis of the moderate body of literature investigating this topic. Four reference CCS power station configurations were examined: (i) An ultra-supercritical pulverised coal (USC-PC) power station with post-combustion amine based CO_2 capture, (ii) A natural gas fired combined cycle (NGCC) power station with post-combustion amine based CO_2 capture, (iii) An integrated coal gasification combined cycle (IGCC) with pre-combustion amine scrubbing technology, and (iv) A pulverised coal oxyfuel power station.

Core flexibility aspects were assessed such as: turndown capability, ramp rates, part load efficiency, and the ability for cycling (i.e. start-up and shut-down). For the NGCC, IGCC, and USC-PC power station it was found that ramp rates and part load efficiencies are not significantly affected by the integration of the CO_2 capture unit. Solely at oxy-fuel power stations the boiler ramp rates (typically 4-5%/min) could be constrained by the less flexible Air Separation Unit (ASU - ramp rates of typically 3%/min). This issue, however, could easily be circumvented by making up for the difference in oxygen supplied by the ASU and the volume demanded by the boiler during ramps with previously stored Liquid Oxygen (LOx; around 10tons of LOx are needed for a 50-100% ramp for a 500MWe power station). This amount could be supplied without any additional infrastructure by the around 200tons of LOx that typically would be included in a corresponding plant for a safe change-over from the oxygen to air-firing mode to hedge, for example, against ASU trips (IEAGHG 2012b).

Potential issues associated with the availability of the CO_2 capability have been identified predominantly during the start-up of NGCC, USC-PC and oxyfuel CCS power stations. When deploying amine scrubbing CO_2 capture techniques the delayed availability of steam supply for warming of the regenerator inhibits the early on regeneration of rich solvent and hence provision of lean solvent to the absorber for capture (i.e. 1-4hrs; IEAGHG 2012b, Domenichini et al. 2013, Ceccarelli et al. 2014). At the oxy-fuel power station the relatively inflexible ASU limits a quick start-up and supply of pure oxygen to the boiler which is fundamental to the oxyfuel CO_2 capture process. Nevertheless, both issues can be resolved by storing significant quantities of lean solvent and LOx that enables CO_2 capture operation even during start-up with limited production of steam or oxygen. At amine based CO_2 capture facilities a second option is to install a heater at the regenerator for production of steam at times the steam power cycle has not yet ramped up.

Further, IEAGHG (2012b) suggests that the turndown ratio of the power unit is not significantly affected by the CO_2 capture process. In line with other studies it was found that the operating envelope of the power stations can even be increased when shifting the parasitic power penalty associated with the capture process (e.g. for solvent regeneration, or production of oxygen or hydrogen) in time and in response to electricity price signals, by exploiting this additional degree of freedom. As such, rich and lean solvent storage tanks can be installed when amine scrubbing technology is deployed. By supplying lean solvent from a tank to the absorber, CO_2 capture can be sustained without incurring a significant parasitic load penalty associated with the regeneration of rich solvent, boosting the electricity output for example at times of high electricity prices. The stored rich solvent can be regenerated at later times of medium or low electricity prices reducing the exported power to the system through an additional parasitic load while staying online to provide reserve and inertial services to the grid. This can be useful, for example, at high penetrations of intermittent renewable power that need fast reserve backup power and inertial response at a low power footprint on the network. Similarly, by using a LOx buffer storage the high energy consumption of the ASU can be avoided at times of high electricity demand and prices boosting the power output at sustained CO_2 capture operation. By operating the ASU at full load while ramping down the boiler to minimum load (i.e. storing the excess produced oxygen) a negative power footprint on the system can even be created, whilst delivering fast response reserve to the power system as well as significant levels of inertia. Hydrogen storage at IGCC power plants can be used to deliver similar services.

Alternatively shutting off the PCC capture plant entirely to recover the energy penalty associated with CO_2 capture is frequently considered, for example to increase the operating envelope of the power stations boosting power output at times of high electricity prices when doing so offsets the costs for the increased emissions.

Two different types of compressor configurations are typically considered for preparing the captured CO_2 flow for transportation: (1) axial inline compressors; and (2) integrally geared compressors. Both configurations can be equipped with a fixed speed drive, or with a variable speed drive in order to support the flexible operation of the system. Both types of compressor systems typically can ramp up and down within second to only few minutes (e.g. 1-2min for the systems proposed in IEAGHG 2011). As these ramp rates are significantly faster than the flow rate changes that can be expected from common CO_2 sources such as power stations (typically ramp rates of 3-5%/min; Domenichini et al. 2013) compression units do not impose an additional constraint in this regard.

A commonly mentioned constraint (Sanchez Fernandez et al. 2016, Gonzales Diaz 2016, Liese and Zitney 2017, Luedtke 2004, IEAGHG 2012b) to flexible operation for all respective power station configurations, however, relates to the turndown limit of the CO_2 compressors which usually lies at around 70% load. Nevertheless, several solutions exist to enable energetically efficient operation also at lower loads. These options range from deploying variable speed compressor systems, over partial recycling of the flow, to

installing multiple smaller compression systems instead of one large one, which can consecutively be shut off at lower loads, enabling close to design operating conditions for the remaining online compressors even at low loads. Alternative compressor part load control strategies that, however, come with significant energetic penalties are partial flow recycling, suction pressure throttling or outlet pressure throttling (Luedtke 2004).

For the above mentioned reasons Brouwer et al. (2015) does not even distinguish explicitly between the flexibility characteristics of base power stations with or without carbon capture capability in a study investigating the operational flexibility of power plants in low carbon power systems.

In a further contribution Ceccarelli et al. (2014) dynamically simulates a gas fired power station with PCC amine based CO_2 capture during common power station transients such as load changes, start-ups and shutdowns. Similarly to IEAGHG (2012b) the authors demonstrate that the main constraint to flexible operation is related to the availability of steam during the first 2hrs of start-up operation that undermines the ability of the plant to capture the produced CO_2. For a commercial 400MWe CCGT cycling power station the authors estimate that this effect could lead to additional yearly residual emissions of 8%. Similar measures as in IEAGHG (2012b) are discussed to mitigate this effect (i.e. solvent storage tanks, additional boiler for early on steam generation). Overall, Ceccarelli et al. (2014) concludes that the flexibility of a mid-merit CCGT does not need to be limited by addition of a post-combustion CO_2 capture facility.

This confirms earlier experimental findings by Knudsen et al. (2009) based on the CASTOR/CESAR amine scrubbing post combustion CO_2 capture pilot project which concludes that the CO_2 capture system "*will be as flexible as the power plant*" (p. 19).

2.2.1.2. Industry

The literature exploring the expected production profiles of cement, steel and industrial plants, as well as discussing how these could affect the flexibility requirements of CO_2 capture facilities is, to date, very limited. Only two sources have been identified briefly examining the topic (ZEP 2017, IEAGHG 2016).

In general it can be expected that the majority of industrial plants have more stable operating profiles than power plants operating in low carbon energy systems. This is likely to be driven to a large extent by the more predictable load requirements (i.e. at least on time scales of hours to a few days), and the durable and storable nature of the final product. Regular shut-downs for example over weekends, however, are conceivable for some industrial applications. Dependent on the application, the competitiveness of the process, and the market conditions, some industrial facilities might further be offline for several months over the year. ZEP (2017) and IEAGHG (2016) briefly examine several types of large industrial CO_2 emitters that are discussed in the following.

When looking at CO_2 flows from natural gas processing and ethanol plants it is expected that they vary on a monthly or weekly basis reflecting underlying demand patterns (IEAGHG 2016). Particularly in the case of ethanol production high prices of the raw material (e.g. corn in years of low harvest) can undermine the business case of the process resulting in idling of plants, as has previously been observed in the US (IEAGHG 2016).

Similarly, hydrogen production facilities are expected to run predominantly at a constant load, with hydrogen pipelines being able to absorb large quantities of excess production as well as to make up for deficient production (IEAGHG 2016). Additional hydrogen interim storage capacity in the form of geological storage could be installed which according to IEAGHG (2016) could "*permit[s] the plants to operate steadily at an optimal rate when possible or vary rates because of internal conditions when necessary. Ultimately, this should reduce variations from the plant*" (p. 35, IEAGHG 2016). In line with this, Strbac et al. (2018) suggests in a study exploring decarbonisation of the UK heat sector that large scale hydrogen storage facilities, even in geological formations, would be more cost-effective than installing a significantly larger fleet of hydrogen production plants for satisfying peak demand.

According to IEAGHG (2016) some cement plants may only run for a month at a time, and only once every few months. It is, however, questionable whether cement and industrial facilities with such low capacity factors will be equipped with CCS capability. It is further acknowledged, particularly in the case of the cement industry, that the stationary production of cement can still imply flue gas flows of varying volumes and CO_2 concentrations, for example when the plant switches between operating in the interconnected mode (when the raw mill is operating) and the direct mode (when the mill is not operating). IEAGHG (2016) suggests that, depending on its age and type, raw mill maintenance can be as often as every 7-10 days. During this process CO_2 is still produced for heating the kiln, however, at substantially reduced volumes of "*perhaps half*" the amount (p. 30, IEAGHG 2016). ZEP (2017) even suggests that switching between operating modes on a daily basis could be conceivable. Other factors that can influence volumes and composition of the produced CO_2 at cements plants are type of fuel, type of clinker, type of raw meal (limestone), and the amount of air leakage (ZEP 2017).

Overall, it seems reasonable to expect that the variability of produced CO_2 flows from large industrial applications is either comparable (e.g. cement) or lower (e.g. gas processing, hydrogen, ethanol plants) than of CCS power stations operating in low carbon electricity systems. Since CO_2 capture technologies considered for industrial applications are similar to the ones considered for power stations (Romano et al. 2013, Leeson et al. 2017), it is also expected that the potential constraints to flexible operation, as well as the available options to overcome these are similar (e.g.: installing solvent storage, LOx or hydrogen buffer storage tanks; installing an additional boiler for steam production in the early phase of start-ups; installing several parallel compressor trains to enable efficient compression even at low loads).

This section has carried out a review of the operating flexibility and requirements of the benchmark CO_2 capture technologies at power stations and industrial facilities. A detailed review of the operating flexibility of other promising future capture technologies such as calcium or chemical or chemical looping or polymeric membranes could not be identified in the literature, although ZEP (2017) indicates that it is likely to be comparable to today's benchmark technologies. Although carrying out such an assessment is considered highly relevant and valuable it goes beyond the scope of the present study. Nevertheless, the review performed in this section has shown that there are no obvious bottlenecks or showstoppers to flexible operation when using the reference capture technologies at power stations or industrial facilities. The CO_2 capture processes are generally expected to be able to support the flexible operating requirements of the underlying power generation or industrial processes without imposing significant additional constraints. Although some concerns exist surrounding the availability of the CO_2 capture process during plant start-ups measures exist mitigating this issue. Since the CO_2 capture process constitutes no obvious limitation to flexible operation, the downstream CCS process chain's ability to operate flexibly can, hence, be expected to be largely driven by the load profiles of the CO_2 sources themselves (i.e. power stations or industrial facilities).

2.2.2. Transportation

Once CO_2 has been separated out in the CO_2 capture facility unit it still needs to be compressed and dried for making it ready for transportation. As mentioned in section 2.1 common transportation ways are by pipeline, ship, truck or train, with pipeline transport being considered to be most cost effective for large quantities as long as distances are not excessive (e.g. within a few hundred kilometre; IPCC 2005, Mohitpour et al. 2012, IEAGHG 2012, Onyebuchi et al. 2018).

CO_2 transportation via pipelines has been practised at scale since approximately the 1950s for the purpose of EOR (Mac Dowell et al. 2017). In 2014, 3,000 miles of CO_2 pipelines were in existence transporting a volume of around 60MTPA in 113 EOR projects in the US alone, with 120 of these projects existing world-wide (NETL 2014, Advanced Resources International 2011). CO_2 transportation via pipelines can, therefore, be considered a relatively mature technology. A major challenge, however, remained of understanding pipeline fluid behaviour with impurities present in the flow. Even small amounts of impurities such as N_2, O_2 or H_2 can significantly shift the phase boundaries and create uncertainties to whether the flow in the pipeline can be maintained in single phase (usually dense phase, for cost-effective transportation). Two phase flow can lead to slug flow, greatly increasing pressure drops, and other difficulties in operation such as damaging effects on pressure booster stations and cavitation (Wetenhall et al. 2017a, Bilio et al. 2009 Mechleri et al. 2017a, Martynov et al. 2015, Nimtz et al. 2010). It is hence widely acknowledged that two-phase flow should be avoided (McCoy and Rubin 2008, IEAGHG 2010).

Components (i.e. impurities) whose critical temperature and pressure lie above that of pure CO_2 will create a two phase region of the fluid mixture below the vapour-liquid phase boundary of pure CO_2 (e.g. N_2, O_2, Ar, H_2). Conversely, components with critical temperatures and pressures lower than those of pure CO_2 will create a two-phase region above the vapour-liquid phase boundary of pure CO_2 (e.g. NO_2, SO_2; Wetenhall et al. 2014b, Porter et al. 2016, Onyebuchi et al. 2018).

Other impurities such as sulphur species (e.g. H_2S, COS, SO_2, SO_3) pose corrosion risks, particularly in the presence of free water (Porter et al. 2016). Similarly, NO_x species as combustion by-products pose a corrosion risk as they can form nitric acid. Of the range of metal trace impurities potentially present in CO_2 flows mercury is receiving particular attention due to the corrosive effects it has on a number of metals. Further, hydrogen poses the risk of embrittlement of steel pipes (Porter et al. 2016). Finally, water represents a common impurity in CO_2 flows and presents a significant risk, particularly at contents over the solubility limit in CO_2, where it can lead to the formation of in situ carbonic acids (Porter et al. 2016), clathrate hydrate formation (Cole et al. 2011) and condensation (Serpa et al. 2011, Uilhoorn 2013). For a more detailed review the reader is referred to (Porter et al. 2016, Wetenhall et al. 2014a, Wetenhall et al. 2014b, Onyebuchi et al. 2018).

Nonetheless, the required knowledge about the relation between CO_2 quality and its behaviour in the pipeline has advanced substantially in the recent years, "*allowing CO_2 quality effects to be taken into account*" (ZEP 2017, p. 4). Recent developments in the databases of physical properties of CO_2 mixtures coupled with advancements in software has enabled detailed steady-state as well as transient assessments of the most important flow conditions (ZEP 2017).

Although the issue of potentially frequently varying flow rates feeding into CO_2 pipelines has been realised for several years (IEAGHG 2010), no major concerns towards flexible operation have been raised (IEAGHG 2016). At off design conditions the same constraints apply in general than at full load. As such, the operating pressure envelope must be respected along the pipeline length to avoid two-phase flow and the exceedance of the maximum operating pressures. Further, the purity specifications must be respected in order to limit corrosion, enlarging of the phase envelope, the formation of hydrates, etc.. Finally, the maximum velocity limit of the pipeline needs be respected for avoiding excessive erosion. Frequently this velocity limit, however, is not of practical concern as the flow velocities are kept relatively low for avoiding large frictional pressure drops that would require a higher number of pressure boosts along the pipeline length (i.e. increasing operational as well as capital costs).

In contrast to steady state operation at full load, variable flow rates automatically come along with transient flow conditions. Care needs to be taken that these transients do not lead to local pressure spikes or oscillations (e.g. hammer effects) that can damage equipment and lead to local two-phase conditions or cavitation (i.e. formation of vapour cavities/voids in the liquid that can be caused by rapid pressure changes when the pressure is relatively low – when these voids face subsequent higher pressure and implode this can

create strong and damaging shockwaves; IEAGHG 2016). However, when using appropriate control systems this is generally not considered a significant area of concern in the literature. For a range of dynamic simulations of CO_2 pipelines Aghajani et al. (2017) suggests that even complete valve shut-ins at the pipeline outlet over periods of 5s would be acceptable.

Pressure boosting stations are crucial components of many proposed CO_2 T&S systems. They ensure that the flow along the pipeline stays within the predefined pressure envelope, and that a sufficiently high injection pressure is provided. In both functions pumps will need to support the variable operation imposed on the CCS process chain by the CO_2 sources. Pumps are common components in the process industry and the large majority of them utilise some kind of flow control mechanism (Tolvanen 2007). The most common flow control methods are: Throttling, alternating 'on/off' operation, and variable speed drive pumps (Tolvanen 2007). Particularly in larger systems that require regular part-load operation variable speed drive pumps are frequently deployed due to significant energy and consequently operating cost (Tolvanen 2007). Variable speed drive pumps also allow for the smooth transition between states avoiding potentially harmful hammer effects. As such, variable speed drive centrifugal pumps were considered as the preferred pumping technology in the White Rose UK CCS Demonstration Project (Capture Power Limited 2016b) as well as in the American Electric Power Mountaineer CCS II Project (American Electric Power 2011). Since variable speed drive pumps are standard components in the process industry these are not expected to restrict flexible operation of CO_2 T&S systems.

Although pipeline based transportation is considered the base case for GB CO_2 T&S systems within this study, offshore transportation via ship is a widely considered alternative to offshore storage sites. Due to the non-continuous and batch-wise nature of this transportation method the flows in the individual subsystems are by design intermittent. The main concern related to this intermittency is related to the offloading of the pressurised and cooled CO_2 (commonly transportation of CO_2 near the triple point at around -50°C is suggested; Skagestad et al. 2014, Brownsort 2015) that can lead to cyclical very low temperatures in injection wells. To avoid the integrity risk associated with these conditions different offloading and injection methods are generally considered (Skagestad et al. 2014, Brownsort 2015, GCCSI 2011b). These comprise direct injection from the ship into a buoy (e.g. Submerged Turret Loading system), or indirect injection via floating or fixed injection facilities. A requirement of heating of the subcooled CO_2 to around -15°C to +20°C is typically recommended that could be carried out either on the platform or on the ship itself for mitigating extreme cyclical temperature sings and associated problems at the injection site (Brownsort 2015, GCCSI 2011b). A detailed review of the problems associated with variable flow rates in transportation networks based on ship transport goes beyond the scope of this thesis. For more information on the topic the reader is referred to (Skagestad et al. 2014, Brownsort 2015, GCCSI 2011b).

In conclusion, this section has shown that CO_2 transportation via pipeline is a relatively mature technology. Constraints to flexible operation are similar to when operating at full load steady state and design conditions. They include staying within predefined pressure envelope of the fluid and respecting erosional flow velocities. Additionally, fast transients causing hammer effects and cavitation within the pipeline caused for example by rapid valve shuts should be avoided. This, however, does not constitute an area of significant concern in the literature particularly when using appropriate control technologies. Pressure booster stations neither pose an additional constraint to flexible operation of CO_2 T&S systems, when designed adequately and when using appropriate part load control strategies. Transportation systems relying on ship transport are inherently characterised by non-continuous and batch-wise operation, which exaggerate cyclical and intermittent flow conditions at the individual subsystems. The main concern to this intermittent operation is, however, related to the integrity of the injection wells due to the large cyclical temperature swings they would regularly face. Although the detailed review of ship based transportation systems and the related intermittency issues go beyond the scope of this study, several offloading options were identified which are generally considered for mitigating the resulting issues (Skagestad et al. 2014, Brownsort 2015, GCCSI 2011b).

2.2.3. Injection

Well drilling and completion technology is the most important cost driver in the oil and gas industry (ZEP 2017). Even small interventions particularly at offshore wells can lead to significant project cost increases (Spitz 2016, Capture Power Limited 2016a). Being a crucial component in the process chain it is, hence, of fundamental importance to CCS projects to ensure the integrity of injection wells over their lifetimes. Whilst CO_2 injection has been carried out for several decades for the purpose of Enhanced Oil Recovery (EOR; IEAGHG 2016) experience with strongly time-variable CO_2 flows and the impact on well integrity is, to date, still very limited. This is on one hand due to the application of EOR which requires a relatively constant and predictable supply of CO_2, and on the other hand due to the commerciality of most EOR projects. As a consequence there is only very little relevant information available in the public domain literature, even in the face of some projects that potentially experience strong and frequent flow rate fluctuations such as the Aquistore project in Canada (Aquistore 2015). Yet, there is strong evidence that frequent variability of CO_2 flows can have significant deleterious effects on the integrity of CO_2 injection wells, as will be discussed in the following.

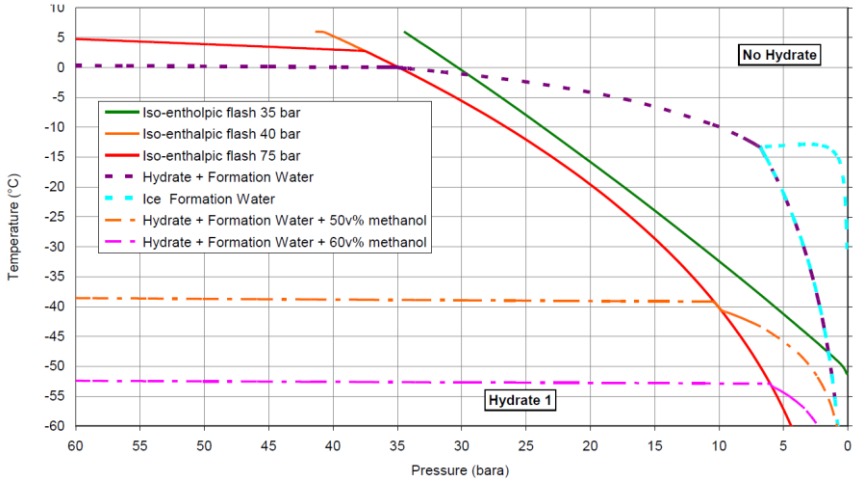

Figure 2.5: Comparing Joule Thomson cooling curves and hydrate formation areas for different concentrations of methanol present in the formation water surrounding the well bottom hole (EON 2012a).

In particular, there are several risks associated with the frequent flexible operation of injection wells that need to be considered. These include the risk of (1) clathrate hydrate formation; (2) of cracking of cement and wellbore materials; (3) of hydrogen embrittlement of well materials; (4) of oscillations and vibrations; and (5) of reduced lifetimes due to cyclic thermal stresses. These risks are particularly prevalent when two-phase flow is present within the well. This can happen for example at low loads when the backpressure from injection falls off, or at low reservoir and consequently wellhead pressures (e.g. depleted oil and gas fields). At such conditions CO_2 can flash across the wellhead choke valve from upstream pressures of typically above 85-90bar. The substantial expansion of the fluid into two-phase or gaseous flow comes along with a significant Joule-Thomson (JT) cooling effect, which, dependent on the pressure drop, can lead to fluid temperatures of -20°C or lower in the well (Shell 2015, Li et al. 2015). This effect is illustrated in Figure 2.5. The diagram shows the temperature drop associated with isenthalpic flashes (no heat exchange with the environment is considered) of pure CO_2 which, for example, could occur over the wellhead choke valve. It can be seen that a sudden pressure drop of CO_2 at 6°C and 42bar to 15bar leads to temperatures of around -28°C. This strong cooling effect is the major driver of the significant risks associated with regular injection well cycling that will, one by one, be reviewed in the following.

2.2.3.1. Clathrate hydrate formation

Clathrate hydrates are crystalline solid inclusion compounds in which small guest molecules (typically gases) are trapped in cages of hydrogen bonded water molecules (Ripmeester and Alavi 2016). Under high pressures, low temperatures, and a sufficiently high water

concentration (i.e. with free water present in the flow) hydrates can form that consist of CO_2 molecules trapped in a water based lattice (Bouillot and Herri 2016). There are three known common hydrate structures (type 1, type 2, type H; English and MacElroy 2015). Carbon dioxide usually forms type 1 hydrate structures (English and MacElroy 2015). Figure 2.6 illustrates for different condensed water (CW) concentrations in CO_2 the pressure and temperature regions under which hydrates (type 1) form (i.e. see within and/or to the left of solid lines). For reasons of reference, a very wide free water content limit of around 50-600ppm is generally suggested for transportation of CO_2 in pipelines that would consequently need to be handled by the downstream injection wells (Onyebuchi et al. 2018, IEAGHG 2010).

The previously presented Figure 2.5 has shown the temperature drops caused by isenthalpic flashes of pure CO_2 from 6°C and various pressures (i.e.: red, green, and orange solid lines). The figure additionally shows the pressure and temperature ranges in which hydrates can form when CO_2 comes into contact with formation water (on the example of conditions at the Kingsnorth CCS demonstration project; EON 2012a) mixed with different concentrations of methanol that can be injected as a hydrate formation inhibitor. Looking at the isenthalpic flash curves in Figure 2.5 (i.e. solid red, orange and green lines) it can be seen that the risk of low temperatures and hydrate formation is biggest when the pressure drop across the well head choke valve is largest. This happens at low loads (i.e. start-ups, shut-downs, continuous operation at low loads) when pressures downstream of the wellhead choke valve are low, due to the reduced (or missing) backpressures in the well.

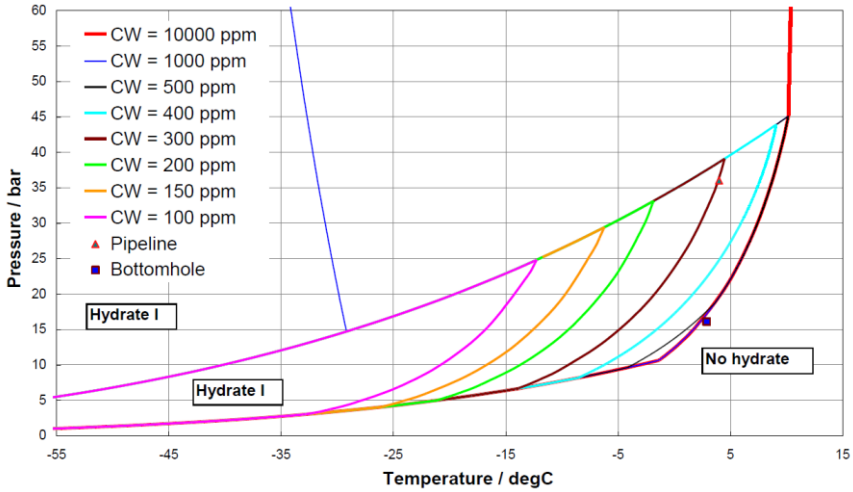

Figure 2.6: CO_2 and water hydrate phase envelopes (EON 2012a).

When hydrates form they can plug flow paths and interrupt operation (Shell 2015, McNeil 2014), which can be very costly even for short amounts of time (Spitz 2016). Once they have formed and clog flow paths they are difficult and time consuming to remove. Although it is difficult to access real data and information from commercial CO_2 injections projects, the formation of hydrates and their blockage of a well has been experienced at the American Electric Power (AEP) Mountaineer Plant Product Validation Facility (PVF) and

confirmed in a personal communication to the author (McNeil 2016, Sminchak et al. 2014). A particularly sensitive area of operation in regards to hydrates is the start-up after a period of complete well shut in. During the shut-in formation water can backflow and migrate into the well increasing the risk of hydrate formation once CO_2 flow is ramped up during start-up, particularly when no hydrate formation inhibitors are used (methanol or MEG - i.e.: monoethyleneglycol; IEAGHG 2016).

It is, therefore, of fundamental importance to avoid the formation of hydrates that can hamper the integrity and operability of injection wells. This can be done, for example, by reducing the water content in the CO_2 to very low levels (which, however, can be particularly difficult during start-ups after periods of well shut-ins due to formation water backflow), or by adding hydrate inhibitors such as methanol and MEG to the flow. Nevertheless, both options can come at significant additional costs when required continuously or regularly. Alternative indirect options should, therefore, be considered that tackle the issue by avoiding pressure and temperature regions in which hydrates form, for example by minimising the time wells need to operate at two-phase flow conditions. The identified options that can be deployed are discussed in more detail in Chapter 4.

2.2.3.2. Cracking of cement and wellbore materials

When operating regularly in the two-phase region of the well (i.e. with flashing taking place across the wellhead choke valve due to low pressures at the well head; e.g. caused by cycling or continuous operation at low loads) the well completion (i.e. installation in the borehole to make the well ready for operation) material is exposed to large temperature variations. These thermal load and temperature swings have a significant effect on near wellbore casing, cement and formation stresses. Over time the steel, cement and rock will repeatedly expand and contract in volume and also relative to each other due to different thermal expansion coefficients (De Andrade et al. 2014). This can create and enlarge fractures, fissures and radial cracking threatening the integrity of the well completion over the desired infrastructure lifetime (Spitz 2016, De Andrade et al. 2014, Li et al. 2015, Nygaard et al. 2014).

Several authors have assessed the integrity risk induced by repeated cyclic thermal stresses at lab-scale or via modelling (Albawi et al. 2014, De Andrade et al. 2014, Lund et al. 2015, Roy et al. 2016, Aursand et al. 2017, Nygaard et al. 2014). Consistent with other authors Lund et al. (2015) concludes that "*large temperature variations may be expected during CO_2 injection, and this may lead to significant stresses and possible damage to the annual seal […of the well…]*" (p.164). Although a number of small scale experiments have been performed the risks and effects of cyclic thermal stresses over projected infrastructure lifetimes of 25–30 years have not yet been fully understood (ZEP 2017). As a consequence CO_2 injection well operating limits in terms of the frequency or magnitude of flow variations are also, as of yet, undefined.

2.2.3.3. Hydrogen induced embrittlement of well material

When CO_2 flashes across the wellhead choke valve due to low pressures at the wellhead, the concentration of volatile components of the mixture in the gas phase increases. This can lead to problems related to increased concentrations of H_2S and H_2 that can lead to corrosion and hydrogen induced embrittlement of the well material (IEAGHG 2016, Carroll et al. 2016, Spitz 2016). Atomic hydrogen can penetrate into the well material and accumulate at cracks reforming to H_2 (Yen and Huang 2003). This will increase the local pressure in the material which can promote cracking of the material (Yen and Huang 2003). It also makes the material more susceptible to fatigue failure (Mohtadi-Bonab et al. 2016). However, H_2 and H_2S are only expected in CO_2 flows from pre-combustion power plants and in some industrial applications (Porter et al. 2015). For CO_2 from post-combustion power plants and oxy-fuel plants this phenomenon is not expected to represent a risk.

2.2.3.4. Oscillations and vibrations

Vibrations can be classified into steady-state and dynamic transient vibrations of which the dynamic transient vibrations are usually more severe (Rao 2006). The increased requirement for ramping amplifies the risk associated with transient vibrations and oscillations. This is particularly the case when flashing happens across the wellhead choke valve, as it leads to large changes in fluid velocity and density over the valve, or when operating the wellhead with pressures and temperatures close to the critical point (Spitz 2016). The phase change in the well might lead to instability of the flow, cavitation and oscillations within the well that are undesirable (Ramamurthi and Sunil Kumar 2003).

2.2.3.5. Reduced lifetime due to cyclic thermal stresses

The sum of the above effects can lead to reduced lifetimes of CO_2 injection wells. Particularly the significant number of expected thermal cycles lead to uncertainties regarding their performance and expected lifetimes (Skagestad et al. 2014). Given the lack of experience in the thermal cycling of CO_2 injection wells, and the small amount of information shared in the publically available literature, it is unclear how many thermal and pressure cycles injection wells will accept (IEAGHG 2016, Skagestad et al. 2014). This area of research has, hence, been identified as being of fundamental importance for the overall integrity and operability of the CCS process chain (ZEP 2017).

Reduced lifetimes of injection wells would directly lead to additional costs of the system. These would be incurred either through the need for additional maintenance work to be undertaken (e.g. more work overs and interventions needed), or by the requirement for drilling and installing more wells for injection given their reduced lifetimes.

Since large uncertainties exist regarding the extent of the lifetime reductions that flexible operation of injection wells implies, the follow up costs associated with early degradation that this leads to are, as of yet, undefined. These and other additional costs associated with flexible operation such as increased insurance costs due to higher risk premiums will need to be compared to the costs of mitigating the lifetime hampering processes. This can be done for example through balancing CO_2 flows upstream in the transportation network, or by enabling the wells to cope better with CO_2 flow variability. The available options are discussed in more detail in Chapter 4 of this thesis.

Overall, the review in this section has shown that there are several issues to consider when cycling CO_2 injection wells frequently, or when operating them at low loads. All of the identified effects that are associated with variable CO_2 flow rates and that can have a negative impact on the wells integrity are at least exaggerated by two-phase flow occurring at the wellhead, and the strong JT cooling effect that this can imply. This can happen particularly at low storage reservoir pressures such as when injecting into depleted oil and gas fields (exaggerated if storage reservoirs is at low depth), and at low injection flow rates that do not provide sufficient backpressure for the fluid to stay in single liquid phase over the entire length of the well. Although methods exist to safely operate wells at all required load points the repeated and cyclical stresses imposed by variable flow rates can result in early degradation of wells affecting their integrity. The early degradation can lead to significant follow up costs if a higher number of well interventions for maintenance are needed, or if more wells need to be drilled and installed due to shortened life spans. To date, due to a combination of lack of operating experience and research, it is uncertain how many thermal and pressure cycles the wells are able to support. Whilst CO_2 injection has been carried out for several decades for the purpose of EOR the lack of operating experience with highly time-varying CO_2 flows is due to the application of EOR which requires a relatively constant and predictable supply of CO_2. Further, due to the commerciality of most projects information in the public domain literature is even scare about projects where high CO_2 flow rate variability is likely, i.e. such as the Aquistore project in Canada.

The high costs associated with the installation and maintenance of particularly offshore wells make it useful to look for options that mitigate the lifetime hampering processes. Such options could, for example, consist of minimising the times injection wells need to operate at low loads by balancing CO_2 flows upstream in the transportation network, or of enabling wells to operate more flexible. The identified options are discussed in more detail in Chapter 4.

2.2.4. Storage

Several different aspects need to be considered when it comes to variable injection rates into geological stores. These are summarised in the following.

Storage capacity

A small number of studies exist in the literature assessing via modelling the impact of varying CO_2 injection rates on the pressure and injectivity responses of geological saline storage reservoirs (Kolster et al. 2018, Bannach et al. 2015, Wiese et al. 2010, Farhat and Benson 2013). Wiese et al. (2010) performs numerical simulations examining the impact of temporal variations of CO_2 injection into a saline aquifer through a single well based on conditions of the Ketzin CCS injection project in Germany. Mimicking the potential CO_2 flow variability from a lignite coal power station, the study finds that in the long term the flow variability has only little effect on the storage capacity and pressure response of the reservoir. Farhat and Benson (2013) present a technical assessment of a saline aquifer being used as an interim CO_2 storage facility. This could, for example, be useful for providing a smooth and steady flow rate of CO_2 for EOR projects even in the face of time variable CO_2 production and capture. Analysing the reservoir behaviour the study concludes that variable CO_2 injection and production imposes no additional risks compared to those typically experienced in CCS projects. The pressure build up associated with variable injection was found to be comparable to a counterfactual case of constant injection (Farhat and Benson 2013). Similarly, Bannach et al. (2015) performs a study on the feasibility of large scale industrial CO_2 injection into a saline aquifer in the Volpriehausen Sandstone in North Germany. A main focus of the study lies on assessing the effect of daily and seasonally varying injection rates. The study concludes that varying injection rates have most impact on overall injectivity within the first years of operation. With increasing lifetime the dynamical pressure spread compared to the respective constant injection scenarios becomes marginal. Kolster et al. (2018) evaluates the effect of varying CO_2 injection rates into the Southern North Sea Bunter Sandstone saline aquifer. In line with the previous studies, the authors find that varying the frequency and amplitude of CO_2 injection rates has only a small impact on the pressure response of the reservoir and the plume migration. Kolster et al. (2018) concludes that as long as the total amount of injected CO_2 that would be injected over several decades is represented in the model, there is no particular need to include more granular variations of CO_2 flows, at least for first order modelling typically performed for whole system analysis.

Halite precipitation

Other literature suggests that dependent on the reservoir characteristics (e.g. formation of caprock and migration of CO_2 plume) care must be taken that the cyclical injection of CO_2

into saline aquifers does not lead to excessive halite (i.e. salt) precipitation in the near wellbore region, since this could significantly reduce the injectivity of the well (Spitz 2016, IEAGHG 2016). This effect is a result of the strong ability of dry CO_2 to dissolve water. Hence, when CO_2 enters the aquifer it not only pushes the brine deeper through the pores into the reservoir, but it also dissolves some of the water component in the brine leaving behind salt precipitate. At periods of shut-in the brine, however, pushes back to the near wellbore area. This phenomenon is particularly pronounced in reservoirs in which the CO_2 plume migrates away from the near well bore due to its buoyancy, the shape of the caprock, and the placement of the well (Spitz 2016). Over many repeated cycles of injection and shut-in the accumulation of halite precipitate in the pores of the near well bore region can hamper the injectivity and the volumes of CO_2 that can be injected through the well. Although the phenomenon of halite build up can be remediated to some extent through water wash intervention, restoring the full initial injectivity again is difficult (Spitz 2016).

At the Snøvit project a higher than predicted pressure response by the reservoir in the face of injection has subsequently been found to be a likely effect of halite build-up due to repeated injection and shut-in cycles during the early phase of the project caused by logistical difficulties encountered with the upstream LNG gas processing unit that supplied CO_2. This eventually led to the abandonment of a well (IEAGHG 2016).

It should be noted, however, that an appropriate storage site development can promote a store's ability to operate in a cyclical manner (e.g. wells are drilled in a manner that restricts the CO_2 plume migrating away from the near wellbore region; Spitz 2016). Further, with increased volumes of CO_2 being injected into the reservoir the brine gets pushed out to regions in the reservoir from where it is unable to push back into the near wellbore region during the durations of well shut-ins, which additionally mitigates the issue.

Thermally induced fractures

Some uncertainty exists surrounding the potential for thermally induced fractures caused by injection of relatively cool CO_2 into the warmer reservoirs. Fractures of the reservoir rock can open up flowpaths for the CO_2 and as such can increase the injectivity of the well. Nevertheless, when fractures penetrate into the caprock they can undermine the sealing ability and the storage integrity of the overall reservoir. Several studies, therefore, investigate the effects that thermally induced fractures can have on the reservoir and the sealing integrity of the caprock formations (Goodarzi et al. 2015, Vilarrasa and Laloui 2016, Bonneville et al. 2014, Shell 2015b). The studies generally conclude that although thermally induced fractures can be expected as a result of injection of cool CO_2 into the reservoirs these would usually be confined to the near wellbore region and as such they would be very unlikely to affect the sealing ability of the caprock. It should be noted, however, that these studies consider an injection temperature of usually higher than 20°C. None of the studies examine significantly lower CO_2 injection temperatures over extended periods in time caused by two-phase flow and the related JT cooling effect at the wellhead. Overall,

however, the topic of thermal fracturing as a results of low CO_2 injection temperatures has not been identified as an area of significant concern in the literature, which possibly can be explained by the large flexibility that exists surrounding the design and placement of wells in reservoirs (e.g.: distance to caprock) which can mitigate the negative effects.

Maximum injection pressures

As a further constraint to flexible operation, near wellbore pressure levels need to be constrained during injection to avoid endangering caprock integrity. This automatically leads to maximum injection flow limits that need to be respected at on and off design flow conditions.

Impurities

It remains to note that varying levels of impurities that can come along with variable CO_2 flow rates can impact the geological store, although this is likely to be reservoir specific and depends on the mineralogical and fluid compositions and the type and amount of impurities (IEAGHG 2016). The effects can range from slight dissolution that creates microvoids to mineralisation that can block pore space (IEAGHG 2016). Non-condensable impurities in CO_2 generally have the effect of decreasing the density of the fluid which would lead to a reduction in the total available storage capacity (IEAGHG 2016). It becomes clear that it is important to control the purity of CO_2 both at design and off-design conditions.

Increased residual trapping under cyclical operation

Finally and most recently, concerns have been raised that cyclical injection into saline aquifers can impair the injectivity of the storage sites (Edlmann et al. 2019). The authors of Edlmann et al. (2019) note that limited experimental data exists on cyclical CO_2 and water/brine injection. The experiments that have been performed "*generally do not extent beyond two cycles*" (p.1). For the first time in the literature their study, therefore, analyses the flow behaviour of CO_2 and brine over six alternating injection cycles. The injection of brine in the experiment represents invasion of brine into the near wellbore region in real saline aquifers when injection of CO_2 is interrupted. The results show that "*for both the CO_2 and water injection cycles, the differential pressure increases with each injection cycle and that … [this] effect is progressive*" (p.1). In other words, it is found that the injectivity of the well progressively deteriorates over several CO_2-brine injection (/invasion) cycles to the point that the authors urge that the anticipated "…*loss of injectivity must be incorporated in the injection strategy"* at real CCS projects, and that *"careful management of cyclic injection*" will need to be carried out. Figure 2.7 illustrates the increase in differential

pressure required in the study for injecting CO_2 and water, respectively, over 6 investigated injection cycles.

The underlying reasons for the deteriorating injectivity caused by cyclical injection lie in the different respective physical properties of the multiphase flow, and ultimately in increased levels of residual trapping taking place. Edlmann et al. (2019) shows that in the test system representative of a saline aquifer, water aheres better to the sandstone surfaces within the rock than CO_2. Water can, therefore, be described as the 'wetting' fluid in the system. During injection of CO_2 the water content as the wetting fluid in the rock gradually decreases since it gets pushed out into the reservoir, eventually being present only as a thin film surrounding edges of the pores. This remaining water is termed irreducible water saturation. When CO_2 injection is interrupted and brine pushes back into the rock, e.g. into the near wellbore region, some of the non-wetting phase, i.e. CO_2, becomes gradually disconnected through capillary 'snap off'. This CO_2 is pushed into smaller pores where it is trapped and effectively becomes immobile. This process is commonly referred to as 'residual trapping'. By blocking flow pathways it subsequently becomes harder for either fluid to push through the rock. Ultimately this leads to higher pressure differentials required for injection of both water or CO_2. Since the maximum allowable injection pressure for maintaining the integrity of the caprock is not significantly affected this leads to an impaired injectivity of the wellbore.

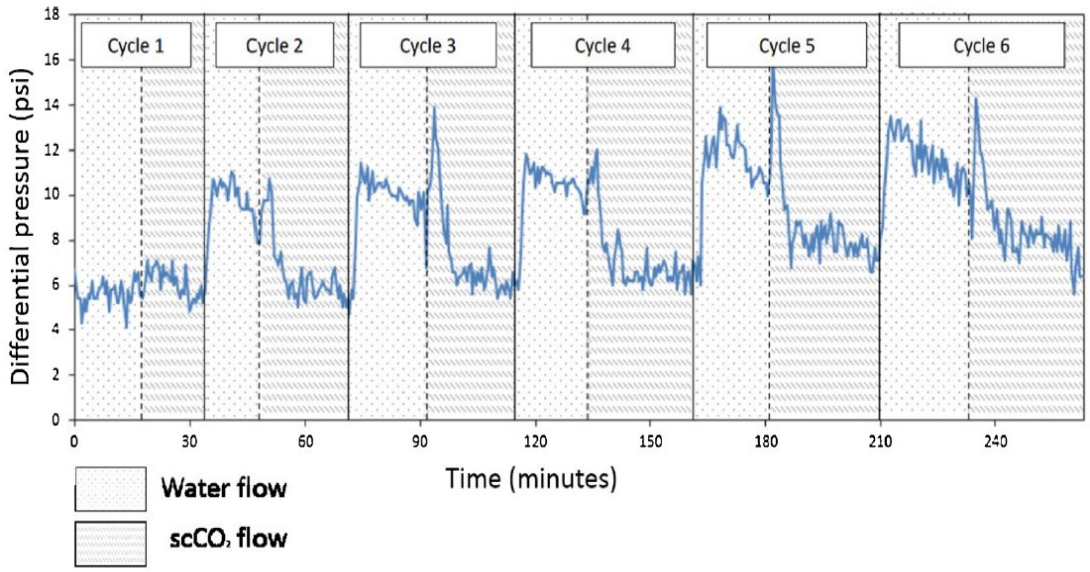

Figure 2.7: Differential pressure required for injection of water and supercritical CO_2 flow over several consecutive injection cycles (Edlmann et al. 2019).

Figure 2.3 in section 2.1 has illustrated that residual trapping increases storage security over structural and stratigraphic trapping. The authors of Edlmann et al. (2019) acknowledge that their finding could potentially be used to increase storage security in saline aquifers via cyclical operation. However, this would need to be carefully balanced with the negative effects it has on the injectivity of the wellbores (Edlmann et al. 2019).

The extent to which increased residual trapping impairs injectivity of wellbores at saline aquifer reservoirs when exposed to more than six injection cycles is, to date, still unclear and requires further research to be carried out. For more detailed information about residual trapping as an effect of cylic injection patters the reader is referred to (Edlmann et al. 2019).

Given that the underlying reason for the wellbore injectivity hampering effects of increased residual trapping and halite precipitation are similar, i.e. the repeated cylical invasion of the near wellbore region of CO_2 and brine, it would also be expected that the ways of mitigating these effects by taking appropriate design measures would be similar. For instance, wells could be drilled in a way that prevents fast migration of CO_2 away from the wellbore, in order to mitigate the repetitive and alternating invasion of both fluids into the near wellbore region. However, the availability of this option would likely dependent on store's specific features (e.g. presence of dome which can prevent migration, or other secondary flow barriers). Further, the effectiveness of this option is uncertain, particularly since no information in the publically available literature could be identified surrounding this topic.

Overall, the review in this section has shown that flexible operation of geological CO_2 stores generally seems feasible when carried out in a controlled manner. There are, however, several risks to consider. The main concerns relate to the risk of halite precipitation in the near wellbore region and increased residual trapping as a consequence of cyclical operation. Both effects can substantially hamper injectivity of wellbores. Whilst the negative effects of halite precipitation have been observed in real operation and options exist to mitigate this effect (e.g. wells are drilled in a manner that restricts CO_2 plume migration away from the near wellbore region; water wash operation), the finding of increased residual trapping hampering well injectivity is only relatively recent. Although design options mitigating this effect could exist the lack of quantification of the latter effect on injectivity constitutes a significant risk to real projects and needs further exploration through experiments and modelling. In the long term, several studies in the literature suggest that neither storage capacity or plume migration is significantly hampered by time-variable or cyclical injection. Finally, the potential for thermally induced stress fracturing of the reservoir rock as a consequence of large quantities of cool CO_2 entering a warmer reservoir is investigated in several studies. At injection temperatures of higher than 20°C the studies conclude that the potential for thermally induced fractures of the formation rock is confined only to the near wellbore area, with little risk to impact the sealing ability of the caprock. No studies could be identified in the literature examining this effect under worst case conditions with a phase change and the JT related cooling effect being present at the wellhead. Nevertheless, it should be noted that thermally induced fracturing has not been considered a significant risk in the small body of literature examining flexible operation of CCS storage reservoirs that has developed in recent years. This can possibly be explained by the fact that large flexibility exists surrounding the design and placement of

injection wells in the reservoirs (e.g. distance to caprock) which can mitigate this stress related issue.

2.3. Conclusions

Forming the basis for the remainder of this thesis, the present chapter has reviewed the ability of all major CCS process chain subsystems to operate in a flexible manner. Individual detailed summaries were given at the end of the respective subsections and shall not be repeated in full. A brief summary of the whole chapter is, nevertheless, provided in the following.

In general this chapter has shown that no significant constraints to flexible operation have been identified in the literature relating to CO_2 capture facilities when supporting the flexible operation required by the underlying base CO_2 producing process (e.g. power station or industrial facility). Although concerns exist surrounding the availability of the CO_2 capture capability during start-ups, as well as in regards to the turn down ratio of CO_2 compressors, options exist to overcome both issues.

Further, no significant constraints to flexible operation were identified in pipeline based CO_2 transportation systems. Similarly to when operating at nominal load conditions, pressure boundaries need to be respected also at off design conditions, as well as impurity specifications. Appropriate control technologies should be deployed to avoid hammer and cavitation effects. These could be caused by rapid transients for example resulting from valve slams. When transportation of CO_2 via ship is considered several technological uncertainties still exist, predominantly associated with the frequent and intermittent offloading and injection operation that implies large and cyclical temperature differences stressing the involved equipment. More research still needs to be performed on this topic.

Most issues associated with flexible operation of CCS infrastructure are related to CO_2 injection wells. Potential issues when cycling wells include the risk of hydrate formation, of cracking of cement and wellbore materials, of hydrogen induced embrittlement of well material, of oscillations and vibrations, and of reduced lifetimes resulting from the combination of these effects, as well as of the cyclical thermal stresses that flexible operation can imply. All of these effects are particularly prevalent when a phase change occurs over the wellhead choke valve and two phase flow is present at the wellhead. This can happen, for example, at low loads when the backpressure from injection falls off, and in particularly at low reservoir pressures leading to low wellhead pressures. It should be noted that the presence of two-phase flow at the wellhead regardless of injection load is highly dependent on the reservoir characteristics (i.e. pressure and depth). Particular concerns relate to depleted oil and gas fields that as a result of their low reservoir pressure are prone to promoting two-phase flow in the well, that can be even exaggerated when reservoirs are located at large depths. When two-phase flow is present in the well the combination of the described effects and in particular cyclic thermal stresses can lead to early degradation of

materials and lifetime reductions. Since injection wells are fundamental and costly components of the CCS process chains it is in the interest of operators to ensure their integrity, either by mitigating the described lifetime hampering effects or the consequences these can have on the equipment. Options could consist of minimising the times injection wells need to operate at off design and low load conditions that promote two-phase flow by balancing CO_2 flows upstream in the transportation network, or by enabling wells to operate more flexibly through various sophisticated operating and design options for wells. For more on these options the reader is referred to Chapters 4-7.

On the storage side the main concerns relating to time-variable and cyclic operation at saline aquifers are the risks of halite precipitation and increased residual trapping in the near wellbore region. Both effects could substantially hamper the injectivity of the wellbores, threatening the success of CCS projects if lower CO_2 volumes than captured can be pumped into the reservoir. Particularly halite precipitation is an effect that has previously been observed, and operating and design options exist to mitigate its negative effects on the injectivity of wellbores. The occurrence of increased levels of residual trapping as a consequence of cyclical operation is a relatively recent finding. Initial results suggest that even as little as six cycles can degrade injectivity of a wellbore significantly. Although it is reasonable to believe that a higher number of cycles will further impede injectivity, the extent of this effect urgently needs to be explored in more detail in follow-up research. Reducing CO_2 flow variability in the upstream network, as investigated in chapters 4-7 of this thesis, could therefore in addition to benefitting injection wells also ensure the long term integrity and injectivity of saline aquifer reservoirs.

3. Unit Commitment Economic Dispatch Model for the GB Electricity System

3.1. Introduction & Rationale

As one of the largest industries to decarbonise the power sector has a very high potential for application of CCS technology. As such the requirements and operating patterns of CCS technology and infrastructure are likely to be shaped to a significant extent by the needs of the power generation sector. To understand the required operating patterns of CCS technology it is, therefore, essential to examine the role and behaviour of CCS power stations operating in future low carbon electricity systems. This chapter draws on a unit commitment economic dispatch electricity system model developed by Bruce (Bruce 2015, Bruce et al. 2015, Bruce et al. 2014) and Stanojevic (2011) to investigate the role and operating regimes of CCS power plants in GB low carbon electricity system scenarios. The GB electricity system was chosen as a suitable case study due to the comparatively high likelihood for deployment of CCS, as well as the availability of extensive and high resolution historical datasets for weather and electricity demand. Whilst an improved understanding of the role and operating patterns of CCS power stations in future low carbon energy systems is a core aim of this chapter, a further main result is the characterisation of CO_2 flow profiles that are captured in the respective scenarios and that will consequently need to be accommodated by the downstream CO_2 transportation and storage networks. The extensive characterisation of CO_2 flow profiles represents an important novelty in the academic literature. Energy system modelling studies examining operation of CCS plants generally do not evaluate CO_2 flow profiles that are captured and sent to the T&S infrastructure, as no constraints from the downstream system are typically considered. However, since this assumption has been challenged by several authors (Lund et al. 2015, Jensen et al. 2014, Spitz et al. 2017; see also Chapter 2) the understanding of CO_2 T&S system feed flow patterns has significantly gained in importance. The improved understanding of CO_2 inflows regimes can help CO_2 T&S network designers to design the system according to the expected operating patterns. It is only when the requirements for CO_2 T&S networks are understood that the system (and CCS process chain more generally) can be designed efficiently.

The chapter is organised as follows: Section 3.2 presents other work in the literature examining the operating role and operating patterns of CCS power stations in future low carbon energy systems. It also offers some background on the basic concepts helping to understand power system operation in general. Section 3.3 describes the unit commitment economic dispatch model that has been deployed in this study for reaching the set research objectives. Section 3.4 presents the range of investigated future GB electricity system scenarios. Section 3.5 discusses the limitations of the deployed model. Section 3.6 presents and discusses the results. Section 3.7 examines sensitivity cases. Section 3.8 concludes.

It should be noted that the work presented in the main body of this chapter has previously been published in the Special Issues of the 9th Trondheim CCS conference in the International Journal of Greenhouse Gas Control (Spitz et al. 2018).

3.2. Literature review and Background

This section provides a relevant background on power system modelling in general, as well as a review of the literature in order to understand the body of work that has formed examining the interaction of CCS power stations with the wider energy system. Section 3.2.1 starts off outlining basic power system fundamentals. Section 3.2.2 discusses expected changes of the energy system landscape in the transition towards low carbon power systems. Section 3.2.3 describes the value that CCS technology can offer to future power systems. Section 3.2.4 provides an overview of the existing state of knowledge surrounding the operating role and operating behaviour of CCS power stations in low carbon electricity systems. Subsequently, section 3.2.5 presents the modelling techniques commonly used for energy system applications.

3.2.1. Power System Fundamentals

Traditional power systems have been characterised by conventional thermal generators such as nuclear and fossil power stations satisfying a relatively predictable and repetitive daily demand profile. The electricity network operator would usually organise the dispatch of these generators according to the 'merit order' in the attempt to minimize the cost required to meet demand (Chalmers 2010a). In short, the merit order ranks the available conventional generators according their Short Run Marginal Costs (SRMC), with the lowest SRMC plant ranking highest in the order (see also Figure 3.1). Power stations would be called upon to generate electricity according to the merit order list to satisfy demand at any hour t, with the plant ranking lowest in the list but being online and delivering power to satisfy demand being called the 'marginal generator'. In a well functioning electricity market it would be expected that electricity prices closely relate to the SRMC of the marginal generator (Chalmers 2010a). Graphically, this price is determined by the intersection of the merit order or electricity supply curve with electricity demand at any time t (see Figure 3.1).

As a consequence of this dispatching strategy generation units could be classified into plants ranking very high in the merit order and hence running predominantly full load (base load plants), mid-merit plants that need to load follow extensively to fill the gap between changing demand levels and the base load power supply, and peaking plants that are only called upon at times of peak electricity demand (Staffell and Green 2016). Traditionally, these plant types differed strongly in their cost structure. Base load plants typically came at a high capital costs, however, they could recover these cost over a high number of running

hours at low operational (/marginal) costs. Mid merit plants generally had medium capital and operational costs. Peaking plants were relatively cheap to build but had high operational costs and only comparatively low run times.

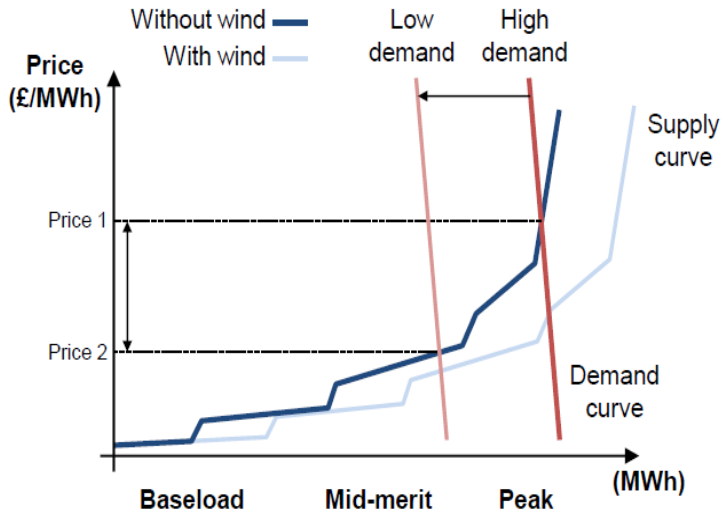

Figure 3.1: Merit order variability as a function of the availability of wind power resource (Bruce 2015).

To ensure the security and quality of the electricity to the consumer power network operators need to procure balancing services. These ensure that electricity demand and supply is closely matched at any time t, to prevent the system frequency from deviating significantly from its design value. In Great Britain the system operator National Grid (NG) is legally required to control the frequency in a narrow band around 50Hz (National Grid 2016a). Amongst the most important balancing services contracted by National Grid to achieve this are frequency control and contingency reserve (upwards and downwards). Both services are used to hedge the power system against unexpected changes of supply and demand (e.g. forecasting error, unexpected failure of plant, etc.) by providing sufficient amounts of quickly available back-up capacity to restore the nominal frequency after a contingency event. An overview over the timeframes of the balancing services procured by the GB network operator (National Grid) is given in Figure 3.2.

National Grid traditionally distinguishes between primary, secondary and high frequency response services (Bruce 2015, National Grid 2016a). High frequency response is deployed within 10s to reduce the system frequency after an initial positive frequency deviation. Primary frequency response is deployed within 10s of a low frequency event and must be able to limit frequency deviations to -0.5Hz after a normal infeed loss for up to 20s, and to -0.8Hz after an infrequent infeed loss (National Grid 2016a). Secondary frequency response takes over and is delivered within 30s of the initial low frequency event. It must be available for a minimum of 30min. To restore the system frequency back to pre-contingency levels a combination of spinning and standing reserve is typically used (Bruce 2015, Silva 2010, Wood et al. 2013).

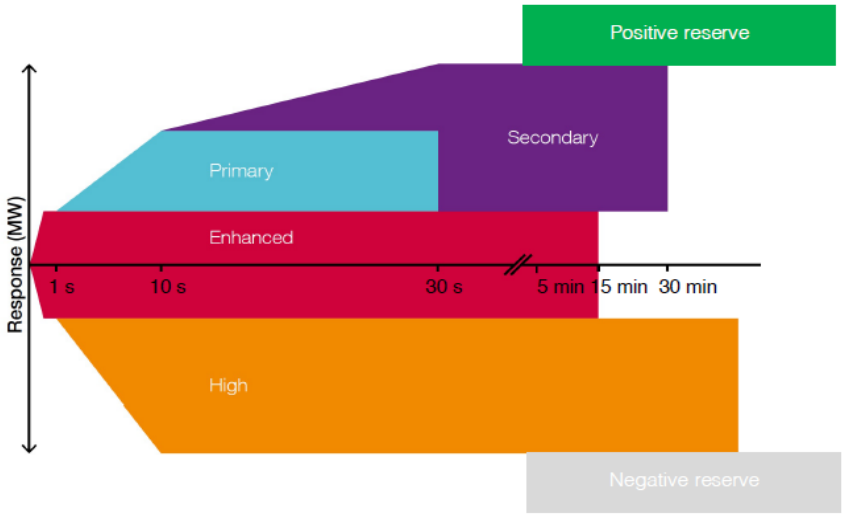

Figure 3.2: Timeframes of balancing services procured by National Grid (Vázquez Villamor 2017 based on National Grid 2016b).

Traditional power system operators frequently procure a sufficiently high reserve capacity to cover the largest credible loss in generation (e.g. largest generator capacity) as well as short term deviations and forecast errors in demand. However, with large amounts of VRE on the network operators of future systems will need to schedule reserve to cover the combined forecast errors and short-term fluctuations in demand as well as wind output (Bruce 2015).

In the face of declining system inertia as a consequence of the increased presence of non-synchronous generation (e.g. VRE) on the network, NG has recently introduced the additional service of the Enhanced Frequency Response (EFR; Vázquez Villamor 2017, Greenwood et al. 2017). This service delivers power within 1s of registering a negative frequency event. It includes both primary and secondary response timescales.

System inertia is an important parameter characterising the ability of the power system to limit the Rate of Change of Frequency (RoCoF) at contingency events. Inertia is usually provided by the rotating masses of synchronised conventional generators preventing the system frequency from changing too rapidly and significantly from the design value as a response to imbalances in supply and demand (Bruce 2015).

For more information about power system fundamentals the reader is referred to Kirschen and Strbac (2004) and Wood et al. (2013).

3.2.2. Future Power Systems

Variable Renewable Energy (VRE) and the need for back-up capacity

Driven by the need for decarbonisation and a long term sustainable low carbon economy the power system is expected to undergo large changes over the next decades. Of particular concern is the integration of low carbon renewable power generation technologies. As such large sums of money are directed towards investment into renewable energy technologies accounting globally for around $316 billion in 2016 (IEA 2017b). This compares to $117 billion that have been invested into fossil fuel power generation in the same year (IEA 2017b). Investment into solar and wind power alone contributed with around $261 billion (Bloomberg New Energy Finance 2018). It is expected that by 2022 30% of the globally produced electricity is generated by renewable sources, which given the vast scale is a substantial increase from 24% in 2016 (IEA 2017c).

Whilst undoubtedly an important part of any decarbonisation strategy, a challenge with the integration of renewable power generation is the intermittent and non-dispatchable nature of some technologies with the highest deployment potential such as solar power and wind power (referred to in the following as Variable Renewable Energy, i.e. VRE, power technologies).

In contrast to flexible and firmly dispatchable conventional generators the power output of renewable power generators is highly dependent on the availability of the underlying VRE resource (e.g. wind speeds or solar insolation). For example, wind farms can only produce electricity as a function of the time variable wind resource availability, and the most competitive solar technologies can only produce electricity at times of solar insolation.

This implies the need for increased amounts of backup capacity for periods of high demand or low electricity supply due to the unavailability of VRE sources. Whilst energy storage can contribute to providing such back-up capacity, particularly by transferring produced VRE sourced power to times in which it is most needed (e.g. times of high demand or low supply), there remain large uncertainties about its cost, economics and ultimately deployment level (Schmidt et al. 2017). Energy storage is likely to play a significant role by shifting around power supply within a day, and accross several days. However, the large amounts of power demanded across the system make it challenging for energy storage to provide the necessary backup power particularly for extended periods of low VRE resource availability. CCS power stations are well suited to close this gap in low carbon power generation capacity. While not as capitally intensive as nuclear plants, CCS power stations are firmly dispatchable, low carbon, and potentially more flexible.

Time variability of the merit order function

The large amounts of non-dispatchable VRE power available in future low carbon energy systems at close to zero SRMCs blur the lines of the more categorised power systems of the past. Whilst in traditional systems generation units could be classified comparatively accurately into base-load, mid merit and peaking plants according to their relatively constant position in the merit order, this will be more challenging in the future. This is due to VRE technologies that turn the traditionally stiff merit order supply curve into a time variable function of VRE resource availability:

When VRE resource is available, these technologies take in a place high up in the merit order due to their very low marginal costs (close to zero), relegating all other conventional generators with higher SRMC to lower positions. However, when the VRE resource is not available, conventional generators move back up in the merit order. This time variability of the merit order is illustrated in Figure 3.1.

It has been observed that the interplay between VRE resource availability and the merit order leads to overall lower electricity spot prices (Keay 2016; and as also suggested by the merit order model: intersection of supply and demand leads generally to lower equilibrium prices). Further, the time-variability of the merit order function also undermines capacity factors of conventional generators.

Dependent on the penetration of VRE technologies conventional generators can in this way lose their traditionally secure spot as base-load/mid merit generators. With fewer operating hours to recover any incurred fixed or capital expenses, conventional generators face diminishing business cases in many traditionally designed markets. This effect has been observed in real power markets, where the diminishing business cases of conventional generators detract investment and lead to capacity shortcomings (for more on this the reader is referred to Keay 2016).

Due to the non-dispatchability of VRE technologies and their high, nevertheless, time dependent position in the merit order (i.e. when available), the term ‘net demand’ has been coined. Net demand is what is left of total demand after deduction of the available power supply from the non-dispatchable VRE sources at any time t, as outlined in Formula (1). The net demand profile can also be thought of as the amounts of demand that firmly available and dispatchable power generators on the network need to meet. Whilst the total demand profile is comparatively predictable (especially in the past, however, this is less certain in the future with smart technologies, electric vehicles, energy storage, Demand Side Response, etc.; EIA 2011, UK BEIS 2018a) the large amount of intermittent VRE supply on the grid is expected to make the net demand curve significantly more volatile in future systems.

$$D_t^{net} = D_t - W_t - S_t \quad (1)$$

Where	*t*	*is time*
	D	*is electricity demand*
	W	*is wind power output*
	S	*is wind power output*

This will put a lot of strain in terms of flexible operation on the firmly dispatchable generators higher up in the merit order (e.g. CCS power stations that need to balance electricity systems by achieving a continuous balance in supply and demand/net demand; IEAGHG 2017). While the provision of flexibly dispatchable power at times when VRE sources get unavailable is one main task of these generators other major tasks include the provision of firm and flexible reserve capacity as well as of sufficient amounts of inertia.

Inertia and frequency control

The provision of sufficient amounts of inertia to limit the RoCoF (Rate of Change of Frequency) at contingency events has traditionally not been a problem with power supply predominantly from synchronised conventional generators. However, with non-synchronous VRE technologies gradually displacing large amount of conventional thermal plants this has been an area of concern of System Operators (SO) such as National Grid (National Grid 2016b). The problem can be amplified with increased reliance on high voltage direct current (HVDC) interconnectors particularly in island systems such as in GB (Vázquez Villamor 2017). Eventually these factors can lead to limits being imposed on the penetration of non-synchronous generation, which is an approach already followed in some countries (EirGrid and SONI 2015). National Grid in GB has indicated that a minimum amount of inertia is required in the GB system, and that curtailment will be necessary of VRE power generation at periods of low demand in order to keep conventional generators online in the system to provide sufficient amounts of inertia (National Grid 2016b, Vázquez Villamor 2017).

The efficient integration of VRE into the system has been an area of intense research, amongst other things to limit the expensive curtailment of renewable generation. As such, a focus has been the creation of 'synthetic' or 'virtual' inertia that can mimic the effect of large synchronous generation units in contingency events. For example, while power convertors are not usually required to react to grid frequency variations, they could be asked to act upon frequency deviations in real time by managing the power flow into the system (Vázquez Villamor 2017). Several methods of providing synthetic inertia have been studied in the literature. Tielens and Van Hertem (2016) report for example that PV is able to provide the inertia either when in combination with fast-acting storage, or by operating below its maximum achievable power output (i.e. by being de-loaded and operating at part load). Highly accurate controls, however, would be needed.

Similarly, wind turbines have demonstrated their ability to deliver additional power output boosts at short time-scales when being controlled by fast reacting power electronics that can initiate in contingency events that the kinetic energy stored in the blades (as well as in the gearbox and generator) is turned into power. By using adequate controls variable speed wind turbines can contribute with inertia constants of 2-6s, which is in a similar magnitude as for large conventional power stations (2-9s; Grainger and Stevenson 1994). Inertia constants indicate the amount of time generators can deliver nominal amounts of power by only using the stored kinetic energy stored of its rotating mass (Morren et al. 2006). Some system operators such as the Hydro-Quebec in Canada have for this reason reinforced their grid code to exploit the synthetic inertial balancing capabilities of wind turbines (Daly et al. 2015).

However, due to the measuring delay that needs to be taken into account (i.e. time between the converter realising a high RoCoF and acting on it) other system operators have been reluctant to follow this step. National Grid consequently clearly distinguishes between synchronous and synthetic inertia, treating the possible contribution of wind to system inertia merely as potentially fast-acting frequency response, rather than as possible contribution to the system inertia (National Grid 2016b). Nevertheless, NG is actively researching in improved control systems that allow the contribution of wind power to frequency response services (National Grid 2016b, Vázquez Villamor 2017). Other studies highlight the importance of this step by demonstrating the potential of wind power to provide frequency services in the GB power system (Teng and Strbac 2016). Whilst the sustained de-loading (i.e. curtailing) of wind turbines for providing upward response is generally considered to be uneconomical, the service is regarded as promising and cost-effective only when wind turbines are forecasted to be curtailed. Nevertheless, the inherently unreliable nature of wind and the measuring delay are some of the major hurdles that system operators are still seeking to overcome.

Having outlined some of the key challenges of future low carbon power systems it becomes clear how CCS power stations can offer high value to these systems. As flexibly dispatchable power generators at comparatively low capital cost and carbon intensity CCS power stations could be the backbone of future energy systems by delivering back-up power whenever needed, even for longer time periods, as well as the required amounts of reserve and system inertia to stabilise the network. As such, CCS power stations contribute to all areas of the energy trilemma: security of supply, affordability, and sustainability from an emissions perspective. The high value that CCS power stations can deliver to future energy systems as found by a range of studies in the literature is discussed in further detail in section 3.2.3.

3.2.3. Value of CCS

The high expected value of CCS power stations to future low carbon energy systems is highlighted in several studies. The IPCC expects that the global total discounted mitigation

costs for reaching a 450ppm CO_2 concentration scenario (consistent with a 2°C global warming scenario with at least 66% probability) will be 138% higher when CCS is not available in the mix of climate mitigation technologies (IPCC 2014). The Low Carbon Innovation Coordination Group (LCICG) estimates a reduction of energy system costs of £100-500 billion when CCS is available in the portfolio of low carbon power generation technologies (LCICG 2012).

Whilst the value of CCS and its deployment potential is widely accepted in the literature it contrasts with the slow uptake of the technology both in industry and the power sector. In the power sector this can be explained to a large extent by the lack of legislative or financial drivers to deploy a relatively new and consequently financially risky technology that can provide many of the flexibility services (i.e. balancing and back-up services) that under current market designs conditions are not sufficiently enumerated (Strbac et al. 2015). For example, even though it has been identified as a challenge by SOs there are currently no evident market incentives, apart from individually contracted agreements with the SO, for promoting high-inertia generators (IEAGHG 2017). On the other hand the slow uptake of CCS in the power sector is likely to be at least partially a consequence of existing but misleading power generation valuation techniques that do not accurately represent the value of a technology to the wider electricity system.

For example, traditional decision making metrics and technology valuation metrics are mainly cost based and only focus on the individual technology (Heuberger et al. 2017). A frequently used tool for comparison of the cost-competitiveness of power generation technologies is the Levelised Cost of Electricity (LCOE) metric. It is a simple and intuitive metric that takes into account capital and operational expenses over the lifetime of a plant, as well as the expected electricity, and compares technologies on a £/MWh basis. It was undoubtedly a very practical metric in many 20th century electricity systems comprising nearly exclusively flexibly dispatchable power stations in the portfolio (Heuberger et al. 2017). However, although still relied upon (e.g.: UK BEIS 2018) the LCOE has lost most of its meaning today, as it does not take into account neither the price and supply variability of electricity, nor the impact that one generators' operation has on the electricity system in terms of reliability and operability (e.g. necessary back-up capacity, balancing and inertial needs, undermined capacity factors of other plants; Lew et al. 2013, Larsson et al. 2014, Heuberger et al. 2017, Ueckerdt et al. 2013). The omission of the additional indirect costs associated with the integration and accommodation of VRE technologies into the power system leads to inadequate results and a distorted comparison when assessing the costs and values of different technologies to the electricity system based on the LCOE (IEAGHG 2017).

Ueckerdt el al. (2013) consider that in an interconnected system power generators influence and depend on each others' services. The authors analyse the effects of a growing share of VRE supply on the electricity market dynamics in the attempt to capture their "integration costs" with a 'System LCOE' metric. The study concludes that these

“integration” or “profile costs” consist of back-up costs, full-load hour reduction costs and overproduction costs (Ueckerdt et al. 2013).

In a further attempt to overcome the drawbacks of the LCOE and trying to capture the complex interdependencies of different power generation technologies on the reliability and operability of the system, the U.S. Energy Information Administration introduced the Levelized Avoided Cost of Electricity (LACE; EIA 2018). The LACE expresses the system wide avoided cost that can be achieved by a power sector specific project levelised by the expected power output of the project over its lifetime (EIA 2018).

The works of Lamont (2008), Lamont (2013) and Strbac et al. (2012), Pudjianto et al. (2014) have relatively recently started to develop a system wide approach to valuing technologies through mathematical modelling and whole system optimisation. Building on this approach IEAGHG (2017) most recently performed an extensive assessment of the value of CCS power stations to UK future low carbon electricity systems. The authors define the value or ‘System Value’ (SV) of a technology as the reduction in Total System Cost (TSC) that results from the integration of one capacity unit of that technology (i.e. in £/kW) into the system. The centrepiece of their work is a Mixed Linear Integer Program (MILP) allowing for both the Generation Expansion Planning (GEP) and the optimal dispatch of generators via a Unit Commitment formulation (UC; for more details on these modelling techniques see section 3.2.5). Under consideration of environmental, system reliability, and operability constraints the TSC is calculated and compared for different electricity system scenarios.

In this way the authors demonstrate that the SV of a technology is a strong function of both the penetration of that technology in the electricity system, as well as of the electricity system conditions itself (e.g. deployment levels of other technologies, emission and reliability constraints, etc.). The study further finds that the optimal mix contains substantial levels CCS capacity deployment ranging from 21-41GW, dependent on the exact CCS technology utilised and future scenario (i.e. 2030 or 2050). The determined value of different CCS technologies varies between £500-800/kW and £150-300/kW at low and high deployment rates, respectively. A main reason for the high calculated value of CCS power stations is that they allow the integration of higher levels of VRE renewables without violating any reliability and operability constraints. In general, the TSC falls with high penetration of renewables due to lower operating costs (as long as the reliability and operability can be secured cost-effectively). The study, therefore, demonstrates how CCS is not competing against but rather operating in synergy with renewable technologies in future low carbon systems.

Strbac et al. (2015) takes a similar approach when examining the system integration costs of different technologies and the optimal capacity mixes for the British power system. The optimal mix, Strbac et al. (2015) finds, depends to a high degree on the level of flexibility in the system. High system flexibility (e.g. through high levels of storage available or generators with high operating flexibility) allows the integration of high levels of VRE capacity that generally drive down system costs. CCS is predominantly valuable at very low emission intensities (e.g. 50g/kWh) and low available levels of system flexibility, which is a

consequence of its high operational flexibility and dispatchability. As the only evaluated technology CCS was found to have a negative system integration cost throughout most analysed scenarios. Besides the greater controllability of CCS plants this has to do with the fact that additional CCS capacity on the system does not increase the requirements for ancillary services for balancing the system. In contrast, an increased reserve requirement of 2-22% is expected to be required as a function of the VRE installed capacity due to the higher volatility and larger forecasting challenge of the net demand profile (UKERC 2006, UKERC 2016, Holttinen et al. 2014, Brouwer et al. 2014, Heuberger et al. 2017).

Another study assessing the optimal capacity mix and values of different technologies in future GB scenarios was undertaken by the Energy Research Partnership (ERP 2015). Similarly to the previous studies it finds that the value of a technology depends to a large extent on the available capacity mix. Nevertheless, in contrast to previous studies ERP finds that the optimal capacity mix consist predominantly of nuclear capacity, with neither wind nor CCS being in the optimal portfolio. The sharp contrast between the optimal capacity mixes determined by IEAGHG (2017) or Strbac et al. (2015) and ERP (2015) illustrate the very high sensitivity of the results to underlying cost assumptions – as acknowledged by both Strbac et al. (2015) and ERP (2015).

The University College London (UCL) Energy Institute has carried out work on behalf of the Sustainable Development Solutions Network (SDSN) and Sustainable Development and International Relations (Pye et al. 2015) assessing cost effective deep decarbonisation pathways for the UK. The study provides an overview of a large range of UK power system scenarios that have recently been studied by different research bodies, advisory bodies, consultancies, as well as the UK governments Department for Energy and Climate Change (i.e. UKERC, CCC, DECC, POEYRY, Anable). Although the level of the deployment of CCS in the power sector varies throughout the summarised studies its contribution in nearly all scenarios is substantial (Pye et al. 2015).

Finally, GB system operator National Grid finds that renewables, CCS and nuclear capacity are the fundamental technologies when transitioning to a low carbon future (National Grid 2016c). The cost optimal mix for the UK by 2050 NG expects to consist of 100GW of renewables, 20GW of CCS and 22GW of nuclear capacity (National Grid 2016c). Seeing CCS as a relatively cheap electricity flexibility tool NG expects the technology to supply approximately a quarter of demand throughout the scenarios that are in accordance with the UK emission targets (National Grid 2016c, p.145, p.169). According to NG and based on the Energy Technologies Institute the 2050 UK emission targets can be met without CCS, however, only with a significant cost increase of 50-100% (National Grid 2016c, Energy Technologies Institute 2014).

Overall, the studies presented in this section have highlighted the strong case for CCS and its widely accepted place in future low carbon energy generation portfolios. The high value that CCS presents to future power systems is a consequence of CCS power stations being able to contribute to all three areas of the energy trilemma: adequacy, reliability and operability. Further, CCS power stations do not increase the balancing requirements of

electricity systems, and their operational flexibility facilitates the integration of higher levels of VRE, which generally drives down the system costs due to lower operational costs. In this way CCS power stations are able to operate in synergy with VRE rather than competing with them.

3.2.4. Operating patterns of CCS plants in future energy systems

Whilst the role of CCS plants in future energy systems is relatively well defined (as described in section 3.2.2-3.2.3), the operating patterns of CCS power stations in future low carbon systems are less well understood. As of yet, there is only a limited amount of literature investigating the operating patterns of CCS plants in future low carbon energy systems, their flexible capabilities, and the consequences these may have on the operating behaviour (Brouwer et al. 2015, Van der Wijk et al. 2014, Mac Dowell & Staffell 2016, Oates et al. 2014, Bruce et al. 2015, Bruce et al. 2014, Mechleri et al. 2017b). The relevant literature will be presented in the following.

Mac Dowell & Staffell (2016) classify the studies, modelling the interaction between CCS plants and the electricity market, into three levels of complexity:

1. Operation of a CCS power station(s) can be evaluated under a predefined pattern of prices (e.g. historical prices of electricity, fuel or carbon);
2. An electricity system scenario ('snapshot') can be modelled by choosing a profile for electricity demand and a power generation portfolio (incl. CCS plants), that will meet demand according to a dispatch procedure; or
3. A dynamic scenario for the future can be created, that is driven by underlying policy and investor behaviour. A coupled power system investment and dispatch model first determines the optimal power generation portfolio, and subsequently the detailed operational dispatch of the power plants.

Several studies model CCS power plants, in particular the value of flexible capture operation ('solvent storage' and capture plant 'bypass'), under predefined (mostly historical) price patterns (Oates et al. 2014, Cohen et al. 2011, Chalmers et al. 2009, Husebye et al. 2011, Mechleri et al. 2017a, Van Peteghem and Delarue 2014). 'Bypass' describes the operational mode of the CCS plant when the capture unit is switched off, resembling operation of a fossil fuelled power station without CO_2 capture capability. 'Solvent storage' refers to the technique at post-combustion CCS power plants of delaying the energy-intensive step of solvent regeneration to later points in time in order to boost electrical output when electricity prices are high. However, given that these studies are typically based on historical price patterns they are not necessarily able to predict operating patterns under the significantly different conditions expected in future low carbon energy systems.

Other studies taking the second and third approaches focus on examining the operating profiles and role of CCS power stations in future energy systems (Brouwer et al. 2015, Van der Wijk et al. 2014, Mac Dowell and Staffell 2016, Bruce et al. 2015, Bruce et al. 2014, Bruce 2015). They generally conclude that CCS plants will need to operate in a flexible, load following (i.e. responding to changing demand levels by adjusting power output) manner in future energy systems in order to balance the large penetrations of renewable power generation.

Nevertheless, very little consideration is given in any of the above studies to whether the future CO_2 transportation and storage (T&S) systems can cope with the large and potentially frequent and irregular fluctuations in CO_2 feed flow rates that the projected operating profiles of CCS power plants imply. The studies generally assume no downstream constraints to flexible operation of CO_2 T&S networks. However, only very few (e.g.: Oates et al. 2014, Ceccarelli et al. 2014, Mac Dowell and Staffell 2016) of these studies consider or even acknowledge the possibility of constraints to flexible operation imposed by downstream CO_2 transportation and storage systems. Concerns, however, have been raised about whether this assumption is justified.

In order for future CO_2 T&S networks to be designed efficiently, it is imperative to rigorously analyse and understand the operating conditions the networks are likely to face.

This chapter therefore addresses this gap in the literature by characterising CO_2 flow regimes feeding into CO_2 T&S systems across a range of future low carbon energy system scenarios for the case study example of Great Britain (GB) with varying penetrations of renewable energy.

Before discussing the unit commitment economic dispatch electricity system model used for the purpose of this study in more detail (section 3.3), section 3.2.5 gives a short overview of the different modelling techniques available for energy systems.

3.2.5. Energy System modelling techniques

Energy system models have been used extensively over the last decades to study and optimise the operation and composition of power generation portfolios. The idea to approach this optimisation task by means of mathematical modelling dates back to the early 1920s (Happ 1977, Li et al. 1997). Today, there is a large range of energy system modelling tools that are used to assess electricity system operation and requirements over a range of different time frames and temporal solutions (Conejo et al. 2010). Some of the most common techniques will be discussed in the following.

Unit Commitment (UC)

Every electricity system containing more than a single generator faces the problem of unit commitment (UC; Happ 1977). UC describes the possible dispatch of power generators over time in terms of power output in order to meet consumer demand. To minimise the production and start-up/shut-down costs of all generating units electricity system operators have sought to optimise the dispatch for many years.

The aim of UC models is, in general, to assist with this goal by determining the optimal dispatch schedule of the available generators to meet demand in the most cost economic way. Traditional UC look ahead and decide which generating units to commit (switch 'on' or 'off') and how much power and spinning reserve to dispatch. Parameters that are taken into account by UC models are operational costs and constraints of individual units, as well as the level of electricity demand that needs to be met. Two perspectives from which UC problems can be typically solved are from the system perspective (total system costs are minimised) and from the power plant operators perspective (to maximise individual profits by optimal production scheduling; IEAGHG 2017).

There are many variations of UC formulations emphasising different aspects of the system. For example, certain UC models focus on generation adequacy and reliability. Different metrics are usually used to assess power systems in terms of reliability, such as the Loss of Load Expectation (LOLE), Loss of Load Probability (LOLP) and Loss of Energy Expectation (LOEE). For an overview of the different aspects of power systems UC focus on the reader is referred to (IEAGHG 2017) and the references therein.

Traditionally, UC formulations have been solved for conventional power generators for which fuel costs are the dominant operating expense (IEAGHG 2017). However, more recently UC have been adapted to study the impact of variable renewables on the power system operation (Bruce 2015). Stochastic UC models, for example, simulate the variability and uncertainty in power systems with significant levels of renewable energy supply (Ma et al. 2013, O'Dwyer and Flynn 2015).

Economic Dispatch

A concept very closely related to UC is that of Economic Dispatch (ED). UC and ED differ in their considered time horizon, as well as their technical granularity and perspective (Kirschen and Strbac 2004, IEAGHG 2017). Whilst UC typically plans out the possible dispatch options in advance over a certain time period (e.g. a day or week in hourly discretisation) in order to make sure that a sufficient number of generators are available online, the ED determines the exact dispatch of the generators based on a more detailed cost structure in real time (e.g. every minute). In this way the ED determines the status of the individual generators after the UC has provided suggestion for the dispatch that are feasible taking into account the longer term planning context (e.g. of several hours or weeks). Whilst the UC is usually formulated as Mixed Integer Linear Programs (MILPs) ED

models are usually in the form of Linear Programs (LPs) or Non-Linear Programs (NLPs; IEAGHG 2017). Even though transmission losses are generally not included in ED models, they can be included in the form of Optimal Power Flow (OPF) models which are a sub-type of ED models (Bruce 2015).

Solving Techniques

Solving methods for UC and ED problems continue to be an area of extensive research. Ongoing improvements are made with the aim of reducing computational effort, solution time as well as optimality and accuracy of the results. There are two main strategies typically used for solving the described optimisation problems. They can be solved by using (i) heuristics, or by using (ii) detailed mathematical modelling guaranteeing convergence to the optimal solution.

Heuristics usually improve solution time by trading in accuracy and optimality of the solution. This solution method can outperform mathematical optimisation where a problem cannot be posed in closed mathematical form. Further, it can be particular helpful in large systems where the 'curse of dimensionality' makes it infeasible to compute all unit commitment combinations to find the optimal least-cost solution. Heuristics that are commonly used are priority listing, simulated annealing, particle swarm, tabu search, evolutionary and fuzzy algorithms (Simopoulos et al. 2006, Frangioni et al. 2008, Bhardwaj et al. 2012, Xia and Elaiw 2010, IEAGHG 2017).

Priority lists can be used to emulate the merit order by ranking generators according to their SRMC, with the lowest cost generator being dispatched first. If this predetermined order is used to commit generators until net demand is met, a dispatch strategy can be achieved with a reasonably high degree of optimality as Staffell and Green (2016) shows. Priority lists can, however, also rank generators dynamically according to full load average costs, commitment utilisation (Sheble and Fahd 1994), or flexibility (Bruce 2015).

The second strategy to solve UC and ED problems relies on rigorous mathematical modelling procedures to find the optimal solution(s). Common methods applied to UC are the Lagrangian Relaxation (Zhu 2009, Wang et al. 1995, Frangioni et al. 2008), Dynamic Programming (DP; Li et al. 1997), Interior point method (Han and Gooi 2007) or the Branch & Bound and Branch & Cut methods (Viana and Pedroso 2013). The Lagrangian Relaxation approximates the solution by iteratively incorporating constraints into the objective function and weighing them with Lagrangian multipliers. These multipliers are repeatedly updated until the determined solution is within the defined tolerances (IEAGHG 2017). Dynamic programming makes use of decomposition procedures. It is frequently used in multi-stage decision making processes. Branch & Bound and Brach & Cut are other state of the art methods that are used by modern commercial solvers (IEAGHG 2017).

Variations and Extensions of traditional UCED models

There are a large number of variations for implementing UC problems (Hobbs et al. 2001). They can come, for example, with additional constraints to consider environmental, security or operability aspects of the system. Another form of traditional UC models considers besides operational aspects also capacity planning. Unit Construction and Commitment (UCC) models seek to minimise the operational costs of existing units, as well as the investment costs for additional units under given emission and reliability constraints over long planning time horizons of usually several decades. UCC models can be used for both transmission as well as generation capacity planning. However, the complexity of modelling increases significantly (Palmintier 2013).

For a detailed review of different UC formulations for varying applications (i.e. UC and optimal investment, UC with CCS, UC with energy storage) the reader is referred to (Bruce 2015) as well as (IEAGHG 2017). For a review of a range of different methods that can be used for implementing UC formulations the reader is referred to Sheble and Fahd (1994) and Bhardwaj et al. (2012).

3.3. Model description

The present study utilises a unit commitment and economic dispatch (UCED) model based on Bruce et al. (2015) and Stanojevic (2011). UCED modelling is a sophisticated and mature method for examining power system operation as well as the operating profiles of individual power stations under consideration of technical operating constraints of individual generators (e.g. ramp rates, minimum up/down times, min. and max. power output, reserve contributions) as well as the overall system (e.g. reserve requirements).

For specified power plant portfolios and wind regime inputs, the model optimizes for each time-step (hourly discretisation) the dispatch of available thermal plants according to a least cost merit order approach (operating costs). The approach considers technical generator as well as system constraints to identify feasible future operating scenarios. After identifying feasible operating scenarios it chooses the available least cost option by deploying a priority based dynamic programming enumeration method. Operating profiles, realised operating costs, and CO_2 emissions are calculated on an hourly basis for all thermal plants over the simulated time period (one year in this study). The model was realised in MATLAB. For a detailed description of the model the reader is referred to Bruce et al. (2015).

Although capable of considering any number of different plant types, the model is specified for the purpose of this study to consider only nuclear, NGCC (Natural Gas Combined Cycle) and OCGT (Open Cycle Gas Turbine) power stations as thermal generators. No unabated coal fired power plants are considered, in line with UK government predictions for the year 2024 and later (UK BEIS 2017a). NGCC plants can be specified in the model to simulate

NGCC plants equipped with CO_2 capture capability (NGCC-CCS plants). Post-combustion CO_2 capture (PCC) technology with a constant capture rate of 90% is assumed for these plants for whenever the PCC unit is operated. The possibility of temporarily switching off the PCC unit for recovering the energy penalty associated with CO_2 capture is discussed only within a sensitivity case in subsection 3.6.7.3. The capture rate of 90% is chosen to be consistent with the majority of the literature, although it is realised that capture rates beyond 90% can be as or more cost-effective, particularly for monoethanolamine (MEA) based capture technologies. It is assumed that only those NGCC plants with highest baseline power plant efficiency (LHV) are fitted with CCS capability, to reflect CCS becoming a standard component in future new-build NGCC power plants. A minimum stable generation load of 40% is assumed for all conventional power stations.

3.4. Scenario selection and input data

A set of high resolution (3x3km) wind speed data for GB is available for the years 2002-2010 from Hawkins (2012). Based on locations of existing wind farm sites, sites under construction, sites under planning, and accounting for wake losses, electrical losses and technical availability, the available wind power generation profiles have been calculated. Power curves are assumed according to Bruce (2015). After assessing the data, wind data from the years 2008, 2004 and 2010 has been selected for illustrative high, medium and low wind speed scenarios. In the following these scenarios will be referred to as the 'high', 'medium', and 'low' wind speed scenario, respectively. Wind data and historical demand data remain coupled for all respective years due to the strong correlation and complex interdependencies between weather patterns and electricity demand. Historical demand data is taken from (National Grid 2015a) and has been normalised and weather corrected according to the methodology presented in Bruce (2015), for better inter-yearly comparison of dispatch profiles.

A wind power generation capacity of 15GW, 30GW and 45GW is assumed in the low, medium and high wind deployment scenarios, respectively. These levels reflect the current amount of installed wind capacity in the UK (15.6GW; RenewableUK 2017), and the medium and high wind deployment scenarios forecasted by the GB transmission system operator (National Grid) for 2035, respectively (National Grid 2016c). In line with government predictions for 2035, nuclear capacity is assumed at 17.1GW (UK BEIS 2017a). The minimum level of synchronised generation is set to 15GW to ensure sufficient system inertia for maintaining the rate of change of frequency within acceptable limits (National Grid 2011, 2013).

A grid average annual CO_2 emission intensity of 60g/kWh and 100g/kWh is selected in the reference scenarios, in line with UK Government targets (UK BEIS 2017a) for 2028 and approximately 2050, respectively. This represents a significant reduction in the average emission intensity level of 420g/kWh in 2015 (UK DECC 2016). A higher emission intensity

of 140g/kWh is chosen as an illustrative sensitivity case. CCS capacity is adjusted between the different scenarios in order to reach the required CO_2 emission intensity, on average over the year, after taking into account the available wind power generation for each scenario. This is implemented by assuming CO_2 capture capability on as many NGCC plants as needed to reach the targeted emission intensity.

NGCC and OCGT capacity is adjusted in every scenario to reach a de-rated generation capacity of at least 65.8GW. This capacity constraint is set to allow for a de-rated capacity margin of 6.5% over the average annual peak demand over the evaluated years of 60GW, as well as for covering a largest credible in-feed loss of 1.8GW (Ofgem 2013, 2014). This is to maintain a comparable yet realistic generation fleet across all wind scenarios for satisfying historical demand levels. The technology-specific availability factors are based on (National Grid 2016d) and are provided in Table 3.3. A flat availability curve is assumed for thermal generators across the year.

A cost-optimal split between NGCC and OCGT gas-fired capacity is calculated, based on (UK BEIS 2016) assumptions for capital, operational, and CO_2 costs as well as operational lifetime data, and a discount rate of 7.5%. This leads to an NGCC load factor threshold of 11%, below which it is more cost effective to build and operate an OCGT instead of an NGCC plant to satisfy power demand. It is assumed that the capacity market and the provision of balancing services deliver sufficient incentives to operate at the assumed load factors. Any residual demand and reserve requirement that can not be met with the respective power generation fleet, due to low wind resource availability during peak demand times, is assumed to be met by Demand Side Response (DSR) procured by the system operator for this purpose (National Grid 2016e).

Technical, techno-economic and economic parameters are selected consistently to represent a 2035 scenario, although it is recognised that some sensitivity scenarios (e.g. 60g/kWh emission intensity and 45GW wind power capacity) might be more realistic for later years in the century. The scenario with 30GW wind power generation capacity, 100g/kWh emission intensity and wind and electricity demand data from 2004 will be referred to as the ‘Base case’. A summary of all core scenarios considered in this study is provided in Table 3.6 in subsection 3.6.1.

Fossil power plant full load efficiencies on a LHV basis are interpolated between lower and upper limits based on Gas Turbine World Handbook (2013) and Brouwer et al. (2015), to reflect gradual advances in technology over time (see Table 3.1). Part-load efficiency penalties for fossil power plants are according to Brouwer et al. (2015).

Upward and downward reserve requirements are set to cover unexpected changes in wind output and electricity demand resulting from forecasting uncertainties within 3.5 standard deviations (3.5σ) or 99.95% of events. This is consistent with a reliability standard of security of supply of 3h per year used by the GB system operator National Grid (Loss of Load Expectation Risk metric; National Grid 2014). Reserve is further scheduled according to the largest credible in-feed loss of 1.8GW (Ofgem 2013, 2014). System reserve

requirements can be met through a combination of synchronous spinning and non-synchronous standing reserve (Wood et al. 2013). An allocation of 1.5σ as spinning reserve and 2σ as standing reserve is assumed based on Silva (2010).

Further technical, techno-economic and economic input data is summarised in Table 3.3-Table 3.5. Technical input data such as ramp rates, minimum and maximum power output of individual generators, minimum up and down times are needed to inform the UCED model about the technical feasibility of dispatching individual generators for meeting net demand at any time t during the simulation period. Techno-economic and economic data such as fuel prices, ramping costs and costs associated with carbon capture is required by the model to optimise and find a least cost dispatch approach of the individual generators over the simulation period under consideration of technical and system constraints. For further information about the way individual technical, techno-economic and economic parameters are used within the UCED model the reader is referred to Bruce et al. (2015).

Throughout the core modelled scenarios onshore and offshore wind power are considered as the only VRE technology. This allows studying the effect of wind induced variability on the power system in detail, and is considered reasonable in the GB context with wind power being considered the dominant VRE technology in the future. A sensitivity study exploring the effect the addition of solar capacity has on power system scenarios with varying amount of wind power penetration is, however, provided in a sensitivity case of this study (section 3.6.7.1).

Table 3.1: Base power plant full load efficiency data (LHV).

Capacity type	Full load LHV efficiency	Reference
Nuclear Plant	36.7%	Bruce 2015
NGCC	62.1-59.5%	Brouwer 2015; Gas Turbine World 2013
OCGT	41.8-37.5%	Brouwer 2015; Gas Turbine World 2013

Table 3.2: Fuel and CO_2 prices.

Resource	Price	Reference(s)
Natural Gas	£21.2/MWh_{th}	BEIS 2016
Uranium	£3.5/MWh_{th}	Based on Bruce 2015; Brouwer 2016
CO_2	£101.1/tCO_2	BEIS 2016

Table 3.3: Generator availability factors per technology type (based on National Grid 2016b and 2016c).

Capacity type	Availability Factors
Nuclear	90%
NGCC-CCS	90%
NGCC	90%
OCGT	94%
Wind	22%

Table 3.4: Technical and techno-economic parameters for thermal plants (based on Bruce 2015 except when specified differently).

Parameters				
		Nuclear	NGCC	OCGT
$P_{g,min}$	Minimum power output (MW_e)	620	360	225
$P_{g,max}$	Maximum power output (MW_e)	1550	900	565
ρ_g^{up}	Ramp up rate (MW_e/h)	4650	300	600
ρ_g^{dn}	Ramp down rate (MW_e/h)	4650	300	600
$UT_{g,min}$	Minimum up time (h)	24	3*	1
$DT_{g,min}$	Minimum down time (h)	24	3*	1
$c_{g,t}^{fuel}$	Cost of fuel (£/MWh_{th})	3.5	21.2	21.2
e_g^{CO2}	Emission factor (tCO_2/MWh_{th})	0	0.2267	0.2267
$c_g^{O\&M}$	Variable O&M cost (£/MWh_e)	0.5	2.5	5.0
$c_g^{ramp,up}$	Upwards ramping cost (£/MW_e)	5.0	5.0	5.0
$c_g^{ramp,dn}$	Downwards ramping costs (£/MW_e)	5.0	5.0	5.0
$c_g^{start,fixed}$	Fixed start-up cost (£)	100000	10000	5000
$F_g^{start,cold}$	Fuel consumption during cold start-up (MWh_{th})	5000	1500	400
τ_g^c	Thermal cooling constant (h)	8	12	24
$c_g^{shut,fixed}$	Fixed shut-down cost (£)	25000	2500	12500
F_g^{shut}	Fuel consumption during shut-down (MW_{th})	1250	375	100

*based on Hentschel et al. (2016), DIW (2016), Van den Bergh and Delarue (2015).

Table 3.5: Technical and techno-economic parameters for post combustion CO_2 capture units (based Bruce 2015).

Post-combustion capture plant parameters		
$P_g^{capt,fixed}$	Fixed CO_2 capture plant power consumption (MW_e)	25
$Y_{g,min}^{capt}$	Minimum CO_2 capture rate (-)	0
$Y_{g,max}^{capt}$	Maximum CO_2 capture rate (-)	0.90
$q_g^{capt,op}$	Energy requirement to capture 1 tonne of CO_2 (MWh_{th}/tCO_2)	0.27
$c_g^{O\&M,capt}$	CO_2 capture plant variable operation and maintenance (£/tCO_2)	1.5
c^{solv}	Cost of MEA solvent (£/kg)	2.0
$c_{g,t}^{trans}$	CO_2 transport and storage (£/tCO_2)	10.0
D_g	Total solvent degradation rate (kg/tCO_2)	1.5
D_g^{th}	Solvent degradation rate cause by thermal effects (£/tCO_2)	0.1

3.5. Limitations

Before presenting the results in section 3.6, several limitations to this study should be noted. Firstly, although it is widely recognised that a significant decarbonisation of the economy requires decarbonisation of industrial processes, including through CCS, no CCS from industrial sources is considered within this study. Depending on the operating regimes of the industrial facilities, this can either smooth out or amplify CO_2 flows feeding into T&S networks. Secondly, neither the electrification of transport nor the effect of smart grids on electricity demand levels and patterns is considered. These technologies have the potential to change demand patterns significantly and, again, either increase or decrease the flexibility in output required from CCS power stations. Thirdly, no energy storage is considered. The effect of energy storage on CO_2 flow patterns is uncertain. Although energy storage has the potential to smooth out operating profiles of fossil power plant at times, it might equally amplify these at other times. Fourthly, the study assumes that wind and demand patterns will remain similar over the coming decades. Finally, no geographical distribution of individual generators is considered. The network is modelled as a single bus system. No transmission constraints are considered, as they go beyond the scope of this thesis.

With large uncertainty about the deployment levels of the mentioned technologies, and considering these caveats, the present study provides a useful baseline estimate of the operating flexibility likely to be required by future CO_2 T&S systems. It is only when the requirement for operating flexibility is better understood, that the additional costs associated with managing the operational issues that flexible operation imply can be minimised.

3.6. Results

3.6.1. CCS capacity required for the given scenarios

Table 3.6 summarises all modelled core scenarios in this chapter (excluding sensitivity cases). It serves as a reference table throughout this study as it shows the amount of CCS capacity that is required and installed in the respective core scenarios for reaching CO_2 emission intensity targets of 60g/kWh, 100g/kWh and 140g/kWh, under the assumption of different amounts of installed wind capacity and 'medium' wind speeds. An emission intensity of 140g/kWh could not be reached with 45GW of installed wind capacity, as the CO_2 emission intensity reaches a maximum of 107.3g/kWh without CCS plants being considered, as indicated in the corresponding field. Throughout all scenarios the nuclear capacity is at 17.1GW, as discussed in section 3.4. A detailed summary of the required NGCC and OCGT capacity to reach the de-rated capacity margin of 65.8GW is provided in

Appendix A1. Further a summary of the nominal (i.e. maximum) CO_2 flow rates captured collectively by the CCS power stations in the respective UCED scenarios is presented in Table 3.7.

Table 3.6: CCS capacity required to reach emission intensity for different wind scenarios for base year ('medium' wind speeds).

Installed Wind Capacity Scenario	CO_2 Emission Intensity Scenario		
	60g/kWh	100g/kWh	140g/kWh
15GW	20.2GW	12.3GW	7.0GW
30GW	14.0GW	7.0GW	0.9GW
45GW	8.8GW	0.9GW	0.0GW (*107.2g/kWh)

*Realised CO_2 emission intensity in brackets when intended intensity cannot be reached due to constraints.

Table 3.6 indicates that 7.0GW of CCS capacity is required in the base case (30GW wind, 100g/kWh CO_2 emission intensity). This compares to 14.0GW and 0.9GW of CCS capacity for the low and high emission intensity scenarios respectively, with 30GW of wind capacity being available. At 45GW of installed wind capacity the required amount of CCS capacity decreases, while it increases with less installed wind capacity. This compares to a total thermal capacity of around 61-69GW throughout the respective scenarios.

Table 3.7: Maximum (i.e. nominal) CO_2 flow captured collecticely by all CCS power stations deployed in the respective UCED scenarios.

Installed Wind Capacity Scenario	CO_2 Emission Intensity Scenario		
	60g/kWh	100g/kWh	140g/kWh
15GW	60.5MTPA	36.6MTPA	20.9MTPA
30GW	41.9MTPA	20.9MTPA	2.6MTPA
45GW	26.1MTPA	2.6MTPA	0MTPA

3.6.2. Time profiles (power and CO_2 flows)

Figure 3.3 displays the aggregate power output curves of CCS-equipped power stations over the month with the lowest (February) and highest (June) required power generation variability in the base case.

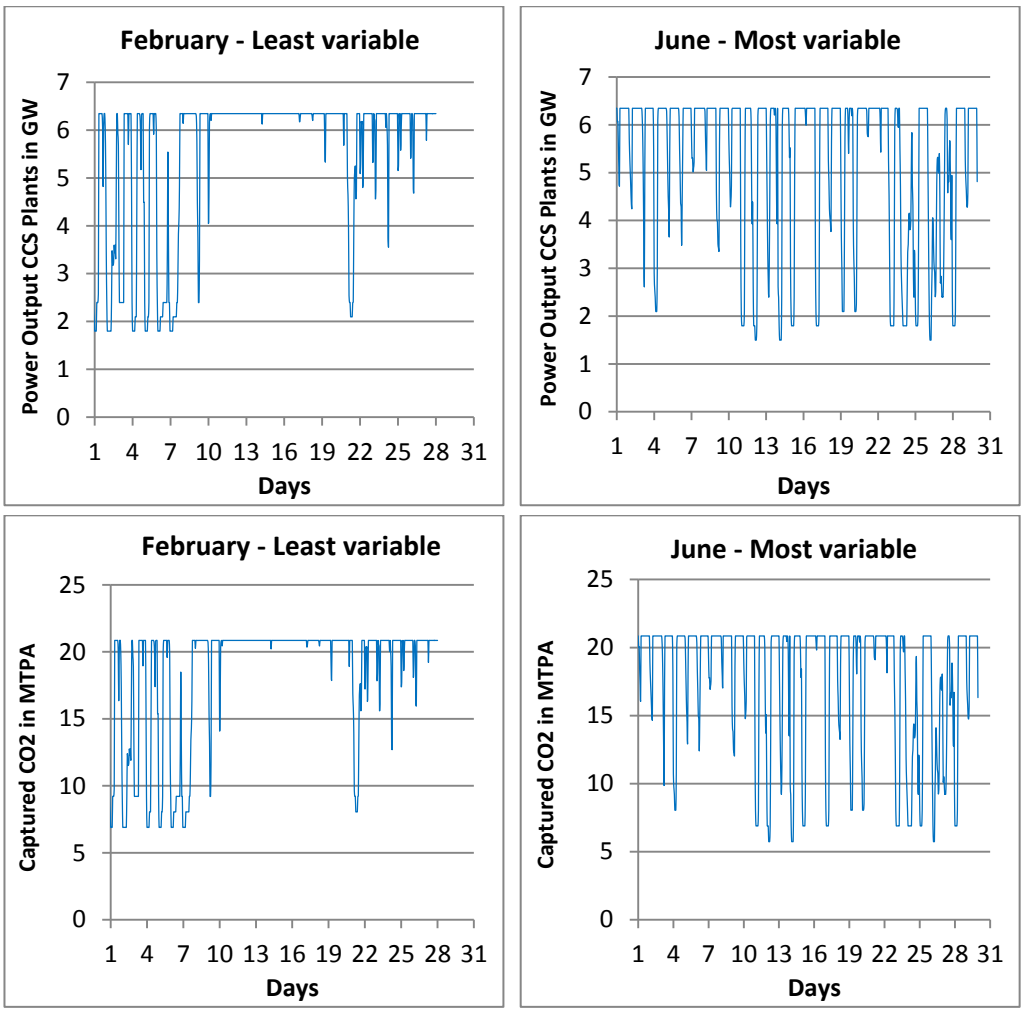

Figure 3.3 (top): Collective power output of CCS power stations in month with lowest (left) and highest (right) fluctuations in base case ('medium' wind speeds, 30GW wind, 7.0GW CCS, 100g/kWh).

Figure 3.4 (bottom): Time profile of collectively captured CO_2 in month with lowest (left) and highest (right) fluctuation in base case ('medium' wind speeds, 30GW wind, 7.0GW CCS, 100g/kWh).

*The discrepancy between installed CCS capacity and the maximum delivered power in Figure 1a is an effect of the assumed availability of 90% for NGCC-CCS plant over the year (see section 2.2 and Table 3.3).

It is notable that even in the month with the lowest variations, CCS power stations need to load follow substantially to compensate for imbalances between net electricity demand (total demand minus power supplied and dispatched from wind farms) and supply. This load following operation manifests in cyclic operation of CCS power plants, including the shifting between production of high levels of electricity (typically during daytime) and low levels of electricity (typically at night).

Figure 3.4 shows the aggregate amount of CO_2 produced by the PCC facilities based on the operating profiles of Figure 3.3. The time profiles of CO_2 production resemble the profiles of electricity generation; however, they also reflect the part-load efficiency losses of the thermal generation fleet. Again, variations in CO_2 production can be observed, often on a

daily basis, although the amplitudes of the variations are somewhat less pronounced than for the electricity production profiles.

Similarly to the previous figure, Figure 3.5 and Figure 3.6 show the aggregate CO_2 production profiles over a representative ('average') month of the base year (October) for a range of emission intensity and installed wind power scenarios. Figure 3.5c shows the same data line on two different scales (y-axes) to facilitate comparison with Figure 3.6b.

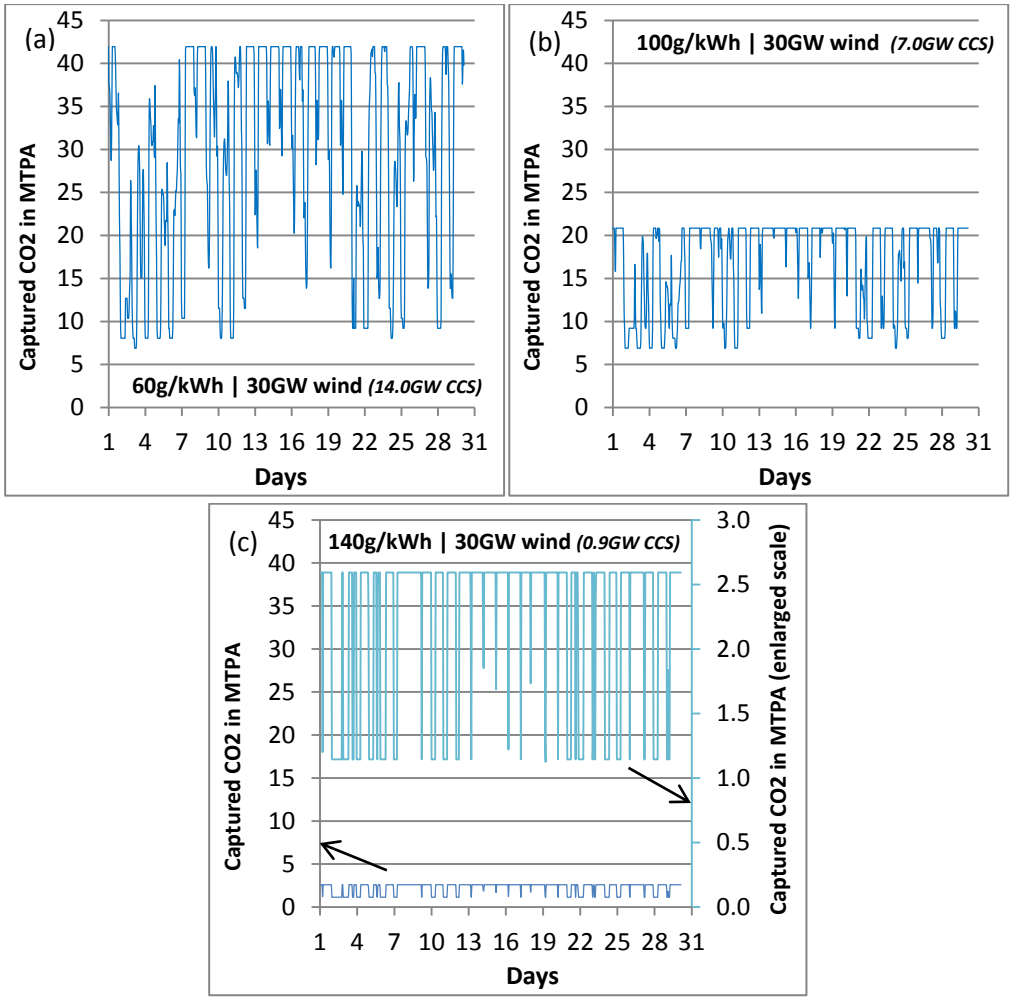

Figure 3.5: Time profile of captured CO_2 in representative month for 30GW installed wind capacity in 60g/kWh (a), 100g/kWh (b) and 140g/kWh (c) emission intensity scenario for 'medium' wind speeds. *

*CO_2 collectively captured by CCS power plants in respective scenarios. Note that different numbers of CCS plants are necessary to reach respective CO_2 emission intensities in different scenarios.

The following core observations can be made when comparing the profiles of captured CO_2:

- The absolute levels of CO_2 captured in the scenarios are very different. This is due to the different amounts of CCS capacity installed in the scenarios (see Table 3.6 for installed CCS capacities).

- In some scenarios, the amount of CO_2 captured oscillates predominantly between two levels (Figure 3.5c and Figure 3.6b), while in others changes in flow rates are more 'variable in size' (Figure 3.5a and Figure 3.6a). Oscillating flow profiles occur when the CCS fleet is comprised of only a few plants (e.g. <4) that tend to collectively adapt their output between full and minimum load to respond to changes in the relatively narrow net demand band that they cover (i.e. in which they need to load follow) based on their merit order position. 'Variable in size' load changes (Figure 3.5c and Figure 3.6b) occur when the CCS fleet is larger, and automatically covers a greater net demand range in which the plants need to load follow, producing more variable output. CO_2 T&S networks for large CCS power station clusters therefore need to be designed for a more continuous infeed flow range than networks for only a few CCS power stations.
- The relative and absolute spread (difference) between the maximum and minimum CO_2 flow rates in the respective scenarios grows with increasing deployment of CCS capacity, magnifying the amplitude of the largest flow rate fluctuations. Whilst a factor of 2.3 between minimum and maximum CO_2 flow rates characterises this spread in scenarios with small CCS fleets (Figure 3.5c and Figure 3.6b), this ratio indicating the size of the largest flow fluctuations rises to 3.6 and 5.9 in scenarios with large CCS fleets (Figure 3.5a and Figure 3.6a). Larger flow rate fluctuations are generally more difficult for T&S networks/injection wells to handle (in particular when two-phase flow develops across the wellhead at low relative flow rates as a consequence of the reduced backpressure from injection – see Chapter 2).
- The variability of CO_2 flows feeding into the T&S networks is substantial regardless of wind capacity and emission intensity scenario, even though the CO_2 flow profiles in the respective scenarios have individual characteristics.

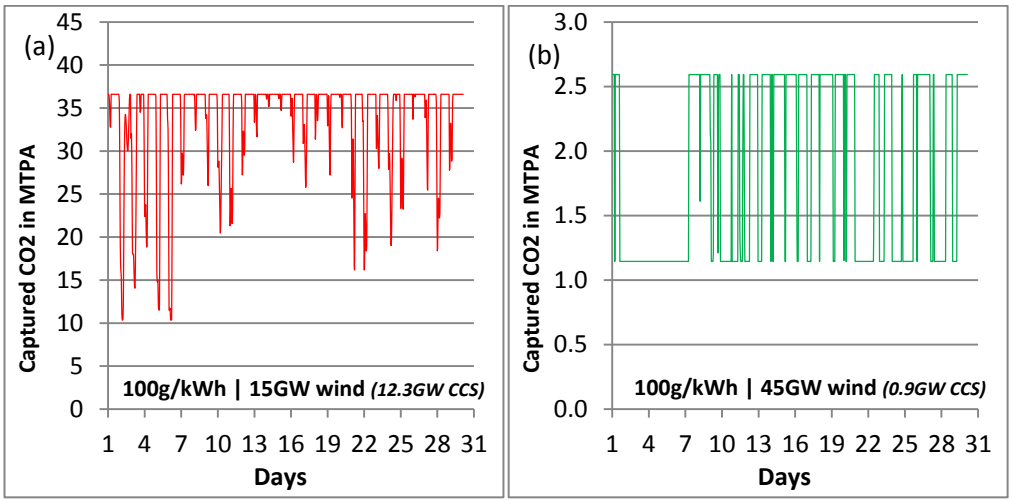

Figure 3.6: Time profile of captured CO_2 in representative month for 15GW (a - red) and 45GW of installed wind capacity (b - green) in 100g/kWh emission intensity scenario for 'medium' wind speeds. *

*CO_2 collectively captured by CCS power plants in respective scenarios. Note that different numbers of CCS plants are necessary to reach respective CO_2 emission intensities in different scenarios.

3.6.3. Flow duration curves

To explore the behaviour of CO_2 flows over an entire year, Figure 3.7 illustrates the 'flow duration curves' for all nine core scenarios. The curves can be thought of as captured CO_2 duration profiles, similar to Figure 3.5 and Figure 3.6, however, over the entire base year and stacked along the x-axis from high levels of CO_2 captured (left) to low levels of CO_2 captured (right). In this work, they will be referred to as CO_2 flow duration curves (FDC), as they indicate the amount of CO_2 that will need to be accommodated as feed-flows by future downstream CO_2 T&S systems, for the given amounts of time of the year. This comes with the assumption that no balancing of CO_2 flows will be performed within the boundary of the power plants.

In all modelled scenarios the nominal (maximum) amount of CO_2 is captured over a significant proportion of time of the year (Figure 3.7). While in the high emission intensity scenario (c), this is the case for 292-311 days of the year, dependent on wind deployment scenario, this number drops to 220-262 days in the medium (b), and 148-161 days in the low emission intensity scenarios (a). The decrease in the number of days the plants are delivering nominal amounts of CO_2 reflects the decrease in average utilisation factors of CCS plants in lower emission intensity scenarios, due to the large number of CCS plants required to reach low emission intensities. When many CCS plants are installed (i.e. installed CCS capacity is high), a significant fraction of the available CCS plants will only be required to operate and therefore capture CO_2 at periods of high net demand, which represent a relatively small fraction of time over the year. This consequently has a negative effect on their average capacity factor[1]. This compares to high emission intensity scenarios that require fewer CCS plants, which, however, typically operate large fractions of the amount of time over the year, as they are rarely constrained off the network due to low net demand. A summary of the capacity utilisation factors of the T&S systems in the individual scenarios is provided in Table 3.8.

[1] NB: Generally the size of the CCS fleet in the low emission intensity scenarios could be reduced without compromising on CO_2 emissions if capture rates of PCC units beyond 90% were considered. This would mitigate the aforementioned negative effect on capacity utilisation caused by comparatively large CCS fleets. However, deviating the capture rate of operating PCC units from 90% is outside the scope of the current study.

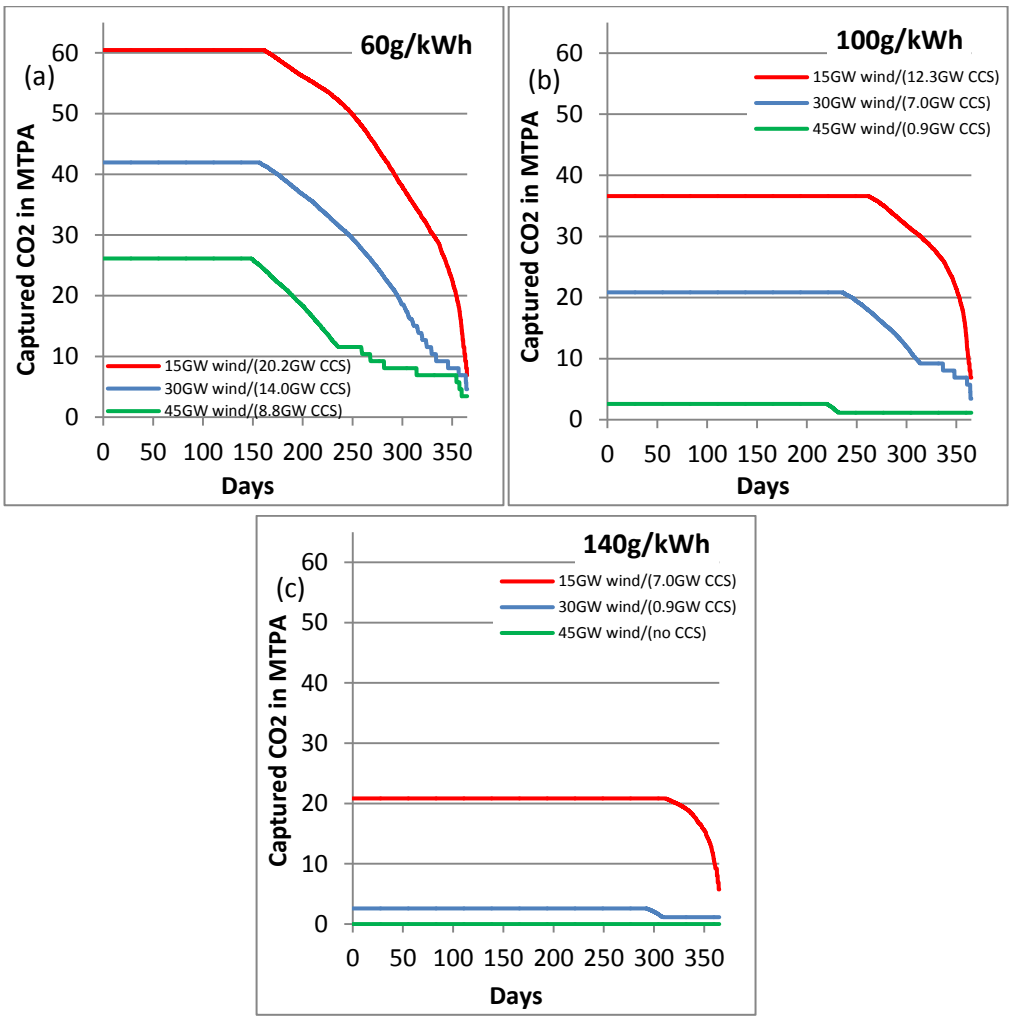

Figure 3.7: CO_2 capture duration profile for 15GW (red), 30GW (blue), 45GW (green) wind capacity in 60g/kWh (a), 100g/kWh (b), and 140g/kWh (c) CO_2 emission intensity scenario for 'medium' wind speeds.*

*CO_2 collectively captured by CCS power plants in respective scenarios. Note that different numbers of CCS plants are necessary to reach respective CO_2 emission intensities in different scenarios.

The shape of most FDCs in the 15GW and 30GW installed wind power scenarios is similar. After an initial plateau of the curve on the left side of the diagram, the curves drop with increasing gradient towards the right, reaching a common level in the low and medium emission intensity scenarios. The indentations on the right of the FDCs represent individual CCS plants of the thermal fleet shutting down. The 45GW installed wind power (green) curves in all scenarios, as well as the 30GW wind power (blue) curve in the high emission intensity scenario, plateau on the right side of the graph at a lower level. This is due to significant levels of upwards spinning reserve provision required from CCS plants with high penetrations of intermittent wind power to hedge the power system against unexpected and fast increases in net demand or shortfalls of supply (e.g. generator failure), leading to sustained operation of these plants at minimum load. Upwards spinning reserve is provided by thermal plants by operating below their respective maximum output levels (e.g. at minimum stable generation load) enabling them to quickly ramp up their power output

when needed. A trend can be observed towards higher levels of reserve provision required of CCS plants at higher levels of wind penetrations, which is indicated by extended plateaus of the corresponding FDCs on the right side of the diagrams.

Table 3.8: Calculated capacity utilisation factors of T&S systems in individual core scenarios.

Installed Wind Capacity Scenario	CO_2 Emission Intensity Scenario		
	60g/kWh	100g/kWh	140g/kWh
15GW	84.7%	93.7%	97.2%
30GW	77.6%	86.2%	90.3%
45GW	69.6%	78.8%	No CCS

In no scenario with actual CCS capacity installed, does the produced CO_2 flow drop to zero for a significant amount of the time. This is on one hand again due to the role of thermal power stations as reserve providers, which means that some CCS units ranking lowest in the merit order list (i.e. low operational costs and hence very cost competitive due to low CO_2 emissions and high CO_2 emission costs; just outperformed on operational cost basis by renewable and nuclear power) never get constrained off the grid and instead operate continuously at minimum stable load at low net demand levels to provide sufficient upward spinning reserve. On the other hand, having no periods of zero CO_2 flow is an effect of the constraint of a minimum level of synchronised generation of 15GW that it is assumed needs to be met by thermal generators throughout the year, to ensure sufficient inertia on the power system to limit the rate of change of frequency (as outlined in section 3.4).

Overall, the analysis of absolute levels of CO_2 captured by CCS power station demonstrates a strong time variability of CO_2 flows across all modelled scenarios. Furthermore it shows that utilisation factors of CCS power stations and their reserve provision behaviour is highly dependent on the wider generation capacity mix, in particular the size of the CCS fleet and the penetration of wind power. Although a lower level of capacity utilisation of CCS infrastructure, including T&S systems, is not a problem by itself, it increases the cost per tonne of CO_2 abated, thus reducing the relative economic value of CCS vis-à-vis other low carbon policy options.

3.6.4. Changes in CO_2 flows (Variability)

While the potential utilisation of CO_2 T&S systems can be very well described with FDCs it is also important to consider the short-term variations in the amounts of CO_2 captured by the power stations that will feed into future T&S systems. This is because it is not only the absolute level but also the size and frequency of variations in feed flow rates that can present significant challenges and operational risks to CO_2 T&S networks when the injection and storage infrastructure needs to be operated flexibly (i.e. see Chapter 2 or Spitz et al. 2017).

The following two sections explore short-term variations in CO_2 collectively captured by CCS power plants in the respective scenarios. Section 3.6.4.1 focuses on net changes in captured CO_2 over different time intervals, on a rolling basis over the year. While short term variations can dampen out and be absorbed over the length of the pipeline system (particularly if active CO_2 balancing is considered within the transportation network), longer term or 'average' variations in CO_2 flow over several hours will propagate through the entire network, having a direct (although time-delayed) impact on downstream CO_2 injection profiles. Section 3.6.4.2 therefore explores (for selected cases) changes in the average amount of CO_2 captured over two consecutive time blocks of 6hrs, again on a rolling basis over the year. 6hrs is chosen as the base case for analysis as this period is considered sufficient for changes in CO_2 feed-flows to have an effect on injection profiles downstream. This corresponds to the amount of time that the FEED study team of the Peterhead CCS demonstration project in the UK (Shell 2015a) estimated that the system operator of their proposed T&S system would have to react to a fault in the downstream injection and storage system, by adjusting/stopping the feed flow rate to the transportation pipeline (of 102km length, 20 inches or 508mm outer diameter; Shell 2016).

3.6.4.1. Net variations

In order to investigate flow variability in the respective UCED scenarios flow rate changes over 6hr periods are calculated in this section according to formula 2 and on a rolling basis over the base year. The approx. 8760 load changes over the base year in each UCED scenario are subsequently stacked according to their amplitude in Figure 3.8. The figure consequently visualises flow variability by illustrating the number of times (in thousands) the net change in CO_2 flow captured collectively by the CCS power stations over time periods of 6hrs (rolling basis over the year) reaches a certain amplitudes (relative to nominal flow).

$$A_t = \frac{|(F_t - F_{t-6})|}{F_{nominal}} \qquad t \in \{7, 8 \dots 8760\} \tag{2}$$

Where A_t *is flow rate change amplitude at hour t*
F_t *is flow rate at time t*
F_{t-6} *is flow rate at time t-6*
$F_{nominal}$ *is nominal flow rate in respective UCED scenario (see also max. flow in respective scenarios in Table 3.7).*

Basing the analysis on net flow variations between two points in time, on a rolling basis over the year, allows demonstrating flow variability at the wellhead if zero flow balancing capacity is available in the CO_2 T&S network, e.g. in the form of buffering capacity of pipeline. This is a realistic case when the pipeline already operates close to its pressure limits (maximum and minimum) and has very limited scope to vary pressure levels and fluid

densities in order to act as an interim buffer store for balancing flows. This can happen for example at very long distance pipelines with infrequent pressure boosting stations, or at pipelines accommodating very high flow rates relative to their economic design flow rates leading to high pressure drops and by extension utilisation of large parts of the allowable pipeline pressure envelope even at regular pipeline operation. For more background on pipeline operation and simulation the reader is referred to Chapter 5.

Finally it should be noted as a caveat that there is a kind of flow variability that this metric cannot capture: Repetitive cyclic flow variations with a cycle duration of 6hrs. To exclude that the metric systematically underestimates flow variability the analysis has been performed by adapting the metric and considering flow variations also over time periods of 1hr and 12hrs (see Figure 3.9). Additionally internal analysis of flow changes over varying time periods has shown that flow rate changes over 6hrs periods are well within the wider trend, and do not systematically underestimate flow variability by ignoring a cyclical CO_2 profile with cycle durations of 6hrs.

Based on the same calculations, and considering all CO_2 flow changes over 6hrs-periods on a rolling basis over the base year (approx. 8760), Table 3.9 summarises how many of them have an amplitude of 0-5%, >30%, and >50% of nominal flow in the respective scenarios.

Figure 3.8 and Table 3.9 show that at lower emission intensities, load changes occur more frequently and have higher amplitudes. This can be explained by the larger number of CCS plants required in lower emission intensity scenarios, which implies that more CCS plants need to load follow leading to relatively frequent and large load changes, compared to CCS plants running predominantly base-load when fewer plants are installed in higher emission intensity scenarios. When only few CCS plants are installed, in high emission intensity scenarios, they only rank very low in the merit order (i.e. low operational costs and hence very cost competitive due to low CO_2 emissions and high CO_2 emission costs). These CCS plants are, therefore, less likely to be constrained off the grid (or be required to load follow) compared to the situation in low emission intensity scenarios, where many CCS plants are installed, some of which rank comparatively high in the merit order.

It is notable that in the low and medium emission intensity scenarios (Figure 3.8a and Figure 3.8b), flow remains constant (i.e. 0% rel. load change) significantly more often in the 45GW wind capacity case than in the 30GW and 15GW wind capacity cases. This is expected for two complementary reasons: first, as fewer CCS plants are deployed in the 45GW wind capacity scenario, and more power is supplied by zero emission wind power, the larger remaining carbon budget is used by non-CCS NGCC plants for load following, enabling more steady generation from CCS plants. Second, the role of thermal power stations as reserve providers means that some CCS units ranking lowest in the merit order list (outperformed on operational costs basis only by nuclear plants, of all thermal power stations) never get constrained off the grid and instead operate continuously at minimum stable load at low net demand levels to provide sufficient upwards reserve. Given that there are fewer CCS plants deployed in the 45GW wind capacity scenario than in other wind

scenarios with larger CCS fleets, this role as a reserve provider can apply to a large share of them at the same time, the consequence being a steadier CO_2 flow.

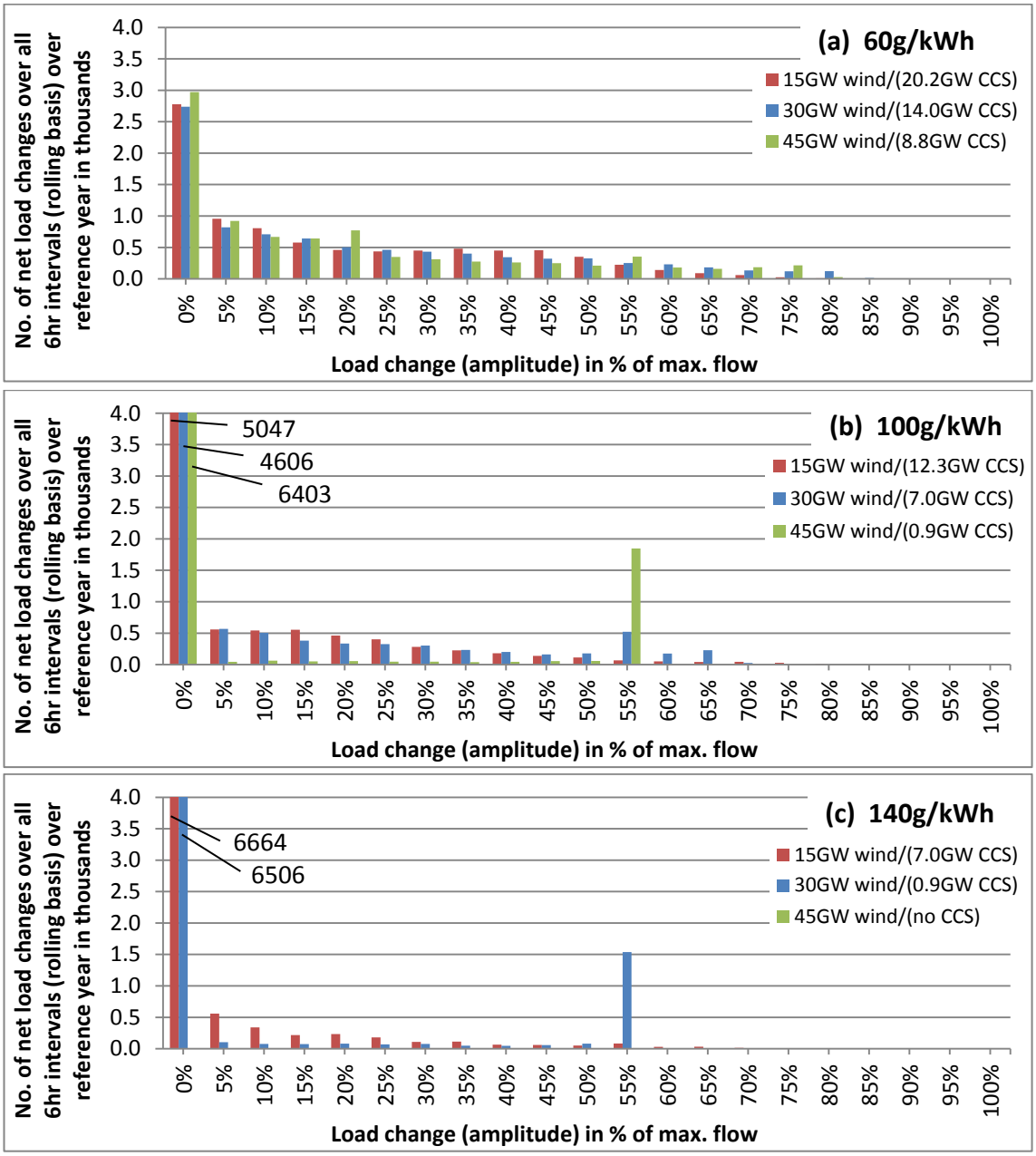

Figure 3.8: Number and relative size of net changes in CO_2 collectively captured by CCS power stations over 6hrs periods (rolling basis) over base year for 15GW (red), 30GW (blue), 45GW (green) wind capacity in 60g/kWh (a), 100g/kWh (b), and 140g/kWh (c) CO_2 emission intensity scenario, for 'medium' wind speeds.*

*For illustrative reasons some columns were cut off at 4000. The sum of all columns in each respective scenario equals approx. 8760 as a consequence of how graphs were calculated (rolling basis over year).

**Note that different numbers of CCS plants are necessary to reach emission intensity targets in respective scenarios.

Similarly, it can be seen in Figure 3.8, that two scenarios (100g/kWh emission intensity and 45GW of installed wind power; 140g/kWh emission intensity and 30GW of installed wind

power) show a spike at a load change amplitude of 55% of nominal flow. This load change amplitude corresponds to ramping of the CCS plants between full load and minimum load (and vice-versa). The spikes occur due to the small size of the CCS fleets in the respective scenarios: the net demand range in which the small CCS fleets can load follow at their given position in the merit order, leading to load change amplitudes other than 0% and 55%, is very narrow and reached only infrequently. Therefore, whenever net demand fluctuations require CCS plants in the respective scenarios to load follow, they are most likely to collectively ramp between full and minimum load (where they are likely to remain for reserve purposes as long as net demand is low). This effect explains why scenarios with high wind penetrations and a very small CCS fleet tend to lead to more extreme feed flow-rate fluctuations (i.e. either no change or very large relative change in flows) to CO_2 T&S systems.

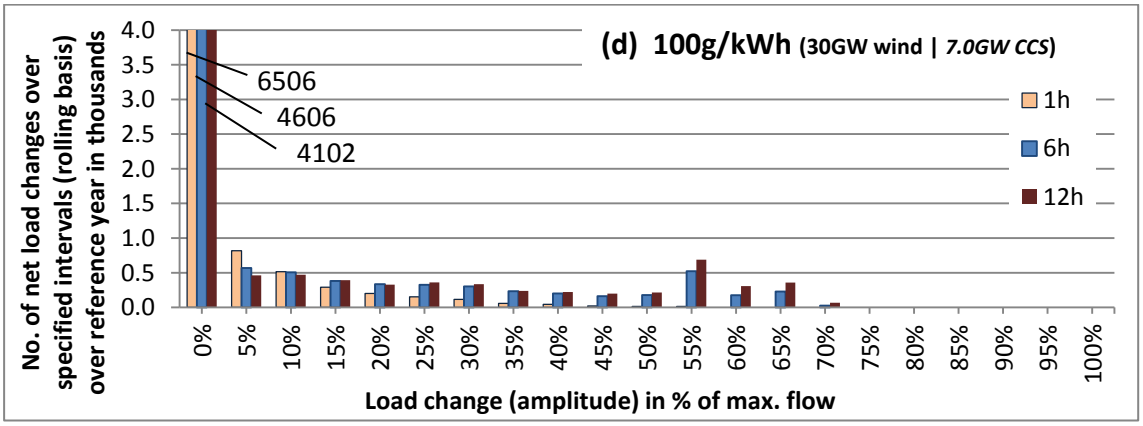

Figure 3.9: Number and relative size of net changes in CO_2 captured by CCS power stations in base case ('medium' wind speed scenario, 30GW wind, 100g/kWh) over time periods of 1hr (beige), 6hrs (blue) and 12hrs (dark red) (rolling basis over year) (d).

*For illustrative reasons some columns were cut off at 4000. The sum of all columns in each respective scenario equals approx. 8760 as a consequence of how graphs were calculated (rolling basis over year).

**Note that different numbers of CCS plants are necessary to reach emission intensity targets in respective scenarios.

Figure 3.9 illustrates that load change amplitudes generally increase when calculated over longer time intervals. The pattern and load change levels within this sensitivity case show that the amplitudes presented in Figure 3.8 are not exceptionally high. Load change amplitudes and frequencies calculated over 6hrs time periods are, therefore, not an effect of atypically high load swings over quarterly day periods, given similarly shaped daily demand time profiles, but instead fit into the wider trend.

Table 3.9: Amplitudes (in % of nominal flow) and frequencies of net flow rate changes over 6hrs periods (rolling basis over year) in % of the total number of net flow rate changes over the year, for respective scenarios.

Rel. flow change (Amplitude)	0% -5%			>30%			>50%		
Scenario	15GW	30GW	45GW	15GW	30GW	45GW	15GW	30GW	45GW
60g/kWh	37.6%	36.3%	42.4%	28.9%	30.4%	25.9%	8.2%	13.8%	14.1%
100g/kWh	61.2%	55.2%	73.4%	11.8%	21.3%	23.7%	3.3%	11.9%	21.4%
140g/kWh	79.8%	74.9%	No CCS	6.0%	20.6%	No CCS	2.1%	18.1%	No CCS

Overall, Table 3.9, Figure 3.8, and Figure 3.9 show that load changes greater than 30% or 50% over time periods of 6hrs are no exceptions, but happen on a regular basis in 21% and 12% of all considered 6hrs load changes in the base case, respectively. Future CO_2 T&S networks should be designed to cope with the resulting variable feed-flows. Although the results were calculated for the example case study of the GB electricity system, qualitatively the results are expected to hold true for other low carbon energy systems with large contributions of intermittent, as well as significant contributions from nuclear power.

3.6.4.2. Variations in average CO_2 flow over two consecutive periods

While short term 'net' variations can dampen out and be absorbed over the length of the pipeline system, particularly when active flow balancing is performed by manipulating the pressure levels and densities in the pipeline (i.e. linepacking), longer term variations in CO_2 flow averaged over the course of several hours will have a directly associated, although time-delayed, impact on downstream CO_2 injection profiles. Representative for other emission intensity scenarios, Figure 3.10 shows the frequencies and amplitudes of the variations between the average amount of CO_2 captured over two consecutive time intervals of 6hrs (again on a rolling basis over the year), for the respective core scenarios. The average flow rate change amplitudes were calculated according to equation (3), and stacked according to frequency and size along the x-axis. Adding up the size of the columns for the respective scenarios would consequently result in 8749.

$$\overline{A_t} = \frac{\left|\frac{1}{6}[F_t + F_{t+1} + \cdots + F_{t+5}] - \frac{1}{6}[F_{t-1} + F_{t-2} + \cdots + F_{t-6}]\right|}{F_{nominal}} \qquad (3)$$

$$t \in Z\,[7 \ldots 8755]$$

Where $\overline{A_t}$ *is average flow rate change amplitude at hour t*

F_t *is flow rate at time t*

F_{t+1} *is flow rate at time t+1*

F_{t-1} *is flow rate at time t-1*

$F_{nominal}$ *is nominal flow rate in respective UCED scenario (see also max. flow in respective scenarios in in Table 3.7).*

Table 3.10 summarises how many of the 8749 average load changes have an amplitude of 0-5%, >30%, and >50% of nominal flow in the respective scenarios.

Whilst the 'net variability' analysis in section 3.6.4.1 can be seen as a conservative analysis of the flow changes that can be expected at the wellhead if there is zero flow buffering capacity available in the CO_2 T&S network, the 'average flow variability' analysis in this section can be seen as a more representative analysis demonstrating flow changes that can be expected at the injection well level if there is some level of flow balancing capacity available in the CO_2 T&S network.

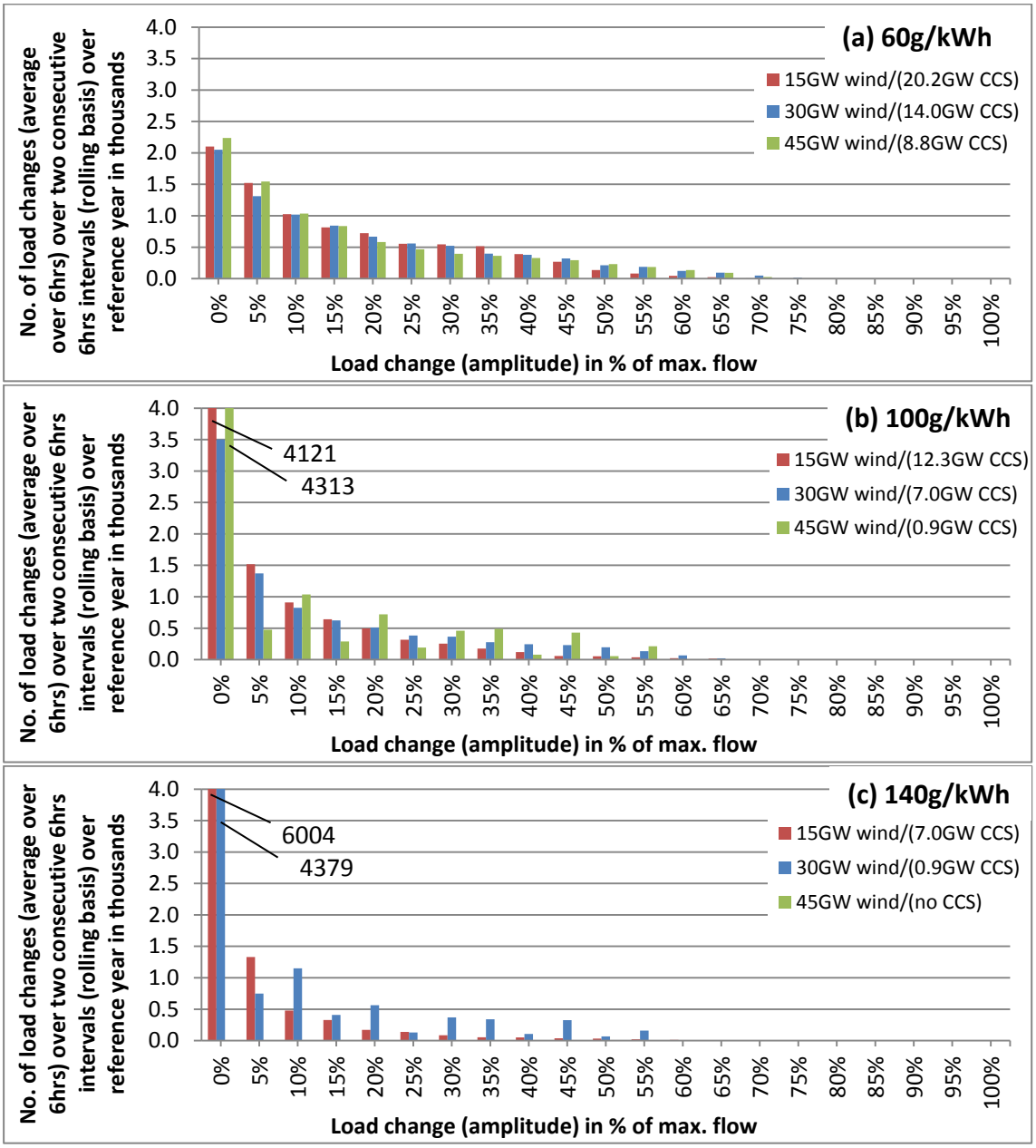

Figure 3.10: Number and relative size of net changes in average amount of CO_2 collectively captured by CCS power stations over 6hrs periods (rolling basis) over base year for 15GW (red), 30GW (blue), 45GW (green) wind capacity in 60g/kWh (a), 100g/kWh (b), and 140g/kWh (c) CO_2 emission intensity scenario, for 'medium' wind speeds.*

*For illustrative reasons some columns were cut off at 4000. The sum of all columns in each respective scenario equals approx. 8760 as a consequence of how graphs were calculated (rolling basis over year).

**Note that different numbers of CCS plants are necessary to reach emission intensity targets in respective scenarios.

A similar trend can be observed in Figure 3.10 as in Figure 3.8 and Figure 3.9, with the frequency of the load changes decreasing at higher amplitudes. Most notably it can be seen that the average load changes are less extreme compared to the net load changes in section 3.6.4.1. However, even when assessing the CO_2 flow changes averaged over two consecutive 6hrs time blocks the variability remains substantial.

This indicates that flow rate variations are often on the basis of fluctuation cycles that extend over more than 2x6=12hrs, and that are likely heavily influenced by a common daily demand profile (as indicated also by two shifting of CCS plants in Figure 3.3). This would in turn mean that it can be harder to balance the flow fluctuations, as more balancing capacity is needed to balance flows over longer time scales.

Overall, the modelling presented in this section suggests that injection wells in future CO_2 T&S networks will likely be confronted with frequent and irregular fluctuations in CO_2 feed flow rates. The extent of these, however, is subject to the availability and effectiveness of balancing options, such as line-packing.

Table 3.10: Amplitudes (in % of nominal flow) and frequencies of average flow rate changes over two consecutive 6hrs time blocks (rolling basis over year), in % of the total number of average changes over the year, for respective scenarios.

Rel. flow change (Amplitude)	0-5%			>30%			>40%		
Scenario	15GW	30GW	45GW	15GW	30GW	45GW	15GW	30GW	45GW
60g/kWh	33.2%	31.6%	35.0%	19.7%	23.1%	21.3%	8.5%	13.7%	13.0%
100g/kWh	59.1%	49.6%	51.5%	6.9%	15.3%	14.8%	2.9%	8.8%	8.4%
140g/kWh	78.5%	54.6%	No CCS	2.9%	12.1%	No CCS	1.5%	6.9%	No CCS

3.6.5. Low Flow Period Analysis

A particular concern for operators of CO_2 T&S networks are periods of low inflows into the system – see also Chapter 2, Shell (2015a), or Spitz et al. (2017). Under certain injection and reservoir conditions this can lead to two-phase flow in the injection wells which over time can degrade their integrity (see Chapter 2). This can, for example, happen at reduced flow rates when the decreased or missing backpressure from injection leads to lower wellhead pressures. Particularly injection into depleted oil and gas reservoirs is known to promote two-phase flow due to the low reservoir pressures (Pale Blue Dot Energy 2016). However, also injection into saline aquifers at low flow can lead to two-phase flow (Capture Power Ltd. 2015a). In the context of CCS in the UK, ETI (2014) suggests that around 43% of the de-risked storage capacity exist in the form of DOGRs, with the remainder existing in the form of saline aquifers. The portfolio of storage sites selected in Summit Power (2017) in a study exploring cost effective T&S network options for the East Coast of the UK consists of DOGR and saline aquifers with a split of around 62%/38%. Since periods of low flow are problematic for maintaining the integrity of injection wells and reservoirs their frequency and durations are explicitly analysed and characterised in the following.

Below which relative flow rate two-phase flow prevails is highly reservoir and injection site specific (Sanchez Fernandez et al. 2016a). For example, at the Peterhead CCS demonstration project in the UK it was predicted that flashing would occur if flows dropped below 60% of design flow (Shell 2015c; Goldeneye storage reservoir, depleted gas field). In contrast, for injection wells at the White Rose demonstration project in the UK it was estimated that flashing would only be a problem in the early phase of injection, and only at low flow rates (e.g. below 10%) and purities (Capture Power Ltd. 2015a; Endurance storage site, saline aquifer).

Periods of low flow (in the following referred to Low Flow Periods - LFPs) in this section are defined as times in which the flow of CO_2 captured collectively by all PCC plants in the respective UCED scenario falls under 50%, 30% or 10% of the nominal flow. For an overview of the nominal CO_2 flow rates in the respective UCED scenarios the reader is referred back to Table 3.7 in section 3.6.1. The broad range of numbers considered reflects the large variation and uncertainty surrounding the actual level of relative flow rates at which two-phase flow will occur. The exact number is not only highly reservoir and injection site specific, but also changes over time as the reservoirs are filled up (Capture Power Ltd. 2015a). The frequency and the time-durations of all LFPs in the individual core UCED scenarios are plotted in Figure 3.11. Table 3.11-Table 3.13 quantify the cumulative number of LFPs in the core scenarios lasting longer than Xhrs.

The analysis presented in Figure 3.11 and Table 3.11-Table 3.13 shows that in general the frequency and duration of LFPs increases with wind deployment levels, and at lower average emission intensity targets.

At 15GW of installed wind capacity up to 170 and 43 LFPs can be observed, respectively, in the reference year when defined as periods of flow below 50% and 30% of nominal flow. No periods with CO_2 inflows into the T&S system below 10% of nominal exist. This is consistent with the analysis of the Flow Duration Curves performed in section 3.6.3. As explained in the previous section the reason for this is the minimum thermal generation constraint of 15GW of the electricity system model (to ensure adequate amounts of inertia), as well as the requirement to provide sufficient amounts of spinning reserve that prevents CCS plants ranked highest in the merit order from shutting down and producing no CO_2 flow. At lower emission intensities, i.e. when CCS fleets get larger, the frequency and duration of LFPs generally increases. This is an effect of the increased nominal CO_2 flow level in lower emission intensity scenarios combined with the fact that a larger fraction of the CCS fleet needs to load follow. As a consequence low relative flow levels are reached more frequently. With more than 97% a large majority of the predicted LFPs across all 15GW wind deployment scenarios endure, however, only for less than 10hrs. This is an important finding since it implies that when CO_2 flow balancing capacity is available to bridge LFPs with durations of up to 10hrs (e.g. via line-packing or solvent storage, see Chapters 4-7 of this thesis) a large majority of low flow periods at the injection level could potentially be avoided, minimising possible damage to wells and storage sites.

At medium installed wind capacity levels (30GW) the number of LFPs significantly increases, particularly at high emission intensities (140g/kWh) where up to 231 LFPs can be observed over the examined reference year. At low emission intensities (60g/kWh) the number of LFPs when defined as periods with flows below 30% of nominal flow increases strongly to 143 - compared to 43 with 15GW of wind capacity installed. Overall, the duration of more than 87% of the observed LFPs across all 30GW installed wind capacity scenarios stays below 10hrs. Three LFPs exist across these scenarios that last for more than 40hrs. This can be traced back to extended periods of low net demand levels during the summer period.

At high installed wind capacities (45GW) LFPs are getting more frequent with up to 263 and 191 of these events existing, respectively, in the reference year when defined as periods of flow below 50% and 30% of nominal flow. To a large extent the increase is due to the occurrence of a larger number of relatively long LFPs extending over more than 10hrs. At 100g/kWh emission intensity, yet, there are no periods with flow dropping below 30% of the nominal rate. This is an effect of the single available CCS plant ramping exclusively between full and minimum load, exporting a minimum of 56% of its nominal flow at all times (when operating at minimum load at 40% electrical output). Due to its high position in the merit order this CCS plant does not shut down, for reasons explained in section 3.6.3. In contrast, at 60g/kWh emission intensity there are significantly more LFPs with a duration of 3-8hrs, when defined as periods with flow below 30% of nominal flow than when defined as periods of flow below 50% of nominal flow. Although this can seem counterintuitive at first this is a consequence of extended periods of flow below 50% of maximum flow being counted multiple times as shorter LFPs when LFPs are defined as <30% of nominal flow. This can happen, for example, when flow levels are persistently below 50% of nominal flow, however, alternate in between below and above 30% of maximum flow. In the low and medium emission intensity scenarios (i.e. 60g/kWh and 100g/kWh, respectively) flow levels remain below 50% of nominal flow for over 40hours for 13 times over the year. These extremely long events of low flow coincide with periods of low demand/high wind speeds both in the summer and the winter. Finally, the trend holds that a majority of the LFPs observed across all 45GW wind capacity scenarios last for less than 10hrs - more than 66%.

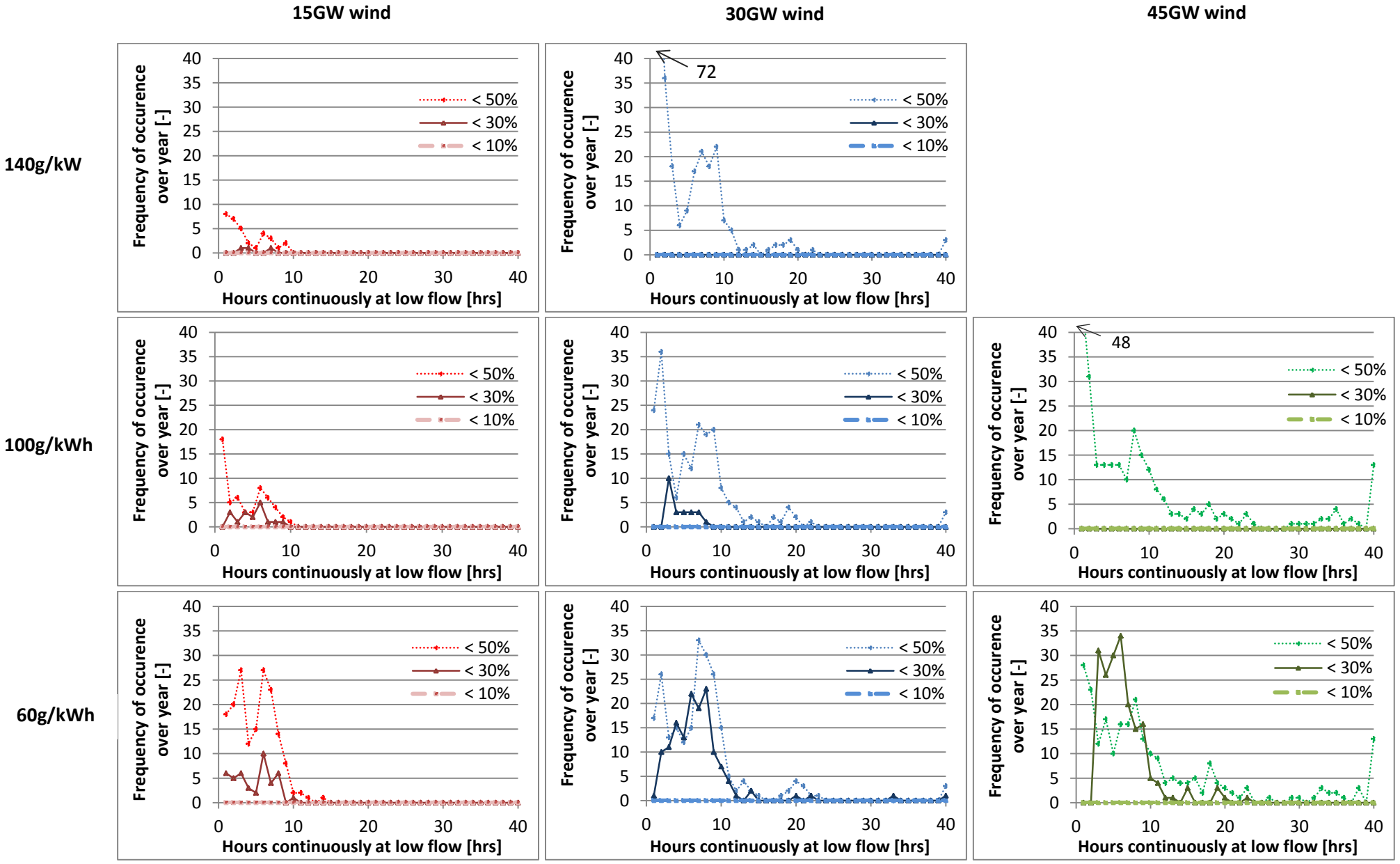

Figure 3.11: Frequency and duration of low flow periods for 140g/kWh (top), 100g/kWh (middle), 60g/kWh (bottom) emission intensity scenario with 15GW (red), 30GW (blue) and 45GW (green) of installed wind capacity. For different definitions of low flow periods see legends.*

*Note that different numbers of CCS plants are necessary to reach 100g/kWh emission intensity.

Overall, the analysis in this section has shown that the number and duration of LFPs generally increases with higher wind deployment, and in lower emission intensity scenarios. Across all core modelled scenarios the large majority of LFPs endure only less than 10hrs. If CO_2 flow balancing capacity is available upstream of injection wells to bridge periods of 10hrs this could potentially greatly reduce the number of periods of low flow through the wells and any possible associated damages.

Table 3.11: Cumulative number of Low Flow Periods (LFPs) extending over more than Xhrs across all core modelled scenarios. LFPs defined as periods of flow lower than 50% of nominal flow.

	>0hrs			>5hrs			>10hrs			>25hrs			>40hrs		
Scenario	15GW	30GW	45GW	15GW	30GW	45GW	15GW	30GW	45GW	15GW	30GW	45GW	15GW	30GW	45GW
60g/kWh	170	231	248	78	148	158	4	29	82	0	3	28	0	3	13
100g/kWh	56	202	263	21	106	145	0	26	75	0	3	29	0	3	13
140g/kWh	33	248	no CCS	10	107	no CCS	0	22	no CCS	0	3	no CCS	0	3	no CCS

Table 3.12: Cumulative number of Low Flow Periods (LFPs) extending over more than Xhrs across all core modelled scenarios. LFPs defined as periods of flow lower than 30% of nominal flow.

	>0hrs			>5hrs			>10hrs			>25hrs			>40hrs		
Scenario	15GW	30GW	45GW	15GW	30GW	45GW	15GW	30GW	45GW	15GW	30GW	45GW	15GW	30GW	45GW
60g/kWh	43	143	191	21	92	104	0	11	14	0	2	0	0	1	0
100g/kWh	17	23	0	8	7	0	0	0	0	0	0	0	0	0	0
140g/kWh	3	0	no CCS	1	0	no CCS	0	0	no CCS	0	0	no CCS	0	0	no CCS

Table 3.13: Cumulative number of Low Flow Periods (LFPs) extending over more than Xhrs across all core modelled scenarios. LFPs defined as periods of flow lower than 10% of nominal flow.

	>0hrs			>5hrs			>10hrs			>25hrs			>40hrs		
Scenario	15GW	30GW	45GW	15GW	30GW	45GW	15GW	30GW	45GW	15GW	30GW	45GW	15GW	30GW	45GW
60g/kWh	0	0	0	0	0	0	0	0	0	0	0	0	0	0	0
100g/kWh	0	0	0	0	0	0	0	0	0	0	0	0	0	0	0
140g/kWh	0	0	no CCS	0	0	no CCS	0	0	no CCS	0	0	no CCS	0	0	no CCS

3.6.6. Start-ups and shut-downs

Figure 3.12 displays the average number of start-ups carried out by CCS plants in all nine core scenarios, respectively, over the reference year. Start-ups would directly lead to large step changes in the amount of CO_2 that is being fed into the downstream T&S system. The columns are stacked with different colours according to how long the plants had been shut-off before start-up (in hours).

The number of start-ups per CCS plant decreases persistently in the higher emission intensity scenarios. This is intuitive, as the higher the allowed emission intensity, the lower the number of CCS plants required. These CCS plants would be stacked up next to each other on the low side of the merit order (due to low operational costs including for CO_2 emissions; just next to nuclear plants), and thus they are less likely to shut-down due to their ability to provide power at a very competitive (low) operational cost. They are also less likely to shut-down for reserve purposes, being the only gas fired power stations

online. In contrast, in scenarios with many CCS plants, even if they are stacked up on the low end, some of them are comparatively high in the merit order, which requires them to load follow and start-up/shut-down extensively.

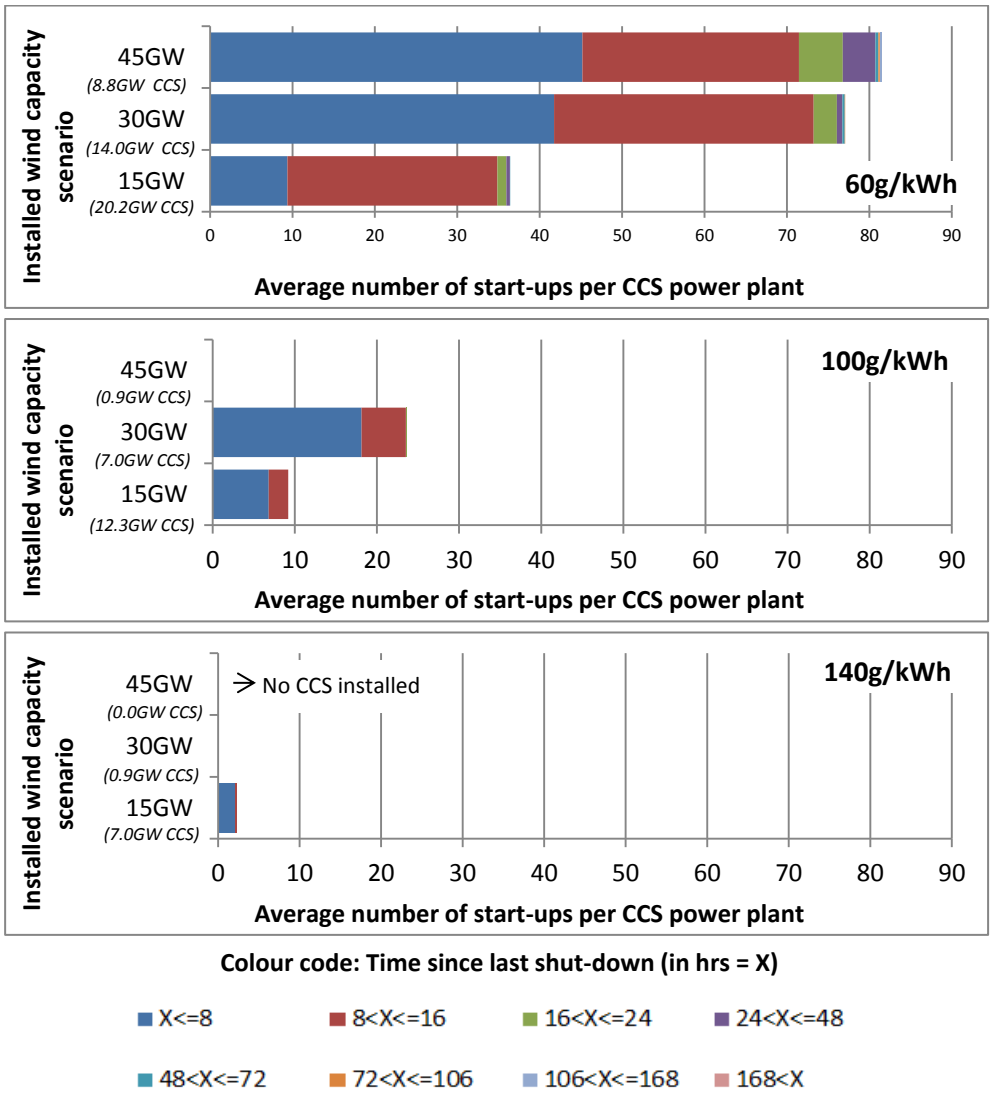

Figure 3.12: Number of average start-ups per CCS power plant in 60g/kWh (top), 100g/kWh (middle) and 140g/kWh (bottom) CO_2 emission intensity scenarios for different installed wind capacities in the base year. Columns are stacked in different colours to indicate time since last shut-down (see colour code above).*

*Note that number of CCS plants is different between the cases.

This reasoning also explains, in the medium emission intensity scenario, the relatively high start-ups in the 30GW installed wind capacity case compared to the 45GW case. While in the 30GW case there are around 9 CCS plants in the capacity mix that run according to a net demand profile that is heavily influenced by the variable power output of the available wind generation capacity, the only CCS plant implemented in the 45GW case is hardly ever constrained off the grid due to its role in providing reserve. The lower penetration of wind power in the 15GW case leads to less variability of the net demand curve. Together with

the relatively high number of CCS plants in this scenario, this leads to a lower average number of start-ups per CCS plant compared to the 30GW case.

The high number of CCS plants across both the low and intermediate merit order range in the low emission intensity scenarios, across all wind deployment cases, makes the number of start-ups more dependent on the variability of the net demand curve. As this variability is in turn driven by the penetration of wind power generation, the number of start-ups is higher in the 45GW installed wind capacity case compared to the 30GW and 15GW cases.

Overall, Figure 3.12 shows a clear trend towards increasing numbers of start-ups in scenarios with lower emission intensities, irrespective of the wind deployment scenario. An average number of start-ups between 36 and 81 in the 60g/kWh scenario indicates even significantly higher numbers for CCS power stations that are comparatively low in the merit order. Given that start-ups and shut-downs are associated with additional costs for the power plant operator (e.g. fixed start-up/shut-down costs to account for wear and tear and additional fuel consumption) this suggests that in future low-carbon energy systems dominated by variable renewable power, on/off and part load performance of CCS fossil fuel power plants may become as or even more important than the traditional performance objective of full load efficiency, requiring substantial changes to power station design. Further, this implies the requirement for future CO_2 T&S systems to be able to cope with a high number of step changes in flow when accommodating CO_2 from CCS power stations operating in low carbon electricity systems.

3.6.7. Sensitivity cases

The following subsections explore some key sensitivities of the results. Given the high number of assumptions that were made when creating and modelling the core scenarios presented over the previous sections, this section takes the analysis a step further by identifying and exploring key sensitivities and the effect these have on the results.

The key sensitivities examined in the following subsections are (i) The inclusion of solar generation in the capacity mix; (ii) Varying yearly demand and weather (i.e. wind) data; and (iii) The option for temporarily switching of the PCC capture plant at NGCC-CCS power stations to recover a large fraction of the energy penalty associated with CO_2 capture at periods of high electricity prices, an option which in the following will be referred to as ‘capture plant bypass’. Further, the influence of varying thermal efficiencies (LHV) of conventional generators, and the impact of the required levels of spinning reserve provision on CO_2 flows is examined in Appendix A1-A2.

3.6.7.1. Solar

Solar power plays an important role in the portfolio of power generation technologies available to meet climate targets across many countries. In 2017 12.9GW of solar power (PV) was installed in the UK (UK BEIS 2018b), with up to 25GW and 40GW expected for 2025 and 2050, respectively (National Grid 2017a).

Although solar power generation is more predictable than wind power generation and has lower capacity factors (Vázquez Villamor 2017), it has the potential to significantly influence the operating patterns of CCS power stations. To examine the extent to which the addition of solar power capacity to the energy system affects the variability of CO_2 flows feeding into T&S systems three core scenarios are chosen to be studied in more detail:

- The base case (30GW wind, 100g/kWh emission intensity),
- The medium wind & low emission intensity scenario (30GW wind, 60g/kWh),
- The high wind & low emission intensity scenario (45GW wind, 60g/kWh).

The rationale behind selecting the base case as well as two low emission intensity scenarios with medium and high wind deployment, is that only when GB is stringent about reaching its climate goals it will deploy both wind and solar capacity to a sufficiently high level that the availability of solar capacity can significantly impact the operating profiles of CCS power stations. The high wind deployment (45GW) and low emission intensity scenario, with maximum solar deployment (45GW in this study) serves as an upper benchmark within this study as to how the aggressive deployment of wind and solar capacity can impose variable CO_2 flows being exported by CCS power stations to the downstream T&S infrastructure.

Solar capacity is added to the outlined core scenarios in increments of 15GW from 0-45GW with the remainder of the thermal generation fleet being unchanged to simplify any subsequent comparison.

It is assumed in this study that the solar portfolio consists solely of PV. This is deemed reasonable in the UK due to the limited ability of the solar resource to generate the high temperatures required in large-scale solar thermal systems (Lew et al. 2013). The available solar power output time-series is calculated by multiplying cumulative installed capacity by hourly capacity factors developed by (Pfenninger and Staffell 2016) and based on the second version of the Modern-Era Retrospective Analysis for Research and Applications (MERRA-2). The MERRA-2 dataset provides long-term hourly observations with a spatial resolution of 50 km along with improved radiance observations compared to the previous version, MERRA-1 (Vázquez Villamor 2017). From this reanalysis dataset (Pfenninger and Staffell 2016) modelled the PV output for several years calculating hourly capacity factors. The authors applied a bias correction and validated the obtained results against empirical measurements of real PV site power outputs and national outputs provided by the UK transmission system operator National Grid. As a technology with close to zero marginal costs (Bruce 2015) solar power output is deducted similar to wind power output at any time t from gross demand (Vázquez Villamor 2017), to create the net demand profile that is

satisfied by the conventional power generation fleet under consideration of system and generator constraints. For a more detailed description of the integration of solar power generation capacity into the deployed UCED model the reader is referred to (Vázquez Villamor 2017).

As the addition of solar PV generation capacity does not contribute to the winter peak demand (National Grid 2015b) the de-rated capacity margin of the overall power generation portfolio remains constant in the respective scenarios. With more renewable capacity available in the energy system to satisfy the yearly demand profile the average CO_2 emission intensity, however, falls with increasing additional solar deployment, as indicated in Table 3.14.

Table 3.14: Reduction of average CO_2 emission intensity as a consequence of the availability of solar generation capacity.

	'Base Case' 30GW wind|100g/kWh	Medium wind & Low EI 30GW wind|60g/kWh	High Wind & Low EI 45GW wind|60g/kWh
15GW solar	-14.1%	-18.2%	-18.3%
30GW solar	-24.4%	-28.7%	-29.4%
45GW solar	-30.9%	-34.4%	-35.5%

The resulting so called 'solar scenarios' are analysed in the following according to the same metrics as established in sections 3.6.3-3.6.5.

Flow Duration Curves

Figure 3.13 shows the FDCs for all evaluated solar scenarios. It can be seen that the maximum amount of CO_2 captured in the respective scenarios remains unchanged, regardless of the amount of installed solar capacity. This is a consequence of the unchanged fleet of conventional (and CCS) generators when solar capacity is added. The main change induced by the availability of solar capacity is related to the expected undermined capacity factors of conventional generators leading to extended periods of CCS plants operating at their respective minimum load limits, producing only relatively small CO_2 flows. The yearly minimum flow level is, however, unaffected.

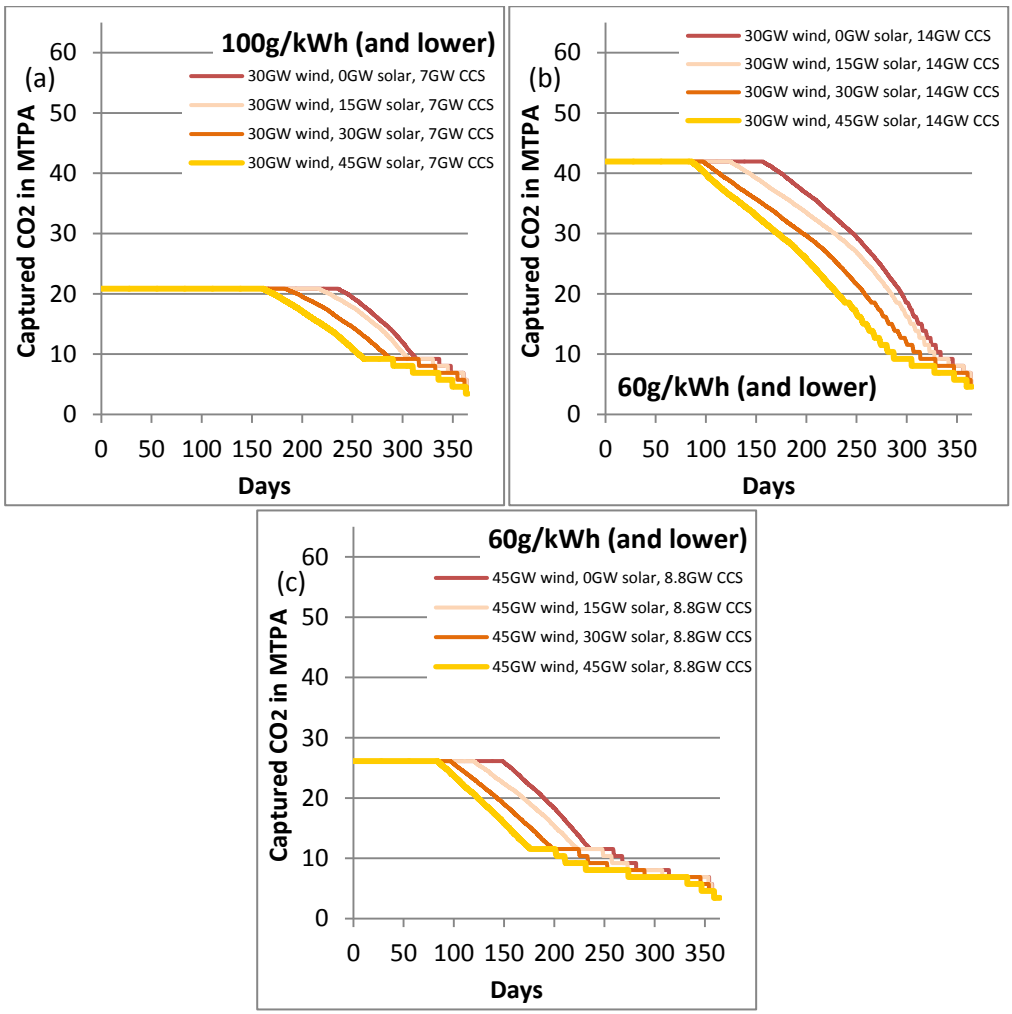

Figure 3.13: CO_2 capture duration profile for 0GW (red), 15GW (beige), 30GW (orange), 45GW (gold) installed solar capacity in 30GW installed wind|100g/kWh emission intensity scenario (a), in 30GW installed wind|60g/kWh emission intensity scenario (b), and in 45GW installed wind|60g/kWh emission intensity (c) scenario scenario, for 'medium' wind speeds.*

*Note that different numbers of CCS plants are necessary to reach emission intensity targets in respective scenarios.

Variability

Similar to section 3.6.4, Figure 3.14 illustrates the frequency and amplitudes of the net changes of CO_2 flows over 6hrs periods on a rolling basis over the base year. The chart was created following the methodology outlined in section 3.6.4.1. It can be observed that generally size and frequency of the load change amplitudes are similar when solar is added to the generation fleet (beige, orange, gold) and when it is not (red). Most notably, the frequency of zero flow changes (amplitude of 0%) decreases the more solar there is on the system. Further, flow changes generally get less extreme when solar is added to the system (with the exception of the 45GW installed solar capacity scenarios). To understand the

reason behind these effects it is helpful to reconsider the characteristics of solar power generation.

Solar generally has the effect of reducing the net demand level at times of high insolation, i.e. during times of daylight and particularly over the warmer (e.g. summer) months. The phenomenon of solar reducing net demand levels during the day at times of high insolation is referred to 'duck curve' phenomenon based on the shape of the resulting net demand curve (see also Denholm et al. 2015). Dependent on the exact interplay between demand and weather (e.g. solar insolation, hours of daylight) the phenomenon has different effects over the year, in particular as a response to the changing interplay between morning and evening demand peaks with the hours of sunlight and insolation during the day. For example, while in the winter both morning and evening demand peaks lie in the dark hours of the day, with solar capacity being unable to contribute to satisfying demand levels at all, in the summer solar kicks in during the very early stage of the morning demand peak reducing it drastically or even eliminating it at high solar deployment levels (45GW). In the spring and autumn solar is able to contribute to the morning demand peak, however, only at a later stage and not as effectively (due to lower insolation), leaving a reduced but significant net demand peak for the conventional generators to deal with. The effect of solar on the cycling requirement of CCS plants and consequently the variability of the resulting CO_2 flows is, therefore, a complex function of the interplay between supply and demand as well as the time of the year.

The reason for fewer zero flow change periods becomes obvious when considering that zero flow changes over 6hrs occur frequently at periods of high sustained net demand (i.e. during day time) when the CCS fleet operates at nominal load for an extended periods of time at nominal load. A significant deployment of solar generation interrupts many of these periods of sustained high power output of CCS plants by displacing them during periods of high solar insolation.

The generally reduced number of flow changes with very high amplitudes (except in the base case with 45GW of solar power capacity available), particularly in the low emission intensity scenarios, can be traced back to the undermined capacity factors of CCS power stations with the availability of solar capacity. Operating overall at a reduced load level, any load change from a medium load level to the upper or lower output limit is smaller than if the load change had taken place between the limits directly. This effect is particularly pronounced in low emission intensity scenarios that are characterised by large CCS fleets with generally lower capacity factors compared to the medium and high emission intensity cases, as can be seen in Figure 3.13. The effect is less pronounced in the illustrated medium emission intensity scenario.

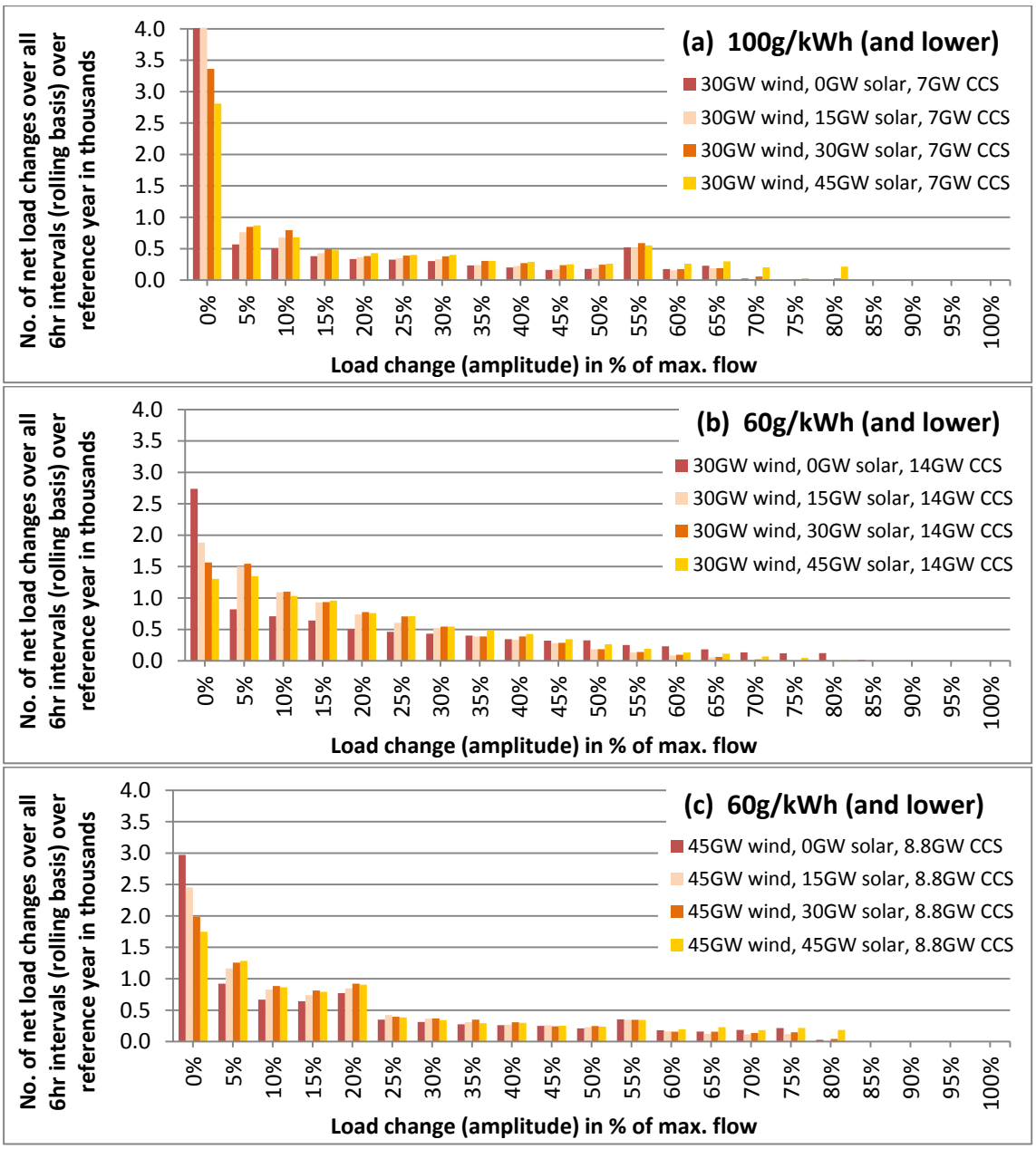

Figure 3.14: Number and relative size of net changes in CO_2 collectively captured by CCS power stations over 6hrs periods (rolling basis) over base year for 0GW (red), 15GW (beige), 30GW (orange), 45GW (gold) installed solar capacity in 30GW installed wind|100g/kWh emission intensity scenario (a), in 30GW installed wind|60g/kWh emission intensity scenario (b), and in 45GW installed wind|60g/kWh emission intensity scenario (c), for 'medium' wind speeds.*

*For illustrative reasons some columns were cut off at 4000. The sum of all columns in each respective scenario equals approx. 8760 as a consequence of how graphs were calculated (rolling basis over year).

**Note that different numbers of CCS plants are necessary to reach emission intensity targets in respective scenarios.

In the medium emission intensity case with 45GW of solar capacity installed (Figure 3.14a), in contrast, a significant number of load changes can be observed with very high amplitudes (e.g. >65%). Whilst the above explanations are still valid the increase number of load changes with extreme amplitudes can be traced back to the spring and autumn periods when a very high solar output kicks in approximately at the morning peak and depresses

net demand to very low levels until late afternoon or even early evening when the evening demand peak sets in. In this way there are specific time periods of the year when very high levels of solar deployment (e.g. 45GW) lead in fact to a higher volatility of net demand, with more frequent load changes at extreme amplitudes.

Overall, however, the frequency and amplitudes of load changes stay comparable across the evaluated solar deployment cases.

Low Flow Periods

Figure 3.15 presents a LFP analysis similar to the one carried out in section 3.6.5, however, with 30GW of solar added to the scenarios as a sensitivity case. The graphs show that the frequency and duration of LFPs are similar when solar is present in the capacity mix and when it is not. Across all cases there is a slight increase in the number of LFPs that last around 3-8hrs and 15-20hrs. Nevertheless, consistent with previous analysis the large majority of LFPs last for less than 10hrs. Henceforth, the conclusion holds that with flow balancing capacity of up to 10hrs upstream of the injection wells the number of times they need to operate at low flow can be greatly reduced.

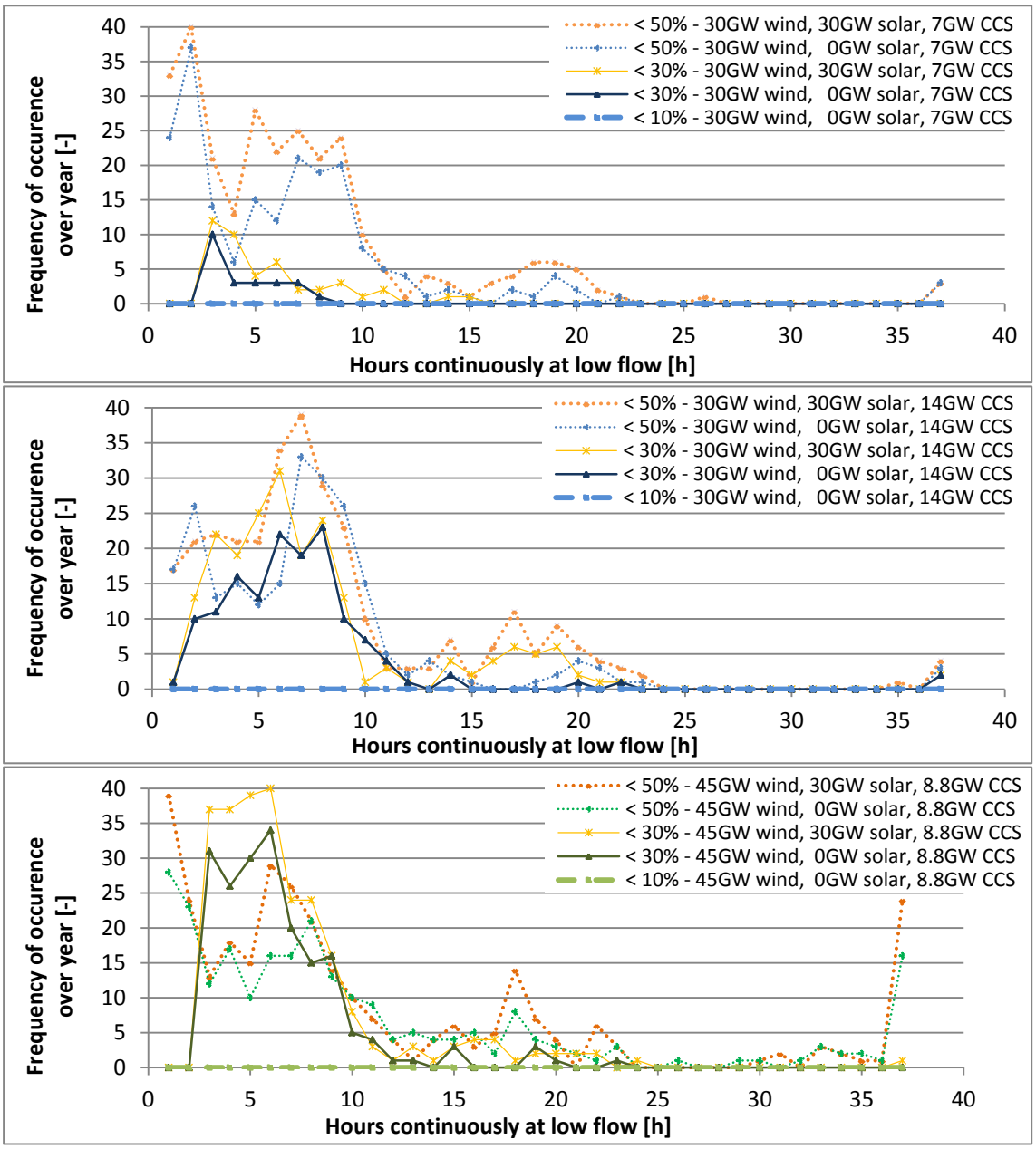

Figure 3.15: Frequency and duration of low flow periods for varying installed solar capacities and scenarios with 30GW installed wind|100g/kWh emission intensity scenario (a), in 30GW installed wind|60g/kWh emission intensity scenario (b), and in 45GW installed wind|60g/kWh emission intensity scenario (c). For installed solar capacity and different definitions of Low Flow Periods see legend.*

*Note that different numbers of CCS plants are necessary to reach 100g/kWh emission intensity.

3.6.7.2. Variability in high and low wind year

The previous analysis has been carried out with demand and weather data from a 'medium' wind speed reference year. This section expands the analysis by examining how the results

vary over different wind speed scenarios (i.e. years), and hence, how applicable the previously discussed findings are for different years. Similarly to previous sections the analysis comprises the comparison of FDCs, variability of CO_2 flows, and LFPs. Three different wind speed scenarios with demand and weather data from the years 2010, 2004 and 2008 are analysed representing a 'low', 'medium', and 'high' wind year as discussed in section 3.4.

Two core scenarios have been chosen for examination of the effect of different wind speed scenarios on operating patterns of CCS stations:

- The base case (30GW wind, 100g/kWh emission intensity),
- The high wind deployment & low emission intensity scenario (45GW wind, 60g/kWh).

The scenarios have been chosen to represent an 'average' or 'most like' reference case (base case), as well as more extreme case in terms of VRE deployment and emission intensity target.

Flow Duration Curves

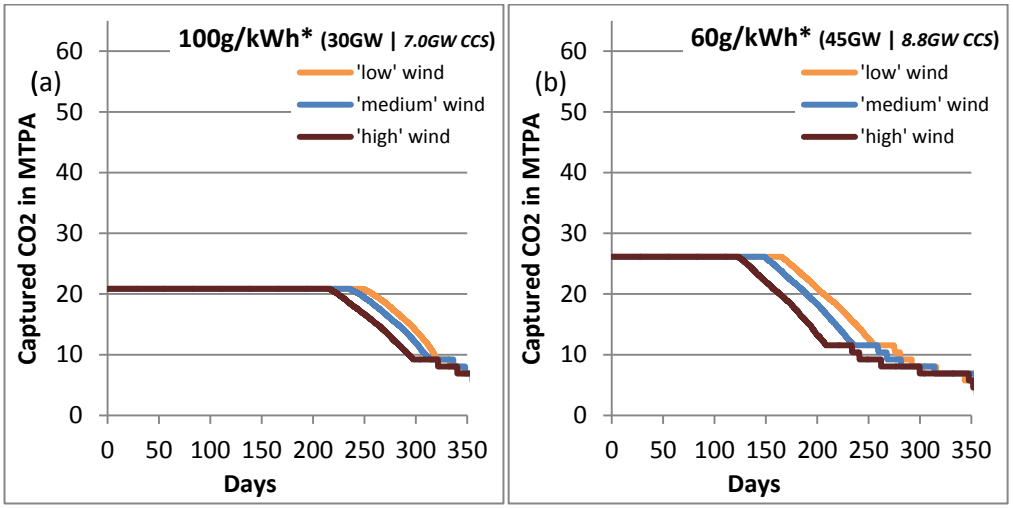

Figure 3.16: CO_2 capture duration profile for the 'low' (orange), 'medium' (blue), and 'high' (brown) wind speed scenario, in 30GW installed wind capacity and 100g/kWh emission intensity scenario (a), and in 45GW installed wind capacity and 60g/kWh emission intensity scenario (b).

*Note that emission intensity in low and high wind speed year deviates from 100g/kWh and 60g/kWh, respectively, as indicated in below paragraph.

Looking at Figure 3.16 it shows that FDCs look similar across the investigated wind speed scenarios. While CCS power stations produce less electricity and hence CO_2 in the high wind speed scenarios (brown curves) due to the high availability of wind power, they need to compensate the gap in power production in the low wind speed scenarios (orange curves). This effect also leads to an emission intensity that deviates by -6.8% and +12.8% compared

to the base case (i.e. left diagram, blue curve) in the high and low wind speed scenarios, respectively, as the power generation fleet remains unchanged. The deviation of average emission intensity accounts for -9.0% and +22.2% in the high installed wind capacity and low emission intensity scenario (i.e. right diagram). Similar to what was observed in section 3.6.3 CCS power stations never collectively shut in across all scenarios. The minimum CO_2 flows remains constant over the considered wind speed scenarios.

Variability

Figure 3.17 illustrates the variability of CO_2 flows across the considered wind speed scenarios. The chart was created following the methodology outlined in section 3.6.4.1. Overall, the figure shows that frequency and amplitudes of load changes are very similar across the examined years. The occurrence of high or low wind years, therefore, does not necessarily have the effect of increasing or reducing the variability of flows feeding into CO_2 T&S networks. The frequency of zero flow change events is, however, reduced in the examined years with higher wind resource availability.

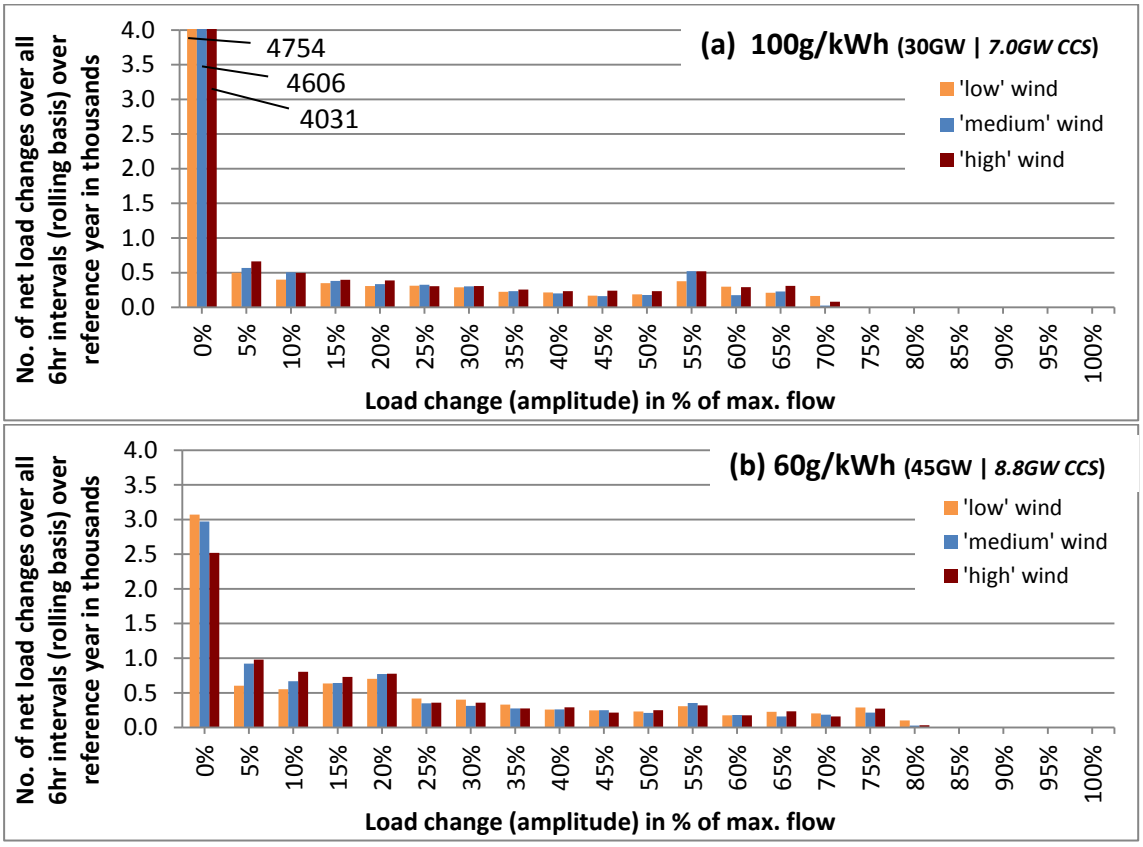

Figure 3.17: Number and relative size of net changes in CO_2 captured by CCS power stations for the 'low' (orange), 'medium' (blue), and 'high' (brown) wind speed scenario for 30GW installed wind capacity and 100g/kWh emission intensity (a) and for 45GW installed wind capacity and 60g/kWh emission intensity (b) (rolling basis over year).

*For illustrative reasons some columns were cut off at 4000. The sum of all columns in each respective scenario equals approx. 8760 as a consequence of how graphs were calculated (rolling basis over year).

**Note that emission intensity in low and high wind speed year deviates from 100g/kWh and 60g/kWh, respectively, as indicated in previous subsection.

Low Flow Periods

Figure 3.18 displays the number and duration of LFPs over the respective wind speed scenarios. The top row of diagrams analyses the effects of varying wind speed scenarios for the base case, whilst the lower row analyses the respective effects in the high installed wind capacity (45GW) and low emission intensity scenario (60g/kWh). The analysis follows the methodology outlined in section 3.6.5. The general trend is that the duration and frequency of occurrence of LFPs increases with increasing wind intensities. However, the trend is neither very strong nor consistent. As such, the number of LFPs defined as flows smaller than 30% of the nominal rate is slightly lower in the 'medium wind' case than in the 'low wind' case. The increase in the number and duration of LFPs from the 'medium wind' case to the 'high wind' case is somewhat more pronounced. The general conclusion that a majority of LFPs last for less than 10hrs holds true across all investigated wind speed scenarios.

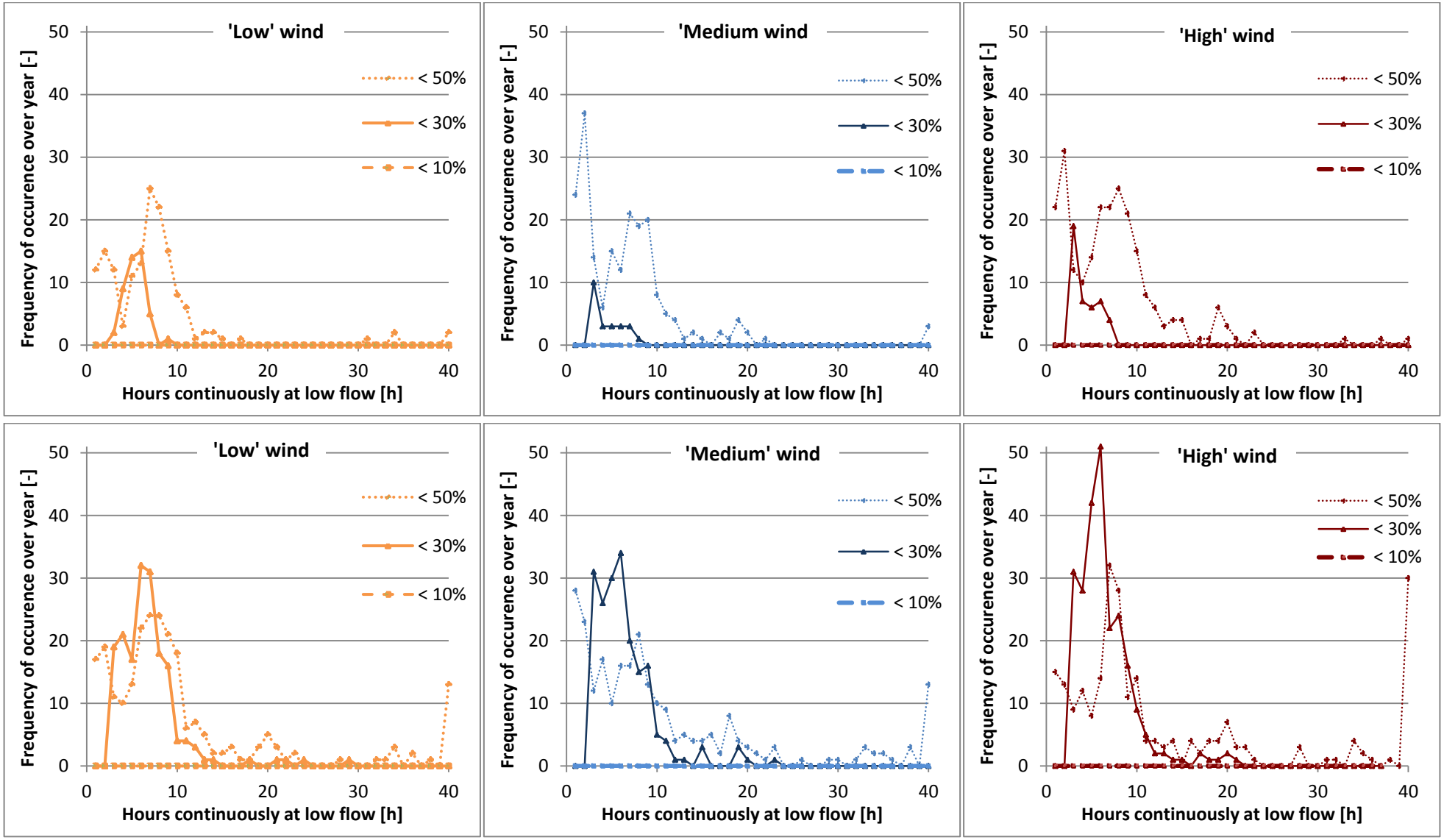

Figure 3.18: Frequency and duration of low flow periods for 'low' (orange), 'medium' (blue), and 'high' (brown) wind speeds for 30GW installed wind capacity and 100g/kWh emission intensity (top) and for 45GW installed wind capacity and 60g/kWh emission intensity (bottom). For different definitions of low flow periods see legends.*

*Note that emission intensity in low and high wind speed year deviates from 100g/kWh and 60g/kWh, respectively, as indicated in previous paragraph.

3.6.7.3. Capture plant bypass

Figure 3.19 compares FDCs for constant capture with FDCs when flexible capture operation is allowed. Flexible capture here refers to the operation of the CCS power station when the CO_2 capture unit is switched off and the base power plant recovers all but a small fraction of the energy consumption of the capture plant (i.e. 'bypass') in order to increase its power output when this is economically favourable (i.e. electricity prices are high enough to offset the increased costs for emitting more CO_2). There is ongoing policy uncertainty regarding the structure of market incentives to encourage the deployment of CCS (Errey et al. 2014) and hence how this may affect the behaviour of CCS plants.

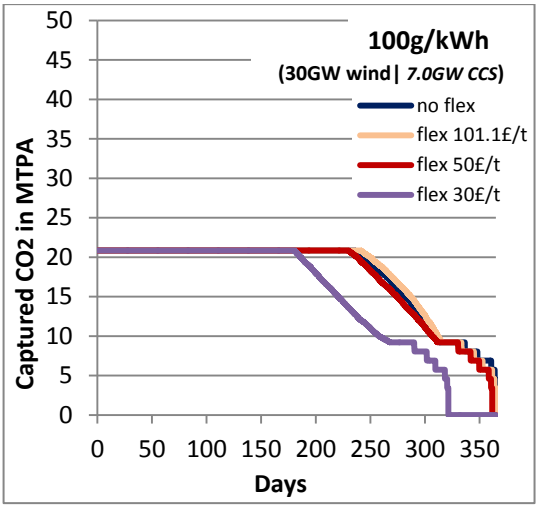

Figure 3.19: CO_2 flow duration curves for constant capture (blue) and flexible capture with carbon price of 101£/tCO_2 (beige), 50£/tCO_2 (dark red) and 30£/tCO_2 (purple) for 7.0GW of CCS capacity installed.

The blue curve in Figure 3.19 represents the base case with constant capture, while the beige, the red and the purple curves illustrate the flexible capture scenario with an identical power generation portfolio and CO_2 prices of 101.1£/tCO_2 (as projected by UK BEIS - 2017a - for 2035), £50/tCO_2, and £30/tCO_2, respectively. Due to a sufficiently high CO_2 price (making flexible capture comparatively unattractive) the blue and the beige curves resemble each other very closely, with the main difference being a slightly longer sustained operation at nominal CO_2 flow in the flexible capture scenario, that comes along with a slight decrease of the CO_2 flows produced at part-load operation, and a significantly lower minimum flow rate (0.0MPTA; for 6hrs over the year). This trade-off between marginally longer operation at nominal load and reduced output at part-load operation suggests that the flexible capture option is predominantly used for provision of spinning reserve. When the option of flexible capture is available, fast shut-downs of the capture plant can free capacity that can be used for provision of reserve (Chalmers 2010, Van der Wijk et al. 2014), as well as for avoiding start-ups of gas generators for only short periods, which is both associated with additional costs for start-up/shut-down operation and additional emissions.

This finding is confirmed by the CO_2 emission intensity dropping by 1.1g/kWh, at carbon prices of 101.1£/tCO_2, when flexible capture is allowed.

At lower future CO_2 prices flexible capture becomes economically more attractive, particularly at times of high electricity prices (Chalmers 2010, Van Peteghem and Delarue 2014). This is reflected in the shape of the corresponding (red and purple) FDCs that indicate that the CO_2 capture plants are shut off for a relatively small (red curve) and more substantial (purple curve) amount of time (approx. 82h and 1046h of 8760h of the year, respectively) producing no CO_2 when they would under constant capture operation produce the nominal amounts. Times of zero flow that usually correspond to periods of high electricity prices are likely to increase CO_2 flow variability substantially. Whilst the positive effect of an increased amount of spinning reserve offered by CCS plants in the flexible capture scenarios counterbalances the increased emissions during periods of capture plant bypass at carbon prices of 50£/tCO_2, the annual average emission intensity increases by around 6.9g/kWh when carbon prices are low (30£/tCO_2).

Overall, the sensitivity case shows that the option for capture plant bypass has the potential to increase the variability of CO_2 flows and times of zero flow significantly, but only at relatively low future carbon prices (e.g. 50£/tCO_2 or lower).

3.7. Changes in flow patterns with additional sources of CO_2

Finally, it remains to discuss in the broader context of the energy system and emission reductions how CO_2 flow variability in the T&S system can change with different types of CO_2 sources being present in the network.

In general the power sector is only of several large sectors of the economy that needs to be decarbonised (see Figure 3.20), and that is likely to feed CO_2 into T&S networks. With certain sectors of the economy being classified as 'hard to decarbonise' such as aviation and agriculture (as well as certain parts of industry) it remains to other sectors, such as buildings, transportation, power and waste, to achieve virtually a complete decarbonisation by 2050 (CCC 2016). The Committee on Climate Change (CCC 2016) predicts that if the UK's climate targets are to be met emissions of the latter sectors need to be reduced from around 288 MtCO_2 in 2015 to well below 30 MtCO_2 by 2050. Particularly heat has been identified as a crucial sector to decarbonise, contributing with around 32%, or 159MtCO_2, to total UK emissions in 2015 (UK BEIS 2018c). Figure 3.21 illustrates the importance of decarbonising heat by comparing the UK's primary energy demand in 2010 for electricity and heat, latter of which is used primarily for domestic heating (62%), non-domestic heating of buildings (21%), and process heat in industry (Chaudry et al. 2015). Efforts have consequently focused in recent years on identifying cost effective pathways to decarbonise the heat sector.

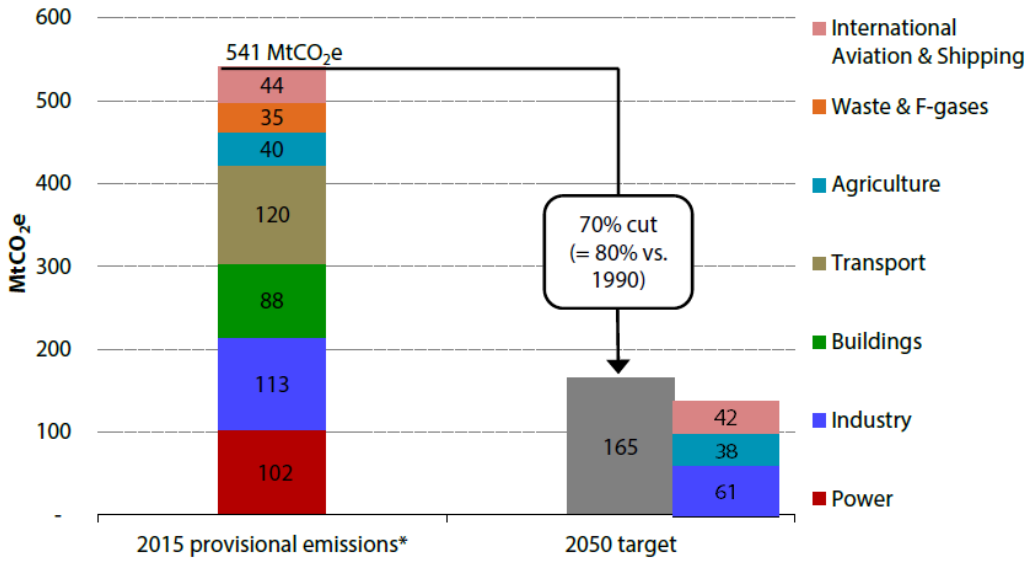

Figure 3.20: The carbon budget and 'hard-to-reduce' sectors (right) after cost effective abatement options have been taken into account. (CCC 2016).

It is by now generally acknowledged that the most cost-effective ways of decarbonising heat is either by using hydrogen as an energy vector, via electrification, or via a combination of both CCC (2016, 2018; see Figure 3.22). When choosing decarbonisation via hydrogen large amounts of this zero-carbon energy carrier need to be generated. If abundant amounts of cheap power and low carbon power were available this could be achieved via electrolysis. A more cost-effective way, however, would be to produce hydrogen from methane via Steam Methane Reforming (SMR) or Auto Thermal Reforming (ATR), with large amounts of CO_2 being produced as a by-product. In order to ensure a sustainable hydrogen based economy a large majority (e.g. 90-100%) of this produced CO_2 would need to be captured and stored via CCS. The Committee for Climate Change predicts CO_2 flows of up to 150MTPA when choosing hydrogen based decarbonisation of the heat and wider energy sector (covering transport, industry and buildings; CCC 2016). CO_2 flows captured from SMR or ATR plant would, however, likely be more stable for achieving high capacity utilisation factors of the facilities. Strbac et al. (2018) predicts in a case study investigating decarbonisation of the UK heat sector via hydrogen that installation of around 20TWh of hydrogen storage capacity would be optimal as this reduces the required hydrogen production capacity necessary for meeting peak demand by over 60% (only 103GW required instead of 260GW). Energy system costs as an effect could be cut by around £13billion/year (Strbac et al. 2018). IEAGHG (2016) suggests that the large buffering capabilities of hydrogen pipelines could "*permit the [hydrogen reforming] plants to operate steadily at an optimal rate when possible or vary rates because of internal conditions when necessary"* (p. 35, IEAGHG 2016). It is, however, unclear whether the last study considers the large seasonal fluctuations in hydrogen demand.

If electrification is chosen as the pathway for decarbonising heat enormous investments into the power generation sector can be expected. Strbac et al. (2018) suggests that

decarbonising the heat and electricity sector via electrification leaving residual emissions of only 30Mt requires a cost effective power generation fleet with a generation capacity of 460GW. This future fleet, the authors propose, would be strongly dominated by renewable capacity, with around 145GW of PV power and 110GW of wind power. Dependent on the size of the CCS fleet resulting from its strong ability to provide firm and flexible power, the CO_2 flows from the power sector are likely to follow similar patterns as described in this work (it is realised that demand and supply patterns might change in the future, as discussed in more detail in section 3.5; however, the quantitative consideration of these effects go over the scope of this thesis).

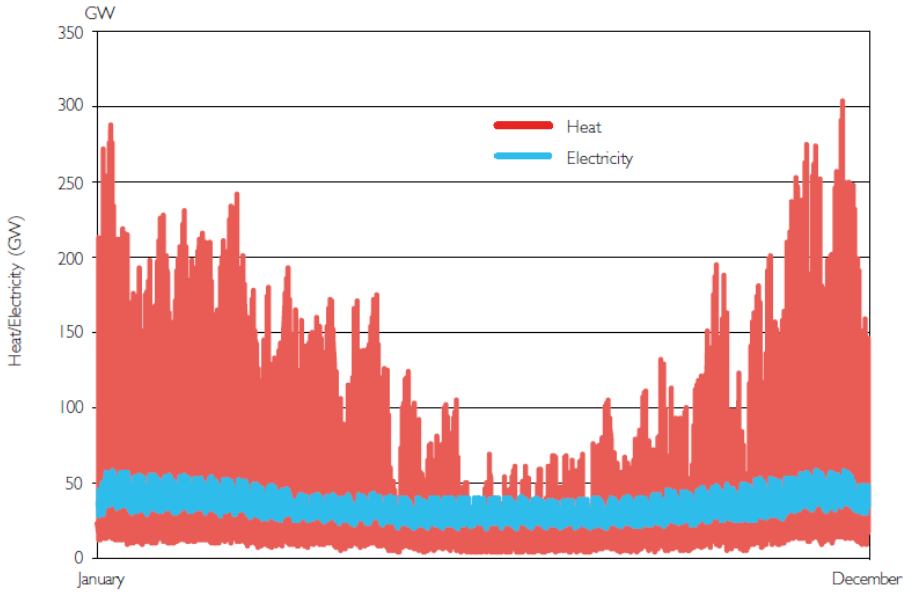

Figure 3.21: Variation of heat and electricity demand throughout the year (UK DECC 2012).

Even if a complete hydrogen or electricity based decarbonisation of the heat sector are options worth considering, the most cost-effective option is likely to be a hybrid of both systems (Strbac et al. 2018). This hybrid system would likely have both large quantities of variable CO_2 flows from power plants, and more constant flows from hydrogen production plants.

Independent of heat and power decarbonisation BEIS further predicts that CCS in industry has a deployment potential of 23MtCO2/y by 2050 (UK BEIS 2017b). It becomes clear that CCS on power is only one of several sources likely to produce large quantities of CO_2 flows destined for permanent geological storage. Although there is little information in the public domain literature about CO_2 flow variability from other sources, as also briefly discussed in section 2.2.1, they are in general likely to me more stable. The analysis presented in the current study focusing on CO_2 flow variability from the power sector can, therefore, be seen as a conservative baseline scenario with high CO_2 flow variability in the system which is not mitigated by other sources providing a constant CO_2 supply.

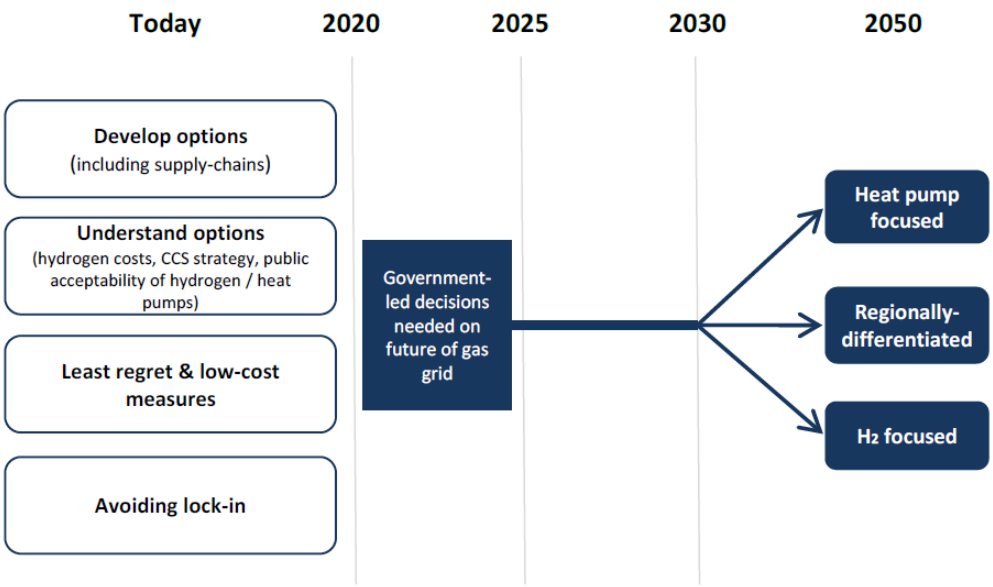

Figure 3.22: The need for strategic and timely government led decisions on the decarbonisation pathway for the heat sector (CCC 2016).

3.8. Conclusions

This chapter has investigated the operating behaviour of CCS power plants in an example energy system (based on the GB system) with 15GW, 30GW and 45GW of installed wind power generation capacity (corresponding to around 18%, 31% and 42% of total installed capacity). The study informs researchers, policy makers and planners involved in designing future CCS systems about the operating requirements, and variability of CO_2 flows that can be expected of CCS power stations. These will consequently need to be accommodated by downstream transportation and storage infrastructure. This presents a novel and relevant contribution to the literature, as it is only when the requirements for operating flexibility are better understood, that the implications and the potentially additional costs associated with managing the operational issues that flexible operation imply can be minimised. In particular, the chapter has shown that:

1. Different combinations of wind and CCS power capacity can be deployed to achieve the respective annual average emission intensity targets. The individual scenarios lead to significantly different operating profiles of CCS power stations, and consequently time profiles of captured CO_2 that will feed into downstream T&S systems.
2. The capacity utilisation of the required T&S system reduces in lower emission intensity scenarios. This will lead to increased costs of the system on a per-tCO_2 throughput basis, thus reducing the relative economic value of CCS vis-à-vis other low carbon policy options.

3. High variability of CO_2 flow rates feeding into future CO_2 transportation and storage (T&S) networks can be expected over the entire year, and across nearly all scenarios. In the base-line scenario, 21% of net changes over 6h-periods were greater than 30% of the nominal flow, and 12% of the changes were greater than 50% of the nominal flow.
4. In general, CCS plants will experience more load changes over 6-hour periods, and changes of greater amplitudes, under low emissions intensity scenarios, due to the greater number of CCS plants required to achieve these targets, some of which will have to load follow.
5. The overall variability of captured CO_2 flows is less dependent on wind capacity than it is on the target emissions intensity. CCS plants will operate more frequently at stable base-load under high wind capacity scenarios, as fewer CCS plants are required to meet emission targets, and more of the carbon budget is available for use by load-following non-CCS NGCC plants. However, at times of very high wind output, even these few CCS plants may have to be constrained down to minimum load, resulting in changes of high (>50%) amplitudes, from full to minimum load and back again. It is unclear whether accommodating such high amplitude changes will be more or less costly than coping with more frequent lower-amplitude changes, underlining the importance of further research to investigate the economics of such trade-offs.
6. The variability of load changes averaged over two consecutive 6-hour periods (selected to provide an indication of the possible smoothing effect of line-packing) is less extreme, with fewer periods of larger amplitude changes and also fewer periods of zero change. However, variability remains substantial under all considered scenarios. This indicates that many CO_2 flow fluctuations are on the basis of cycles extending over more than 12hrs, which will automatically lead to a higher requirement for CO_2 balancing capacity (compared to short term fluctuations), if large and frequent load changes at the injection well level are to be avoided.
7. Dependent on the exact definition the number of LFPs that T&S systems face over the year can be substantial, particularly at high or medium wind penetration levels (up to 248 and 263, respectively). Across all core modelled scenarios the large majority of LFPs endure, however, only for less than 10hrs. If CO_2 flow balancing capacity is made available upstream of injection wells in order to bridge periods of low flow for up to 10hrs, this could potentially drastically reduce the number of LFPs at the injection well level, mitigating the risk of any associated possible damages.
8. The frequency of CCS plants starting-up (and shutting-down) is a very strong function of the target emission intensity, and to a much lesser extent of the installed wind capacity scenario. Whilst in the high target emission intensity scenarios CCS plants have on average less than 3 non-maintenance related shut downs per year, this number increases substantially to around 65 times per year across low target emission intensity scenarios. This suggests that in future low-

carbon energy systems dominated by variable renewable power, greater attention will need to be paid to on/off and part load performance in CCS fossil fuel power station design. Further, this implies a requirement for future CO_2 T&S systems to be able to cope with a high number of flow rate step changes when accommodating CO_2 from CCS power stations operating in low carbon electricity systems.

9. In general, the variability of wind speeds/intensities across different years has the potential to influence the capacity utilisation of CCS power stations. In high wind years the capacity utilisation and hours at full load of CCS power stations drops, while it rises in low wind years. The levels and trends regarding CO_2 flow variability and duration and number of LFPs, however, are not impacted fundamentally.
10. Similarly, the addition of solar capacity to the generation portfolio leads to depressed capacity factors of CCS power stations (7-12% lower across the evaluated wind deployment and emission intensity scenarios with 30GW of additional solar capacity). Even though the effect of solar capacity on CCS power station load curves varies across different seasons of the year, as an effect of the complex interplay between weather (e.g. hours of sunlight) and electricity demand, the overall variability in terms of frequency and amplitudes of load changes of CCS power stations stays comparable across the evaluated scenarios. Whilst time durations are similar, the cumulative number of annual LFPs somewhat increases when adding solar capacity in the evaluated cases (e.g. LFPs are on average around 30% more frequent when adding 30GW of solar generation capacity across considered scenarios).
11. The option for flexible capture could change CO_2 flow profiles considerably towards higher variability, but only at relatively low future carbon prices (e.g. approx. 50£/tCO_2 or lower).
12. CCS on power is only one of several sources likely to produce large quantities of CO_2 flows destined for permanent geological storage. There is little information in the public domain literature about CO_2 flow variability from other sources. In general, it is expected that they are more stable. For hydrogen production, representing potentially another dominant source of CO_2 in future GB energy systems for example for decarbonising the heat sector, constant production rates are expected to improve cost economics by enabling better infrastructure capacity utilisations. Although there remain large uncertainties about CO_2 flows from industrial CCS facilities the durable nature of many produced goods and the comparatively slow (market) drivers dictating load fluctuations suggest a lower short term flow variability than can be expected from the power sector. Overall, however, it is recognised that CO_2 flow variability from other type sources remains a gap in the literature that still needs to be better understood.

Although the observed variability of captured CO_2 flows at CCS power stations operating in low carbon GB electricity system scenarios would be unlikely to cause any particular concerns for transportation networks, they do raise serious technical issues associated with

cycling of injection wells and storage reservoirs (see Chapter 2, or Spitz et al. 2017). A number of options exist to enable injection wells to operate more flexibly that are discussed in Chapter 4. Alternatively, CO_2 flow rate fluctuations can be balanced and smoothed out at various points upstream in the system. Any such solutions are, however, likely to come at an increased cost and/or decreased efficiency (see Chapter 4).

When transferring the learnings from this study to other energy systems it should be noted that demand data, wind data, and their interplay may be country specific. Other energy systems may have wind or renewable resource distributions that complement demand profiles in different ways, or power systems that are able to absorb more/less supply from renewables. The general findings of this study are nevertheless expected to hold for many different energy systems.

The present study provides a baseline estimate of the operating flexibility likely to be required by future CO_2 T&S systems, but further research in all of the areas outlined in section 3.5 (including the effect of energy storage, electrification of transport, smart grids, other energy sources etc.) would be useful in order to improve our understanding of future flexibility requirements. Line-packing studies building on Aghajani et al. (2017) that rigorously examine the extent to which pipeline networks can be used to smooth out and absorb feed flow-rate variations would be particularly useful. One such study is presented in Chapter 5 of this thesis. This enables more accurate determination of the extent to which CO_2 injection wells and storage reservoirs will need to accommodate varying flow rates, or alternatively, the extent to which additional flow balancing capability needs to be installed.

The key take-away message for policy-makers and planners to be aware of is that CCS is unlikely to be utilised predominantly at steady-state base load operation. Flexible operation of CCS infrastructure is likely to be required to some degree. This implies additional costs to manage or mitigate the damaging downstream (e.g. wellhead) effects of CO_2 flow variations, either at the power plant or within the transportation network, which will only be minimised if operating flexibility is better understood and anticipated at the system design stage.

4. Options to mitigate issues associated with CO_2 flow variability

Having outlined the issues associated with regular CO_2 injection well and storage reservoir cycling in Chapter 2, as well as the requirements for flexible operating of CO_2 T&S networks for accommodating feed flow variability from the electricity sector in Chapter 3, this section presents options with which these issues can be mitigated or overcome. The options can be classified according to where in the T&S process chain measures are taken.

Section 4.1 examines solutions allowing injection wells, as the main limiting factor to flexible operation, to operate in a more flexible manner and with a wider operating envelope. Section 4.2 investigates options to smooth out CO_2 flow rate variability by balancing CO_2 flow rates within the boundaries of CCS power stations. Finally, section 4.3 reviews options to balance CO_2 flow rate variability within the transportation network mitigating any downstream injection well issues associated with variable operation. Although it is expected that some of the issues surrounding increased levels of residual trapping and halite precipitation caused by cyclical flow rates injected into saline aquifer reservoirs can be at least mitigated by appropriate reservoir design and well placement, as previously discussed in Chapter 2, balancing flow rates upstream in the network would additionally help to reduce the remaining risks and uncertainties associated with variable flow rates at the storage level.

It should be noted that the review presented in this chapter is largely based on a conference paper (Spitz et al. 2017) presented by the author at the Greenhouse Gas Technologies 13 conference in Lausanne, Switzerland, in 2016. For the purpose of this thesis the review has, however, been refined and extended.

4.1. Options for improving operational flexibility of CO_2 injection wells

Constituting one dominant constraint to flexible operation, a logical attempt to improve the operational flexibility of the overall CCS system is to improve the flexible capabilities of CO_2 injection wells. Indeed there are several options available for increasing the operational envelope of injection wells. Alternatively options exist for minimising the damaging effects critical periods of two-phase flow have on the equipment. The options can broadly be distinguished into operational and design solutions. They are discussed in subsections 4.1.1 and 4.1.2, respectively.

4.1.1. Operating solutions

4.1.1.1. Optimal start-up and shut-down time

Start-ups and shuts-downs are critical periods in the life of injection wells as the low or missing backpressure from injection can lead to a gas cap developing at the wellhead

(depending on depth and pressure of reservoir). When passing through this state of the system CO_2 flashes across the wellhead choke valve. This comes along with a strong Joule-Thomson (JT) cooling effect, which can endanger the integrity of the well, particularly when repeated frequently (Shell 2015, Li et al. 2015; see also Chapter 2).

During these two-phase flow transients the minimum temperature of the well completion material is dominated by the interplay of the heat exchanged with the cold CO_2 through convection (cooling effect), and the heat exchange with the warmer surrounding materials such as the casing, cement and rock though conduction (heating effect; Li et al. 2015). There exists an optimum start-up and shut-down time that minimises the temperature drop of the well material. This optimal time is a trade-off between allowing for sufficient time for heat-exchange with the environment to occur (heating effect), and the time it takes for the well completion[2] and surrounding materials to be cooled down excessively by the cold CO_2, since this would reduce heating effect via heat-exchange through conduction (Li et al. 2015). By modelling an injection well based on conditions of the Goldeneye depleted reservoir (i.e. considered for long term CO_2 storage within the Peterhead UK CCS demonstration project in the UK) Li et al. (2015) finds optimal start-up and shut-down times of 5s and 10min, respectively. The Shell FEED study team of the Peterhead CCS demonstration project suggested regular start-up and shut-in times of 30min, which is a compromise between limiting temperatures drops at the wellhead, as well as avoiding excessive fluid speeds and hammer effects taking place along the well (Shell 2015a). By considering the optimal time for start-ups and shut-downs, the temperature drop of the well completion material can be limited mitigating some of the lifetime hampering effects outlined in Chapter 2 (e.g. cyclical thermal stresses).

It should be noted, however, that this strategy is suitable only during start-up and shut-down operation. It is not suitable when there is a need for continuous operation at low loads with flashing taking place across the wellhead choke valve caused by low wellhead pressures as a result of low amounts of CO_2 being supplied by CO_2 capture facilities upstream in the network.

4.1.1.2. Addition of MEG or Methanol

Monoethyleneglycol (MEG) and methanol are hydrate formation inhibitors. Their addition to the flow shifts the hydrate formation area of the mixture to higher pressures and lower temperatures. The substances can be added to the CO_2 mixture before injection and in order to avoid the risk of hydrates forming in the injection well due to low temperatures (Shell 2015, Capture Power Ltd. 2016). It should be noted, however, that the continuous injection of MEG and Methanol during operation at low-loads when flashing is taking place across the well-head choke valve is likely to be economically unviable due to the large required volumes. This is particularly true when injection is taking place off-shore. Further,

[2] The well completion is the installation in the cemented borehole to make the well ready for operation.

the addition of sufficient amounts of MEG or Methanol does only prevent hydrate formation, and does not mitigate other integrity hampering effects caused by two-phase flow such as cyclical thermal stresses.

4.1.1.3. Additional injection of nitrogen

In order to minimise flashing when a gas cap is present at the top of the well, additional amounts of nitrogen can be injected. By increasing the total flow volumes through the well and into the reservoir the backpressure in the well is increased. When injecting sufficient amounts of nitrogen single phase flow can be ensured at the wellhead, preventing flashing and avoiding the associated risks (Capture Power Limited 2016a). Again, the additional injection of nitrogen over extended periods of time is likely to be economically challenging, particularly for offshore operation due to the high volumes that would be required. Nitrogen is chosen being relatively cheap and practically an inert gas under the given conditions (Oldenburg 2003).

4.1.1.4. Managing a portfolio of wells

Maximum flow capacities of CO_2 injection wells range typically from 1-2MTPA (Kolster et al. 2018, Capture Power Limited 2016a). This compares to CO_2 flow volumes of large-scale CCS projects of frequently 1MTPA or higher. The nominal flow rates at the White Rose and Peterhead UK CCS demonstration project were expected to be 2.68MTPA and 1MTPA, respectively (Shell 2016, Capture Power Limited 2016b). Particularly in CCS networks of a certain size operators, therefore, have the option of managing the portfolio of injection wells according to their individual specific needs and limitations. For instance, the operator could choose to react to periods of low CO_2 supply by shutting in as many wells as required for ensuring sufficient flow in the remaining online wells, to allow these to operate within their preferred operating envelope, and at sufficiently high flow rates to avoid two-phase flow. He could further take turns in shutting in wells. This would distribute the additional stress that shut-ins and start-ups have on the affected equipment. This approach would limit the amount of time any respective injection well in the network would need to operate at low flow rates and at two-phase flow. Given the high frequency and amplitudes of CO_2 flow rate fluctuations that can be expected from the power sector, as indicated in Chapter 3, the number of shut-ins per well is still likely to stay significant. Further, any well shut-down and subsequent start-up is associated with two transitions through the low flow region of the well, as well as one period of zero injection that comes with own challenges for the storage site (see reduction of injectivity in aquifers as an effect of increased residual trapping caused by cyclical operation, as described in section 2.2.4).

Managing the portfolio of injection wells is, therefore, without doubt an important component when mitigating the risks associated with low or no flow events at injection and

storage sites. Nevertheless, it is evident that avoiding periods of low or zero flow entirely is the preferred option of operators as it enables them to avoid these risks entirely. Chapters 5-7 in this thesis, therefore, provide an important and relevant contribution to the literature by exploring the extent to which two CO_2 flow balancing options, namely line-packing and solvent storage at PCC power stations, can contribute to avoiding low or zero flow periods at the injection level entirely.

4.1.2. Design solutions

There are several design solutions to prevent flashing taking place across the wellhead choke valve even at low loads, mitigating the associated long term integrity hampering effects. All of these options apply the same basic principle of increasing the backpressure in the well completion in order to prevent two-phase flow. They are discussed in subsections 4.1.2.1-4.1.2.5.

It is worth noting that these options can be combined in tailor made new designs. However, due to higher risks associated with more complex design solutions, and high costs associated with well interventions in case of malfunction, a general consensus amongst well engineers is to design early CO_2 injection wells with as little complexity as possible to minimise the potential for failures (Spitz 2016).

4.1.2.1. Remotely actuated ball valve

Ball valves (e.g. Figure 4.1) can be installed in the completion, for example at the lower end of the upper completion (the lower completion is usually referred to as the part of the completion being located in the production/injection zone of the reservoir, whilst the upper completion connects the lower completion with the wellhead), to control the backpressure in the well at lower loads. They can also be used to isolate the pressure in the upper well completion from the reservoir pressure during shut-in. In this way the formation of a gas cap at the wellhead can be avoided at all loads along with the associated integrity risk this would imply. Balls valves can be actuated remotely (Capture Power Ltd. 2016a, Halliburton 2014). However, being an additional and remotely controllable component in the well completion balls valves add to the complexity and cost of the completion. Along with the increased complexity inherently comes an additional risk of malfunction which will be discussed in subsection 4.1.2.5 (see also Spitz 2016, Capture Power Ltd. 2016a).

Figure 4.1: Halliburton lubricator interval control valve (Halliburton 2014).

4.1.2.2. Remotely actuated sliding sleeves

Similarly to ball valves, sliding sleeves can be used to manipulate the flow through the well completion, and even through individual isolated injection zones in the reservoir (see Figure 4.2-Figure 4.3). This flow control again can be useful for controlling the backpressure in the upper completion at low loads or during shut-in. Sliding sleeves can be operated remotely, either electrically, hydraulically or in combination (Bellarby 2009, Sankar and Knabe 2010). They can have binary, multiple or continuous opening positions (Bellarby 2009, Sankar and Knabe 2010). Again, the increased complexity of the configuration leads to higher costs of the completion. The moving parts in the corrosive and exposed environment deep underground, however, further represent a risk of failure inherent to the configuration (Spitz 2016, Capture Power Ltd. 2016).

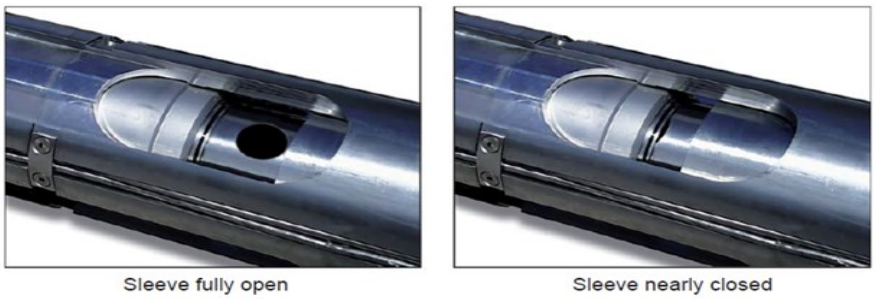

Figure 4.2: Hydraulically actuated sliding sleeve (Bellarby 2009).

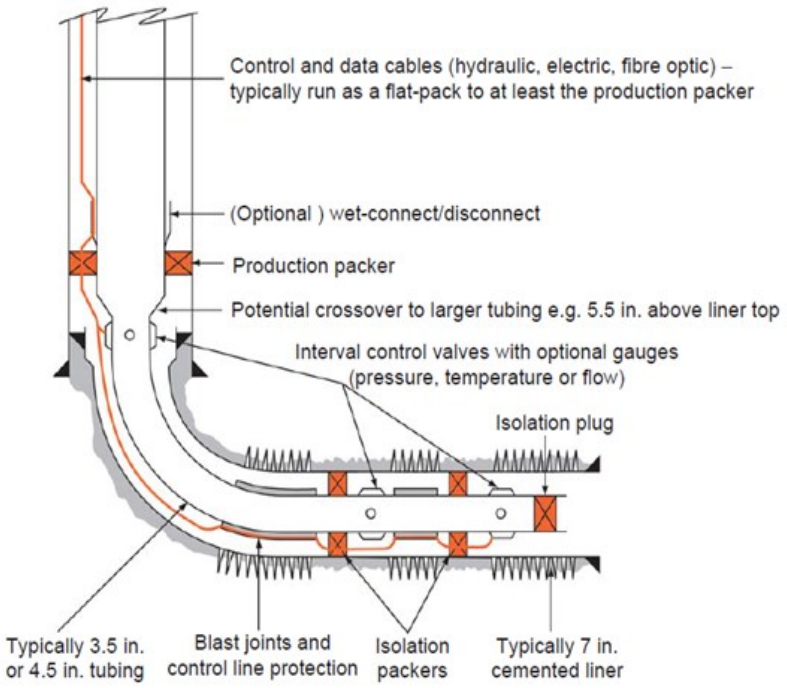

Figure 4.3: Typical cased well downhole flow control completion (Bellarby 2009).

4.1.2.3. Multilateral wells

Multilateral wells consist of a mother well and several well laterals branching off into different parts of the reservoir as illustrated in Figure 4.4. There are several levels of technical advancement of such well configurations as summarised in Figure 4.5. Dependent on the level of advancement Inflow Control Valves (i.e.: ICVs; e.g.: ball valves or sliding sleeves) can be used to control the flow of CO_2 through the individual well laterals. ICVs can currently, however, only be installed in the well's mother bore and not in the laterals (Al-Khelaiwi 2013). Given the inherent reliability issues of moving parts (i.e. valves) in the well completion it might make sense to spread the risk by making several flowpaths available. Multilateral wells come at a significantly increased cost, complexity and integrity risk of the configuration (Bellarby 2009, Spitz 2016). Nevertheless, dependent on the requirements and issues associated with flexible operation of injection wells this technology could also play a role for CO_2 storage ZEP (2017) notes recently.

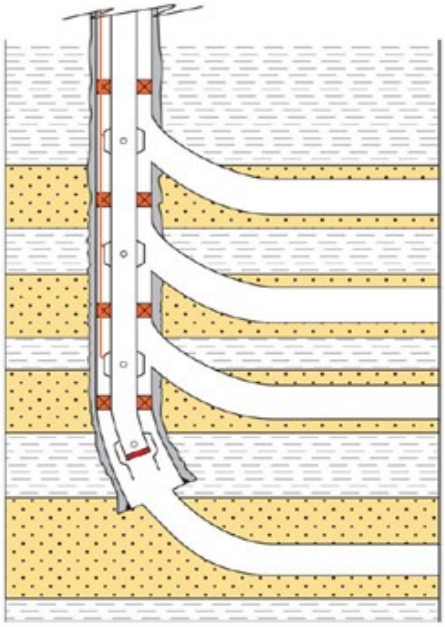

Figure 4.4: Downhole flow control with TAML - Technical Advancement of Multilaterals Code - level 2 multilaterals (Bellarby 2009).

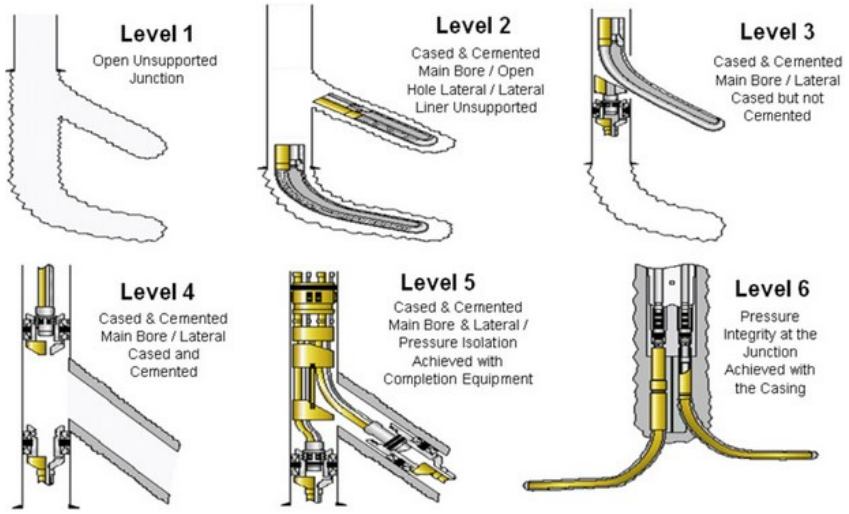

Figure 4.5: Technical Advancement of Multilaterals Code (Drilling Contractor 2011).

4.1.2.4. Dual or multiple tubing string completion

A multiple string completion consists of several tubing strings in the same wellbore casing. The tubing strings can be arranged in parallel or concentrically in another (Capture Power Ltd. 2016, Bellarby 2009). They can be closed in and operated independently from each other (Spitz 2016). This allows injecting CO_2 into two (or more) independent tubing strings with smaller effective diameters. The backpressure in the strings will increase due to a larger relative surface exposure of the CO_2 in two (or more) independent tubing strings

leading to increased friction. This enables single phase operation even at lower injection loads. At very low loads one tubing string can be shut-in, with operation in the remaining tubing string being closer to its respective design point, minimising the operating loads at which flashing takes place across the wellhead choke valve. Figure 4.6 schematically illustrates a typical parallel tubing string configuration in a single well.

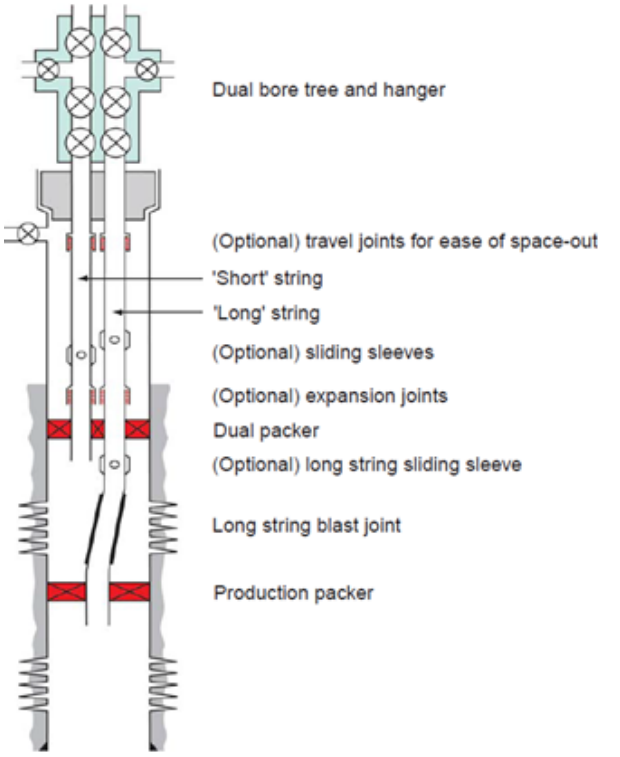

Figure 4.6: Typical dual completion (Bellarby 2009).

4.1.2.5. Reliability and cost data for Inflow Control Valves

Most of the above options to overcome two-phase flow at the wellhead even at very low loads rely on ICVs to manipulate the backpressure. A major concern regarding the deployment of subsurface, remotely controllable ICVs is related, however, to their reliability performance. The increased design complexity of well completions with ICVs inherently comes along with an increased the risk of failures. This is particularly problematic as ICVs are moving parts in a corrosive subsurface environment where intervention and work-over costs can escalate quickly. For example, only the rig hire necessary for well intervention at the White Rose CCS demonstration project was estimated at 155,000-255,000£/day (Capture Power Limited 2016a). Although being of fundamental importance, long term reliability data in the publically available literature is scarce. This is at least partially due to the relative novelty of the technology. The first so called ‘intelligent’ or ‘smart’ well system has been installed at the Snorre oil and gas field in the southern part of

the Norwegian Sea in 1997 (Halliburton 2014). The reliability data that could be retrieved from the publically available literature suggests:

- Mitchell and Skarsholt (2008) state that, when excluding the first installations in the statistics, the survivability rate of the ICVs installed in the Snorre (oil & gas) field in Norway is approximately 85% over a time period of approximately 10 years;
- Al-Khelaiwi (Al-Khelaiwi 2013) suggests that the 5-year survivability for the ICV system is currently 96% for the all-hydraulic control system; and
- Sankar and Knabe (2010) mention an industry wide reliability target exists aiming at 90% of the installed sliding sleeves still being operatable after a time period of 10 years.

It must be noted, however, generally that the reliability data that could be retrieved from the literature has been gathered for ICVs operating in a significantly different environment. While the data was derived for ICVs installed in oil & gas extraction wells that would usually be operated on the basis of several months or even years (Sankar and Knabe 2010, Mitchell and Skarsholt 2008), ICVs for CO_2 injection would face a considerably changed working environment and potentially much more frequent usage (e.g. daily: see variable feed flow rates in Chapter; ZEP 2017). Further, due to the high intervention and work-over costs particularly offshore ICVs for CO_2 injection would likely be required to operate largely maintenance free over the intended infrastructure lifetimes of 20-30 years in order to be economically viable. Whether this can be achieved with further technological advancements on ICVs is, yet, to be determined.

Similarly cost data on ICVs in the literature is scarce. Several sources estimate the typical cost of integrating an ICV into a well completion over the large span of 0.5-2.1M$ (Al-Khelaiwi 2013, Jackson et al. 2008, Robinson 2003). This suggests that the equipment costs for installing ICVs are relatively small compared to the overall costs of wells (costs for drilling and completing 3 wells for the White Rose project was estimated at 68.3M£ - EON 2012b; injection infrastructure capital costs at the Kingsnorth UK demonstration project were estimated at 94.3M£ in the central case within a FEED study - Capture Power Ltd. 2016). The costs are, however, increased by the longer installation time required for installing the system (e.g.: around 0.5M$/day according to Jackson et al. 2008). The largest cost contributions could, nevertheless, likely be the increased insurance costs and/or increased work-over costs due to the lower expected reliability of the overall system (Spitz 2016).

4.1.2.6. Development and deployment of cement and well materials that can withstand cyclic thermal stresses

A significant part of the concerns related to injection well integrity surround the uncertain resistance of well materials to repeated cyclic thermal stresses. The integrity risk is driven by repeated contraction and expansion of well materials with different thermal expansion

coefficients, which ultimately can lead to fractures and loss of sealing ability. Particularly interfaces of materials with different thermal expansion coefficients, e.g. cement and steel, are imperilled. A further approach to mitigate this risk, therefore, relates to developing and deploying materials that are better able to cope with cyclic thermal stresses. ZEP (2017) notes that currently "*the performance of well construction materials is not tested under daily thermal cycling*" (p. 92). Material science could help developing materials with similar thermal expansion coefficients which would assist in avoiding excessive thermally induced stresses (Torsæter et al. 2017, ZEP 2017). Further, materials with high conductivity would avoid large temperature differences in well materials which are the source of detrimental thermal stresses (Lund et al. 2015). The extent to which materials research can help to avoid the thermal stress induced detrimental effects on the well completions is, however, yet to be determined.

4.2. Options on the power plant level

There are other non-well related options to mitigate the risks associated with frequent and irregular fluctuations in CO_2 feed flows to the T&S system. These can be considered alternatives to making changes in the design and/or operation of CO_2 injection wells. They consist of reducing the flow variability by balancing CO_2 flows upstream in the system. "*Owing to the high cost of offshore well interventions…*" and the uncertainties in regards to the injection well and storage response to frequent and variable operation, ZEP (2017) notes that it would be likely that "*operators take a conservative approach and try to minimise on/off cycles*" (p. 91). This could be done, for example, via flow balancing. Dependent on the particular CO_2 capture technology several options are available for balancing flows either within the transportation network or within the boundaries of the power plant itself. The available options will be discussed in the following subsections 4.2.1-4.2.3.

4.2.1. Solvent storage at post-combustion capture CCS power stations

Solvent storage at PCC CCS power stations can allow decoupling of electricity produced by the power unit, and the CO_2 streams produced by the CO_2 capture plant, at least for a certain amount of time (e.g. few hours). This is achieved by the temporary storage of CO_2 within the solvent in a rich solvent storage tank, and by delaying the energy intensive step of regeneration of the solvent to later points in time. Operation of the capture plant is maintained by feeding lean solvent from a dedicated lean solvent tank to the system. The time over which solvent storage operation can be continuously sustained before the need for regenerating rich solvent becomes apparent is determined by the capacity as well as the inventory of the rich and lean solvent storage tanks (for more detailed explanation see Chalmers 2010b, Lucquiaud et al. 2011, Chalmers and Gibbins 2007). A schematic

illustration of the additional rich and lean storage tanks required for solvent storage operation is provided in Figure 4.7.

There are several studies in the literature that explore the economic viability of solvent storage (Cohen et al. 2011, Oates et al. 2014). They all focus on using solvent storage as an indirect energy arbitrage technique that allows achieving higher profits by boosting electrical output of the power plant when electricity prices are high by storing rich solvent, and delaying the energy intensive step of solvent regeneration to a later point in time. When electricity prices and with it the opportunity costs of selling less electrical power the step of regenerating stored rich solvent is carried out. The literature suggests that solvent storage can lead to additional profits in jurisdictions with large and frequent fluctuations in electricity prices (Chalmers 2010a, Cohen et al. 2011, Versteeg et al. 2013, Mechleri et al. 2017b).

By using solvent storage tanks and varying the CO_2 output of the capture unit independently from the power unit, the CO_2 flows profiles exported to the downstream T&S system can be smoothed out. The value of solvent storage as a CO_2 flow balancing option has, to the knowledge of the author, not yet been explored in the literature. Nevertheless, on the example of a weekly predefined cyclical profiles of NGCC-CCS and PC-CCS power stations (IEAGHG 2012b) demonstrates that constant CO_2 flows exported to the downstream T&S system can be achieved even at cyclical operation of the power plant with additional total investment costs of 1.5-3% for the reference plant.

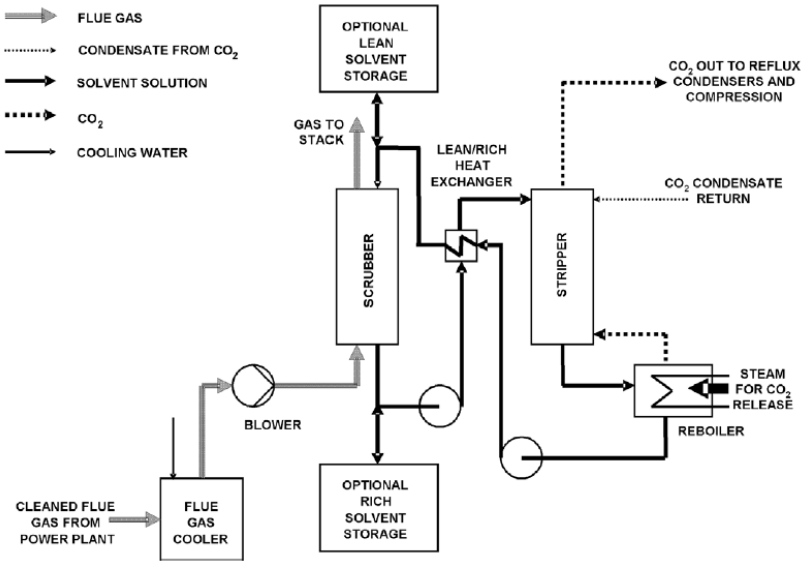

Figure 4.7: Schematic diagram of post-combustion capture plant with optional solvent storage tanks (Chalmers and Gibbins 2007).

4.2.2. Liquid oxygen storage at oxy-fuel combustion CCS power stations

Similarly to post-combustion CCS power stations the most energy intensive step associated with CO_2 capture at oxy-fuel CCS power plants - i.e. the production of pure oxygen in the Air Separation Unit (ASU) - can be decoupled for a certain time from the power generation unit. The installation of a Liquid Oxygen (LOx) interim storage tank allows, for example, operating the ASU at high loads consuming large amounts of power and producing large amounts of excess LOx whilst simultaneously running the power cycle at minimum stable generation. Excess produced LOx is stored in the LOx tank. Overall, the power station in this mode would produce only very small amounts of power (if even) at times at which it is not demanded by the wider electricity system, while maintaining a substantial flow of CO_2 to the downstream T&S system. Capture Power Ltd. in charge of the FEED of the White Rose demonstration oxy-fuel CCS power station in the UK, estimated a minimum stable load level at regular operation of ~25% of the nominal power production (Capture Power Ltd. 2015b). When operating at this load with a fully ramped up ASU almost no power exchange with the wider electricity grid was expected while exporting around 25-35% of nominal CO_2 flow to the T&S network. Similarly, the ASU can be shut-in (/ramped down) whilst running the power generation unit at higher load. If the power cycle is operated at full load, for example in response to high electricity prices, the strongly reduced parasitic energy requirement from the ASU can enable a boost in output as well as in economic profits. By exploiting the flexible operating capability of the ASU at oxy-fuel power stations, CO_2 flow rates exported to the downstream T&S network can be balanced while simultaneously achieving higher economic profits (i.e. similarly to solvent storage technology at PCC capture plants).

The CO_2 flow balancing capacity of oxy-fuel power plants is generally limited by the available LOx storage volumes and the power consumption of the ASU. In the specific design proposed for the White Rose CCS demonstration plant operation of a fully ramped up ASU with power cycle at minimum load (i.e. exporting approx. net zero power at CO_2 flows of around 25-30% of nominal load) could be sustained for up to 8hrs before the LOx storage vessel would reach full capacity (Capture Power Ltd. 2015b). Nevertheless, the LOx storage tank capacity could be further increased if this was needed.

4.2.3. Hydrogen storage at pre-combustion capture power stations

Pre-combustion CO_2 capture technologies involve reacting a fuel with air (or oxygen) and/or steam to produce a synthesis gas (syngas) that is composed of carbon monoxide and hydrogen (Davidson 2011). Once the carbon components are captured in what is generally an energy intensive process (e.g. using amine scrubbing technology) there remains a mixture of (nearly) pure hydrogen that is later combusted in the power generation unit of the plant. Similarly to the methods described above, a hydrogen buffer tank can be installed for decoupling the energy intensive CO_2 capture step, (e.g. using amine capture) from the power generation process consisting of burning the carbon free hydrogen. Again,

similarly to what has been explain in the previous subsections this would allow partially decoupling the production of electricity from the production and export of CO_2 flows. Ultimately CO_2 flows exported to the T&S network could be balanced and smoothed out.

4.3. Options in the transportation network

Options to smooth out CO_2 flow profiles feeding into CO_2 injection wells also exist at the transportation network level, as will be discussed in the following.

4.3.1. Interim CO_2 storage opportunities

Several options for interim storage of CO_2 along the transportation network exist. Temporary buffering of CO_2 can be achieved via large tanks being installed either at the beginning or somewhere along the transportation system. Alternatively, large scale temporary storage can be achieved in underground geological formations as is routinely done in the natural gas industry. In the United States, around 400 sites for temporary underground natural gas storage exist with a storage volume of 4,725 Bcf in 2017 (~$134x10^9 m^3$; EIA 2017). The storage formations used include depleted oil & gas fields, deep saline aquifers, and salt caverns with a storage capacity split of approx. 79%, 11% and 10%, respectively (Alleman 2016). Similarly such formations could be used for interim CO_2 storage. To explore this possibility Farhat et al. (2011) and Farhat and Benson (2013) perform an assessment of the technical feasibility and the economic favourability of temporary CO_2 storage in underground saline aquifers. Although the authors do not identify any major barriers to this technology, they note that water vaporisation can lead to salt precipitation after every production and injection cycle. On the positive side the same effect could, however, lead to a dry out zone around the well which could lead to production and recovery of relatively dry CO_2 when needed. The energy needed for dehydration and re-compression the authors quantify at 88.6kJ/kg (~24kWh/tCO_2) which constitutes approx. 6% of the energy penalty associated with CO_2 capture and compression at NGCC-CCS power stations. Kaufmann et al. (2016) carry out a similar study assessing the potential of aquifers to act as CO_2 buffer stores. In line with the previous studies the authors find that technically the technology would be feasible. However, due to low levels of backproduction in the aquifer considered and the hence low buffer tank 'efficiency' the authors do not recommend this method.

To avoid some of the difficulties and the scale required for geological interim storage, buffer storage tanks could be used. It should be noted that the highest effective working capacity for these tanks can be achieved when there is a phase change taking place when emptying the store (from liquid/dense to gaseous). This would again come along with a JT cooling effect that could lead to some of the similar problems that previously have been described for injection wells. Nevertheless, being more accessible than injection wells it is

expected that the risks and costs associated with handling those issues are comparatively easy to manage.

4.3.2. Linepacking

CO_2 can be buffered in transportation pipelines through line-packing. Since pipelines are installed in many or most CCS systems this might be the most straight forward and cost-effective way for temporary CO_2 storage. Line-packing refers to the action of increasing (decreasing) the pressure levels in the pipeline in order to 'pack' more (or less) of the fluid into the pipeline by compressing (decompressing) it. The process relies on exploiting the compressibility of the fluid and its change in density at varying pressure levels. A diagram illustrating the density of CO_2 as a function of pressure and temperature is presented in Figure 4.8. Line-packing is performed by controlling the flow out of the CO_2 T&S system by a downstream throttling valve (e.g. wellhead choke valve) in response to the given amounts of CO_2 feeding into the system.

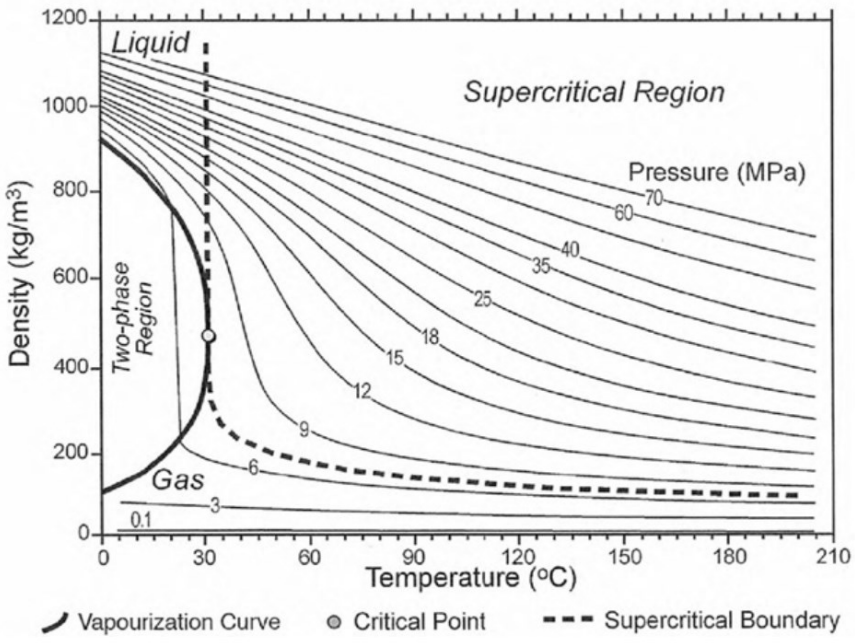

Figure 4.8: Variation of CO_2 density as a function of pressure and temperature (IPCC 2005).

In the natural gas industry linepacking is a routine process to handle the frequently large imbalances between supply (inflow) and demand (outflow) of the commodity required of the transportation system (National Grid 2017b, Tran et al. 2018). In the CCS sector line-packing can be used as an additional degree of freedom to smooth out CO_2 flow fluctuations for the downstream injection wells and storage reservoirs. Care, however, must be taken that the compressibility of CO_2 at supercritical or dense conditions is substantially smaller than that of natural gas when transported. This has a direct negative effect on the line-packing potential of the pipelines. Aghajani et al. (2017), nevertheless,

demonstrates that linepacking times (i.e. the time a pipeline can be filled at nominal flow and a closed outlet valve until the maximum available pressure is reached) of several hours are possible for CO_2 pipelines, at least when they are significantly oversized compared to the flow they need to transport. The linepacking time of a pipeline is a function of the length and diameter of the pipeline, the maximum and minimum allowable pressures, the flow regime, and the temperature and composition of the fluid.

In the absence of studies investigating the flow balancing capabilities of dense phase CO_2 pipelines, Chapter 5 and 6 of this thesis deliver a novel and relevant contribution to the literature by presenting such an analysis. For the first time hydraulic flow pipeline models are soft-linked with CO_2 flow profiles generated by the power sector, as calculated in Chapter 3, to determine the possible contribution of CO_2 pipelines to reducing the variability of flows at the downstream injection wellhead level, and in particular the number of critical low flow periods, ultimately in the effort to mitigate the associated integrity issues and project risks.

4.4. Conclusions

This chapter has reviewed available options that allow mitigating the issues previously outlined in Chapter 2 associated with variable flow rates at the injection and storage level. These options provide designers and operators of CCS networks with different alternatives that exist for ensuring the long term integrity of the downstream infrastructure, mitigating the risk of premature failure and the additional insurance costs and potential follow-up costs that this could imply. The available options can broadly be classified according to the location in the system where they intend to tackle the problem.

At the CO_2 injection well level, several operational options have been discussed, including starting up and shutting in wells in optimal time intervals, adding MEG and Methanol to the flow to prevent the formation of hydrates, and adding significant levels of nitrogen to the flow to boost pressure levels in the well. An important option in networks with several wells is to manage them individually, shutting them in sequentially at low flow rates allowing the remaining online wells to operate within their preferred operating envelope. Nevertheless, even if the cycling load is distributed across several wells this could still imply a significant number of potentially harmful low or zero-flow periods for each respective well.

Several design options have been identified that mitigate issues associated with flexible operation and in particular two phase flow at the injection level. These options commonly aim at manipulating the backpressure in the well whenever necessary in order to avoid two-phase flow at the wellhead. Options include the deployment of remotely controllable ball valves or sliding sleeves, multilateral wells and multiple tubing strings in the well completion, or the development and deployment of well materials that are able to cope

with frequent thermally induced stresses. These different well design options can also be used in combination. Nevertheless, a major concern associated with using sophisticated well design options is, particularly in early phase of CCS deployment, the long term reliability of these systems. A lower reliability of the system can lead to substantially increased insurance premium of the overall process chain. Further, even small problems affecting the operability of the well could lead to significant follow up costs if well interventions are needed particularly at offshore storage sites, or if lifetimes of the wells are reduced.

An alternative to enabling injection wells to cope with flexible operation, for example via expanding their operating envelope, is the smoothing out of CO_2 flow profiles upstream in the system, with the aim of reducing the requirement for injection wells to operate flexibly in the first place. At the power plant level it was found that solvent storage can be used for this purpose at amine based PCC power stations. Similarly LOx storage and hydrogen storage can be used at oxy-fuel and pre-combustion power stations. All these options have in common that they enable the de-coupling of the power production from the production of CO_2, for a time determined by the capacity and inventory of the storage tanks. This can assist in smoothing out CO_2 flow profiles exported to the downstream T&S system, even in the face of frequent and strong variations in electricity demand. At the transportation level storage tanks can be installed. Alternatively, temporary geological storage sites can be developed such as depleted oil & gas fields, saline aquifers or salt caverns which are routinely used in the natural gas industry for large scale interim storage. Another option for balancing CO_2 flow rates is the exploitation of the line-packing capabilities of dense phase CO_2 pipelines. Since pipelines are likely to be inherently installed, and, therefore, available in many CCS networks for the cost-effective transportation of large quantities of CO_2, this might be an obvious starting point for balancing CO_2 flow rates.

Which combination of options will be deployed in future CCS systems is, in the end, a question of practicality and cost-effectiveness. However, it is still unclear, at the time of writing, what methodology would be required for a consistent techno-economic comparison of these options in the wider context of mitigating well related issues associated with variable flow rates.

It is important to note, finally, that the negative effects and the impacts on lifetime of flexible injection well operation have, to date, not yet been fully quantified. Depending on the extent of the integrity risk posed by two phase flow and regular cycling, one possible outcome is possible that, in the future, this risk would be considered sufficiently low and no further measures are taken to extend well integrity. However, in the absence of a strong body of evidence in support of this approach, and considering the large impact that well failure would have on the success of CCS projects, it is likely that a combination of alternative options may prove to be a more successful approach to developing a robust and resilient CCS transportation and storage infrastructure.

5. Line-packing

5.1. Introduction

The previous chapters have characterised the CO_2 flows that can be expected from CCS power stations operating in future GB low carbon electricity systems. They have illustrated the issues associated with variable flowrates in the T&S systems, and the available options to mitigate these. As one of the considered options able to mitigate issues associated with variable flowrates in the T&S system the buffering, i.e. the linepacking, capabilities of dense phase CO_2 pipelines are studied in this chapter. Given that many CCS networks will extensively rely on CO_2 transportation by pipeline, linepacking could potentially provide a relatively straight forward and cost-effective option for balancing CO_2 flow variations. Pipelines, therefore, would be an obvious choice when aiming at following ZEP's (2017) recent advice of building "*capacity and redundancy into a [CCS] system*" that "*copes with volatility in supply and demand of CO_2*". Yet, the extent of the balancing capability of dense phase CO_2 pipelines still needs to be better understood. This is the main objective of the present and the following chapter of this thesis.

The process of linepacking refers to the manipulation of pressure levels within pipelines. By exploitation of the compressibility of the transported fluid and the change in density with pressure, the inventory of fluid within the pipeline volume can be managed. In this way pipelines can effectively act as interim storage vessels, providing potentially significant amounts of operational flexibility to operators of transportation networks. For example, pipelines can be able to sustain high outflows for significant amounts of time even at periods of low or zero inflows when they have been previously packed (i.e. 'filled up'). Equally, pipelines can absorb relatively high inflows for significant amounts of time even at periods of low or zero outflows. The most influential factors determining the achievable linepacking times of pipelines are: (i) maximum and minimum allowable operating pressures of the pipeline, (ii) inflow and outflow regime during the process of linepacking, (iii) the compressibility and heat capacity of the fluid, (iv) the heat transfer into or out of the pipeline, and (v) the state of the pipeline before the activity of linepacking starts (i.e. the level of inventory it contains).

Linepacking is a routine process for operators of natural gas pipelines (National Grid 2017b, Aghajani et al. 2017, Tran et al. 2018). It is used for handling short term imbalances (e.g. frequently inter daily) between supply and demand. Due to the different fluid characteristics and operational conditions the linepacking potential of dense phase CO_2 pipelines is expected to be substantially smaller than for natural gas (Wetenhall et al. 2017, Aghajani et al. 2017).

Although the potential need for CO_2 buffering options in CO_2 T&S networks has been noted by a limited number of authors (Kaufmann et al. 2016, Farhat and Benson 2013, Farhat et al. 2011) studies examining this operating flexibility option are scarce. Only two studies examine the linepacking potential of dense phase CO_2 pipelines (Aghajani et al. 2017, Van der Harst 2017). Both studies define the linepacking time as the amount of time after a

downstream valve of the pipeline restricts all outflow that a specified inflow into the pipeline can be sustained without violating maximum operating pressure limits of the pipeline. Starting off simulations from steady state and nominal flow initial conditions, Aghajani et al (2017) determines the feasible linepacking times for a large range of pipeline parameters and flow conditions. The authors conclude that linepacking times of up to 8hrs are realistic, however, only for large pipelines (e.g. diameter and length) and very low relative flow rates.

Van der Harst (2017) conducts a similar study benchmarking linepacking times calculated in the process simulation tool gCCS (PSE 2014, 2018) against the times presented in Aghajani et al (2017) and determined with the pipeline simulation tool OLGA (Schlumberger 2018). Van der Harst (2017) finds that gCCS typically predicts linepacking times around 30% lower than OLGA. This discrepancy can, however, be largely attributed to different heat transfer models, as is discussed in more detail in section 5.6. Van der Harst (2017) further investigates how the linepacking capabilities of pipelines can be used to smooth out flow variations. For a small set of test sample of cases, he demonstrates how pipelines can be used to convert strongly time varying inflows into relatively smooth outflows.

Similar to the described studies, the present work examines the linepacking i.e. interim storage potential of dense phase CO_2 pipelines. In contrast to Aghajani et al (2017) and Van der Harst (2017), however, this study does not investigate the time periods available to sustain inflows into pipelines at closed downstream valves restricting all outflows. Instead, it focuses on describing the time periods a minimum level of outflow can be maintained from of the pipeline (i.e. 50%, 30% or 10% of nominal flow), for example to the downstream well, even at zero or low inflows (i.e. 20%, 10% or 0% of nominal flow). Assuming initially fully packed pipelines (i.e. full inventory), pipelines are able to sustain outflows higher than inflows for a certain period of time by feeding any discrepancy in flows from the initially stocked up inventory until a minimum allowable pressure in the pipeline is reached. Effectively the pipelines are ‘de-packed’ in this process. The maximum time a pipeline is able to sustain a specified outflow at a given reduced level of inflow is, thereafter, referred to as the ‘line-depacking time’.

Whilst linepacking times have been examined with the objective of determining the time scales operators of CO_2 pipelines have for reacting to a fault downstream at the injection site by ramping down the inflows, the rationale behind examining line-depacking times is to find out the time scales pipelines are able to supply a minimum flow to the downstream injection wells even at no or low inflows. By sustaining a minimum flow into the injection wells even at periods of low or zero CO_2 production some of the risks associated with low flow periods as described in Chapter 2 (e.g. two-phase flow) can be mitigated, and potentially fully avoided. The study, therefore, delivers a novel and important contribution to the literature by quantifying the extent of the buffering capability of dense phase CO_2 transportation pipelines (Chapter 5) and demonstrating how it can be used to avoid critical periods of low flow at the injection and storage level (Chapter 6).

The present chapter is organised as follows: Section 5.2 explains the fundamentals of pipeline modelling. Section 5.3 discusses likely CO_2 T&S network configurations in the GB context. Section 5.4 presents line-depacking times for a large range of generally applicable pipeline scenarios. Section 5.6 validates gCCS as the deployed software in this study for calculating line-depacking times against data from the leading pipeline simulation software OLGA. Section 5.7 describes the detailed methodology according to which the line-depacking simulations are carried out within the gCCS process modelling environment. Section 5.8 presents and analyses the results from the core modelled scenarios. Section 5.9 explores the sensitivity of the results to a number of further influential parameters. Section 5.10 concludes.

5.2. Fundamentals of pipeline modelling

There are several studies in the literature modelling the fluid flow behaviour of dense phase CO_2 pipelines (Martynov et al. 2015, Wetenhall et al. 2014b, Mechleri et al. 2017a, Brown et al. 2015). Although algebraic equations exist for the engineering pipeline design, rigorous flow models based on the differential form of the conservation equations (mass, momentum, energy) are typically used to study fluid flow behaviour in more detail (Martynov et al. 2015). The mass, momentum and energy equations, displayed in equations (4)-(6), are derived from the fundamental conservation laws of fluid mechanics. They form the governing set of equation describing the flow along the pipeline.

$$\frac{d\rho u}{dx} = 0 \tag{4}$$

$$\frac{d\rho u^2}{dx} = -\frac{dp}{dx} - f\frac{\rho u^2}{2D_i} \tag{5}$$

$$\frac{d\rho u\left(h + \frac{1}{2}u^2\right)}{dx} = \frac{4q_w}{D_i} + f\frac{\rho u^3}{2D_i} \tag{6}$$

…where *x is the local coordinate along the pipeline*
D_i is the pipeline inner diameter
u is the local velocity
f is the Darcy friction factor
And q_w is the heat flux at the pipe wall
ρ is the density
p is the pressure
h is the enthalpy

These conservation equations are solved simultaneously usually in an iterative numeric process. Coupled with the pressure drop, temperature change and physical property models for the fluid they represent the set of equations that needs to be solved to determine the fluid properties along the pipeline. A schematic illustration of this procedure is shown in Figure 5.1.

For the purpose of this study the process simulation tool gCCS is used to model the hydraulic behaviour of the CO_2 flow along the pipelines. gCCS is built on the wider process modelling platform gPROMS and is developed by Process System Enterprise (PSE) specifically for the purpose of modelling integrated whole chain CCS system network operation. For more information about the model the reader is referred to PSE (2014, 2018).

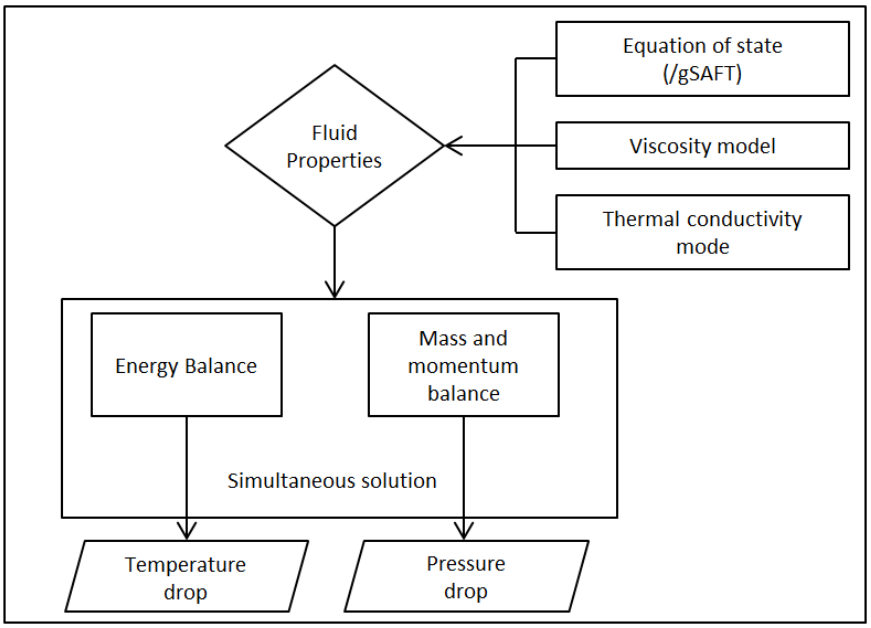

Figure 5.1: Pipeline hydraulic modelling process (adapted from Aghajani et al. 2017).

The property package deployed for the pipeline simulations is the custom made gSAFT tool based on the Statistical Associated Fluid Theory (SAFT). SAFT is an advanced thermodynamic method that is able to predict a wide variety of thermodynamic properties of different mixtures based on physically-realistic models of molecules interacting with other molecules (PSE 2019). The fluid viscosity is calculated using the Pedersen model (Pedersen et al. 1984). Having benchmarked results against values obtained from the alternative LBC (Lohrenz et al. 1964) viscosity model, this is in line with what Wetenhall et al. (2014b) suggests since the Pedersen model tends to always overpredict experimental viscosity data for pure CO_2 allowing for worst-case hydraulic calculations. Fluid thermal conductivity is calculated with SUPERTRAPP (NIST 2007) consistent with other literature (Aghajani et al. 2017, Wetenhall et al. 2017b, Wetenhall et al. 2014b). Although the pressure drop and thermal model deployed by gCCS are not enclosed due to the

commerciality of the product, the model has been extensively validated by Hussein (2017). Hussein (2017) concludes that while the model has difficulties in accurately predicting the temperature profile along the pipeline when benchmarked against real operational pipeline data this is likely an effect of varying soil thermal conductivities that locally deviate from the constant values specified in the model. Hussein (2017), therefore, concludes that gCCS it is a suitable tool for predicting dynamic flow rate responses. Furthermore, gCCS offers more accurate physical property data than other commercial software, Aspen HYSYS and OLGA, in particular for modelling CO_2 mixtures with impurities (Hussein 2017).

As a simplification to the provided pipeline model, the inertial term in the momentum equation is not considered in the core scenarios, but only in a sensitivity case of this study. Neglecting the inertial term in the momentum equation has the effect of linearising the governing set of partial differential equations (Behbahani-Nejad and Bagheri 2008, Chapman et al. 2005). As a result, simulation times are reduced by a factor of approx. 70. This is a necessary step to perform a large number of simulations necessary for the scenario based approach in this thesis. Neglecting the inertial term in the momentum equation is a procedure followed by several authors in the literature when examining flow models or when performing hydraulic flow modelling of water networks or for the oil & gas sector (Behbahani-Nejad and Bagheri 2008, Larock et al. 2000, Masella et al. 1998, Paris 2015). The accuracy of the results is not significantly impacted as is further shown in a sensitivity case in Appendix B2. Line-depacking times stay within 1.1% for the range of benchmarked cases, regardless of whether the inertial term in the momentum equation is being considered or not (see appendix B2). This marginal deviation is considered reasonable in the context of this pioneering study, with an extensive number of realistic modelled pipeline scenarios intending to outline the scale of buffering capability that can be expected to be available from the large range of conceivable future CO_2 transportation pipelines.

5.3. UK future scenarios CCS transportation system scenarios

Several studies in the literature discuss possible and cost effective UK CO_2 T&S network scenarios (Summit Power 2017, ETI 2014, Element Energy 2013). A consensus in the literature is that the formation of CO_2 capture as well as storage clusters can benefit substantially from economies of scale via reducing the number of long distance trunk pipelines (i.e. trunklines) connecting capture and storage clusters. Based on the location of large point emission sources in the UK and the characteristics and available of storage reservoirs Summit Power (2017) developed a detailed set of CO_2 transportation system scenarios which are proposed as being the most cost-economic and feasible, in short the most conceivable, for the purpose of large scale deployment of CCS. The study considers CO_2 storage volumes of up to 75MTPA by 2050.

Figure 5.2 illustrates one representative scenario out of the seven scenarios developed by Summit Power (2017). The scenarios differ with respect to the magnitude of existing infrastructure reuse, the rollout schedules, and the magnitude of CO_2 stored on the UK's

North Sea continental shelf (alternative is on Norwegian continental shelf). Although exceptions exist, the study shows that pipeline lengths in the UK would typically be within the range of 50-200km. It should be noted that pumping stations would usually be installed at the beach crossing for delivering final pressure boosts before long distance transportation offshore, dividing pipelines into an onshore and an offshore pipe. These pumping stations would compensate for previous pressure losses occuring in the upstream onshore pipelines from the point of collection and/or initial compression, and they would deliver the final pressure boosts required for the fluid to overcome frictional losses and offshore pipeline topography to reach the injection platform with a sufficiently high pressure level. Although the Summit Power (2017) study focuses on CCS deployment on the East Coast of the UK, pipeline sizing would likely be similar for West Coast infrastructure given the proximity to suitable storage fields in the Irish Sea where both depleted oil and gas fields and saline aquifers are available. In line with other UK CCS transportation system studies, pipelines of 20-24inch (508-610mm) diameter are proposed for the long distance transportation of CO_2 to the stores. For more detail the reader is referred to (Summit Power 2017).

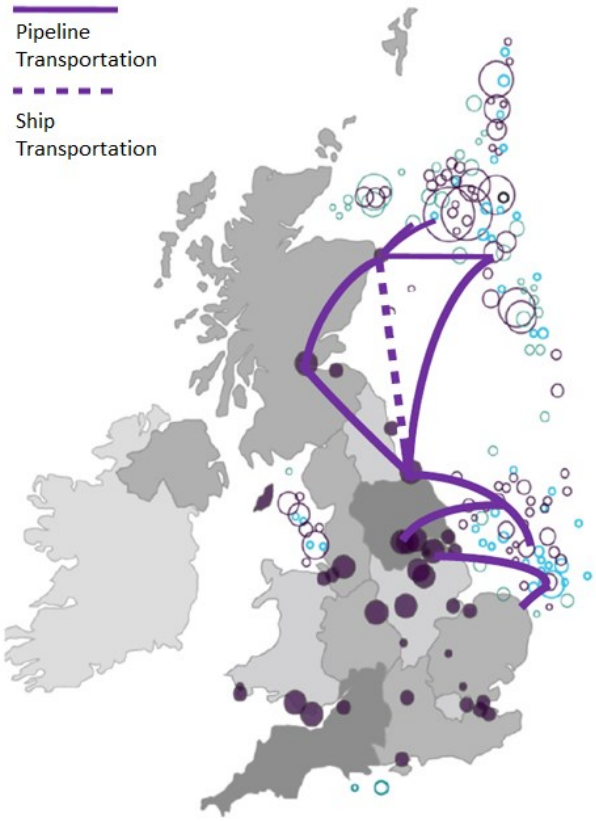

Figure 5.2: GB transportation network scenario as developed for flow volumes of up to 75MTPA by Summit Power (2017). (Adapted from Summit Power 2017).

5.4. Matrix of investigated scenarios and assumptions

Based on the UK CO_2 T&S network scenarios proposed by Summit Power (2017), a set of pipeline scenarios has been developed for which line-depacking times are calculated in the following subsections. Table 5.1 summarises all baseline examined scenarios in this chapter. These will be referred to as the 'core pipeline scenarios' for the remainder of this thesis (i.e. excluding sensitivity cases). Due to the lack of comparable data in the literature, and as a consequence of the large variety of pipelines that are conceivably deployed for transportation of CO_2, the aim of this chapter is to obtain line-depacking times for a large number of pipeline sizes and flow conditions. As key influencing factors affecting line-depacking times, the pipeline length, the outer diameter, the maximum operating pressure, the 'utilisation of pipeline at nominal flow', and the inflow & outflow regime after the line-depacking process starts (at t=0) are chosen for investigation in the core scenarios. Due to the large number of conceivable permutations of the system, 252 core pipeline scenarios are evaluated. This assists in finding underlying trends in the results, and provides fellow researchers, practitioners, and policy makers with a large set of data for related follow-up projects. Consideration has been given when selecting key parameters that pipelines are produced as standard components in discrete nominal pipeline sizes. A justification of the selected parameters and tested cases is provided below. The reference parameters are underlined in Table 5.1.

Table 5.1: Core scenarios for which line-depacking times have been calculated in the following subsections (baseline parameters are underlined).

Length	Outer Diameter	Maximum Operating Pressure	Utilisation of pipeline capacity at nominal flow	Inflow|Outflow after t=0
50 km	508mm	150bar	100%	0%in | 50%out
100 km	610mm	200bar	50%	10%in | 50%out
150 km	914mm			20%in | 50%out
				0%in | 30%out
				10%in | 30%out
				20%in | 30%out
				0%in | 10%out
2	**x 3**	**x 2**	**x 2**	**x 7**
= 252 Scenarios				

Length: Three different pipeline lengths of 50km, 100km, and 150km are evaluated within this study. These pipeline lengths are able to approximate most offshore pipeline lengths proposed in the Summit Power network scenarios (Summit Power 2017). They, therefore, represent a useful set for analysis in the GB context. Only the Teesside-Forties pipeline and the Teesside-St. Fergus pipelines in the scenarios developed by Summit Power (2017) are

significantly longer than 150km. The latter pipeline, however, only exists in one of the 6 scenarios proposed by the Summit Power. In the other scenarios the transport is organised by ship (Summit Power 2017).

Outer Diameter: Three pipeline outer diameters are chosen for evaluation: 508mm, 610mm, and 914mm. Those diameters are within the range of pipeline diameters that are currently operational in the US (Vandeginste and Piessens 2008, Race et al. 2007). Further, these pipeline diameters have been widely considered for transportation of CO_2 in GB (IEAGHG 2013, Capture Power Limited 2015, EON 2011, Summit Power 2017). For example, a 914mm diameter pipeline was proposed by the FEED study team of the Kingsnorth CCS demonstration project (EON 2011). Similarly a 610mm pipeline was suggested by the White Rose CCS demonstration project FEED study team as an anchor pipeline for the proposed Yorkshire/Humber CCS cluster. Although it is realised that Summit Power (2017) suggests that economies of scale are very high for pipeline nominal flow capacities of up to 10MTPA, a 508mm pipeline (~8MTPA nominal flow capacity) is considered in this study to assist with illustrating possible trends in line-depacking times. All considered pipelines diameters are chosen in accordance with standard pipeline sizes as set out by British Standard (BS EN10208-2 2009).

MAOP (/wall thickness): The Maximum Operating Pressure (MAOP) of a pipeline is an important parameter influencing line-depacking times. The higher the MAOP the more CO_2 can be packed into the pipeline by exploiting the compressibility of the fluid without violating pressure limits. A higher initial inventory of fluid in turn enables the pipeline to sustain high outflows at relatively low inflows for longer periods of time. Hence, two different MAOP of 150 and 200bar are chosen for investigation. These MAOPs are in the range of what is typically considered for offshore pipelines (Martynov et al. 2015, Wetenhall et al. 2014a). The MAOP is, however, an indirect parameter in pipeline design. For a given material and pipeline diameter, it can be set for example by selecting an appropriate wall thickness of the pipe. Based on a stress based design criterion the MAOP of a pipeline can be determined according with the following relation (Ghazi and Race 2012, Aghajani et al. 2017, Mechleri et al. 2017a):

$$\sigma_h = \frac{p * D_o}{2 * wt} \tag{7}$$

where the maximum tolerable hoop stress in turn is given by the expression:

$$\sigma_h \leq e * a * \sigma_{SMYS} \tag{8}$$

where e is the weld factor (assumed to be 1 for a seamless pipe; Mechleri et al. 2017a), a is the design factor based on the governing code and operators specification for a CO_2 pipeline, and σ_{SMYS} is the Specified Minimum Yield Stress (SMYS) of the pipeline material in MPa. The design factor is a construction de-rating factor dependent on the location class unit, which is an area extending for 220 yard on each side of the centreline for any

continuous 1 mile length of the pipeline (Mechleri et al. 2017a). Similarly to National Grid Carbon Ltd. a design factor of 0.72 is assumed (Capture Power Limited 2016b), which corresponds to a class 1 location. An SMYS of 450MPa is assumed for a carbon steel pipe in line with Aghajani et al. (2017).

Given that pipelines are routinely produced in nominal sizes and discrete wall thicknesses, any wall thicknesses outside the discrete range of values offered by suppliers (BS EN10208-2 2009) are not considered for practical reasons associated with cost-effectiveness. When wall thicknesses corresponding to MAOPs of exactly 150bar or 200bar are not commercially available for a given pipeline diameter, the next biggest wall thickness is chosen. It should be noted that pipeline MAOP can also be increased by increasing the pipeline SMYS by selecting higher grade materials. Since the outcome on pipeline MAOP would effectively be equivalent to when increasing the wall thickness this options is not evaluated further within this study.

As a consequence, the MAOPs for the range of pipelines evaluated in the core scenarios in this chapter effectively lie in the range of 150-159.5bar and 200-212.7bar, due to the procedure followed. This is clearly indicated in the following when presenting the results (see Table 5.4).

Capacity Utilisation (CU) of pipeline at nominal flow: The optimal amount of CO_2 that is transported at nominal load through a given pipeline is an important parameter for the calculation of line-depacking times. Not only does it decide on how much fluid can be packed into the pipeline initially and the pressure distribution along the pipeline, it also decides on the amount of flow that needs to be sustained at the outflow during the process of de-packing (which is assumed relative to the design flow in this study, see also below in this section). There are different ways of calculating the optimal flow through a pipeline. Vandeginste and Piessens (2008) present an extensive overview of different methods for relating optimal diameter and nominal flow rates. The different methods in the literature can broadly be categorised into two groups: (1) The optimal diameter and flowrates can be correlated under considerations of the pipeline hydraulic behaviour; or (2) they can be calculated on the basis of economics-related equations based on optimal design (Zhang et al. 2006). In reality, the optimal diameter for a given flow (or vice versa: optimal flow for a given diameter) is a trade-off between the capital cost of the pipeline and associated equipment (pumps, valves, etc.), and the operational costs of the system. Whilst the capital costs of the pipeline generally decrease with a reduced pipeline diameter, the opposite is true for the compression/pumping (operating) costs. For transporting the same flow through a smaller pipeline diameter a higher velocity of the flow is generally needed, which increases the pressure drop along the length of the pipeline, hence compression costs and possibly the number of required booster stations. There are different methods for relating optimal diameter and flow rate. This work deploys a hydraulic based design criterion consistent with the majority of other studies in the literature. A pressure drop criterion of 0.25bar/km is chosen based on economic considerations in accordance with Vandeginste and Piessens (2008), Wetenhall et al. (2014), Knoope et al. (2013). For given pipeline

diameters, wall thicknesses, outlet pressures (90bar in this thesis as further discussed in section 5.5), inlet temperatures, compositions, and target pressure drops it was, therefore, possible to calculate the optimal flow rate, i.e. 'nominal' flow rate, based on the hydraulic equations outlined in section 5.2.

For simplicity the optimal flow rate for a given pipeline diameter (508mm, 610mm, 914mm) is calculated for wall thicknesses corresponding to MAOPs of around 150bar. Although pipelines with identical outer diameters but higher MAOPs have higher wall thicknesses, which effectively decreases the internal diameter and in turn reduces the optimal flow rate for a given pressure drop criterion, this marginal effect is neglected. Furthermore, the optimal flow rates for the given pipe diameters is determined for pipeline reference lengths of 100km. The resulting optimal flow rates, rounded to the next .5MTPA, for the individual pipeline diameters are as follows:

Outer diameter: 508mm → 8.0MTPA

Outer diameter: 610mm → 13.0MTPA

Outer diameter: 914mm → 36.5MTPA

The resulting flow rates are within the range of flow rates of operational or planned pipelines with the respective diameters (Knoope et al. 2015, Summit Power 2017, Vandeginste and Piessens 2008). In the following these will be referred to as the 'maximum' or 'design' flow rates for the respective pipeline diameters.

To account for the possibility of oversizing pipelines for operation with a positive effect on the achievable line-depacking times, two different 'flow capacity utilisations' are considered. In one case, the pipeline is designed to carry 100% of the 'maximum' flow as nominal load. In the second case, the pipeline is oversized by design and, hence, carries 50% of the 'maximum' flow as the nominal load. For example, at a flow Capacity Utilisation (CU) of 100%, a pipeline with an outer diameter of 610mm carries 13.0MTPA as a nominal load. In contrast, at a flow capacity utilisation of 50% the same pipeline carries only (13.0MTPA x 50% =) 6.5MTPA as nominal flow.

Inflow|Outflow regime after t=0: The inflow and outflow regime after the line-depacking process starts (t=0) is very influential when determining achievable line-depacking times. The higher the difference between inflows and outflows after t=0, the shorter the time that the process can be sustained by the initial inventory of the pipeline. To take into account the vastly different flow capacities that can be transported by the evaluated pipelines, the inflows and outflows that are sustained after t=0 are expressed as a percentage of the nominal flow rate of the respective pipeline. Due to the large uncertainty regarding the minimum level of flows that should ideally be sustained through the wells at any (up-)time, a broad range of 'minimum outflow' scenarios are investigated: minimum flow is assumed to be (i) 50%; (ii) 30%; and (iii) 10% of nominal flow. In reality, the minimum outflow is determined, for example, by establishing the flow level where two-phase flow prevails.

However, this flow rate is highly dependent on the geological reservoir conditions, and the injection well design (Sanchez Fernandez et al. 2016a). For example, for the wells of the Peterhead CCS demonstration project in the UK (Goldeneye storage reservoir; depleted gas field) flashing (i.e. two-phase flow) was predicted to start if flow dropped below 60% of design flow (Shell 2015c). In contrast, for the injection wells of the White Rose demonstration project in the UK (Endurance storage site, saline aquifer) flashing was estimated to be an issue limited to the early phase of injection, and only at low flow rates (e.g. below 10%) and low purities (Capture Power Ltd. 2015a).

Adding to the complexity of CO_2 T&S networks a large CO_2 trunkline is likely to feed into a number of wells - frequently an injection volume of 1-2 MTPA is considered per well, whilst transportation capacity per trunkline depending on diameter can be as high as 36MTPA (Kolster et al. 2018, Capture Power Limited 2016a). At low loads it would be possible for the network operator to manage the flow rates into the respective wells individually and according to their specific needs (see also section 4.1.1.4). The pipeline network operator could, for instance, chose to shut down individual wells during low flow periods, distributing the remaining flow equally across the operating wells. Alternatively he could choose to operate some wells at higher loads than others if this was found to be beneficial for the specific portfolio of wells. Although it would be insightful to consider this level of granularity, it requires site specific geology data and is beyond the scope of the present study. To approximate a set of realistic 'minimum flow' conditions for a wide range of applications the minimum pipeline outflow scenarios of 50%, 30%, and 10% of the respective nominal flow rate for the pipeline are, therefore, examined.

Line-depacking times can be greatly extended if a minimum inflow is sustained during periods of line-depacking. This minimum inflow can, for example, be provided by industrial sources with a relatively constant CO_2 output, by power stations operating at minimum load, or by e.g. post-combustion capture fossil power generators regenerating significant amounts of previously stored rich solvent (see Chapter 7). To investigate the effect of a minimum inflow even at times of line-depacking three inflow scenarios are evaluated. It is assumed that during the pipeline de-packing process inflows are maintained at either: (i) 20%; (ii) 10%; and (iii) 0% of nominal flow.

Sensitivity Cases

To assess the sensitivity of line-packing times to a range of other influencing factors, Table 5.2 summarises the sensitivity cases that have been analysed throughout section 5.9. Sensitivity case number 1 (subsection 5.9.1) investigates the deviations of available line-depacking times at different surrounding water temperatures, e.g. due to seasonal variations in temperature. Sensitivity case 2 in subsection 5.9.2 quantifies the reduction in line-depacking times when onshore pipelines are used for transportation instead of offshore pipelines. Sensitivity case 3 in subsection 5.9.3 analyses the impact of varying the minimum permissible pressure levels on depacking times. Finally, sensitivity case 4 in

subsection 5.9.4 explores the effect of several common impurities on the achievable depacking times.

Table 5.2: Sensitivity cases for which line-depacking times have been calculated in the section 5.9.

Surrounding Temperature	Onshore vs Offshore	Minimum permissible pipeline pressure	Impurities
6°C	Offshore	80bar	Pure CO_2
10°C	Onshore (*Soil type)	90bar	CO_2 + 2vol% N_2
14°C		100bar	CO_2 + 2vol% H_2
			CO_2 + 2vol% O_2

5.5. Other assumptions

To compare a large set of line-depacking times on a consistent basis several other assumptions are made:

1) The pipeline is fully packed before starting the line-depacking process at t=0. This implies that the pipeline operator has the capacity to predict low flow periods and has sufficient time to prepare for these events by increasing the inventory in the pipeline to its maximum. Low flow periods can be predicted in a similar way that electricity system operators continuously forecast net demand levels several hours in advance. This can be done by estimating gross demand levels with a mix of historical and weather data, and by evaluating the likely contribution of renewables to meeting gross demand. Operating profiles of CCS power stations can then be forecasted and, consequently, CO_2 flow rates feeding into the T&S networks can be predicted.
2) A minimum allowable pipeline operating pressure of 90bar is assumed, based on the value used in the FEED study of the White Rose UK CCS demonstration project for a proposed Yorkshire/Humber transportation trunkline (Capture Power Limited 2015). A minimum pipeline pressure of 80-90bar is generally set for dense phase CO_2 transportation pipelines. This is to provide a safe margin above the critical pressure (73bar for pure CO_2), and for preventing any unexpected and potentially harmful two-phase flow in the system.
3) Further, it is assumed that a pressure of 90bar at the pipeline outlet would be sufficient for injection, or if not, that a pressure booster station at the platform would be able to deliver the necessary pressure boost for injection. Allowing for a high discrepancy between MAOP and minimum allowable pressure of the pipeline allows to achieve high line-depacking times. Necessary platform arrival pressures would vary depending on the design of the system. For the Peterhead UK CCS demonstration project an initial platform arrival pressure of 85bar was predicted (Shell 2015a). For the White Rose project an initial platform arrival pressure of 102-105bar was targeted (Capture Power Ltd. 2015a). Over time, when the reservoir

would fill up and the injection flow rates would be ramped up, this pressure was expected to increase to 160bar (depending on scenario, e.g. how many wells drilled; Capture Power Ltd. 2015a). A booster station at the shore (Barmston pumping station) was planned to deliver the required pressures for the first years of operation. However, the injection platform was specifically designed to fit an additional pumping station as a future proofing strategy in order to provide the option for further pressure boosts in later years (Capture Power Ltd. 2015c). These additional pressure boosts were expected to be necessary in later years to compensate for the increased pipeline pressure drops at higher flowrates, for the increase in injection pressure as the reservoir fills up, and for the expansion of a growing offshore T&S hub. It is thus assumed that similarly to this future proofing strategy of National Grid Carbon, pipeline operators in need for significant line-depacking times would be willing to fit a pressure boosting station (i.e. pumps) on the injection platform for additional pressure boosts for the injection process.

4) The valve shut at t=0 is assumed to happen instantaneously. This compares to a valve shut-in time of 5s in Aghajani et al. (2017). Valve shut-in times of this magnitude do not significant influence line-depacking times, as was confirmed in relevant benchmark simulations in this study.
5) The baseline pipeline type is assumed to be in water (i.e. offshore). This is on one hand due to offshore pipelines being the dominant part of the proposed future UK transportation network scenarios. On the other hand, offshore pipelines can offer significantly higher linepacking and line-depacking times than onshore pipelines due to a substantially faster heat exchange with the environment. As the objective of this work is to illustrate the available operational flexibility options that can balance CO_2 flow rates in the best and most cost-effective way it is considered reasonable to investigate line-depacking times of offshore pipelines as a baseline. A sensitivity case, however, explores the differences in line-depacking times between onshore and offshore pipelines.
6) No concrete coating is assumed in the model of the offshore pipeline. Concrete coating would have the effect of slowing down heat transfer. Whilst for offshore pipelines without concrete coating ambient conditions of the fluid are reached very quickly within the first few kilometres (e.g. 3-5km, see section 5.9.2) this would be expected to occur later along the pipeline length if concrete coating was present, with a potentially negative effect on depacking times. The examination of the effect of concrete coating on pipeline operation including its linepacking capability would require detailed and dedicated modelling and goes beyond the scope of the current study. Nevertheless, this area is pointed out as an important area for future research.
7) Similarly, no thermal insulation is assumed for onshore pipelines as it is expected that construction standards and practises for CO_2 pipelines will be similar to those currently in use for natural gas pipelines (Wetenhall et al. 2017b).
8) For simplicity a flat topography is assumed in this work.

9) Transportation of pure CO_2 is assumed as the baseline scenario. Due to common expected impurities generally decreasing the density of the fluid, transportation of the pure CO_2 can be seen as the worst case scenario in regards to linepacking times (Aghajani et al. 2017, Wetenhall et al. 2014a), and pipeline de-packing times. Sensitivity case 4 (section 5.9.4) explores the effect of common impurities on achievable depacking times.
10) A constant ambient temperature of 10°C along the entire pipeline length is assumed in the baseline scenario. It is representative of yearly average near sea-bed temperatures in areas in the North Sea that are most conceivable for future CO_2 T&S networks (Summit Power 2017, UK MET Office 2014), and of annual average ground temperatures at around 1m depth (Busby 2015). Sensitivity case 1 in section 5.9.1 expands the analysis and explores variations of the results at deviating ambient temperatures.
11) A pipeline inlet temperature of 30°C is assumed consistent with Aghajani et al. (2017), Wetenhall et al. (2017) and Wetenhall et al. (2014b). Pipeline inlet temperature can have a significant effect on pipeline sizing (Race et al. 2012), flow velocities and pressure drops, particularly for relatively well insulated pipelines (e.g. onshore). Due to the rapid heat transfer and fluid temperature adjustment to ambient conditions at offshore pipelines within the first few kilometres (e.g. 3-5km in the pipelines modelled, as illustrated in section 5.9.2) line-depacking times are insensitive to pipeline inlet temperatures. However, as a caveat it should be noted that a possible concrete coating of offshore pipelines would slow down heat transfer, the effect of which is recommended to be examined in future studies.
12) A roughness value of 0.0457mm is selected as the recommended value for a commercial steel pipeline based on Mohitpour et al. (2003) and Boyce (1997). This is in line with other CO_2 pipeline modelling literature (McCoy and Rubin 2008, Vandeginste and Piessens 2008, Wetenhall et al. 2017b, Aghajani et al. 2017). It shall be noted that in particular new pipelines can, however, have roughness values significantly lower.
13) A pipe element length or discretisation length of 500m is assumed throughout all simulations. This is considered as a reasonable discretisation length since benchmark simulations have shown that line-depacking times vary by only up to 0.3-0.5% with discretisation lengths of 250m and 100m, respectively. The time discretisation within the gCCS or gPROMS modelling environment is adaptive and automatically reduces whenever necessary.

A summary of the core parameters and assumptions is provided in Table 5.3:

Table 5.3: Summary of modelling parameters in core scenarios.

Parameter	Value	Unit
Inlet temperature	30	°C
Minimum pressure	90	bar
Minimum platform arrival pressure	90	bar
Inlet Composition	Pure CO_2	-
Surrounding environment	Water	-
Roughness	0.0457	mm
Ambient temperature	10	°C
Topography	Flat	-
Valve closing time	Instantaneous	-
Pipe element length	500	m
Initial Conditions	Steady State	-

5.6. Validation of gCCS for line-packing purpose

An extensive validation of the modelling tool gCCS at normal pipeline operating conditions is performed by Hussein (2017). Hussein concludes that gCCS has difficulties in accurately predicting temperature profiles along pipelines when benchmarked against real operational data. The author attributes this to local variations in soil thermal conductivities. Overall, Hussein (2017) concludes that gCCS is a suitable tool for predicting dynamic flow rate responses (Hussein 2017). Further, gCCS offers more accurate physical property data than other commercial software, Aspen HYSYS and OLGA, in particular for modelling CO_2 mixtures with impurities (Hussein 2017).

To verify that gCCS is equally suitable for the modelling of linepacking and line-depacking processes, simulation results with gCCS are benchmarked against results obtained with the alternative software tool OLGA and presented in Aghajani et al. (2017). OLGA is a leading dynamic multi-phase flow simulation software package originally developed by Statoil and currently offered by Schlumberger (Aursand et al. 2013, Schlumberger 2018). It is widely regarded as the industry standard for the modelling of Oil and Gas transportation via pipeline (Aursand et al. 2013). A relatively recently product module upgrade allows the simulation of transportation of CO_2 (Ruden et al. 2013, Munkejord et al. 2013, Aursand et al. 2013).

Linepacking times for a large range of pipeline scenarios determined by Aghajani et al. (2017) with the software OLGA, as well as the times obtained by performing the equivalent simulations in gCCS are plotted in Figure 5.3. Two different pipeline types are considered in gCCS. Linepacking times for onshore pipelines in a dry sandy soil environment are taken from Van der Harst (2017; blue line). Linepacking times for the equivalent offshore pipelines are modelled as part of this study and are illustrated in green. For the detailed pipeline design specifications and other underlying modelling assumptions the reader is referred to Table B.1-Table B.2 in Appendix B1, or to Aghajani et al. (2017) directly. Whilst steel and soil heat transfer coefficients of 60.55W/m^2/K and 2.595W/m^2/K have been selected in Aghajani et al. (2017) in the OLGA pipeline simulation tool for representing

onshore pipelines (particular soil environment not specified), heat transfer coefficients in gCCS cannot be specified directly and are linked to the pipeline type and surrounding environment selected (e.g. water, sandy soil, clay environment).

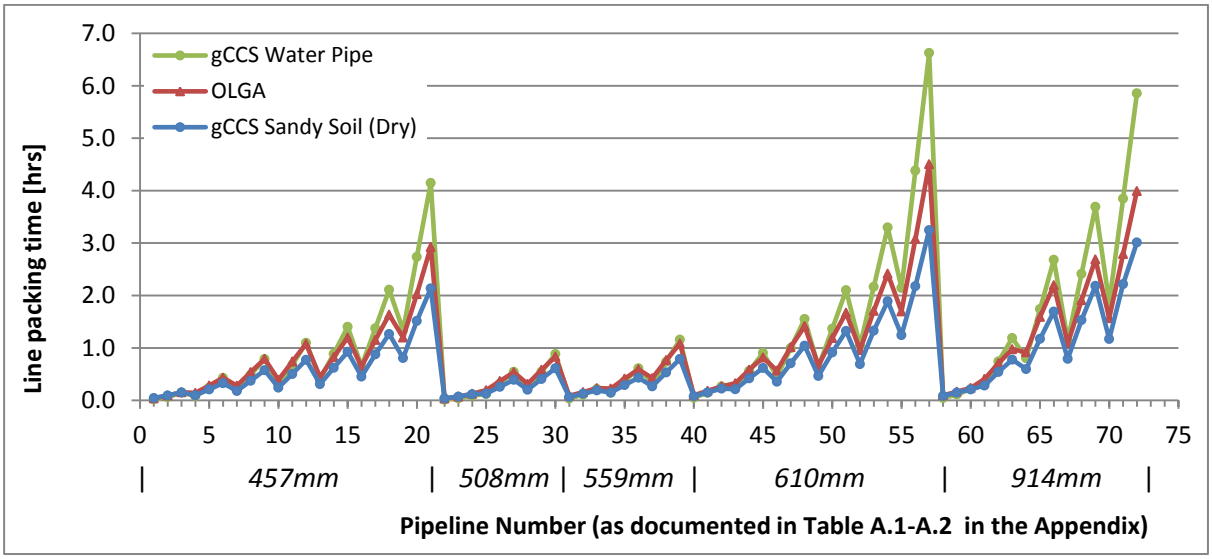

Figure 5.3: Linepacking times for a large range of pipeline types and flow scenarios as predicted by gCCS and OLGA (based on Aghajani et al. 2017, Van der Harst 2017, and own simulations).

It is recognised, finally, that a discrete number (i.e. 75) pipelines have been modelled in the respective process simulation tools. For better visualisation of the trends the datapoints in Figure 5.3 are, however, connected with a continuous line.

Overall, Figure 5.3: demonstrates that linepacking times predicted by OLGA are consistently in between times predicted by gCCS for the onshore and offshore pipeline. After assessing the sensitivities of various other factors on the results (i.e.: dynamics in momentum equation, property data, discretisation) it was concluded that different heat exchange characteristics are the dominant source for the discrepancies between linepacking times determined by OLGA and gCCS. This finding is confirmed by the fact that heat transfer characteristics are the only change between the simulations of onshore and offshore pipelines (blue and green graphs, respectively) in gCCS, which, however, lead to substantial differences in the results. The larger linepacking times can generally be achieved at pipelines with improved heat transfer characteristics. Whilst in OLGA heat transfer coefficients can be specified directly, this is only possible indirectly in gCCS by choosing from a limited set of available pipeline environments (e.g. soil type/onshore or offshore). It is, therefore, not possible to accurately replicate the results from OLGA in gCCS. Nevertheless, the observed trends and scales of linepacking times are consistent.

For the purpose of this work it is, therefore, concluded that gCCS is a suitable tool for assessing the linepacking as well as line-depacking times of CO_2 transportation pipelines.

5.7. Methodology

For completeness the detailled methodology according to which simulations are carried out in gCCS is described in this section. Figure 5.4 presents a schematic illustration of this process. As a first step a steady state simulation is initiated in gCCS at t=0s with assumptions as listed in sections 5.4 and 5.5. For example, the pipeline is operated at its highest allowable pressure level. Pressure drop and flow behaviour are calculated internally in the software according to the equations and methodology described in section 5.2. The steady state operation is continued for 10s in order to ensure the numerical stability of the simulation.

At t=10s the actual line-depacking operation starts. The pipeline inlet flowrate is reduced instantaneously (i.e. step function) at t=10s to either 0%, 10%, or 20% of nominal pipeline flow in line with the specific pipeline depacking scenario (for evaluated scenarios see section 5.4). Simultanously the original specification setting the pipeline outlet flow control valve to 'fully open' (i.e. stem position = 1) is deleted in the model to free up one variable. Instead, a constraint is placed in the model setting the pipeline outlflow to either 10%, 30%, or 50% of nominal flow, according to the specific pipeline depacking scenario (see section 5.4 for scenarios). Effectively the pipeline outlet valve in this way controls outflows and maintains them at the intended level. Since the momentum equation is set to steady state and no inertia is considered (see section 5.5 and Appendix B3 for justification) no sophisticated feedback control loop is required to maintain outflows at the specified level.

The simulation is continued until the discrepancy between pipeline outflows and inflows leads to a drop of the minimum fluid pressure in the pipeline, which is found towards the very end of the pipeline. Once the minimum fluid pressure in the pipeline reaches the minimum allowable pressure limit (i.e. 90bar for pure CO_2, as detailed in section 5.5) the simulation is stopped. The time at which the minimum pipeline fluid pressure reaches the minimum allowable pressure and after which no fluid can be extracted without violating the pipeline operating pressure constraint is called t_{end}. Once t_{end} has been determined the the line-depacking time for the respective pipeline scenario is calculated according to:

$$t_{line-depacking} = t_{end} - 10s \tag{9}$$

The execution schedule determining the modelling process in gCCS for the reference pipeline depacking simulation is provided in Figure B.1 in Appendix B2. A copy of the model as developed in gCCS has further been uploaded to the University of Edinburgh research archive to facilitate replication of the results, and to assist future studies with building on the model.

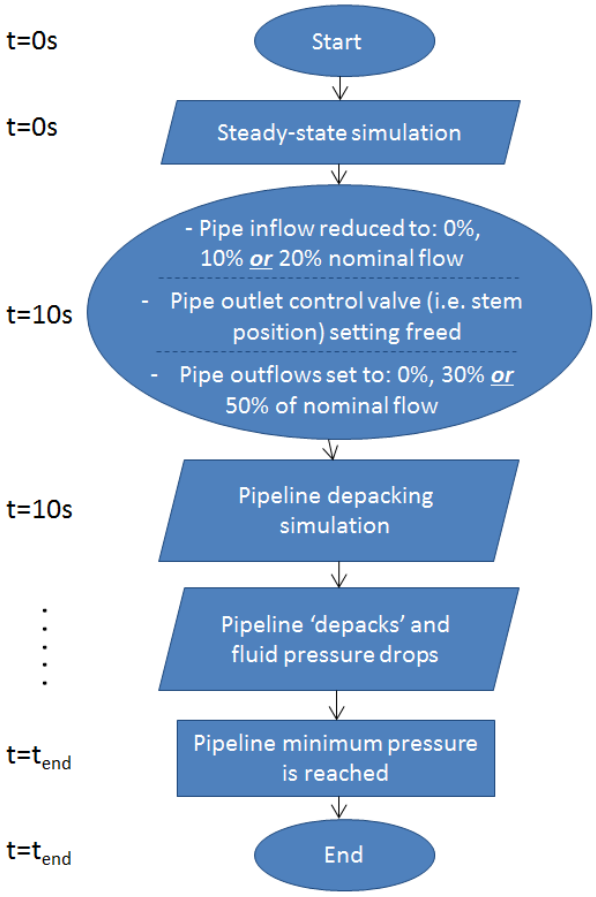

Figure 5.4: Schematics of the simulation schedule implemented in gCCS for carrying out pipeline depacking simulations.

5.8. Results

This section presents and discusses the results of the performed pipeline simulations. Due to the large number of obtained line-depacking times the results are categorised according to the assumed minimum outflows during the pipeline depacking process. Consequently the chapter is organised as follows: Subsection 5.8.1 illustrates available line-depacking times for minimum outflows of 50% of nominal pipeline flow during the process. Subsection 5.8.2 presents feasible line-depacking times at minimum outflows of 30% of nominal flow during the process. Subsection 5.8.3 shows line-depacking times when minimum allowable outflows are set to 10% of nominal flow.

Subsequent analysis is performed in subsection 5.8.4 to investigate the buffer storage capabilities of the individual pipeline types. To quantify both the sensitivities of line-depacking times and buffer storage capabilities of the pipelines to key influential design parameters Artificial Neural Networks (ANNs) are deployed in subsection 5.8.5. Finally, section 5.9 examines the sensitivities of further influential parameters on the results. Section 5.10 summarises and concludes.

5.8.1. Minimum outflows: 50% of nominal flow

Figure 5.5 illustrates line-depacking times for the range of considered pipeline diameters, lengths, MAOPs, and flow capacity utilisations, with a continuous pipeline outflow at 50% of nominal flow after the pipe inflow valve is shut at t=0s. Three inflow scenarios are considered. In Figure 5.5a zero inflows are assumed during the entire line-depacking process. A continuous inflow of 10% and 20% of nominal flow are assumed in Figure 5.5b and c, respectively. For the numerical values of the datapoints illustrated in the diagrams the reader is referred to Appendix B4.

As previously discussed in section 5.4 the MAOPs depicted in Figure 5.5 are indicative. Due to the discrete range of wall thicknesses routinely available from suppliers the MAOPs of the individual pipelines are effectively slightly above 150bar and 200bar, respectively. For a summary of the actual MAOP the reader is referred to Table 5.4.

Table 5.4: Indicative and actual Maximum Operating Pressure (MAOP) as well as corresponding wall thicknesses of considered pipeline types.

	OD 508mm		OD 610mm		OD 914mm	
	MAOP	wt	MAOP	wt	MAOP	wt
'150'bar	159.4 bar	12.5mm	150.8 bar	14.2mm	159.5 bar	22.5mm
'200'bar	204.1 bar	16.0mm	212.5 bar	20.0mm	212.7 bar	30.0mm

Figure 5.5a shows that line-depacking times vary strongly between the individual pipeline types. At outflows of 50% of nominal flow and zero inflows, feasible line-depacking times vary between 0.4-7.2hrs for the considered pipeline types. Line-depacking times increase approximately linearly with pipeline length. The increase is apparent since longer pipeline have higher internal volumes in which CO_2 can be stored when preparing the pipeline for the depacking process. Across all diameters a pipeline of 150km length offers approximately 2.5x times higher line-depacking times than an equivalent pipe of 50km.

In contrast to the high relative changes in line-depacking times at different pipeline lengths, times are comparable for different pipeline diameters. Although this might be surprising at first when considering the significantly higher volumes available in large diameter pipelines that can be used to store CO_2 as preparation for the de-packing process, this effect is counterbalanced by the fact that large diameter pipelines usually have significantly higher nominal flow rates. While a 914mm OD pipeline has a nominal flow of 36.5MTPA at a 100% flow capacity utilisation in this study, the equivalent flow for a 508mm OD pipeline is merely 8MTPA. When expressing both inflows and outflows during the line-depacking process as percentages of nominal flow the achievable line-depacking times turn out to be comparable for pipelines with different diameters. 508mm OD pipelines offer slightly higher line-depacking times than 610mm OD pipes, and notably higher times than 914mm pipes. This was found to be an effect of the heat leaving the fluid significantly faster in small diameter pipes than in pipelines with larger diameter. Due to the higher density at lower

temperatures smaller pipes can pack more CO_2 in preparation for the line-depacking process than large diameter pipeline, at least on a relative basis. Once the line-depacking process starts, smaller diameter pipelines have, hence, a relatively larger inventory to feed from than larger pipes.

Further, the gain in line-depacking times achievable with higher MAOPs and lower flow capacity utilisations at nominal load is substantial. Increases in line-depacking times of around 50%-100% are achievable, regardless of pipeline diameter, when increasing the MAOP from 150-200bar. Similarly, increases in line-depacking times of 100-150% are achievable when oversizing pipelines in terms of flow capacity (i.e. when nominal flow through the pipeline is only 50% instead of 100% of the design flow capacity for the respective pipeline diameter, see also section 5.4).

Notably, the relations between the line-depacking times for pipelines with different MAOPs and flow capacity utilisation (i.e. relation between the blue, red, green and purple curve) are significantly different at the respective pipeline diameters. Whilst the green and the red line are relatively equally arranged between the purple and blue line in the diagram at pipeline diameters of 508mm, they are comparatively closer together at diameters of 610mm. This is a direct consequence of MAOPs deviating from 150bar and 200bar, in order to respect the discrete range of wall thicknesses offered by pipeline suppliers (as previously explained in section 5.4, and illustrated in Table 5.4). Whilst the actual MAOPs of 508mm OD pipes are 159.4bar and 204.1bar, the corresponding values for 610mm OD pipes are 150.8bar and 212.5bar, based on the available pipeline sizes. The actual increase in MAOP is, hence, substantially larger for a 610mm OD pipe when comparing a '150bar' pipeline with a '200bar' pipeline than for a 508mm OD pipe. This directly reflects on the relations between the purple, green, red and blue lines for different pipeline diameters.

Figure 5.5b&c illustrate the available line-depacking times when inflows of 10% and 20% of nominal flow are sustained, respectively, during the line-depacking process. Outflows during the process are kept at 50% of nominal flow. Generally, the trends described for Figure 5.5a hold. As such, feasible line-packing times increase by around 150% for pipelines of 150km pipes compared to pipelines of 50km length. The sensitivity of depacking times to the outer diameters is low. In contrast, line-depacking times increase by around 50-100% when MAOP is increased from around '150'bar to '200'bar. Further, reducing the flow capacity utilisation at nominal flow from 100% to 50% increases line-depacking times by 100-150%.

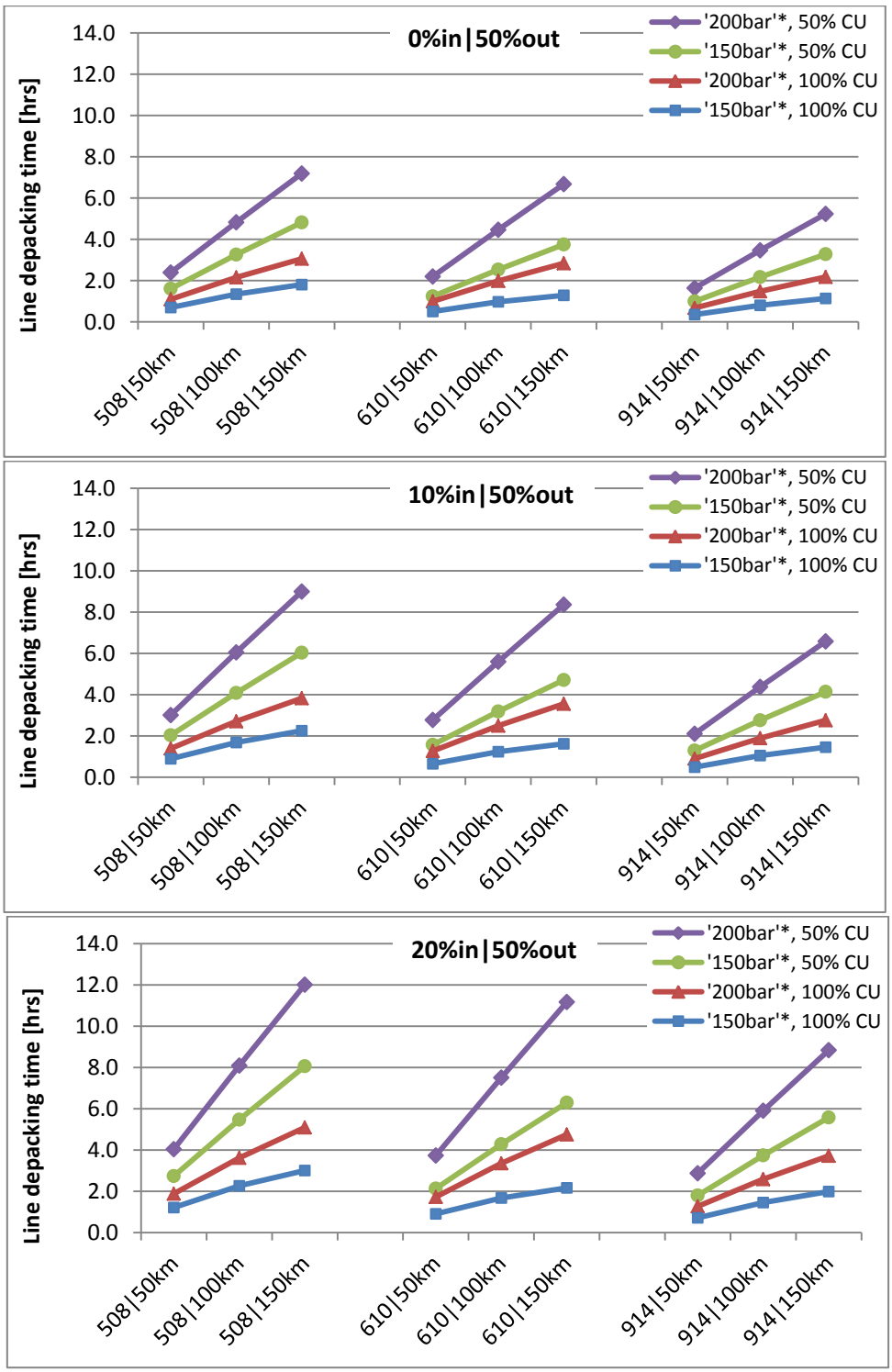

Figure 5.5: Line-depacking times for the range of considered pipeline types for outflows of 50% of nominal flow and inflows of 0% (top – a), 10% (middle – b) and 20% (bottom – c) of nominal flow. For pipeline Maximum Operating Pressures (MAOPs) and Capacity Utilisations (CU) of pipelines at nominal load see legend.

*The MAOPs presented in legend are only indicative - for actual MAOP see Table 5.4.

Comparing the results from Figure 5.5a and Figure 5.5b it can be observed that depacking times increase consistently by around 30% when a minimum inflow of 10% of nominal flow is sustained during the depacking process. This leads to line-depacking times of 0.5-9hrs being feasible dependent on the individual considered pipeline. When a minimum inflow of 20% of nominal flow is maintained during the depacking process, the achievable times increase by around 70% compared to the zero inflow case. Line-depacking times of 0.7-12hrs become feasible.

Overall, the analysis in this section shows that line-depacking times strongly depend on individual pipeline design parameters. There are a number of parameters with the potential to increase achievable line-depacking times by 50-150% each: Length, MAOP, flow capacity utilisation at nominal flow, and the inflow scenario during the depacking process. If the positive effect of several of these design parameters on the depacking times are exploited simultaneously, substantial depacking times of several hours can be achieved, even at relatively high outflows of 50% of nominal flow and short pipeline lengths (i.e. 50km). Line-depacking times of several hours can provide T&S system operators with significant operational flexibility and flow balancing capabilities. By exploiting the buffering capabilities of pipelines, operators of T&S systems could smoothen out CO_2 flows within the transportation system, providing relatively constant outflows to the downstream injection wells and storage sites even in the face of variable inflows. Further, operators could chose to avoid/bridge critical periods of low flow periods at the injection and storage sites by feeding from CO_2 temporarily stored within the pipeline.

5.8.2. Minimum outflow: 30% of nominal flow

This section examines achievable line-depacking times when outflows of 30% of nominal flow need to be sustained during the process. Figure 5.6a displays depacking times for the range of pipeline types considered when zero inflows are provided during the process. Diagrams Figure 5.6b-c display the corresponding depacking times if inflows of 10% and 20% of nominal flow are sustained during the process, respectively. For reasons of consistency the axes across all diagrams in Figure 5.6 are aligned, although it is realised that this obscures comparison of some of the results with Figure 5.5.

Overall, the trends and relationship between Figure 5.6 are very similar to the ones observed in Figure 5.5 in the previous section. They are, therefore, not be repeated in detail.

Due to the lower levels of outflows depacking times in Figure 5.6 are, nevertheless, higher than in Figure 5.5. While they are consistently only around 70% higher in the zero inflow scenario, this gap even substantially widens in higher inflow scenarios as a consequence of the strongly reduced relative discrepancy between inflows and outflows. Consequently line-

depacking times of up to 18hrs and 36hrs are achievable when inflows of 10% and 20% of nominal flow are maintained, respectively, during the depacking process.

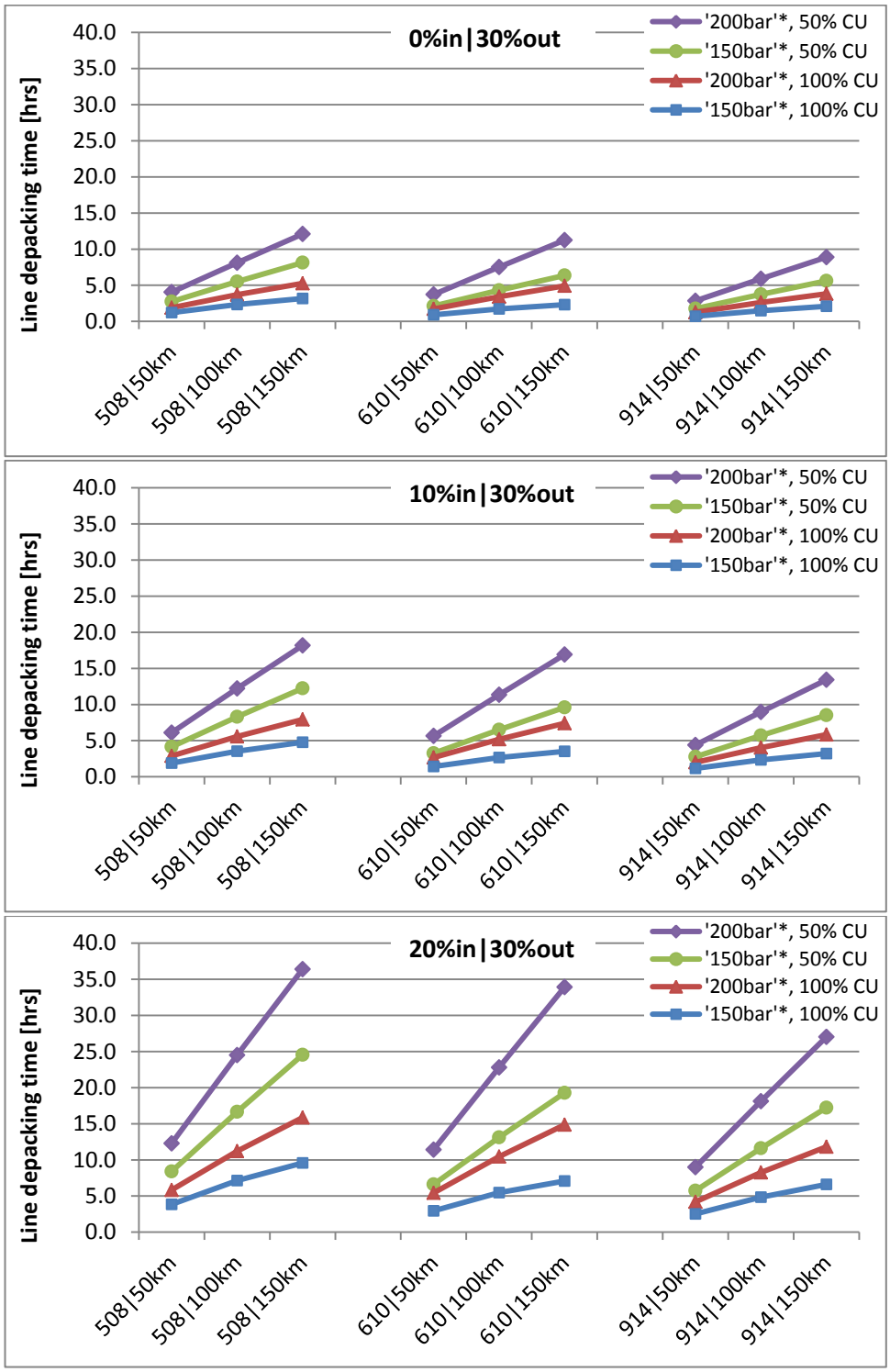

Figure 5.6: Line-depacking times for the range of considered pipeline types for outflows of 30% of nominal flow and inflows of 0% (top – a), 10% (middle – b) and 20% (bottom – c) of nominal flow. For pipeline Maximum Operating Pressures (MAOPs) and Capacity Utilisations (CU) of pipelines at nominal load see legend.

*The MAOPs presented in legend are only indicative - for actual MAOP see Table 5.4.

In general, this section shows that line-depacking times are very sensitive to the level of outflows during the depacking process. Dependent on the inflows, the achievable depacking times can be extended by 70-210% if outflows of only 30% instead of 50% of nominal flow need to be maintained during the process. It is, therefore, of significant importance to determine a cost-effective level of minimum flows that should be respected in CO_2 injection wells for mitigating integrity risks. If minimum required pipeline outflows are approx. 30% of nominal flow, line-depacking times of 10-36hrs are feasible, especially if a level of inflow into the pipe can be sustained during the process.

5.8.3. Minimum outflow: 10% of nominal flow

Figure 5.7 shows line-depacking times for the range of considered pipelines at required minimum pipeline outflows of 10% of nominal flow, and zero inflows during this period. The trends and relations between the datapoints are generally very similar to the ones presented in previous Figure 5.5 and Figure 5.6. At outflows of 10% of nominal flow and zero inflows depacking times of 2.5-36hrs are achievable, dependent on the specific pipeline scenario.

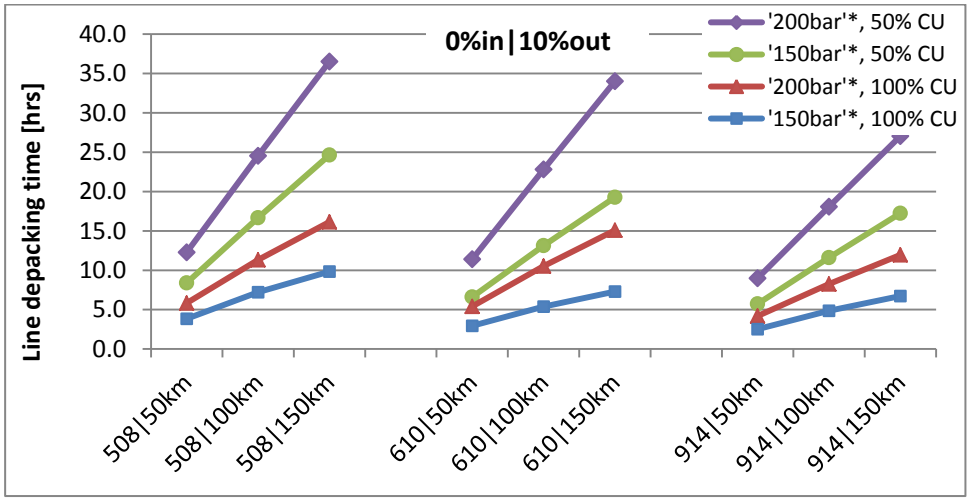

Figure 5.7: Line-depacking times for the range of considered pipeline types for outflows of 10% of nominal flow and inflows of 0% (top – a), 10% (middle – b) and 20% (bottom – c) of nominal flow. For pipeline Maximum Operating Pressures (MAOPs) and Capacity Utilisations (CU) of pipelines at nominal load see legend.

*The MAOPs presented in legend are only indicative - for actual MAOP see Table 5.4.

Notably, the determined line-depacking times in Figure 5.6c and Figure 5.7 look very similar. This suggests that depacking times are primarily a function of the discrepancy between and inflows and outflows, and only a very minor function of the actual relative levels of inflows and outflows. This finding is further confirmed in the following subsections, as well as when comparing the results in Figure 5.5c and Figure 5.6a.

5.8.4. Buffer storage capabilities of pipelines

In order to compare the interim storage capabilities of the considered pipeline types to possible alternative flow balancing options (e.g. storage vessels or interim storage in geological formations as suggested by Kaufmann et al. 2016) the amounts of CO_2 temporarily stored in the pipelines is illustrated in Figure 5.8. The storage volumes are calculated by integrating the discrepancy of inflows and outflows over the total achievable line-depacking periods for the individual pipeline scenarios (i.e. according to formula 10). The calculated storage capacities henceforward will be referred to as the available and effective 'working capacities' of the pipelines, as they describe the amount of CO_2 that can be packed in a fully depacked pipeline, or vice-versa depacked from a pipeline with full inventory, without violating max. or min. pressure limits.

$$\int_{t=0}^{t=Max\_Dep\_t} (Outflows - Inflows)\, dt = Working\ Capacity \tag{10}$$

Where *t* *is time*
Max_Dep_t *is maximum possible line-depacking time in the investigated pipeline scenario*

Figure 5.8 shows that larger diameter pipelines can temporarily store significantly more CO_2. This is intuitive due to the substantially larger available storage volumes. Whilst 914mm OD pipelines have temporary storage capacities of around 890-5600kt, dependent on the respective design (e.g.: length, MAOP, flow capacity utilisation during nominal load), this capacity is lower for 610mm OD (400-2500kt) and 508mm OD (330-1650kt) pipelines. The storage potential of pipelines increases approximately proportional with length.

Although counterintuitive at first, pipelines with identical diameters and MAOPs that only deviate in their flow capacity utilisation at nominal load have slightly different working capacities. These differences can be attributed to the different pipeline flow and inventory conditions at the start of the line-depacking process at t=0. Due to the lower flow velocity in pipelines that use only 50% instead of 100% of their maximal flow capacity at nominal flow conditions, more CO_2 can be initially packed into the pipe as preparation for the depacking process. This is an effect of the lower flow velocities at steady state flow conditions that lead to lower pressure drops in the pipe, and as a result a more even pressure distribution along the pipeline closer to the MAOP compared to a pipeline with higher pressure drops. In this way densities along the full pipeline length are higher, and as a results also the inventory of CO_2 that later during the depacking process can be used to maintain outflows even during periods of low or zero inflows. This effect also explains the increasing discrepancy in working capacities for equivalent OD and MAOP pipelines at higher lengths: Due to the higher absolute pressure drops in longer pipelines the pressure

distribution particularly towards the end of the pipes deviates increasingly from the MAOP, locking the potential to increase densities and hence inventories by maintaining the high pressure levels.

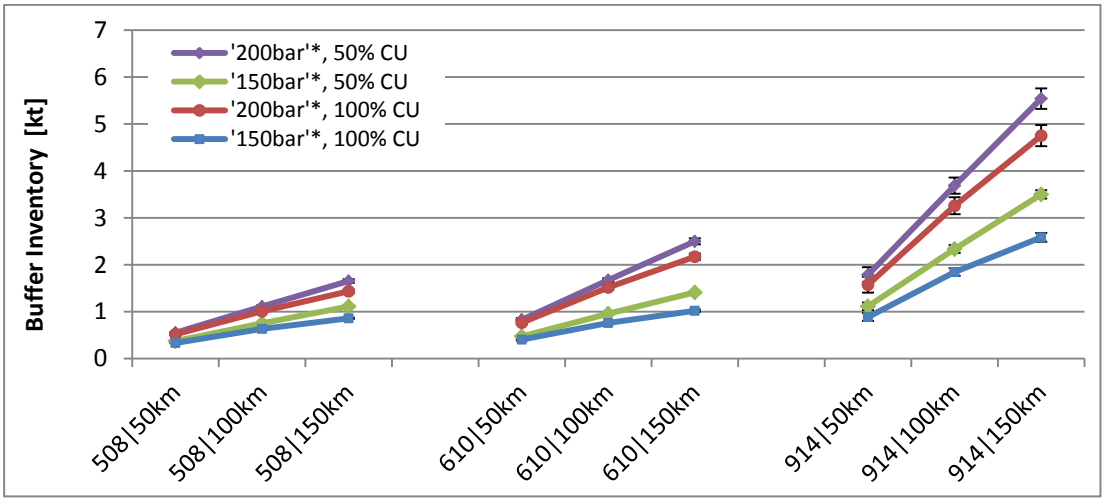

Figure 5.8: Maximum working capacity of pipelines indicating the sizes of equivalent storage tank vessel that could be installed for achieving similar flow balancing capabilities. For pipeline Maximum Operating Pressures (MAOPs) and Capacity Utilisations (CU) of pipelines at nominal load see legend.

*The MAOPs presented in legend are only indicative - for actual MAOP see Table 5.4.

Finally, the error brackets for every data point indicate that the inflow/outflow regime during the line-depacking process marginally affects the available working capacities. This can be explained by low discrepancies between inflows and outflows during the depacking process requiring only relatively low driving forces i.e. pressure differentials over the entire length of the pipeline. As a consequence the pressure distribution at the end of the line-depacking process is more evenly distributed and closer to the minimum allowable pressure (90bar) along the whole length of the pipe, maximising possible pipeline inventory depletion and as an effect achievable depacking times compared to when high driving forces (i.e. pressure differentials) are required for pushing out larger amounts of CO_2.

The fact that the working capacity at offshore pipelines is only marginally affected by the inflow and outflow regime during the depacking process is a very important finding in this section. It forms the basis for a simplified pipeline buffer tank model that is adopted in Chapter 6 for exploring the extent to which linepacking can be used for mitigating the number of annual low flow periods injection wells face as a consequence of variable CO_2 flows being fed into T&S networks.

5.8.5. Artificial Neural Network (line-packing times and storage inventories)

Aghajani et al. (2017) finds in a study investigating linepacking times for a large range of pipeline scenarios that the simultaneous integration of all key design parameters into correlations describing linepacking times could not be achieved with simple regression analysis techniques. This is a consequence of the underlying non-linearities in the results and co-dependencies of the input parameters. The benefit of using sophisticated regression analysis techniques for the purpose of the present study would also be limited, since line-depacking times have only been determined for a low number of discrete design parameters, for example for MAOPs ('150'bar and '200'bar) and for flow capacity utilisations at nominal load (100% and 50%). Even sophisticated regression analysis techniques would not be able to take into consideration some of the non-linearities observed by Aghajani et al. (2017). Instead of using sophisticated regression analysis techniques this study, hence, relies on Artificial Neural Network (ANN) analysis to further quantify the sensitivity of line-depacking times, as well as working capacities, to the key design parameters for the range of considered pipelines. It should be noted that while the dataset with around 252 datapoints is relatively small for training neural networks it has been found that the generated networks have a relatively high predictive capability (see results below in this subsection). They are hence considered sufficient for demonstrating the sensitivity of line-depacking times and working inventories to key influential design parameters of the considered pipelines.

An ANN is a statistical machine learning tool that performs multifactorial analysis on a series of inputs to predict an output. The underlying learning algorithm has originally been inspired by the behaviour of biological neurons in the brain and central nervous system (McCulloch and Pitts 1990, Rosenblatt 1958). An ANN is constructed from several layers of neurons: the input layer, typically a number of hidden layers, and the output layer. In the context of this work the input layer contains information about the pipeline dimensions, the flow capacity utilisation at nominal load, and the inflow|outflow regime during the depacking process.

The output layers consist of information about the achievable line-depacking times, or the working capacities, respectively. By using predetermined 'learning rules' ANNs learn to 'weigh' connections as well as biases between inputs and outputs when being presented with a training dataset. In an iterative process the determined weights and biases are refined. The self-adaptive nature of ANNs enables them to capture complex non-linear relationships between dependent and independent variables without prior knowledge. As such, ANNs are used for a large variety of application areas that have a large number of inputs with complex relationships to each other, as well as to the output.

For the construction of ANNs in this study the commercial MS Excel add-in NeuralTools (version 7.5) has been used developed by Palisade Corporation. NeuralTools is a user friendly and leading tool in its domain regularly used in the academic community (Brooks

and Tucker 2015, Mossalam and Arafa 2017, Vouk et al. 2011, Zhao and Zhao 2017). Whilst there are a large number of network structures available that could be considered NeuralTools specifically supports General Regression Neural Networks (GRNNs) and Multi-Layer Feed-Forward Networks (MLFN) for numeric predictions and function approximations (Palisade Corporation 2015). Both networks types vary in their structure and the activation functions used in the individual nodes to process information from previous nodes and calculate an output value to pass on:

GRNNs

- Consist of four layers, with the number of nodes in the input layer corresponding to the number of input parameters. The second layer, also called pattern layer, consists of as many neurons as there are training cases. The third layer consists of two neurons, the numerator that adds up all the weight values multiplied by the actual target value for each pattern neuron, and the demoninator sums up all the weights of the hidden neurons. Finally, the single neuron in the output layer determines the predicted value by dividing the numerator by the denumerator (Brooks and Tucker 2015, Palisade Corporation 2015).
- The transfer function commonly used in the neurons in the hidden layers is the Gaussian activation function (Al-Mahasneh et al. 2018, Celikoglu 2006).

MLFN

- Consists of the input layer with as many neurons as input parameters, usually 1-2 hidden layers with a varying number of neurons, and the output layer with again one neuron (Brooks and Tucker 2015). Whilst there is technically no restriction on the number of hidden layers most functions, particularly continous functions, can be approximated with relatively high accuracy with only one hidden layer (Zhang and Morris 1998, Cybenko 1989). NeuralTools therefore uses one hidden layer as default. The number of neurons in the hidden layer can further have a large influence on the predictive capabilities of the MLFN. NeuralTools allows either selecting the number of neurons in the hidden layer manually, or searching for the optimal number of nodes by comparing the alternative nets (Palisade Corporation 2015).
- As the transfer function in MLFN networks and for producing outputs of the nodes in the hidden layers NeuralTools uses a sigmoid (S-shaped) activation function, and more specifically the hyperbolic tangent function (Palisade Corporation 2015). The identity function is used as the actication function for the output node (Palisade Corporation 2015).

By selecting the 'Best Fit Method' option NeuralTools trains a number of neural networks with the supported network structures (i.e. GRNN, MLFN with varying number of nodes in hidden layer), compares them based on their predictive capabilities of the data, and suggests the best net based on the residual error analysis. For a more detailed description

about the construction of ANNs the reader is referred to Palisade Corporation (2015, 2018), and Livingstone (2009).

By learning to weigh the connections and biases between the individual neurons in the network, NeuralTools is able to establish the sensitivities of line-packing times to the key influential design parameters, as demonstrated in Figure 5.9. Every generated network is trained by NeuralTools until its convergence after a maximum runtime of 4hrs. It was found by a software internal predictive error analysis that a MLFN with 2 nodes in the single hidden layer is best for predicting line-depacking times based on the provided line-depacking data. In contrast, a GRNN was found to be best for predicting pipeline working capacities based on the input data. Both of these selected 'best nets' will be referred to as ANN_{time} and $ANN_{working\_cap}$ in the following, respectively. Since NeuralTools does not provide prediction equation and biases of the generated networks the numeric input parameters used for training the neural networks are summarised in Table B.3 - Table B.8 in Appendix B4 to facilitate replication of the networks. Further summary tables with additional information about the generated neural networks are provided in Figure B.3 in Appendix B4.

Figure 5.9 demonstrates that the order of sensitivities of depacking time to the key influential parameters is similar to what has been observed in the previous subsections. Both length and capacity utilisation affect linepacking times twice as much as the MAOP, and around 3 times as much as the outer diameter. Since the length of the pipeline is frequently predetermined by the distance between the CO_2 source (or collection point) and the sink (i.e. storage site), this leaves the MAOP, the capacity utilisation of a pipeline, and the OD as free variables available for manipulation when designing pipelines in order to achieve the desired line-depacking times. Interestingly, the flow regime (i.e. inflow|outflow regime) during the depacking process scenario has the greatest effect on the depacking times. This underlines the importance of establishing in more detail the required levels of minimum flow rates at the injection wells for mitigating or avoiding integrity hampering effects.

Figure 5.10 demonstrates that the sensitivities are differently distributed for working inventory. The most influential factors are, by decreasing order, the outer diameter, the pipeline length, the MAOP, the pipe capacity utilisation during nominal flow, and finally the inflow and outflow regime during the depacking process. It shows that the pipeline design parameters are the dominant factors deciding on the pipeline working capacity. Similarly to what has been observed and described in more detail in section 5.8.4 the correlation between the pipeline working capacity and the inflow and outflow regime during the depacking process is very small.

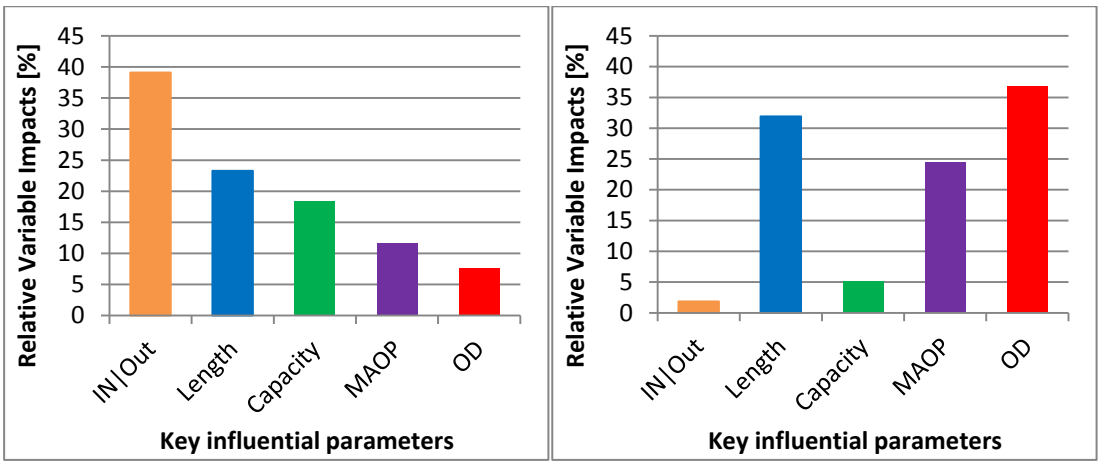

Figure 5.9 (left): Sensitivities of line-depacking times to the key influencing parameters as determined by ANN_{time} (MLFN structure with one hidden layer with two nodes).
Figure 5.10 (right): Sensitivities of working capacity to the key influencing parameters as determined by $ANN_{working\_cap}$ (GRNN structure).

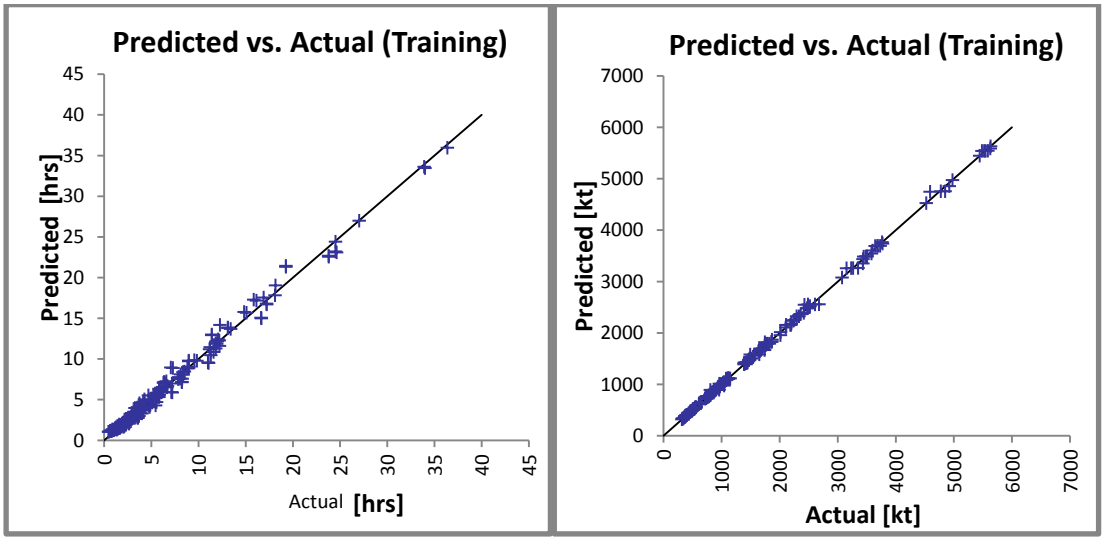

Figure 5.11 (left): Comparison of calculated line-depacking times to times predicted by ANN_{time}. The y=x line indicates perfect agreement.
Figure 5.12 (right): Comparison of calculated working capacity to working capacity predicted by $ANN_{working\_cap}$. The y=x line indicates perfect agreement.

To test the accuracy of the generated ANNs the training datasets of line-depacking times and working capacities (and associated input parameters) is compared in Figure 5.11 and Figure 5.12 with the values that the ANNs would predict. The inserted x-y lines indicate perfect agreement between the predicted and the actual values. Both graphs show good agreement of the predicted values with the actual values. No significant trends indicating overprediction or underprediction can be observed. When testing the ANNs against 15% of the datapoints of the dataset that have been retained from the training procedure, it was observed that the ANN_{time} could predict line-depacking times within 0.5hrs of the actual value in 74% of the cases, and within 1hrs in 95% of the cases. Similarly, $ANN_{working\_cap}$ could predict working capacities within 50kt of the actual values in 77% amount of the cases, and

within 100kt in 85% of the cases. Further graphs illustrating the predictive capabilities of both ANNs can be found in Appendix B5.

5.9. Sensitivity Cases

The above sections have illustrated line-depacking times, working capacities, as well as their sensitivities to a number of key influencing design parameters. The following section expands the analysis and explores how line-depacking times are affected by a range of other parameters that have been assumed constant over the previous sections.

5.9.1. Water Temperature

The temperature of the surrounding water influences the heat transfer between the pipeline and the environment. By influencing the temperature profile of the fluid along the pipeline it has the ability to change the fluid's temperature dependent physical properties such as compressibility and density. This has a direct impact on the achievable line-depacking times. In the core scenarios a surrounding water temperature of 10°C is assumed to represent average near seabed temperature for UK waters in areas with the greatest potential for CO_2 T&S network deployment, as well as average UK ground temperature at approximately 1m depth (Busby 2015). Two sensitivity temperatures of 6°C and 14°C are investigated in this section. These sensitivity temperatures were chosen based on seasonal near seabed temperature variations for areas in the southern and northern North Sea with the largest potential for CO_2 T&S networks, as illustrated in section 5.3. A map illustrating historical (from 1961-1990) and predicted (for 2070-2098) near seabed temperatures for UK waters is provided in Figure 5.13.

Figure 5.14 shows the resulting achievable line-depacking times at different surrounding water temperatures for the reference pipelines with MAOPs of around '150'bar and '200bar', respectively, and flow capacity utilisations of 100% and 50% at different lengths and outer diameters. An inflow|outflow regime during the depacking process of 0% and 50% of nominal flow is assumed, respectively. It can be seen that line-packing times vary consistently around +/-15% at temperature deviations of +/-4°C. In fact higher line-depacking times are achievable at higher surrounding water temperatures. This can be explained by the higher compressibility of CO_2 at higher temperatures. Even though only smaller amounts of CO_2 (mass basis) can be fitted into the pipeline during the linepacking preparation stage with higher surrounding water temperatures (i.e. lower density of CO_2 at higher temperatures), the higher compressibility of CO_2 at these elevated temperatures enables sustaining a sufficiently high driving force for longer periods of time during the depacking process. This is necessary for pushing out the required quantities of fluid through the outlet during the entire duration of the process.

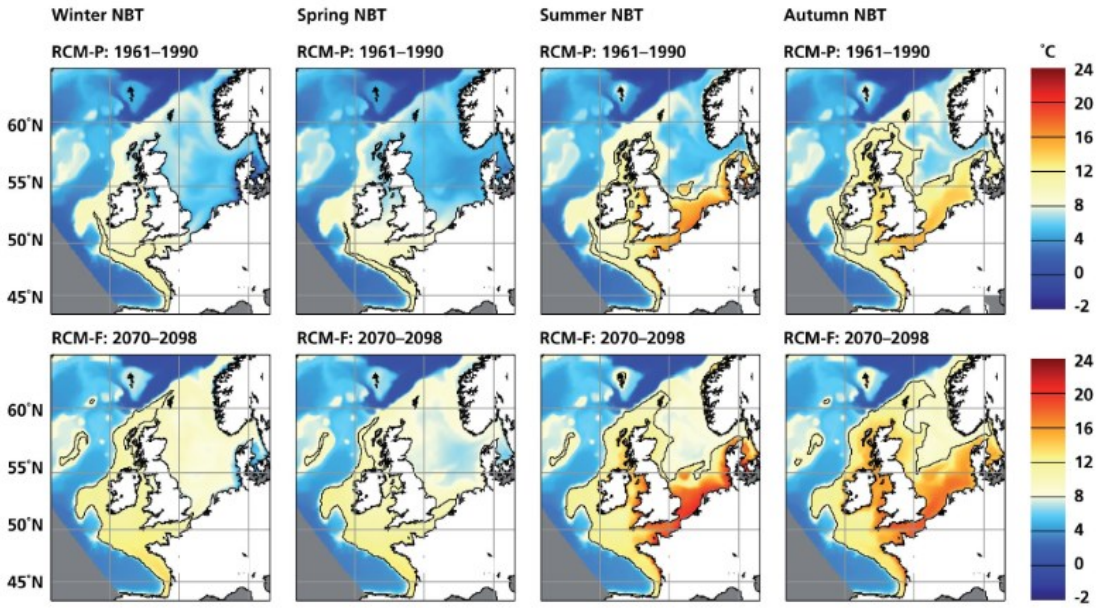

Figure 5.13: Seasonal mean Near sea-Bed Temperature based on historical data (RCM-P; 1961-1990) and as predicted for the end of the century (RCM-F; 2070-2098; UK Climate Projections 2014).

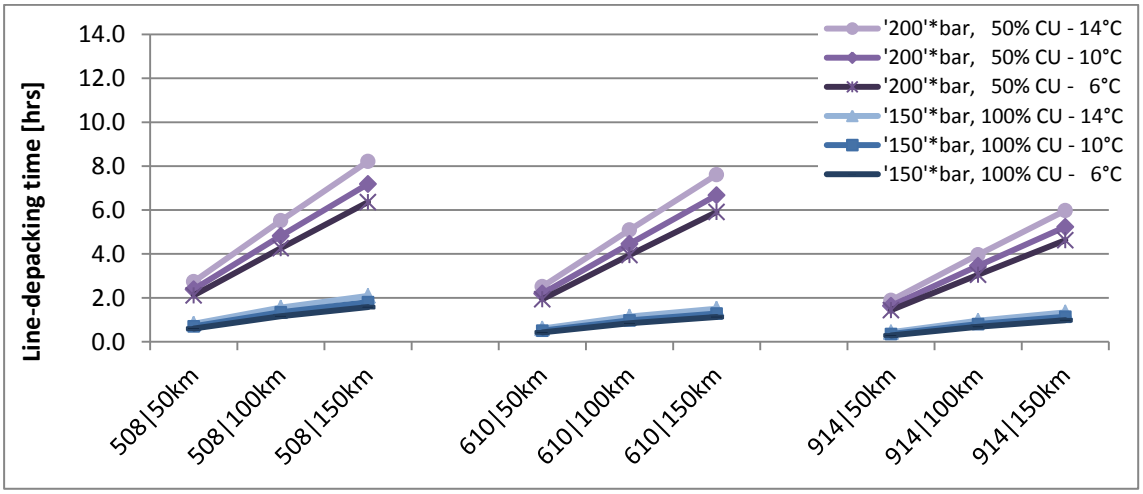

Figure 5.14: Line-depacking times for water temperatures of 6°C, 10°C and 14°C for reference pipelines of '150'bar ('200'bar) Maximum Operating Pressure (MAOP) and 100% (50%) flow Capacity Utilisation (CU), respectively. Outflows (inflows) during depacking process are maintained at 50% (0%) of nominal flow. For interpretation of colours see legend.

*The MAOPs presented in legend are only indicative - for actual MAOP see Table 5.4.

Figure 5.15 explores possible effects of varying water temperatures on line-depacking times under different inflow|outflow regimes during the depacking process. For equivalent pipeline size and flow parameters the diagram confirms that the achievable line-depacking times are around 15% higher at increased (+4°C) surrounding temperatures and 15% lower at decreased (-4°C) water temperatures, regardless of inflow|outflow regime during the depacking process. The general trends between the data points are similar to the ones discussed in the core analysis section of this paper (section 5.8).

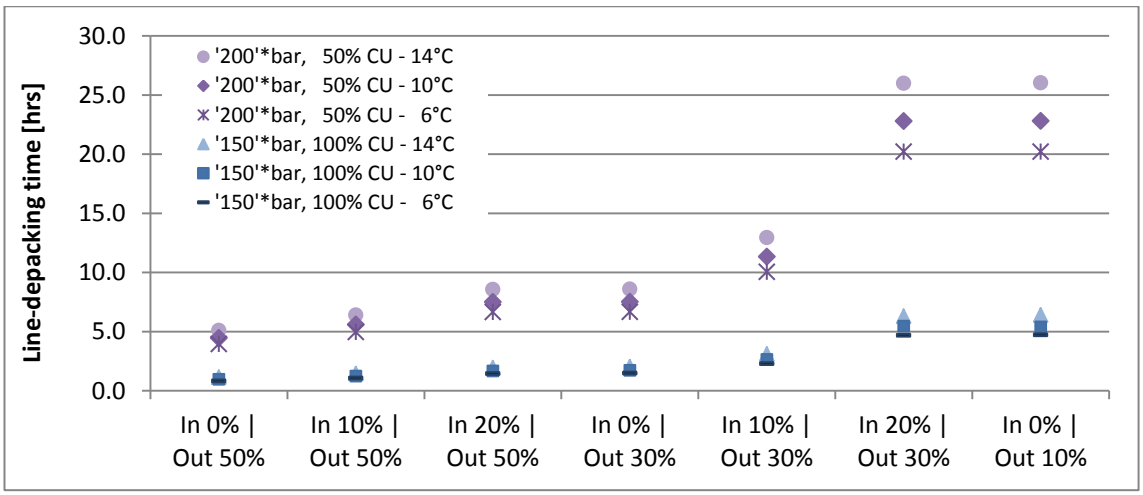

Figure 5.15: Line-depacking times for water temperatures of 6°C, 10°C and 14°C for reference pipelines of 610mmOD, 100km, '150'bar ('200'bar) Maximum Operating Pressure (MAOP) and 100% (50%) flow Capacity Utilisation (CU) for different inflow|outflow scenarios after t=0. For interpretation of colours see legend.

*The MAOPs presented in legend are only indicative - for actual MAOP see Table 5.4.

5.9.2. Onshore versus Offshore

Heat transfer at CO_2 pipelines varies significantly dependent on the type of surrounding material. For example, due to the different heat transfer characteristics the temperature profile within the pipeline deviates substantially in different environments even at similar flow conditions. While the fluid temperature in the reference offshore pipeline falls close to ambient levels within the first approx. 4-5km (see Figure 5.16; blue curve), temperatures decline substantially slower in the equivalent onshore pipelines surrounded by either dry or soaked sandy soil (red and green curve, respectively). In the onshore pipeline in a dry sandy soil environment (red curve) temperatures drop slowest and only by around 5°C over the entire pipeline length as a consequence of the very slow heat transfer with the environment. Similarly, in the equivalent onshore pipeline surrounded by soaked (wet) sandy soil (green curve) with slightly faster heat transfer characteristics temperatures drop only by around 10°C and do not reach ambient levels even after 100km. The temperature slopes are comparable to the ones reported in other studies for onshore dense phase CO_2 pipelines (Witkowski et al. 2014, Mechleri et al. 2017a).

To expand on the analysis, line-depacking times are compared for offshore and onshore pipelines. It is assumed that onshore pipelines are surrounded by sandy soil that is either dry or soaked (i.e. wet; Wetenhall et al. 2014). Figure 5.17 shows the calculated line-depacking times for the reference pipelines with MAOPs of around '150'bar and '200bar', respectively, and a flow capacity utilisations of 100% and 50% at different lengths and outer diameters. An inflow|outflow regime during the depacking process of 0%|50% of nominal flow is assumed.

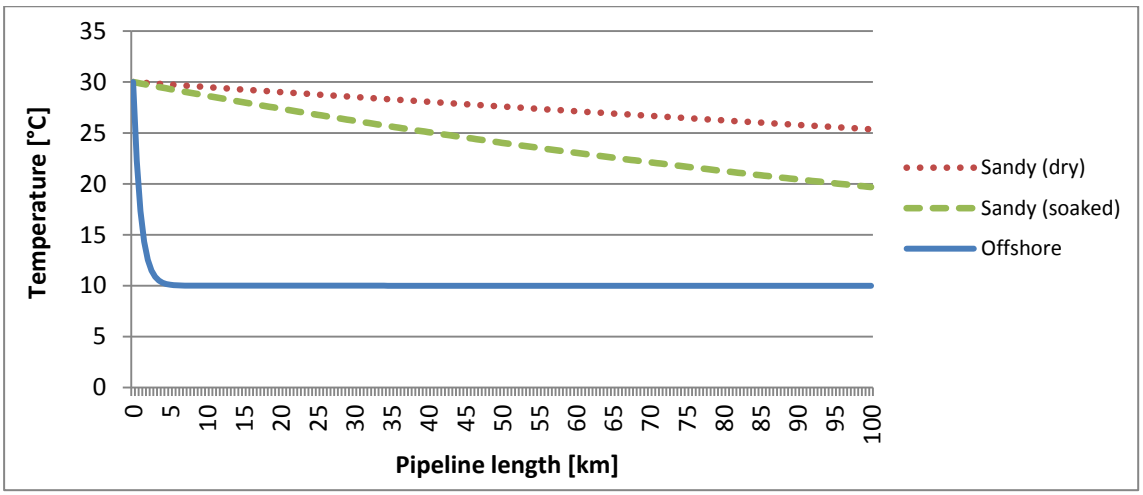

Figure 5.16: Temperature profile at initial steady state conditions at t=0 at start of line-depacking process for reference pipeline (610mm outer diameter, 100km length, '150'bar maximum operating pressure, 100% flow capacity utilisation).

The figure shows that line-depacking times drastically decrease for onshore compared to offshore pipelines. The 50-70% reduction in depacking times for onshore compared to offshore pipes can be attributed mainly to the very different initial steady state conditions at t=0, as illustrated in the above Figure 5.16. With heat leaving offshore pipes much quicker this decreases the temperature and, hence, increases the densities along offshore pipelines, freeing space to fit higher initial inventories of CO_2 during the linepacking preparation phase. The substantially higher initial inventories in offshore pipelines at t=0 overcompensate for the reduced compressibilities at lower temperatures and hence reduced driving forces (to push CO_2 through the outlet) during the depacking process, leading overall to dramatically higher achievable line-depacking times for offshore compared to onshore pipelines.

Interestingly, pipelines in soaked sandy soil environments with comparatively better heat transfer characteristics offer slightly lower line-depacking times than their equivalents in dry sandy soil environments. This appears to be caused by the slightly higher initial inventory of pipelines in soaked sandy soil environments not being able to compensate for the reduced driving force (due to lower temperatures, densities and compressibilities) during the depacking process. Line-packing times, therefore, appear to be a compromise between the initial inventory that can be built up (which is generally higher in pipes with good heat transfer characteristics as temperature and densities are lower), and the compressibility of the fluid in order to maintain high driving forces even during the line-depacking process which is the case in pipelines with better isolation and hence higher temperatures.

It can be observed that the drop in achievable line-depacking times (offshore versus onshore) is less strong for the large pipeline diameter (914mm) when compared to the drop for significantly smaller diameter pipes. This can be explained by the strongly increased volume flows in the 914mm OD pipelines impeding the very quick temperature adjustment

to ambient conditions even for the offshore pipes. Less space is freed for a high initial inventory and, hence, the large diameter offshore pipe has less of an advantage over the comparable onshore pipelines.

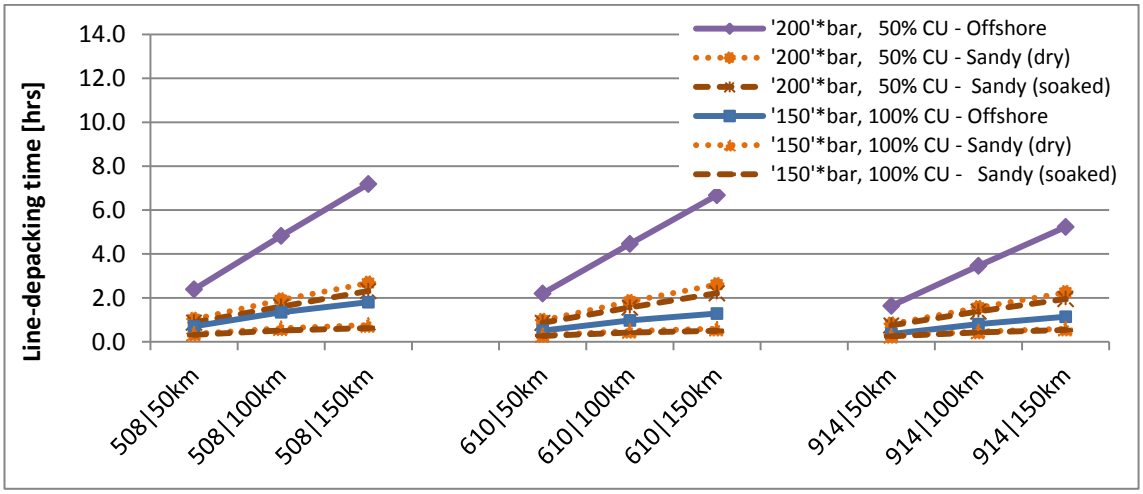

Figure 5.17: Line-depacking times for different surrounding environments for reference pipelines of '150'bar ('200'bar) Maximum Operating Pressure (MAOP) and 100% (50%) flow capacity utilisation (CU), respectively. Outflows (inflows) during depacking process are maintained at 50% (0%) of nominal flow. For interpretation of lines and colours see legend.

*The MAOPs presented in legend are only indicative - for actual MAOP see Table 5.4.

To examine further trends in the results line-depacking times are analysed for different inflow|outflow regimes. The analysis is performed for two reference offshore and onshore pipelines, respectively:

- 610mm OD, 100km length, '150'bar MAOP, 100% flow capacity utilisation;
- 610mm OD, 100km length, '200'bar MAOP, 50% flow capacity utilisation.

Figure 5.18 shows that across all inflow|outflow regimes line-depacking times are between approx. 50-70% lower for onshore than for offshore pipes. Nevertheless, deviating from the trend described in sections 5.8.2 and 5.8.3, the feasible depacking times for onshore pipelines are substantially lower in the 0%inflow|10%outflow flow regime scenario compared to the 20%inflow|30%outflow scenario. Similarly, times are lower for the 0%inflow|30%outflow flow regime scenario than for the 20%in|50%out scenario.

It has been concluded for offshore pipes that line-depacking times are largely a function of the difference between inflows and outflows and not the actual flow levels (relative to nominal flow, also described in sections 5.8.2 and 5.8.3). This, it appears, is not valid for onshore pipelines. Onshore pipelines clearly benefit from a minimum level of inflows when it comes to line-depacking times, even when the difference between inflows and outflows during the depacking stage is identical.

The underlying reason is that at initial steady-state starting conditions the temperature profile along onshore pipes never reaches ambient conditions (see also Figure 5.16). During the line-depacking process, particularly with low or zero inflows and hence heat supply, the fluid in the onshore pipeline cools off substantially, leading to lower temperatures, densities, compressibilities, and consequently significantly lower driving forces for pushing out CO_2 through the outlet. As a result feasible line-depacking times drop. Having a minimum inflow, and as such a 'heat source' during the depacking process is, therefore, particularly valuable for onshore pipelines. Due to temperatures having reached ambient conditions along most of the offshore pipeline already at initial steady state conditions, offshore pipelines do not cool off significantly during the de-packing process. Hence, line-depacking times of offshore pipelines are not impaired by a heat flux out of the pipeline during the process.

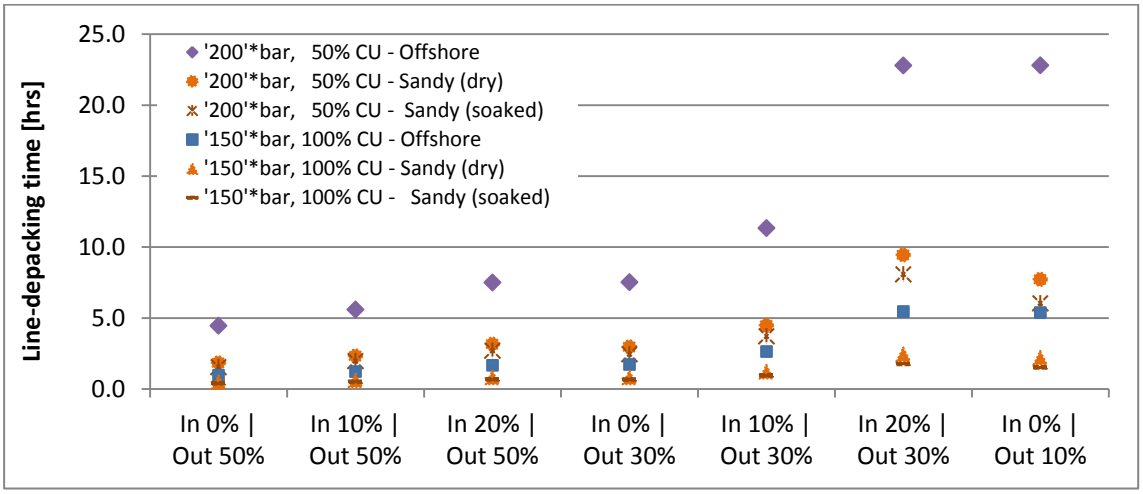

Figure 5.18: Line-depacking times for different surrounding environments for reference pipelines of 610mmOD, 100km, '150'bar ('200'bar) Maximum Operating Pressure (MAOP) and 100% (50%) flow capacity utilisation for different inflow|outflow scenarios after t=0. For interpretation of lines and colours see legend.

*The MAOPs presented in legend are only indicative - for actual MAOP see Table 5.4.

Overall, the analysis in this section has shown that the achievable line-depacking times are a compromise between the initial inventory that can be packed into a pipe (higher at good heat transfer between pipe and environment by reducing temperature and density in the pipe and hence 'freeing space' for further inventory), and the compressibility of the fluid during the line-depacking process (better at high compressibility, i.e. at high temperatures in the pipe caused by low heat transfer between pipe and environment). Due to the very fast heat transfer and the substantially higher achievable initial inventories of offshore pipelines their line-depacking times are around 2-3 times higher than for equivalent onshore pipes. Further, it has been found that whilst for offshore pipelines line-depacking times are largely a function of the discrepancy between inflows and outflows and not the actual flow levels (relative to nominal flow), this is not valid for onshore pipelines. The large quantities of CO_2 that cool off only during the depacking process in onshore pipelines

undermine and shorten the line-depacking process (decreased driving force for pushing CO_2 out of the outlet at decreased temperatures).

5.9.3. Pipeline minimum pressure

The pipeline allowable minimum pressure is a further parameter that can significantly influence achievable depacking periods. If this pressure is reduced and consequently lower residual inventories are allowed in the pipeline (i.e. after the line-depacking process is over), automatically the working capacity increases and, therefore, also the time periods pipelines can sustain high outflows even at periods of low inflows. Higher minimum allowable pressures decrease the available line-depacking times. This section investigates the effect the minimum allowable pressure level has on line-depacking times. As discussed in section 5.5 minimum allowable pressures are usually set to respect a safety margin over the critical pressure of the fluid (73bar for pure CO_2). However, minimum outlet pressures may also be set higher according to the pressures required at the wellhead to maintain a positive flow into the storage reservoir. This sensitivity case, hence, investigates the effect on line-depacking times if the baseline minimum pressure changed from 90bar to 80bar or 100bar, respectively.

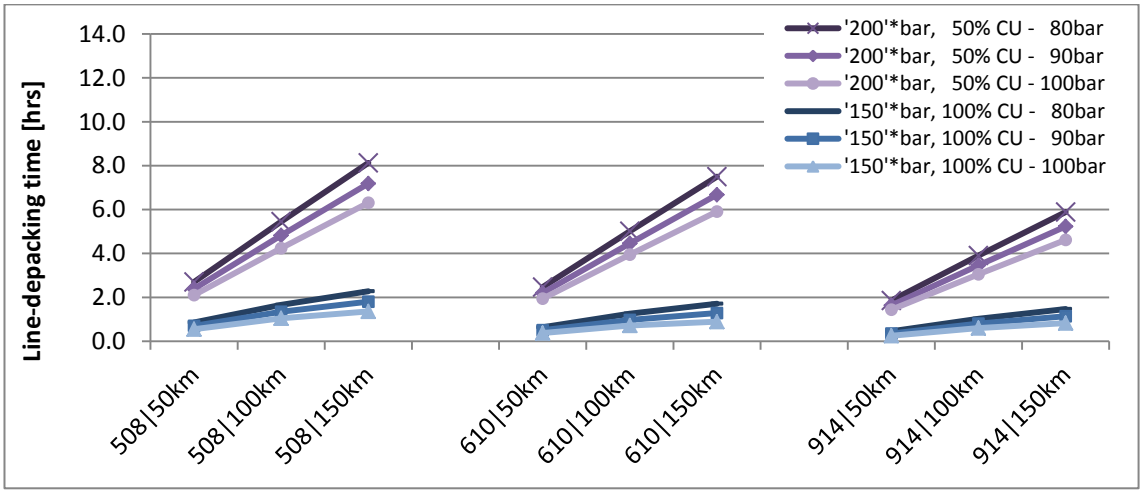

Figure 5.19: Line-depacking times for minimum pressures of 80bar, 90bar and 100bar for reference pipelines of '150'bar ('200'bar) Maximum Operating Pressure (MAOP) and 100% (50%) flow capacity utilisation (CU), respectively. Outflows (inflows) during depacking process are maintained at 50% (0%) of nominal flow. For interpretation of colours see legend.

*The MAOPs presented in legend are only indicative - for actual MAOP see Table 5.4.

Figure 5.19 shows the line-depacking times for the reference pipeline scenarios with MAOPs of around '150'bar and '200bar', respectively, and a flow capacity utilisation of 100% and 50% at different lengths and outer diameters. An inflow|outflow regime of 0%/50% of nominal flow during the depacking process is assumed, similarly to the previous sections. The figure shows that a change in the minimum allowable pressure of -

10bar(+10bar) leads to line-depacking time variations of around +25%(-25%) for pipelines with an MAOP of around '150'bar. For pipelines with higher MAOPs of around '200'bar, line-depacking times change only around +10%(-10%) for a minimum allowable pressure deviation of -10bar(+10bar). This lower relative change in feasible line-depacking times of pipelines with higher MAOPs can be attributed to the fact that these pipelines have a naturally larger allowable operating pressure range and, hence, higher working capacities. A change in the operating range of 10bar does not affect them as much as comparable pipelines with lower MAOPs and consequently smaller pressure operating ranges.

5.9.4. Impurities

Finally, it remains to explore the effect of impurities on line-depacking times. Wetenhall et al. (2014b) and Porter et al. (2015) provide overviews of the range of impurities that can be expected in CO_2 streams from different sources. In general, the impurities commonly expected in future CO_2 transportation systems have the effect of decreasing the density of the fluid. Therefore, it was predicted by Aghajani et al. (2017) that their addition would increase the linepacking capability of pipelines. Some of the most prominent impurities in CO_2 streams from post-combustion, pre-combustion and oxyfuel combustion CCS power stations include N_2, H_2 and O_2 (Hussein 2017). This section investigates the effect on line-depacking times of 2vol% of these impurities being present, respectively, in the CO_2 flow.

Since impurities open up a phase envelope in the phase diagram consideration has to be given that two-phase flow can occur at higher pressures than the critical pressure of pure CO_2. The cricondenbar is the maximum pressure above which no gas or two-phase flow can form. For consistency with the previously performed pipeline simulations a pressure safety margin of 21.8% is assumed above the maximum pressure at which two-phase flow can occur (i.e. cricondenbar). Table 5.5 summarises the cricondenbar for the examined CO_2 mixtures with impurities as well as the resulting minimum allowable pipeline pressure in the respective sensitivity scenarios.

Table 5.5: Cricondenbar for CO_2 mixtures with impurities* and resulting minimum allowable pipeline pressure for sensitivity scenarios.

	Cricondenbar	Minimum allowable pressure	%
CO2 + 2vol% H2	80.1bar	97.6bar	+21.8%
CO2 + 2vol% N2	76.9bar	93.7bar	+21.8%
CO2 + 2vol% O2	78.8bar	96.0bar	+21.8%

*Highest value in disrete range of values describing bubble/dew point curve (1°C resolution) in IEAGHG (2016).

Figure 5.20 illustrates the relative deviation in line-depacking times with impurities present in the flow for the reference pipelines with a MAOP of '150'bar and a capacity utilisation of 100%. Overall line-packing times deviate by +3% to -12%. Whilst depacking times mostly increase due to higher compressibilities with N_2 present in the flow the significantly narrowed pressure operating envelope faced by pipeline operators when H_2 and O_2 are present in the flow depresses depacking times. Generally depacking times decrease with increasing pipeline length with impurities present in the flow. This is a consequence of the higher flow velocities of the fluid (due to the reduced densities caused by common impurities) which lead to higher frictional pressure drops along the pipeline length. Since a larger fraction of the pipeline pressure envelope is utilised at regular operation consequently an even smaller fraction stays available to manipulate pressure levels for linepacking and de-packing operation, ultimately depressing the time periods over which such an operation can be sustained. Similarly the different deviations in achievable line-depacking times upon addition of impurities at different pipeline diameters can also largely be explained by varying pressure envelopes: Whilst for example for the 508mm pipelines with an MAOP of '150bar' the effective allowable operating pressure envelope expands from 90bar-159.4bar (see also Table 5.4) for pure CO_2, and from 97.6bar-159.4bar upon addition of 2vol% of H_2, a much larger fraction of the original operating pressure envelope of the 610mm pipeline of 90-150.8bar for pure CO_2 becomes unusable when 2vol% H_2 is added to the flow (a significantly smaller operating pressure envelope of 97.6-150.8bar remains; see Table 5.4 and Table 5.5).

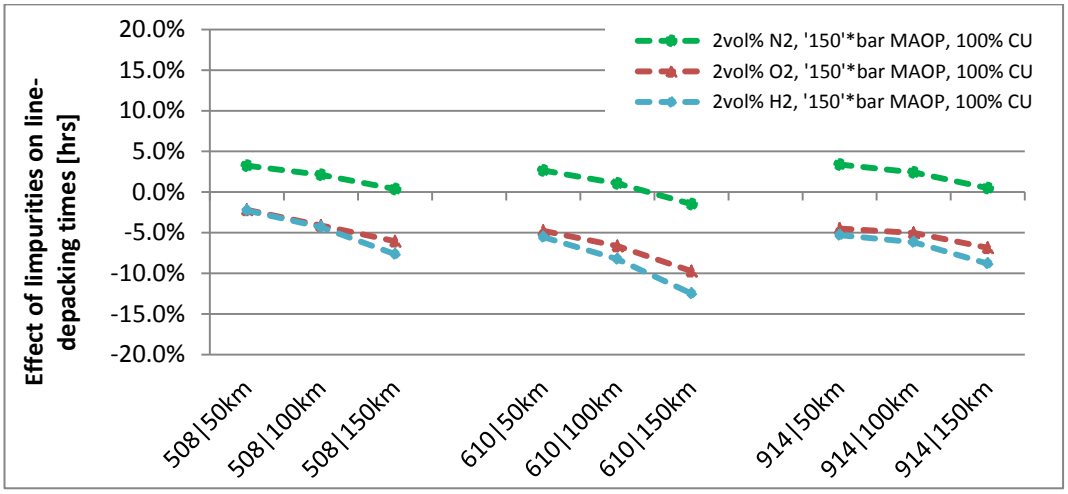

Figure 5.20: Relative deviation of line-depacking times with impurities present in the flow for reference pipelines of '150'bar Maximum Operating Pressure (MAOP) and 100% flow Capacity Utilisation (CU). Outflows (inflows) during depacking process are maintained at 50% (0%) of nominal flow. For interpretation of colours see legend.

*The MAOPs presented in legend are only indicative - for actual MAOP see Table 5.4.

Figure 5.21 presents the deviations in linepacking times upon addition of impurities for the reference pipelines with a MAOP of '200'bar and a capacity utilisation of 50%. It shows that across all reference pipelines the addition of impurities increases depacking times by 1-6%.

The increase in depacking times can be explained by the reduction in the pressure operating envelope through addition of impurities being relatively small compared to the total available pressure operating envelope of the pipeline, that stretches from around 90bar (or somewhat higher with impurities, see Table 5.5) to over 200bar (see Table 5.4 for exact values). The negative effect of the reduction in the operating pressure envelope can consequently be overcompensated by the increased compressibility of the CO_2 with impurities leading to overall higher pipeline-depacking times.

It can be concluded the impact of impurities on available pipeline depacking times is not straight forward and is dominated by two competing effects: i) the higher compressibility of the fluid upon addition of common impurities such as H_2, O_2, and N_2 which positively impacts depacking times of the pipeline; and ii) the reduced effective operating pressure envelope of the pipeline as a consequence of the addition of common impurities and the resulting two-phase flow envelope expanding to higher pressure levels than the critical pressure for pure CO_2. It has been demonstrated in the illustrative sensitivity cases that at pipelines with a relatively narrow operating pressure envelopes (i.e. from around 90-150bar) the first effect tends to dominate depressing achievable line-depacking times. In contrast, at pipelines with a relatively large pressure envelope (i.e. from around 90-200bar) the latter effect dominates in the examined sensitivity cases, and increases line-depacking times by around 1-6%.

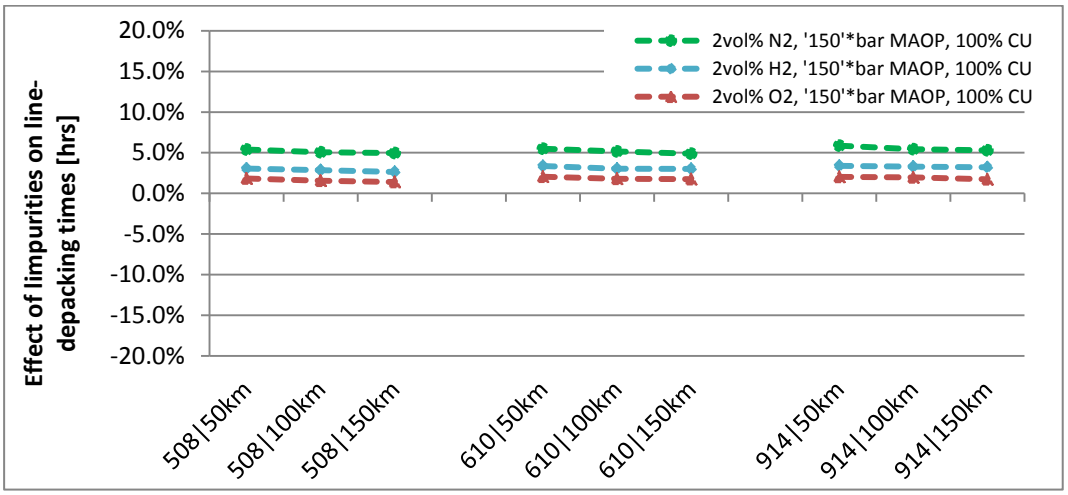

Figure 5.21: Relative deviation of line-depacking times with impurities present in the flow for reference pipelines of '200'bar Maximum Operating Pressure (MAOP) and 50% flow Capacity Utilisation (CU). Outflows (inflows) during depacking process are maintained at 50% (0%) of nominal flow. For interpretation of colours see legend.

*The MAOPs presented in legend are only indicative - for actual MAOP see Table 5.4

5.10. Conclusions

This chapter has investigated the available line-depacking times for a large number of widely applicable pipeline scenarios. The chapter makes a novel and relevant contribution to the literature by quantifying the extent to which dense phase CO_2 pipelines can provide buffering flexibility to operators of CCS networks. This can be used, for example, for balancing frequent and irregular variations in CO_2 flow rates mitigating associated integrity issues at the CO_2 injection and storage level. A range of sensitivity cases were examined expanding the analysis and exploring underlying effects. Several important conclusions can be drawn that can broadly be distinguished into four different categories. These are summarised in the following:

General:

- Key parameters with greatest effect on achievable line-depacking times of CO_2 dense phase transportation pipelines in the order of sensitivity are:
    - Inflow|outflow regime during the depacking process,
    - Length of the pipeline,
    - Flow capacity utilisation at nominal load,
    - Maximum operating pressure (MAOP),
    - Outer diameter (OD).
- Since the inflow|outflow regime and the length of the pipeline are usually determined by the operating requirements of CO_2 sources and sinks, as well as their geographical locations, three key pipeline design parameters remain for manipulation for positively impacting the achievable line-depacking times:
    - Flow capacity utilisation at nominal load,
    - Maximum operating pressure,
    - Outer diameter.
- Pipelines offer only limited line-depacking times when not oversized in terms of MAOP or flow capacity. At minimum permissible outflows of 50% of nominal flow and zero inflows during the depacking process, achievable line-depacking times are around 0.3-1.8hrs, for a range of lengths and diameter.
- However, if either the minimum permissible outflow level is lower or a minimum inflow is sustained during the depacking period - in other words if the difference between inflows and outflows during the depacking process is decreased - more significant line-depacking times of 2.5-10hrs are achievable, even when pipelines are not oversized (e.g. at inflow|outflows differences of only 10% of nominal flow).
- Oversizing the pipelines implicitly by reducing the capacity utilisation at nominal load from 100% to 50%, and by increasing the MAOP from 150bar to 200bar increases feasible line-depacking times by a factor of 3.5-4.5. When exploiting both parameters simultaneously substantial line-depacking times of up to

7hrs/12hrs/36hrs are achievable, at inflow|outflow differences of 50%/30%/10% of nominal flow, respectively.

- Therefore, if the need for line-depacking is considered in the design phase of the pipeline substantial line-depacking times can be achieved.
- Pipelines with such high buffering capabilities are likely to be able to help bridging a significant number of critical low flow periods at the injection and storage level, by feeding into the downstream system at times of low CO_2 supply from the available working capacity. In this way the integrity risk associated with variable flow and low flow rates at the injection and storage level (see Chapter 2) could likely be substantially reduced.

Offshore versus onshore:

- At offshore pipelines line-depacking times are predominantly a function of the differences between inflows and outflows during the depacking process, and not of the actual levels of inflow and outflows.
- Onshore pipelines offer line-depacking times around 50-70% lower than for equivalent offshore pipes. The primary reason for the higher balancing capability of offshore pipelines is the higher inventory at initial fully line-packed steady state flow conditions. This is an effect of the rapid heat transfer in offshore pipelines and fluid temperatures reaching ambient levels after only few (e.g. 4-5km) kilometres. This temperature drop is associated with a significant increase in the density of CO_2, which frees capacity for further inventory to be stored in preparation for a subsequent depacking event.
- In contrast, temperatures along the length of onshore pipelines drop substantially slower resulting from slower heat exchange with the environment. As a consequence of higher temperatures and lower densities, onshore pipelines can only be packed with substantially lower inventories in preparation for subsequent line-depacking. This negatively impacts the achievable line-depacking times.
- Yet, due to higher compressibilities of the fluid at higher temperatures onshore pipelines can sustain a driving force and maintain outflows at lower overall inventories than equivalent offshore pipelines. This has a counteracting and positive impact on line-depacking times.
- Consequently, achievable line-packing times are a compromise between the initial inventory that can be packed into a pipeline (higher at fast heat transfer between pipe and environment by reducing temperature and increasing density of the fluid in the pipe, hence, 'freeing space' for further inventory), and the compressibility of the fluid during the depacking process that enables to sustain high driving forces in order to push CO_2 out the outlet even at low inventories (better at high compressibility, i.e. at high temperatures in the pipeline caused by low heat transfer between pipe and environment).
- Due to these opposing effects pipelines in dry sandy soil environment with slowest heat transfer characteristics offer slightly higher line-depacking times than pipelines

in soaked sandy soil environment with slightly better heat transfer characteristics. However, both pipelines have around 50-70% lower line-depacking times than equivalent offshore pipelines with very fast heat transfer characteristics.

- The balancing capability of onshore pipelines is, further, significantly hampered when the fluid cools off during the depacking process of the pipeline. As a consequence the density of the fluid increases and the compressibility of the fluid decreases. This substantially reduces the driving force for pushing CO_2 through to the outlet, particularly at low overall inventories.
- In contrast to offshore pipelines, their onshore equivalents benefit from a minimum level of inflows during the depacking process. Not only do they stock up inventory, they also act as a heat source for increasing (or maintaining) temperatures and compressibility at elevated levels which positively affects the driving force ultimately responsible for pushing CO_2 through the outlet for longer periods of time even at low inventory.

Other sensitivity cases:

- A change in pipeline surrounding water temperature of +4°C/-4°C was found to influence line-depacking times by around +15%/-15%.
- Similarly, decreasing the minimum permissible pressure from 90bar to 80bar positively influences line-depacking times by around 12-30%, while an increase in the minimum permissible pressure from 90bar to 100bar leads to reductions in depacking times of 12-30%.
- The effect of common impurities such as O_2, N_2 and H_2 on line-depacking times is dominated by two competing effects: i) higher compressibility of the fluid upon addition of common impurities such as H_2, O_2, and N_2 which positively impacts depacking times; and ii) reduced effective operating pressure envelopes as a consequence of common impurities causing a two-phase envelope expanding to higher pressure than the critical pressure for pure CO_2. For pipelines with relatively narrow operating pressure envelopes (e.g. 90-150bar) the former effect tends to dominate, depressing achievable depacking times. At pipelines with a relatively large pressure envelope (e.g. 90-200bar) the latter effect dominates, leading to increases in line-depacking times by around 1-6% in the examined sensitivity cases.

Interim storage inventory:

- Key influencing factors determining the working capacity of a pipeline in the order of priority are outer diameter, length, maximum operating pressure, and capacity utilisation at nominal load. Dependent on the dimensions of the design parameters for offshore pipelines typically considered realistic in the GB context working capacities in the wide range of 335-5540kt can be expected.
- A sufficiently high working capacity could act as a dominant source of operational flexibility to operators of CO_2 T&S systems for balancing flow variability and bridge

critical periods of low flow at the injection and storage level. If necessary, this could be complemented by additional flow balancing options such as solvent storage at PCC-CCS power stations. Both options will be further explored and quantified over the following chapters.

6. Contribution of Linepacking to avoiding Low Flow Periods in Injection Wells

6.1. Introduction

The work presented in Chapter 5 gives an indication of the feasible time periods over which CO_2 pipelines can be expected to sustain the process of depacking, i.e. the process of maintaining relatively high outflows even at periods of low or zero inflows. Key factors and effects have been identified that influence the available line-depacking capability of pipelines. The work in Chapter 5 by itself, however, does not give any indication regarding how useful this option can be in real CO_2 T&S networks for avoiding critical periods of low flow at the downstream injection level. This is a consequence of the assumption in Chapter 5 that at the beginning of any depacking process the pipeline is fully packed. In reality, the pipeline operator may not always have the opportunity to prepare for upcoming LFP periods by packing the pipeline. For example, this would not be possible if periods of low CO_2 flow follow closely onto each other, without being interrupted by periods of high CO_2 inflows that allow stocking up on inventory.

This effect is illustrated in Figure 6.1-Figure 6.4. The figures show time profiles of captured CO_2 flows from Chapter 1, relative to nominal flow, over the entire year in the 'Basecase' UCED scenario (Figure 6.1-Figure 6.2), and in the 'High Wind, Low Emission Intensity' UCED scenario (Figure 6.3-Figure 6.4). The green graphs on the respective diagrams show the time duration in hours since entering the last LFP. For illustrative reasons LFPs are defined as 50% of nominal flow. When zooming in on the period between day 230 and 280 in the reference year in Figure 6.2 and Figure 6.4, it can be seen that LFPs following closely onto each other happen on a regularly basis during times of low net demand. When no significant periods of high CO_2 flows occur following a LFP (e.g. of several hours), pipeline operators are unable to stock up pipeline inventory in preparation for balancing the next upcoming LFP.

The detailed assessment of the extent to which pipelines can contribute to reducing the number of LFPs at the downstream injection level, therefore, requires considering both information about the CO_2 inflows over the year, and about the pipeline's ability to act as a buffer store (i.e. via linepacking & depacking). The present chapter merges the work performed in Chapter 1 and Chapter 5. Specifically, the CO_2 time profiles from the electricity sector generated in Chapter 1 are assessed in conjunction with representative pipeline scenarios building on Chapter 5, ultimately for quantifying how the buffering capability of pipelines can be exploited for reducing the number of critical LFPs downstream at the injection well and storage level. Whilst it would be enticing to compare the number of avoided/remaining LFPs to a number of LFP that is deemed to be acceptable for the infividual well or T&S network it should be noted as a caveat that such an assessment cannot be provided in this study, since the number of allowable LFPs at the injection and storage level is yet unknown. The current study can, however, provide a first step toward this ultimate goal.

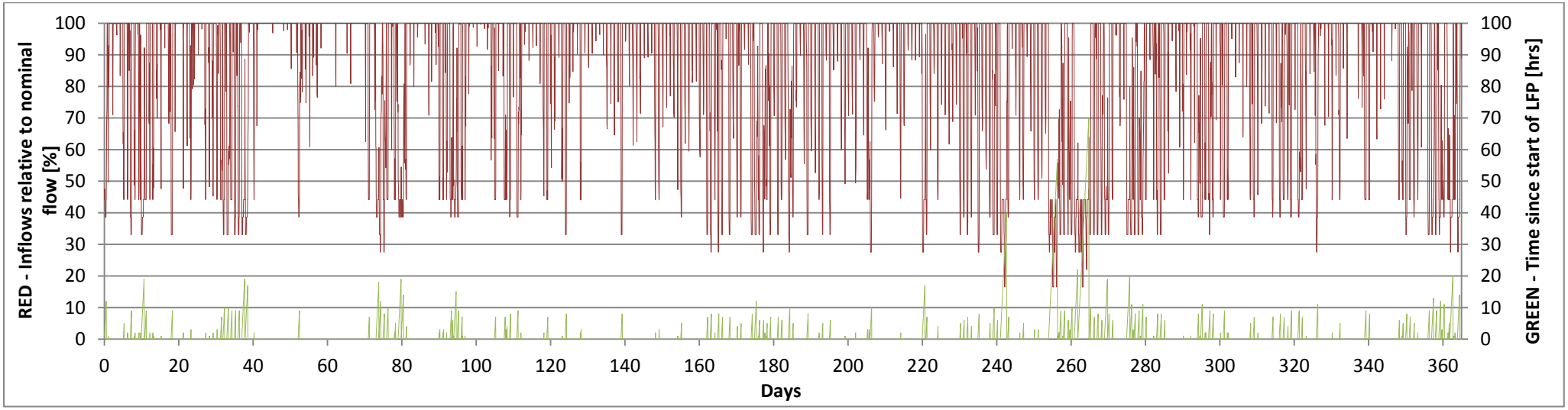

Figure 6.1: Captured CO_2 flow profile in the 'Basecase' UCED scenario (100g/kWh emission intensity, 30GW wind, 7.0GW CCS) over the entire year (dark red), and time duration since entering Low Flow Periods (LFPs; light green – lower curve). LFPs defined as periods of flow below 50% of nominal flow.

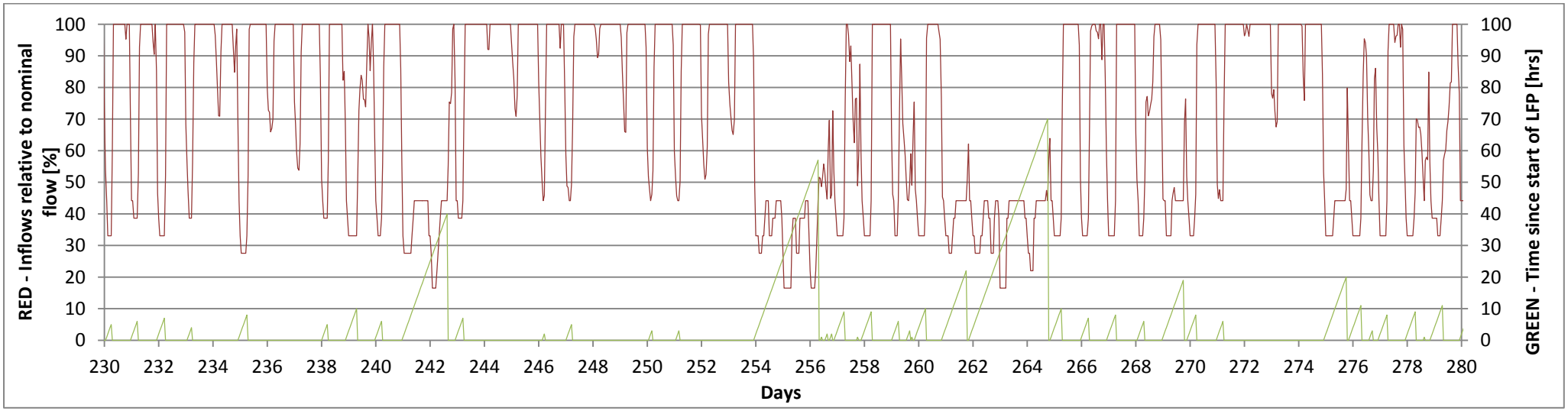

Figure 6.2: Captured CO_2 flow profile in the 'Basecase' UCED scenario (100g/kWh emission intensity, 30GW wind, 7.0GW CCS) over a selected period over the year (dark red), and time duration since entering Low Flow Periods (LFPs; light green). LFPs defined as periods of flow below 50% of nominal flow.

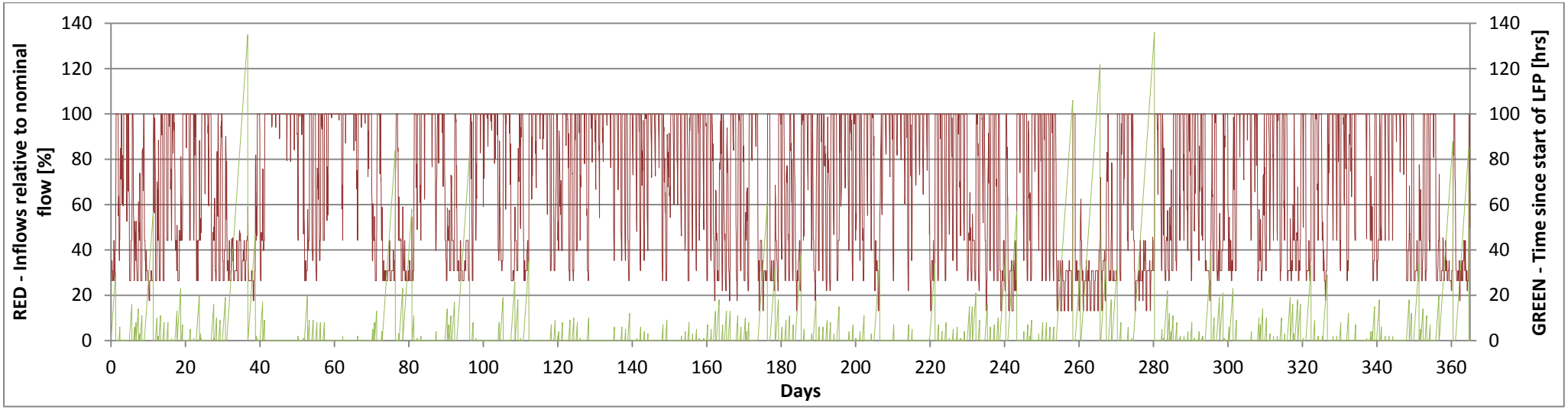

Figure 6.3: Captured CO_2 flow profile in the 'High Wind & Low Emission Intensity' UCED scenario (60g/kWh emission intensity, 45GW wind, 8.8GW CCS) over the entire year (dark red), and time duration since entering Low Flow Periods (LFPs; light green). LFPs defined as periods of flow below 50% of nominal flow.

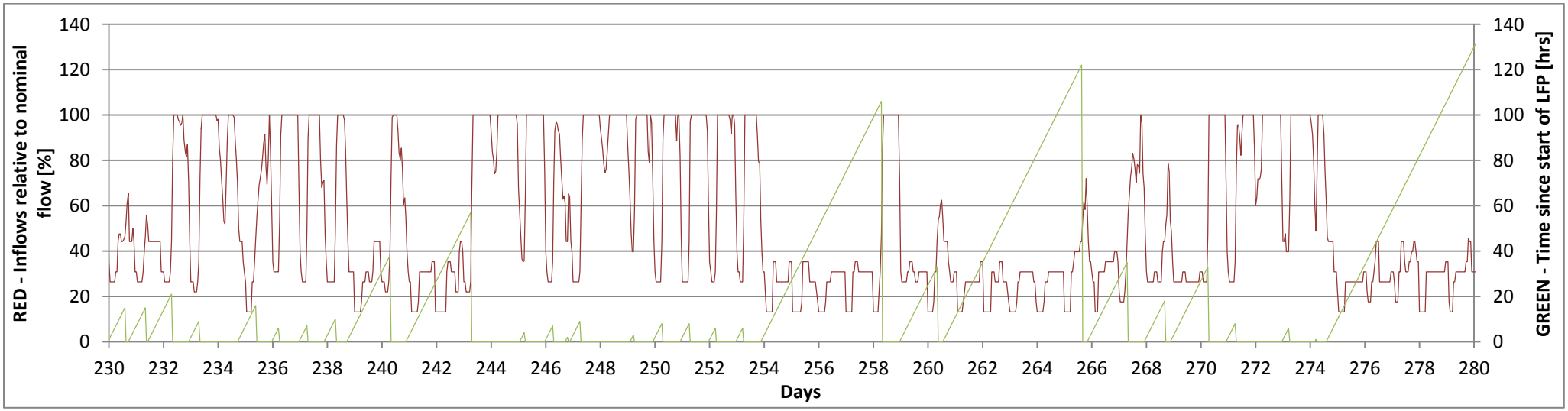

Figure 6.4: Captured CO_2 flow profile in the 'High Wind & Low Emission Intensity' UCED scenario (60g/kWh emission intensity, 45GW wind, 8.8GW CCS) over a selected period over the year (dark red), and time duration since entering Low Flow Periods (LFPs; light green). LFPs defined as periods of flow below 50% of nominal flow.

The present chapter, therefore, delivers an important and novel addition to the literature by informing CCS system designers about the possible contribution of dense phase CO_2 pipelines to mitigating lifetime and integrity hampering effects associated with periods of low or zero flow at the injection and storage level. By extension, the chapter informs CCS system designers about the additional level of effort that needs to be undertaken for procuring flexibility at other parts of the system. The current chapter, therefore, provides a foundation for future studies carrying out a "*system analysis of the whole chain [which] is necessary to evaluate where the capacity for flexibility is to be built in most cost-effectively*" as suggested by ZEP (2017, p. 100).

Due to the significant mismatch between the timescale of interest, i.e. for which generated CO_2 profiles have been obtained (i.e.: yearly and on hourly basis), and the practically feasible simulation timescales for hydraulic modelling of long distance pipelines (i.e.: seconds to a few days), several simplifications had to be made. A simplified buffer store model was developed in this chapter for estimating the possible contribution of pipelines for balancing CO_2 flows. The buffer store model is based on the findings from Chapter 5. In particular it is based on the finding of a nearly constant 'working capacity' of offshore pipelines, regardless of the inflow|outflow scenario during the depacking process. For more information about the methodology the reader is referred to section 6.2.

The chapter is structured as follows: The methodology applied in this chapter is outlined in section 6.2. Section 6.3 lays out the case studies examined. Section 6.4 presents the results. Section 6.5 analyses the sensitivities of the results to several influential input parameters. Section 6.6 provides a brief and illustrative cost example calculation to put the cost of oversizing the pipelines into perspective with the value of the components that could be protected via it, i.e. the injection wells. Section 6.7 summarises and concludes.

6.2. Methodology

To account for the fact that the hydraulic modelling of pipelines can only be performed with reasonable computational effort for several hours to a few days, a simple buffer storage model of the pipeline is adopted in this chapter. The pipeline is modelled as a storage buffer tank with a certain working capacity. As previously discussed the working capacity of a pipeline is defined as the difference in the mass of fluid the pipeline contains when being fully packed, and when being fully depacked. Yet, all operating pressure limits are still respecting in both states. The adopted buffer store model works as follows:

In periods of high inflows the pipeline operator can choose to fill up the working inventory of the pipeline/buffer store by constraining the outflow under the condition that the minimum flow rate at the pipeline outlet/wellhead is respected. The pipeline operator can fill up the inventory to the maximum capacity of the pipeline/buffer tank. This maximum capacity is calculated in advance for the selected pipelines by detailed hydraulic simulations, similar to the ones performed in Chapter 5. During times of low inflows the

pipeline operator can choose to make use of the available working capacity (i.e. inventory) and feed from it for maintaining the flow level at the outlet of the pipeline at the minimum permissible level (either 50%, 30% or 10% of nominal flow based on Chapter 5). The pipeline operator can perform this depacking process as long as the working capacity/buffer tank inventory is able to sustain it. The aim of the operator of the pipeline is to use the available buffer store capacity of the pipeline as effectively as possible to avoid critical LFPs at the pipeline outlet (i.e. wellhead) by balancing the flow. To quantify the contribution of a specific pipeline to avoiding LFP at the wellhead, the number of LFPs at the wellhead when deploying the pipeline as a buffer storage tank is, finally, compared to the counterfactual case when no balancing of flows is carried out.

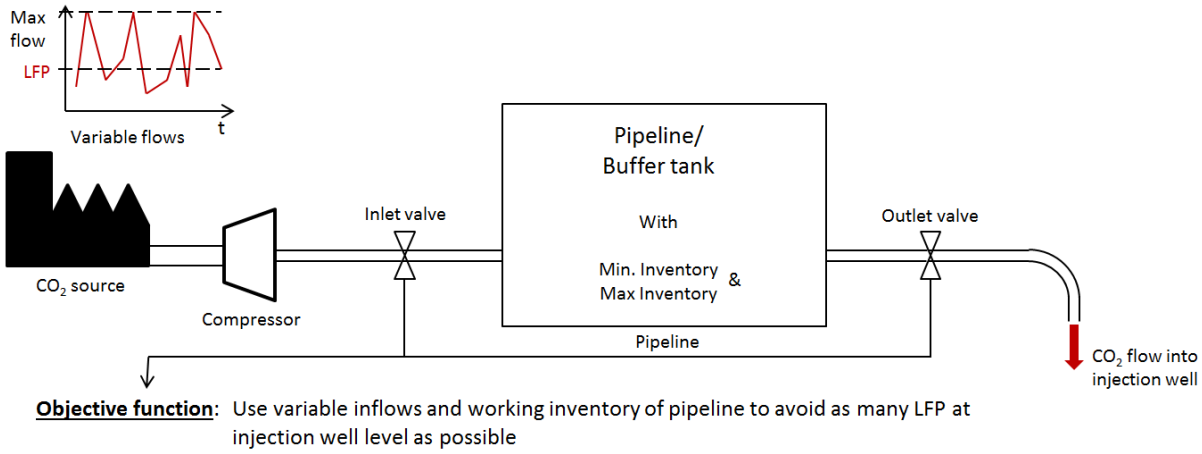

Figure 6.5: Schematic illustration of buffer tank methodology adopted in this chapter.

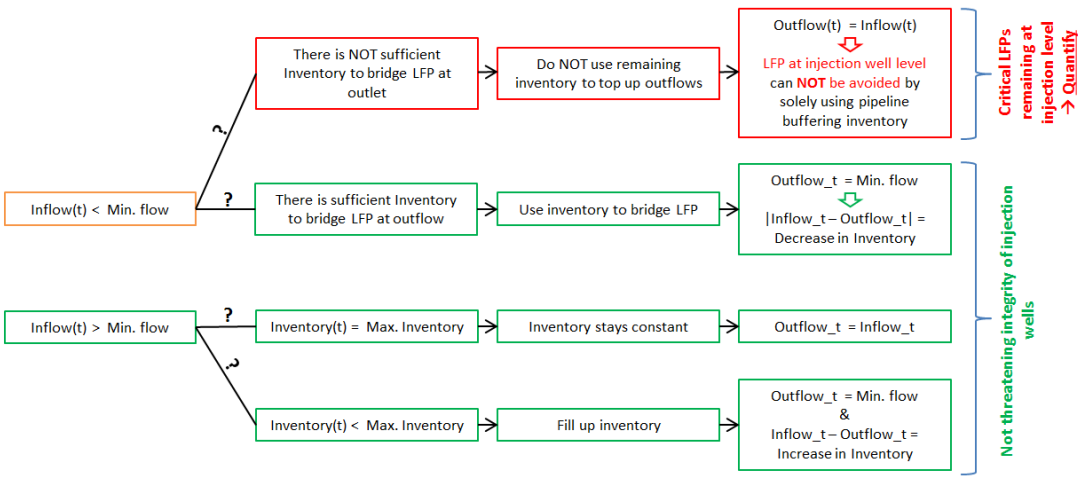

Figure 6.6: Schematic illustration of buffer tank methodology: Determination of whether a low flow period at the injection level can be avoided by buffering flows in pipeline.

The buffer storage tank methodology is implemented in MATLAB. The model has been uploaded and is available from the Research Archive of the University of Edinburgh. A schematic overview of the model is provided in Figure 6.5. Figure 6.6 provides a flowchart of the implemented algorithm.

The simplified buffer tank methodology is considered to be reasonable for the purpose of this chapter based on the finding that the working inventory of a specific offshore pipeline was found to be nearly independent of the inflow|outflow scenario considered during the line-depacking process (see section 5.8.4, and as will be further demonstrated in Figure 6.9). As previously demonstrated in Chapter 5 the applicability of the buffer store model for offshore pipelines is a consequence of the relatively fast heat transfer between the pipeline fluid and the surrounding environment. As a caveat it should, however, be noted that no concrete coating for offshore pipelines was considered in the pipeline simulations in Chapter 5 (as stated in section 5.5). Concrete coating could slow down heat transfer at offshore pipelines, the effect of which would need to be investigated in more detail in future studies. Due to the conservation of mass any working inventory that is taken from the pipeline during the depacking process will need to be packed into the pipeline again at a later point to get the pipeline back close to its initial state.

A number of underlying assumptions were made for carrying out the assessment in the present chapter. These are summarised in the following:

- The baseline CO_2 transportation trunklines are offshore (i.e. with relatively fast heat transfer to the environment).
- The deployed buffer store model for modelling the linepacking & depacking potential of pipelines is applicable.
- The produced CO_2 flows in the respective UCED scenarios are split equally to feed into a number of identical CO_2 trunklines (either into 610mm OD or 914mm OD pipelines - as further outlined in section 6.3).
- The pipeline operator can choose to linepack the trunkline at times of relatively high inflow by partially restricting outflows from the pipe (by manipulating downstream valve). However, during this process the minimum flow constraint must be respected.
- The pipeline operator has perfect foresight. He will prepare for periods of low inflows, whenever possible, by linepacking the pipeline.
- The pipeline operator will utilise the buffer capability of the pipeline and the perfect foresight to avoid as many LFP at the wellhead level as he possibly can.
- There are no significant hydraulic constraints neglected when modelling the linepacking and depacking process of the pipeline similar to a buffer store model. This is considered reasonable given the relatively long timescales considered in the present chapter: Yearly, with flow step changes from the UCED model on an hourly

basis; the hourly step changes could be smoothed out in real systems through flow rate ramps over several minutes.

Having presented the methodology that is applied in this chapter, the next section outlines the scenarios that will be examined.

6.3. Case Studies

There is a large number of CO_2 inflow scenarios available from Chapter 3, as well as pipeline network scenarios that could be considered for analysis within this chapter. Similar to Chapter 5 the present chapter does not go into the depth of designing and analysing GB networks scenarios that consider detailed locations of CO_2 sources and storage sites. Neither are detailed configurations and locations of booster stations and 'feeder' pipelines considered (i.e. smaller pipelines collecting the flow from the CO_2 sources and bringing it to the long distance trunklines). Instead, this chapter focuses on examining the extent to which buffering capabilities of representative GB CO_2 trunklines can help bridging critical LFPs at the injection and storage level. Due to their length and diameter it is expected that long distance CO_2 trunklines will provide the dominant amounts of buffering capability in pipeline based CO_2 transportation networks. In the following, the UCED and pipeline scenarios that are analysed in this chapter are outlined in more detail.

6.3.1. UCED Scenarios

Analysing all previously developed and examined UCED scenarios goes beyond the scope of the present chapter. A choice was made to examine several representative ones. As such, the 'Basecase' UCED scenario is selected for analysis. Additionally, two low emission intensity (60g/kWh) scenarios with medium and high wind deployment (30GW and 45GW) are investigated. The rationale behind selecting these two low emission intensity scenarios is to evaluate the 'worst case' UCED scenarios in terms of variability of CO_2 flows that may need to be handled by T&S networks. The assessment of the extent to which CO_2 flows can be balanced even under worst case variable CO_2 inflow scenarios is of particular interest. Figure 6.7 summarises all core UCED scenarios examined in Chapter 3. The scenarios selected for assessment in the current chapter are highlighted by thick red contours. Figure 6.7 displays the LFP analysis previously presented in section 3.6.5 only for illustrative reasons.

Although the 'High Wind/Medium Emission Intensity' scenario (i.e. 100g/kWh emission intensity, 45GW wind capacity) also demonstrates high variability of CO_2 flows, this case has not been selected for further investigation since it does not present a worst case. This is on one hand due to the small CCS capacity (0.9GW corresponding to around maximum flows of 2.6MTPA), which makes it easier to balance the flows when deploying one of the relatively

large pipelines that are typically considered for long distance transportation of CO_2, since they would be automatically substantially oversized. On the other hand the flow never drops below around 44% of nominal flow in this scenario (as discussed in Chapter 3 – due to balancing and reserve purposes and the small CCS fleet) which will make it comparatively easy to sustain outflows levels above 50% of nominal flow at nearly all times.

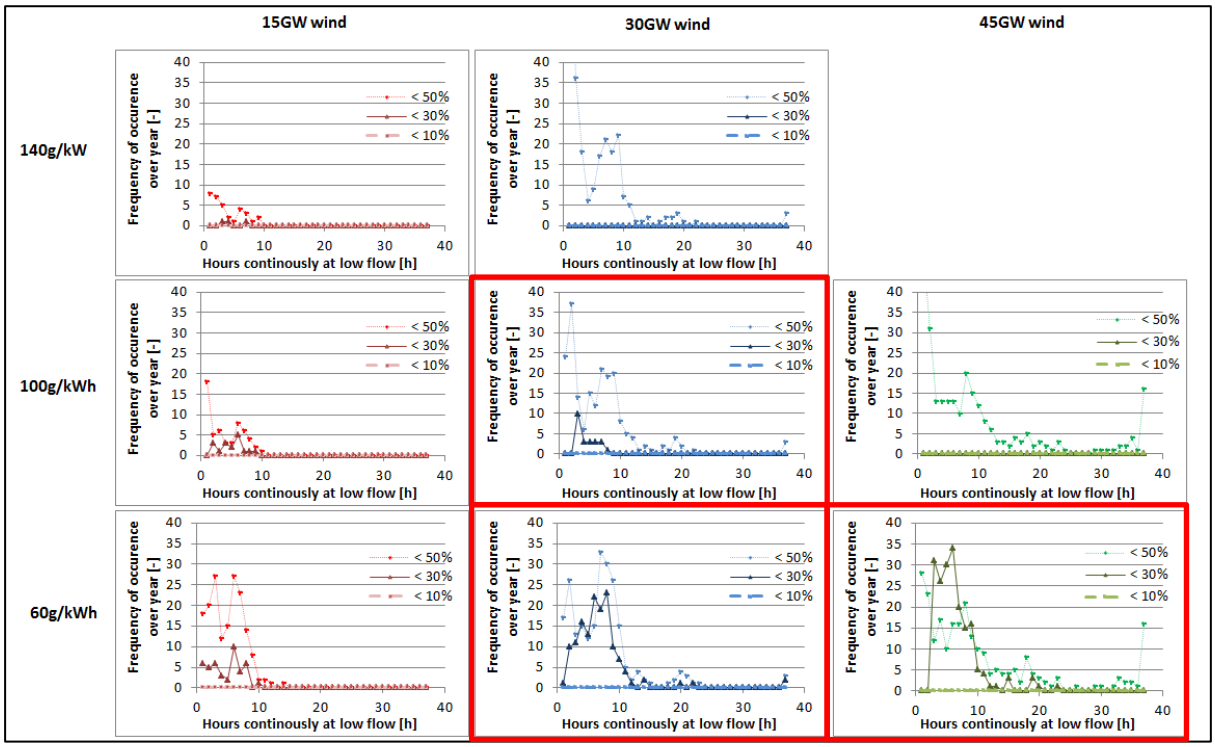

Figure 6.7: Summary of all core UCED scenarios examined in Chapter 3. Diagrams display low flow period (LFP) analysis as previously presented in section 3.6.5. Scenarios with a thick red contour are analysed in this chapter.

6.3.2. Pipeline Scenarios

Similarly to the UCED scenarios there is a large range of conceivable pipeline network scenarios. Two trunkline scenarios are selected: a moderately oversized pipeline referred to as the '610mm OD' pipeline, in reference to its diameter, for transporting carbon dioxide from the CO_2 clusters to the storage clusters; and a strongly oversized pipeline referred to as the '914mm OD' pipeline, for fulfilling the same purpose.

- The moderately oversized pipeline consists of an offshore 100km long pipeline with a MAOP of approx. '200'bar (by following the procedure outlined in section 5.4 a wall thickness of 20mm was chosen which corresponds to a MAOP of 212.4bar).
- The strongly oversized pipeline consists of a 100km long offshore pipeline and a MAOP of around '200'bar (212.7bar following the procedure outlined in section 5.4 at a wall thickness of 30mm).

It is recognised that in reality transportation pipelines could vary substantially in length. Chapter 5, nevertheless, shows that even pipelines of significantly different lengths can have similar or equal line depacking capabilities dependent on the choice of other influential design parameters. For instance, even a relatively short pipeline (e.g. 50km length) can achieve comparable line-depacking times to a long pipeline if other design parameters such as flow utilisation at nominal load, MAOP, and pipeline diameter are selected accordingly.

The choice of one moderately and one strongly oversized pipeline of 100km length for transportation of CO_2 in this chapter is, therefore, considered sufficient for the purpose of this chapter. It is considered representative in a scenario in which the system designer chooses to procure some level of operational flexibility/balancing capability, by oversizing the pipelines either in terms of diameter or MAOP, in order to hedge against various uncertainties in the system.

Looking at the nominal CO_2 flow rates in the examined UCED scenarios (20.9-41.9MTPA) it becomes clear that transportation of all captured CO_2 through one trunkline is not only impractical but also infeasible/uneconomical. This is particularly true in the case of the 610mm OD pipeline which is economically designed for a maximum flow rate of around 13MTPA (see section 5.3). The flow in the investigated UCED scenarios is therefore split equally and fed into several identical pipelines of either 610mm OD or 910mm OD. To ensure that both pipeline types (610mm OD and 914mm OD) are suitable for transportation, the flow in the respective UCED scenarios is fed into as many pipelines as required for not exceeding the maximum design flow capacity of the smaller pipeline (i.e.: 610mm OD pipeline; 13MTPA). Figure 6.8 illustrates this process and summarises all UCED/pipeline scenarios that are analysed in the following. It serves as a reference table throughout this chapter.

An implicit assumption of the scenarios drawn up in the currrent chapter is that the captured CO_2 is collected in several clusters and fed into a very small number of trunklines for long distance transportation to the storage site. This is in line with Summit Power (2017) and several other studies investigating cost-economic CCS deployment ways on a national and large scale in GB (Oxburgh 2016, UK CCUS Cost Challenge Taskforce 2018, Poyry 2017). Splitting up CO_2 flows equally for distribution into two trunklines is considered reasonable as a first approximation for the purpose of this study given large uncertainties about the location of future CCS power stations across the GB.

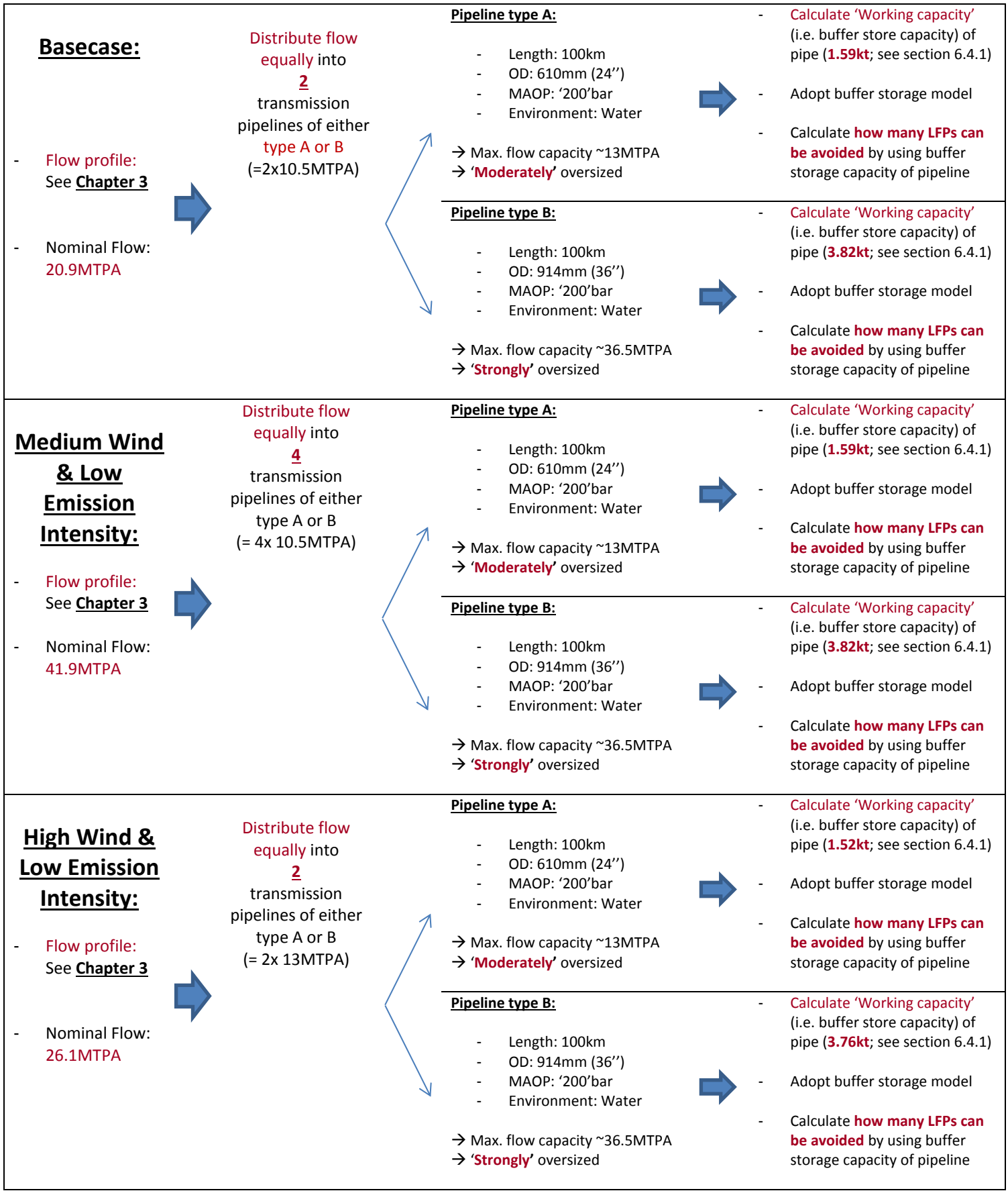

Figure 6.8: Schematic illustration of the coupling of UCED scenarios with pipeline scenarios, for quantifying to what extent the number of low flow periods at injection can be reduced by exploiting the balancing capabilities of CO_2 pipelines.

6.4. Results

Having outlined the methodology and case studies examined in this chapter, this section presents and analyses the results. It is structured as follows: Subsection 6.4.1 determines the working capacities of the respective pipelines. Subsection 6.4.2 presents the LFP analysis for the respective evaluated UCED scenarios, and determines how many of them can be avoided by exploiting the buffering capabilities of the considered pipeline types. Section 6.5 examines the effects of several sensitivity cases on the results.

6.4.1. Working inventory

Figure 6.9 shows the working inventories for both evaluated pipeline types (i.e. 610mm OD and 914mm OD pipelines of 100km length) for different design nominal flowrates and inflow|outflow regimes during the depacking process. The working capacities were determined according to formula 10 in Chapter 5 (subsection 5.8.4). The examined flowrates are chosen according to the maximum flow rates in the examined UCED scenarios, and the number of pipelines they feed into, as illustrated in Figure 6.8. Similar to Chapter 5 and as has previously been explained the working inventory is relatively constant (within 3-6%) for different inflow|outflow regimes during the depacking process. At smaller inflow|outflow discrepancies the working inventory tends to marginally increase as less driving force is needed to push CO_2 out of the pipeline end, and hence a pressure distribution closer to the 90bar minimum towards the end of the depacking process is possible, maximising the inventory reduction during the process.

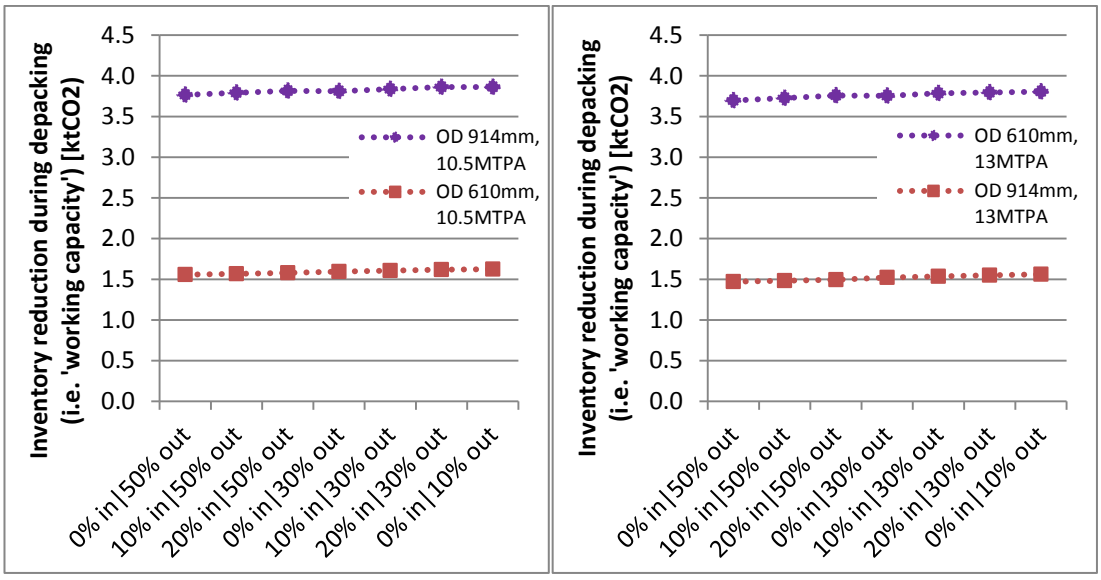

Figure 6.9: Working inventory for '610mm OD' pipeline (914mm OD, 100km, '200'bar MAOP, water environment) as well as for '914mm OD' (914mm OD, 100km, '200'bar MAOP, water environment) pipeline for nominal flowrates of 10.5MTPA (left) and 13MTPA (right), respectively.

For similar reasons the working capacity marginally decreases at higher nominal flowrates and higher inflow|outflow discrepancies (see section 5.8.4). Although this effect is relatively small it is considered in this chapter.

Table 6.1 summarises for the pipeline scenarios considered in the present chapter the (i) nominal flow rate; (ii) the range of determined working capacities at different inflow|outflow scenarios; (iii) the working capacities' deviations as an effect of the considered inflow|outflow scenario; and (iv) the working capacities that have been adopted for the buffer store model in this chapter in the respective pipeline scenarios (bold).

Table 6.1: Summary of working inventories adopted in the buffer store model for coupling UCED and pipeline scenarios.

	Flow through 1 pipe	Working inventory range (dependent on inflow|outflow scenario)	Deviation in working inventory range	Medium working inventory for buffer store model
Basecase	10.5MTPA			
Pipe A		1.56kt-1.62kt	+/-2.2%	**1.59kt**
Pipe B		3.77kt-3.86kt	+/-1.4%	**3.82kt**
Medium Wind & Low EI case	10.5MTPA			
Pipe A		1.56-1.62kt	+/-2.2%	**1.59kt**
Pipe B		3.77kt-3.81kt	+/-1.4%	**3.82kt**
High Wind & Low EI case	13MTPA			
Pipe A		1.47-1.56kt	+/-3.0%	**1.52kt**
Pipe B		3.70kt – 3.81kt	+/-1.7%	**3.76kt**

6.4.2. Number of avoided low flow periods at injection and storage level

This section presents and analyses the annual number of critical LFPs that can be avoided at the injection and storage level when exploiting the balancing capabilities of the reference pipelines. Due to the uncertainty regarding the exact definition of LFPs which would constitute a risk to the injection wells integrity, three different cases have been examined based on previous chapters' analysis. Section 6.4.2.1 examines the number of LFPs that can be avoided via line-packing & depacking when LFPs are defined as periods with flows less than 50% of nominal flow. Section 6.4.2.2 performs the equivalent analysis with LFPs being defined as periods when flows drop below 30% of nominal flow. Section 6.4.2.3 discusses the results when LFPs are defined as times when flows fall below 10% of nominal flow.

As a conservative baseline study and in order to avoid increasing the granularity of the scenarios it is assumed that injection wells are not managed individually at reduced flow

rates (as discussed in section 4.1.1.4), and the flow is distributed equally across the range of operational wells.

6.4.2.1. 50% minimum outflow

Figure 6.10 shows the LFP analysis at the injection level in the 'Basecase' UCED scenario (top), the 'Medium Wind/Low Emission Intensity' (middle), and the 'High Wind/Low Emission Intensity' scenario (bottom), when no balancing is deployed (blue curves), and when the reference pipelines with an OD of 610mm and 914mm OD are available for flow balancing (red curves and green curves), respectively. The diagrams to the left illustrate the frequency of occurrence, and the corresponding durations of LFPs (in hrs) in the respective scenarios. The diagrams to the right show the cumulative number of annual LFPs in the respective scenarios that last for longer than X hours (see x-axis), before and after balancing is deployed.

In the 'Basecase' UCED scenario it can be seen that when no flow balancing is deployed more than 200 LFPs occur at injection level throughout the year, with most LFPs lasting for around 1-10hrs. When balancing capabilities are deployed this number drops drastically to around 32 LFPs at the injection well when the 610mm OD pipelines are available, and to only 7 if the 914mm OD pipelines are available for flow balancing. Diagram a) shows that both pipeline types enable bridging all LFPs that last for less than 8hrs. Both pipeline types are further able to bridge a significant number of LFPs that last for 8-15hrs. Reasons why only some and not other LFPs can be bridged of equivalent durations are that either the inventory of the pipeline could not be filled up as preparation for the LFP (due to other LFPs occurring shortly before), or that higher inflows are provided during some LFPs than for others, counteracting fast depletion of the pipeline working inventory. In the evaluated 'Basecase' UCED scenario only the 914mm OD pipeline is able to bridge LFPs lasting for more than 15hrs.

In the 'Medium Wind/Low Emission Intensity' scenario the number of LFPs at the injection level that occur when no balancing is deployed can be reduced from 231 to 118 and 40, respectively, when pipelines of either 610mm or 914mm OD are available for balancing. This corresponds to reductions of 48% and 83% that are achievable with flow balancing. Nevertheless, these possible reductions are significantly lower than in the UCED 'Basecase' scenario (84% and 97%). Recalling the Flow Duration Curves from section 3.6.3 (Figure 3.7) this can be explained by the fact that in the 'Medium Wind/Low Emission Intensity' case the inflows of CO_2 during LFPs into the T&S system are generally lower relative to the nominal load than in the 'Basecase'. Consequently, the working capacity of the pipelines during LFPs depletes faster and cannot bridge as long time intervals. This effect is also directly linked to the large CCS fleet in the 'Medium Wind/Low Emission Intensity' scenario that is frequently only used at partial capacity (particularly as a consequence of the high levels of intermittent wind energy on the system).

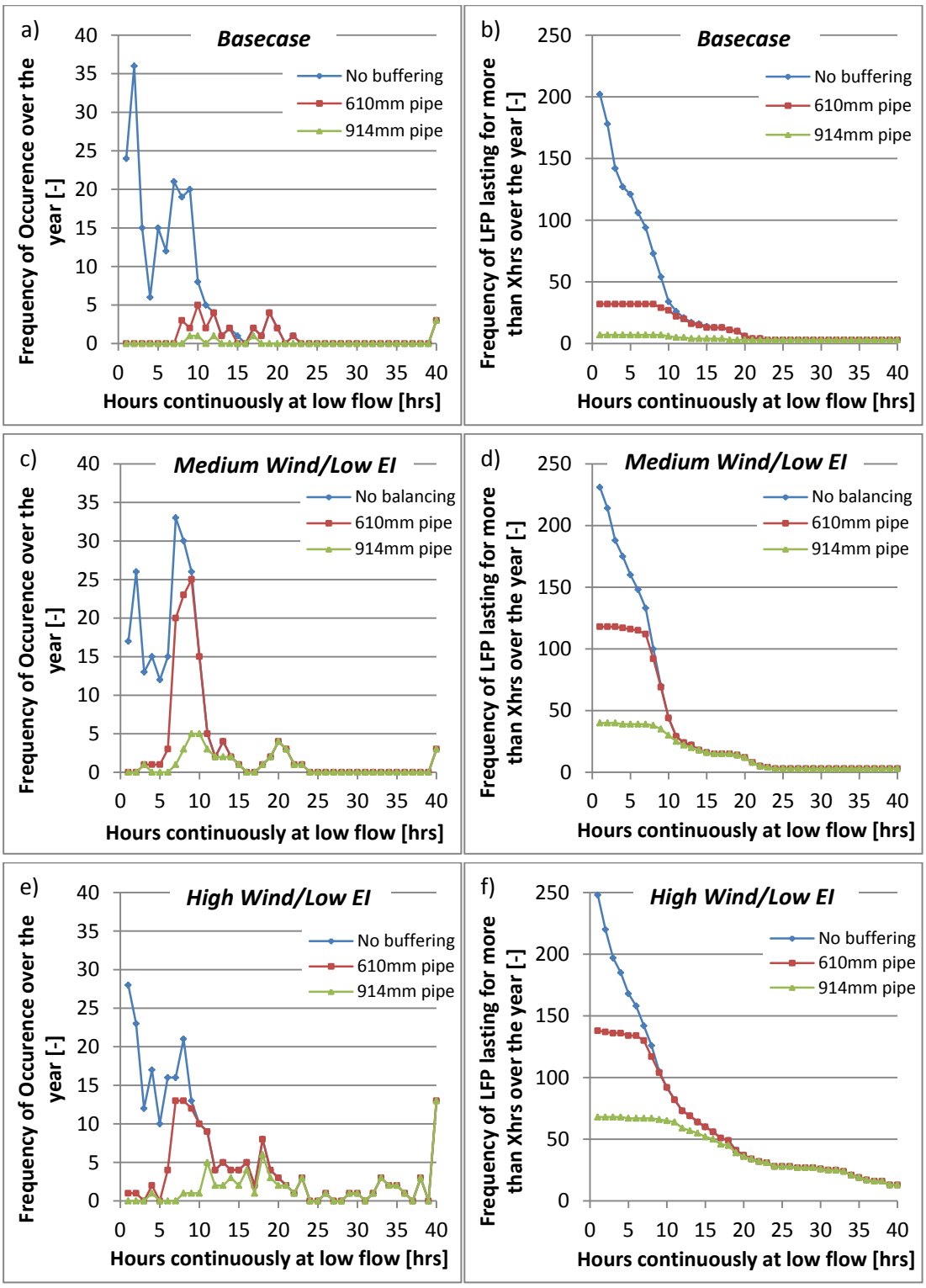

Figure 6.10: Duration and frequency of low flow periods (LFPs) at wellhead in 'Basecase', in the 'Medium wind/Low Emission Intensity', and in 'High Wind/Low Emission Intensity' UCED scenario, if no flow balancing is considered (blue curves), if '610mm OD' pipeline balancing capabilities are exploited (red curves), and if '914mm OD' pipeline balancing capabilities are considered (green curves). Diagrams on the right side show cumulative number of LFPs lasting for longer than X hrs. LFPs are defined as periods of flows below 50% of the nominal rate.

Diagram d) illustrates how both pipeline types are able to bridge most LFPs lasting for up to 5hrs. Pipelines of 610mm OD are able to bridge some LFPs of up to 12hrs duration, whilst the much larger balancing capability of the 914mm OD pipelines enable them to bridge some LFPs enduring for up to 18hrs.

Out of the evaluated scenarios, the number of LFPs is highest in the 'High Wind/Low Emission Intensity' UCED scenario (i.e. diagrams e) and f)). Without any balancing in the transportation network the injection sites face around 248 LFPs over the year. The balancing capabilities of the 610mm or 914mm OD pipelines would enable reducing this number to 138 and 68, respectively. This corresponds to reductions of around 44% and 73%. Although these numbers are smaller than for the 'Basecase' they remain substantial. The reason for the numbers falling compared to the 'Basecase' can be again traced back to the reduced levels of inflows during LFPs that deplete the working inventory comparatively fast. Additionally, LFPs in the 'High Wind/Low Emission Intensity' scenario tend to last for longer times, making it harder for flows to be balanced.

The time durations of LFPs that generally can be bridged with 610mm and 914mm OD pipelines are 1-6hrs and 1-13hrs, respectively. Neither pipeline type is able to bridge a significant number of LFPs extending over longer time periods.

The analysis in this section shows that by making balancing capability available via oversizing of pipelines the number of LFPs at the injection level can be reduced substantially. Whilst in the 'Basecase' the number of LFPs injection wells face can be reduced by 84% and 97% by deploying pipeline of 610mm and 914mm OD, respectively, this number stays high but falls to 44% and 73% in the 'High Wind/Low Emission Intensity' scenario. A main reason for this reduction was found to be the low relative levels of inflows during many LFPs in the evaluated low emission intensity scenarios (see also FDCs in section 3.6.3). This leads to a quicker depletion of the pipeline working capacity, and the depacking process cannot be used to bridge as long LFPs anymore.

6.4.2.2. 30% minimum outflow

This section analyses the annual number of critical LFPs at the injection and storage level and the achievable reductions via pipeline flow buffering when LFPs are defined as times of flow below 30% of the nominal rate. The section is structured similarly to the previous one. Figure 6.11 illustrates the frequency and duration of LFPs at the injection level in the 'Basecase' UCED scenario (top), in the 'Medium Wind/Low Emission Intensity' scenario (middle), and in the 'High Wind/Low Emission Intensity' scenario (bottom), when no balancing is deployed (blue curves), and when pipelines with outer diameters of 610mm and 914mm are available for flow balancing, respectively (red curves and green curves).

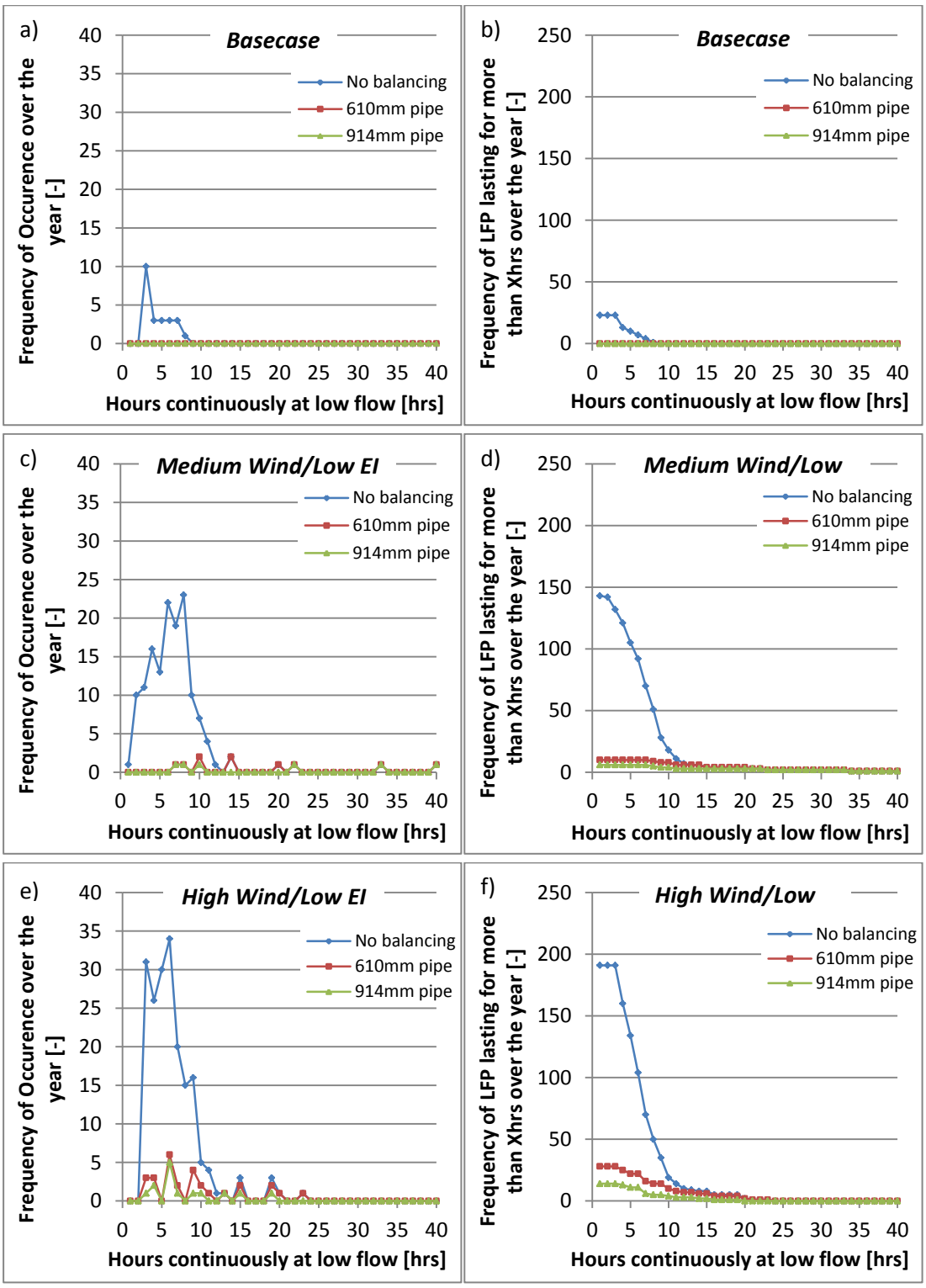

Figure 6.11: Duration and frequency of low flow periods (LFPs) at wellhead in 'Basecase', in the 'Medium wind/Low Emission Intensity', and in 'High Wind/Low Emission Intensity' UCED scenario, if no flow balancing is considered (blue curves), if '610mm OD' pipeline balancing capabilities are exploited (red curves), and if '914mm OD' pipeline balancing capabilities are considered (green curves). Diagrams on the right side show cumulative number of LFPs lasting for longer than X hrs. LFPs are defined as flows below 30% of nominal flow.

Again, the diagrams on the left illustrate the frequency of occurrence and the corresponding durations of LFPs (in hrs). The diagrams to the right show the cumulative number of LFPs that last for longer than X hours (see x-axis).

Looking at diagrams a) to f) it can be seen that, in general, the number of LFPs can be reduced to very low levels across all investigated UCED scenarios. In the 'Basecase' UCED scenario all 23 LFPs can be bridged with 610mm OD pipelines available for buffering. There is, consequently, no benefit when installing the larger 914mm OD pipelines if the aim is to avoid LFPs at injection level.

Similarly, in the 'Medium Wind/Low Emission Intensity' scenario nearly all LFPs can be bridged. The 610mm OD pipelines can reduce the number of LFPs over the year from 143 to 10. Deploying a larger 914mm OD pipeline can bring this number down to 6. These reductions correspond to around 93% and 96%. There is, hence, a marginal benefit of installing the larger pipelines. Both pipeline types are able to bridge LFPs enduring for up to 12hrs. Only the 914m OD pipelines are able to bridge LFPs enduring for up to 20hrs.

In the 'High Wind/Low Emission Intensity' scenario the 610mm OD pipelines are able to reduce the number of LFPs at the injection well level from 191 to 28, whilst the larger 914mm OD pipelines reduce it to around 14. These numbers correspond to reductions of 85% and 83%, respectively. Again both pipeline types are able to bridge most LFPs lasting for up to 12hrs. Only the 914mm OD pipelines are able to bridge most LFPs enduring for up to 20hrs.

Overall, this section shows that when LFPs are defined as any time that CO_2 flow drops below 30% of nominal flow, deploying either of the investigated pipelines with 610mm or 914mm OD, respectively, can reduce the occurrence of such events at the injection wells to very few times over the year, if not to zero. It is shown that both pipeline types achieve comparable performances of avoiding LFPs at the injection well level, with the significantly larger 914mm OD pipelines being only marginally better.

6.4.2.3. 10% minimum flow

The extensive LFP analysis carried out in Chapter 1 has shown how across all investigated core UCED scenarios CO_2 flow never drops below 10% of nominal flow. It has been discussed in Chapter 3 that this is on one hand an effect of the minimum thermal generation constraint (15GW) and on the other hand an effect of CCS power stations never shutting down collectively in order to provide the necessary amounts of reserve to the wider electricity system (see Section 3.6.2). Given that inflows never drop below 10% of nominal flow it will not be an issue sustaining outflows above this level, even with no flow balancing available. With all graphs overlapping with the x-axis providing very little additional information to the reader the corresponding diagrams are omitted.

6.5. Sensitivity Cases

This section examines the sensitivity of the results to certain key input parameters. Three sensitivity cases are examined.

- Sensitivity case 1 evaluates the sensitivity of the results to the minimum thermal generation limit assumed in the UCED model (15GW in the core scenarios) in Chapter 3. There is significant uncertainty surrounding this number, and it can potentially significantly change the results. A lower minimum thermal generation limit leads to reduced inflows of CO_2 during LFPs, with a negative effect on working inventory depletion and the number of LFPs that can be bridged.
- Sensitivity case 2 explores the effect of sustaining an additional level of inflows during low flow periods, in order to fill up the working inventory and ultimately enabling bridging more and longer LFPs.
- Sensitivity case 3 illustrates how the number of LFPs/avoided LFPs changes when the option for bypass is allowed at CCS power stations in response to periods of high electricity prices.

6.5.1. Minimum thermal generation limit

Due to the large uncertainty surrounding the minimum level of thermal generation required on the network for ensuring a sufficient amount of inertia available for stabilising the wider power system in the event of unforeseen short term deviations in demand or supply, a case has been examined exploring the sensitivity of the results to this parameter. Whilst in the core scenarios a minimum thermal generation limit of 15GW has been assumed based on (National Grid 2013) and Vázquez Villamor (2017), a reduced minimum thermal generation constraint of 7.5GW is evaluated in this sensitivity case similar to Vázquez Villamor (2017). The analysis is performed in the following subsections on the example of the 'Basecase' UCED scenario. It should be noted that a main assumption in this section is that nuclear power plants are able and allowed to operate in a load following flexible manner providing also a majority or all of the required reserve to the power system whenever needed. This would be particularly needed at times of net demand falling below the aggregate installed nuclear capacity (17.1GW). As a consequence of the merit order stack dispatch of generators the majority or all other thermal generator types may be shut-in during these times, leaving it to nuclear plants to balance the system. Although traditionally and most widely nuclear power stations are used as baseload power generators there is evidence that nuclear power station can be used for load following as well as for primary and secondary reserve provision (Lokhov 2011, Cany et al. 2016, Jenkins et al. 2018, Loisel et al. 2018, IAEA 2014). In the French power system this is particularly prevalent due to the very high penetration of nuclear power supply, reaching 76% in 2015 (Cany et al. 2016). Cany et al. (2018) reports that as a consequence of increasing contributions of VRE in recent years the share of nuclear power stations being involved in

significant load following operation reached around 40% by 2014. Further, the authors note that many French nuclear power stations provide upward and downward primary and secondary reserve to the system amounting for +-7% of their nominal power output capacity. Flexible operation of nuclear power plants can similarly be observed in the German power market (Cany et al. 2016, Lokhov 2011) allowing for the integration of large amounts of intermittent renewable energy supply. In the UK flexible operation of nuclear power stations could be promoted by improving the technical ability of plans to operate flexibly, by overcoming regulative barriers, and by setting financial incentives.

The following two subsections explore the potential of pipelines to contribute to reducing the annual number of LFPs faced by injection and storage sites via linepacking, with LFPs being defined as periods of flow below 50% and 30%, respectively, of the nominal rate.

6.5.1.1. 50% minimum flow

Figure 6.12 and Figure 6.13 illustrate the duration and frequency of LFPs at injection level in the 'Basecase' UCED scenario if no flow balancing is considered at minimum thermal generation constraints of 15GW (blue curves) and 7.5GW (black curves), respectively, and when the reference pipelines of 610mm and 914mm OD are available for CO_2 flow balancing (blue, red and grey graphs). Whilst the top diagrams show the frequency of occurrence as a function of the duration of the LFP, the lower diagrams display the cumulative number of LFPs that extend for longer than X hrs (as defined on x-axis). LFPs in this subsection are defined as any periods when flows drop below 50% of the nominal rate.

The graphs show that when LFPs are defined as periods of flows below 50% of the nominal rate the frequency and durations of the (unbalanced) LFPs are nearly identical. As a consequence the black and blue graph in both diagrams overlap almost entirely.

When looking at the LFPs that can be bridged via pipeline flow balancing it can be seen, however, that significantly fewer can be bridged at the reduced minimum thermal generation level. The number of LFPs that cannot be bridged rises from 32 to 61 when the 610mm OD pipelines are deployed for flow balancing, and from 7 to 16 when the 914mm pipelines are utilised. Similar to the effects observed in section 6.4 this can be explained by the lower CO_2 inflows into the pipelines during many LFPs, which leads to quicker depletion of pipeline working inventory.

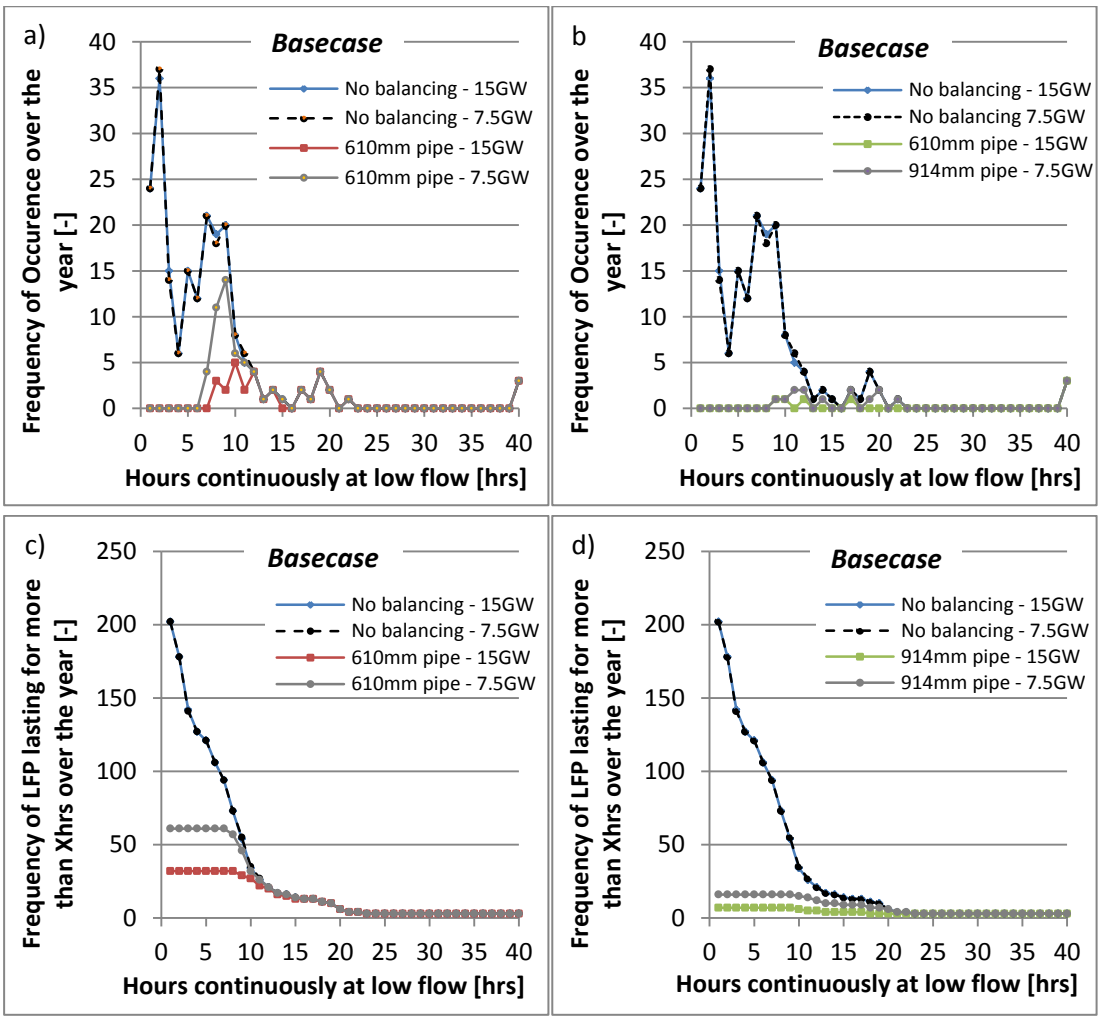

Figure 6.12 (top): Duration and frequency of low flow periods (LFPs) at wellhead in 'Basecase' UCED scenario when no flow balancing is considered and minimum thermal generation limit is at 15GW (blue) and 7.5GW (black), and when pipelines of 610mm and 914mm OD are available for flow balancing, respectively, at a minimum thermal generation limit of 15GW (red and green) and 7.5GW (grey). LFPs are defined as flows below 50% of nominal flow.

Figure 6.13 (bottom): Cumulative number of low flow periods (LFPs) at the wellhead lasting for longer than X hours (see x-axis) in the 'Basecase' UCED scenario when no flow balancing is considered and minimum thermal generation limit is at 15GW (blue) and 7.5GW (black), and when pipelines of 610mm and 914mm OD are available for flow balancing, respectively, at a minimum thermal generation limits of 15GW (red and green) and 7.5GW (grey). LFPs are defined as flows below 50% of nominal flow.

6.5.1.2. 30% minimum flow

Figure 6.14 and Figure 6.15 illustrate the corresponding results when LFPs are defined as periods with flow rates lower than 30% of the nominal rate. In contrast to the previous subsection the frequency and duration of LFPs, when unbalanced, changes significantly as a

result of the changed minimum thermal generation limit. This indicates how frequently CCS power stations were operating and, hence, producing CO_2 flows above 30% of the nominal amount only as a consequence of the minimum thermal generation constraint of 15GW, whereas these flows would not be produced if the limit was lower.

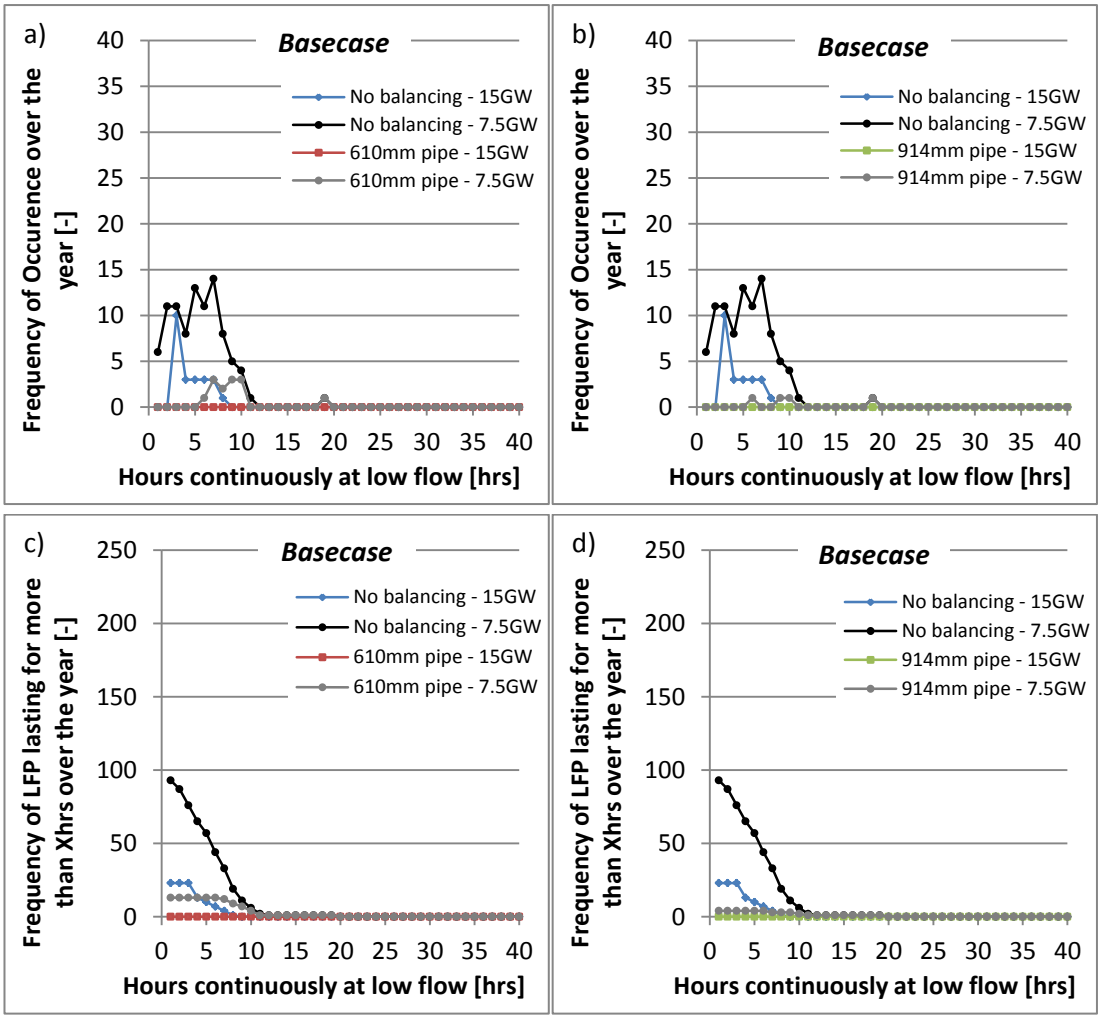

Figure 6.14 (top): Duration and frequency of low flow periods (LFPs) at wellhead in 'Basecase' UCED scenario when no flow balancing is considered and minimum thermal generation limit is at 15GW (blue) and 7.5GW (black), and when the reference pipelines of 610mm or 914mm OD are available for flow balancing, respectively, at minimum thermal generation limit of 15GW (red and green) and 7.5GW (grey). LFPs are defined as flows below 30% of nominal flow.

Figure 6.15 (bottom): Cumulative number of low flow periods (LFPs) at the wellhead lasting for longer than X hours (see x-axis) in the 'Basecase' UCED scenario when no flow balancing is considered and minimum thermal generation limit is at 15GW (blue) and 7.5GW (black), and when the reference pipelines of 610mm or 914mm OD are available for flow balancing, respectively, at minimum thermal generation limits of 15GW (red and green) and 7.5GW (grey). LFPs are defined as flows below 30% of nominal flow.

As a result of the relaxed inertial requirement in the sensitivity case the number of LFPs (when unbalanced) increases from 23 to 93 (by around 300%) when these periods are defined as times of flow rates below 30% of the nominal amount. Whilst the 914mm OD pipelines are able to bridge around 96% of these periods (89 out of 93), the 610mm OD representative pipelines are able to bridge around 86% (80 out of 93) of the events.

Overall, this sensitivity case shows that when LFPs are defined as a relatively high percentage of nominal flow (i.e. 50%) the frequency and durations of these periods do not change much when the minimum thermal generation level is reduced. However, fewer of them can be bridged by the balancing capabilities of the pipelines, which is a consequence of the lower levels of inflows during many LFPs (i.e. due to reduced minimum thermal generation constraint). When LFPs are, however, defined as relatively low percentages of the nominal flow (i.e. 30%) their frequency and number increase significantly at reduced inertial requirements. This is an effect of CCS power stations being able to shut in/reduce their load to a greater extent. Whilst the larger 914mm OD pipelines are still able to bridge nearly all LFPs even at reduced inertial requirement (92-98%), this is not possible anymore with the 610mm OD reference pipelines (reduction of 70-86% achievable).

6.5.2. Additional inflows during low flow periods

This section explores to what extent sustaining an additional level of inflow during LFPs can complement the balancing capabilities of pipelines and assist in reducing the number of LFPs at the downstream injection and storage level. Additional levels of inflows corresponding to 10% and 20% of the nominal flow rate are, respectively, fed into the pipelines in this sensitivity case to add to the regular inflows during LFPs. These additional inflows could be procured, for instance, from power stations being financially rewarded by T&S operators for running at a higher electricity load than required by the power system ultimately for the purpose of providing CO_2 flow balancing to the T&S system. To maintain the balance of electricity demand and supply, intermittent renewable power production could be curtailed, or nuclear power could be ramped down. Alternatively, PCC units operating at part load could utilise their spare capacity for regenerating previously stored rich solvent in order to increase the CO_2 flows that are exported to the T&S system to relatively high levels even at low overall power output (this option is evaluated in detail in Chapter 7). Another option for sustaining relatively high inflows of CO_2 even during LFPs would be to connect some baseload CO_2 generating facilities to the pipeline (i.e. CCS from industry) instead of having exclusively CCS power stations feeding into the system.

In this sensitivity study, the UCED ‘Basecase’ and the ‘High Wind/Low Emission Intensity’ scenarios are considered.

6.5.2.1. 50% minimum outflow

Figure 6.16 and Figure 6.17 illustrate the duration and frequency of LFPs at injection wells in the 'Basecase' UCED scenario if no flow balancing is considered (blue curves), and when the reference pipelines of 610mm and 914mm OD are deployed, respectively, for flow balancing (red and green curves). The different shades of red and green represent different inflow boosting scenarios during LFPs, as expressed in the legend. Whilst the top diagrams show the frequency of occurrence of a LFP as a function of its duration, the lower diagrams display the cumulative number of LFPs that extend for more than X hrs (as defined on the x-axis). The LFPs are defined in this section as times when flows drop below 50% of the nominal rate.

Similarly to Figure 6.2, diagrams a) and c) demonstrate that when the 610mm OD pipelines are utilised for flow balancing the number of LFPs at the injection well level can be reduced from around 202 to approx. 32. If additional inflows of 10% or 20% are procured during the LFPs this number further reduces to 5 and 2, respectively. When the larger 914mm OD pipelines are deployed for flow balancing the number of LFPs at the well can be reduced from 202 to 7. If additional inflows during LFPs of 10% and 20% are sustained this number further reduces to 4 and 1, respectively.

It becomes clear that boosting the inflows into the pipeline at times of low CO_2 supply, even if only by around 10-20% of nominal flow, has the potential to drastically reduce the residual number of LFPs injection wells will face, particularly when used in combination with the flow balancing capabilities of pipelines. Boosting inflows by only 10% of nominal flow during LFPs when simultaneously utilising 610mm OD pipelines for balancing has approximately the same effect than using solely the strongly oversized 914mm OD pipelines for balancing. Both ways allow the number of LFPs at the injection well level to be drastically reduced to very low levels - if not eliminated - even when LFPs are defined very broadly as periods when flow rates drop below 50% of the nominal level.

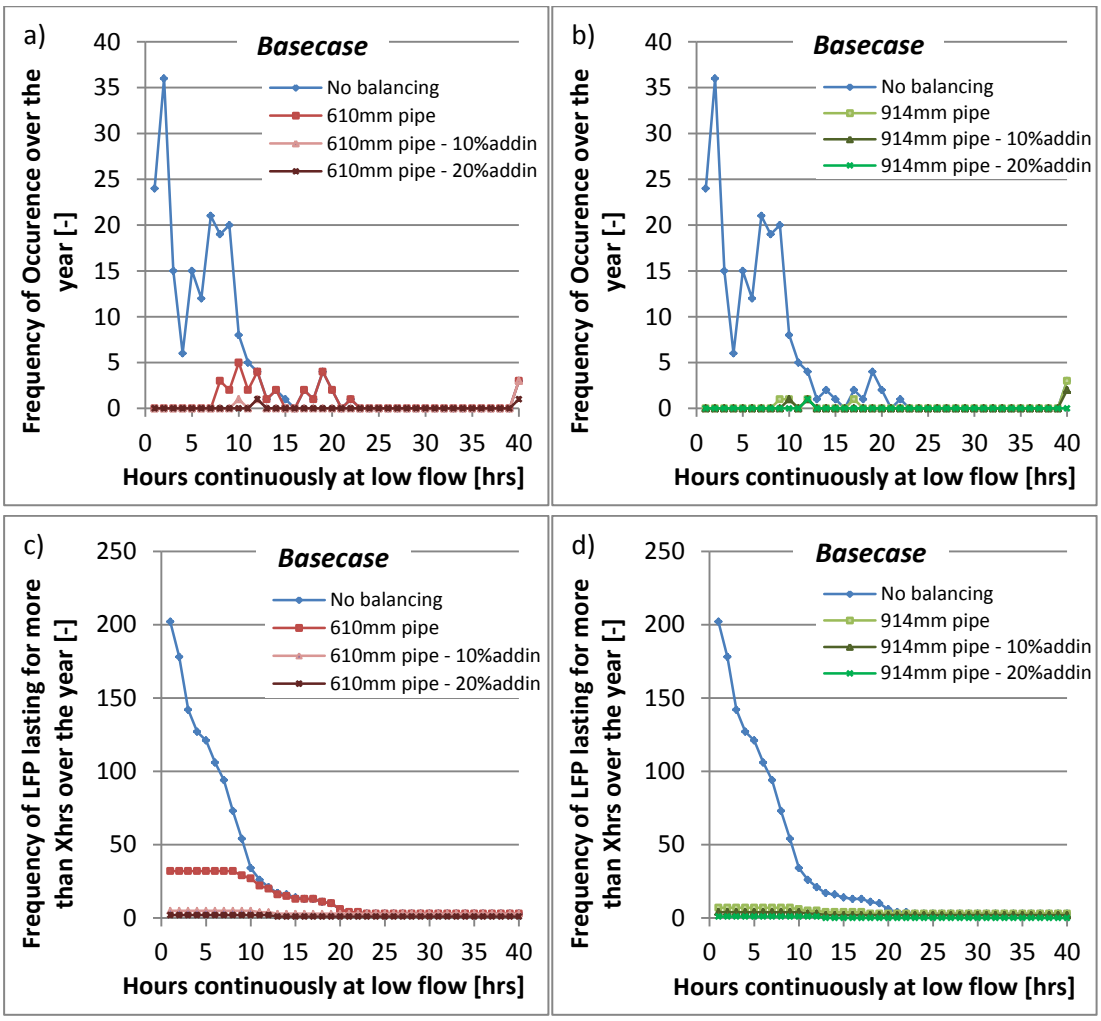

Figure 6.16 (top): Duration and frequency of low flow periods (LFPs) at wellhead in 'Basecase' UCED scenario if no flow balancing is considered (blue), if the 610mm OD pipelines are deployed for flow balancing (red - left), and if the 914mm OD pipelines are deployed for flow balancing (green - right) for different levels of additional inflows during LFPs (see legend). LFPs are defined as flows below 50% of nominal flow.

Figure 6.17 (bottom): Cumulative number of low flow periods (LFPs) at the wellhead lasting for longer than X hours (see x-axis) in the 'Basecase' UCED scenario if no flow balancing is considered (blue), if the 610mm OD pipelines are deployed for flow balancing (red - left), and if the 914mm OD pipelines are deployed for flow balancing (green - right) for different levels of additional inflows during LFPs (see legend). LFPs are defined as flows below 50% of nominal flow.

Figure 6.18 and Figure 6.19 show the resulting diagrams when performing the equivalent analysis on the 'High Wind/Low Emission Intensity' UCED scenario. It can be observed how by deploying the 610mm OD pipelines for balancing purposes the number of LFPs at the injection well can be reduced from 248 to 138. When boosting the inflows during LFPs into the pipe by 10% of nominal flow this number drops to 72. This is a similar level that can be achieved with the larger 914mm OD pipelines (68) without relying on additional inflows. When boosting inflows during LFPs by 20% of nominal flow the number further falls to 20. This is in a similar region than can be achieved by deploying the larger 914mm OD pipelines

when additional inflows of 10% of nominal flow are secured during LFPs (32). Only when deploying the larger 914mm OD pipeline in combination with additional inflows of 20% of nominal flow during LFPs the number of can be reduced by 97% (to 7).

Diagrams a) and b) show that boosting inflows can help bridging some LFPs enduring for longer than 40hrs, particularly when using 914mm OD pipelines, however, at times even when using the 610mm OD pipelines.

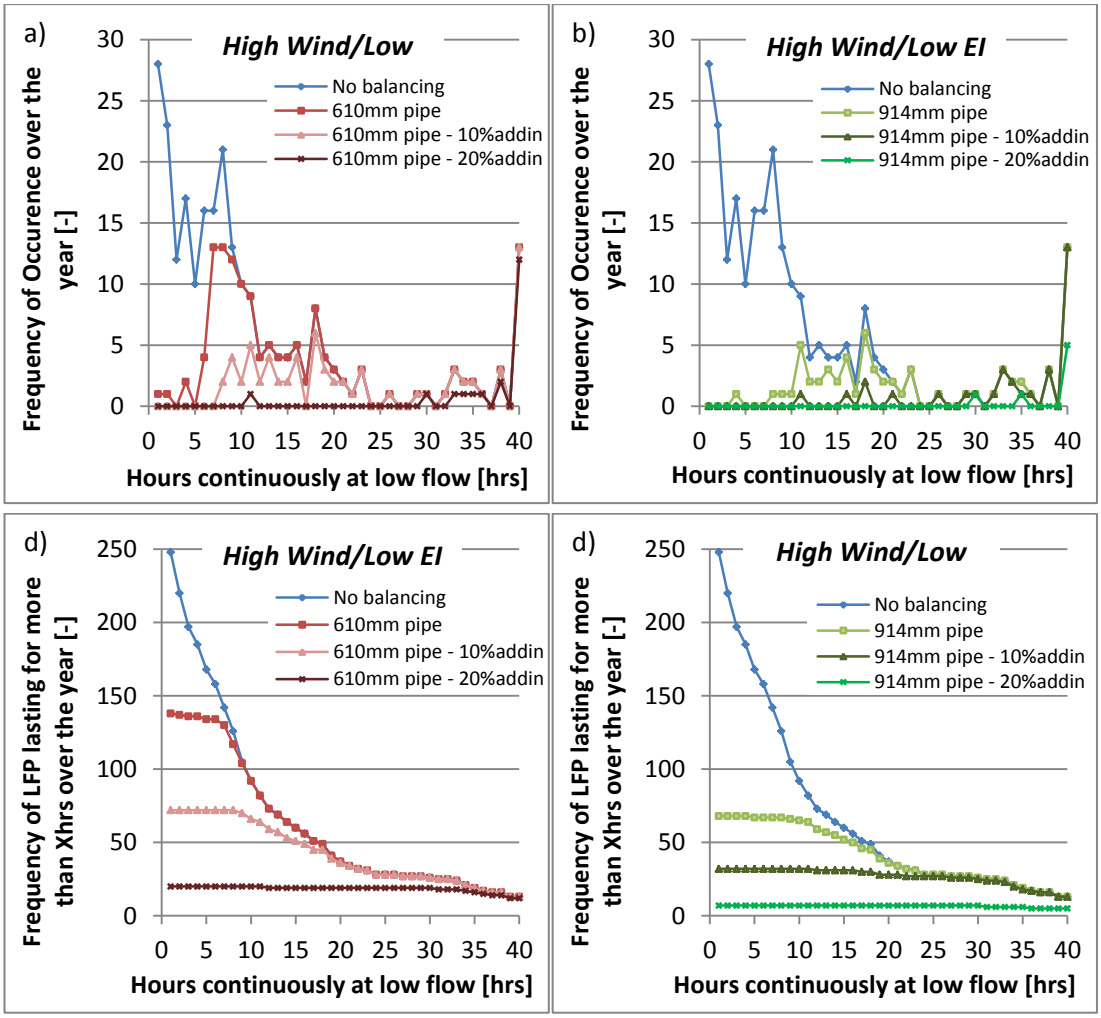

Figure 6.18 (top): Duration and frequency of low flow periods (LFPs) at wellhead in 'High Wind/Low Emission Intensity' UCED scenario if no flow balancing is considered (blue), if the 610mm OD pipelines are deployed for flow balancing (red - left), and if the 914mm OD pipelines are deployed for flow balancing (green - right) for different levels of additional inflows during LFPs (see legend). LFPs are defined as flows below 50% of nominal flow.

Figure 6.19 (bottom): Cumulative number of low flow periods (LFPs) at the wellhead lasting for longer than X hours (see x-axis) in the 'High Wind/Low Emission Intensity' UCED scenario if no flow balancing is considered (blue), if the 610mm OD pipelines are deployed for flow balancing (red - left), and if the 914mm OD pipelines are deployed for flow balancing (green - right) for different levels of additional inflows during LFPs (see legend). LFPs are defined as flows below 50% of nominal flow.

6.5.2.2. 30% minimum outflow

This subsection carries out the equivalent analysis as the previous subsection, however, with LFPs being defined as periods in which flow drops below 30% of nominal flow.

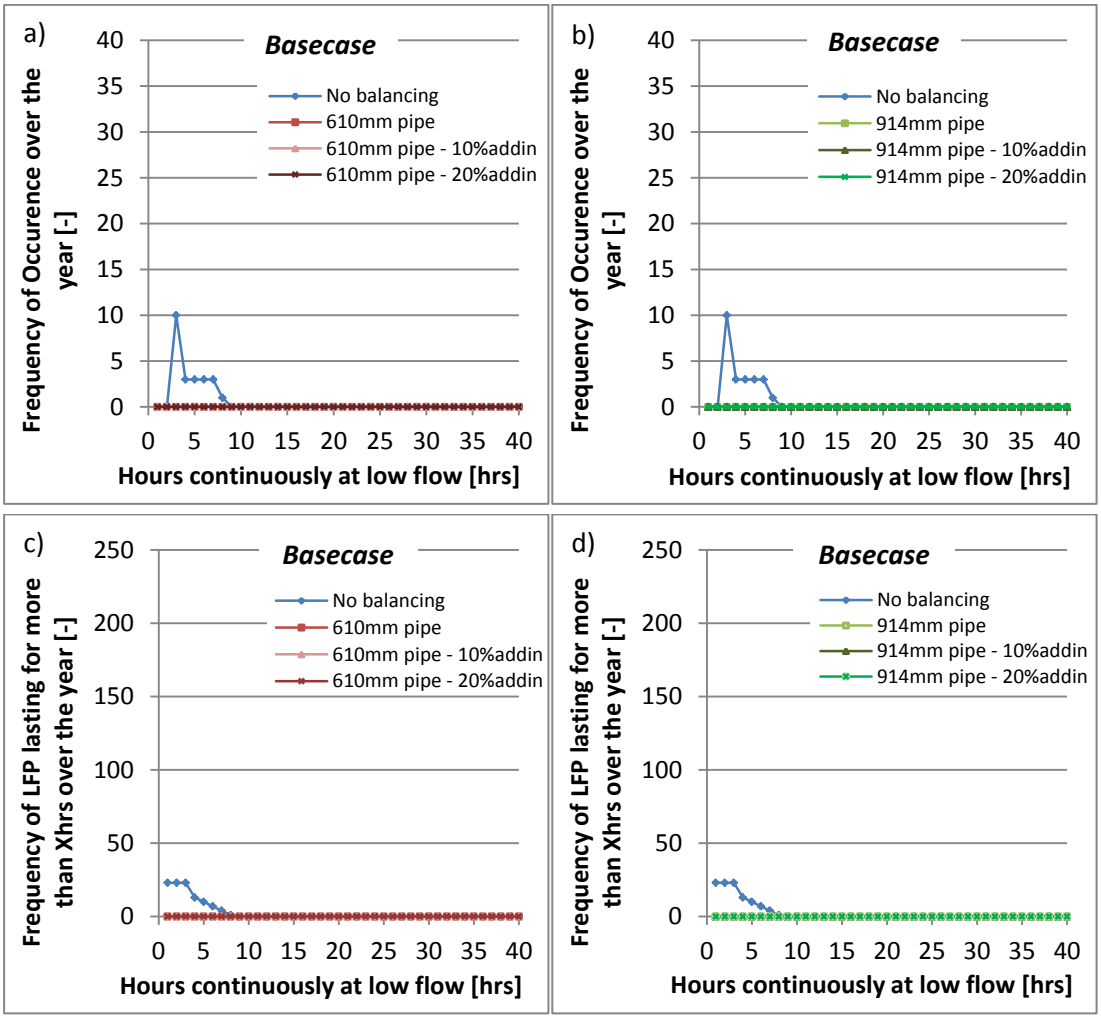

Figure 6.20 (top): Duration and frequency of low flow periods (LFPs) at wellhead in 'Basecase' UCED scenario if no flow balancing is considered (blue), if the 610mm OD pipelines are deployed for flow balancing (red - left), and if the 914mm OD pipelines are deployed for flow balancing (green - right) for different levels of additional inflows during LFPs (see legend). LFPs are defined as flows below 30% of nominal flow.

Figure 6.21 (bottom): Cumulative number of low flow periods (LFPs) at the wellhead lasting for longer than X hours (see x-axis) in the 'Basecase' UCED scenario if no flow balancing is considered (blue), if the 610mm OD pipelines are deployed for flow balancing (red - left), and if the 914mm OD pipelines are deployed for flow balancing (green - right) for different levels of additional inflows during LFPs (see legend). LFPs are defined as flows below 30% of nominal flow.

Figure 6.18 and Figure 6.19 show that in the 'Basecase' UCED scenario all LFPs can be bridged with both pipelines of 610mm and 914mm OD, respectively, even when there are

zero additional inflows during these critical periods. It can, therefore, be concluded that when LFPs are defined as periods with flows below 30% of the nominal rate there is no additional value in procuring additional inflows during LFPs for the purpose of avoiding LFPs at the injection well.

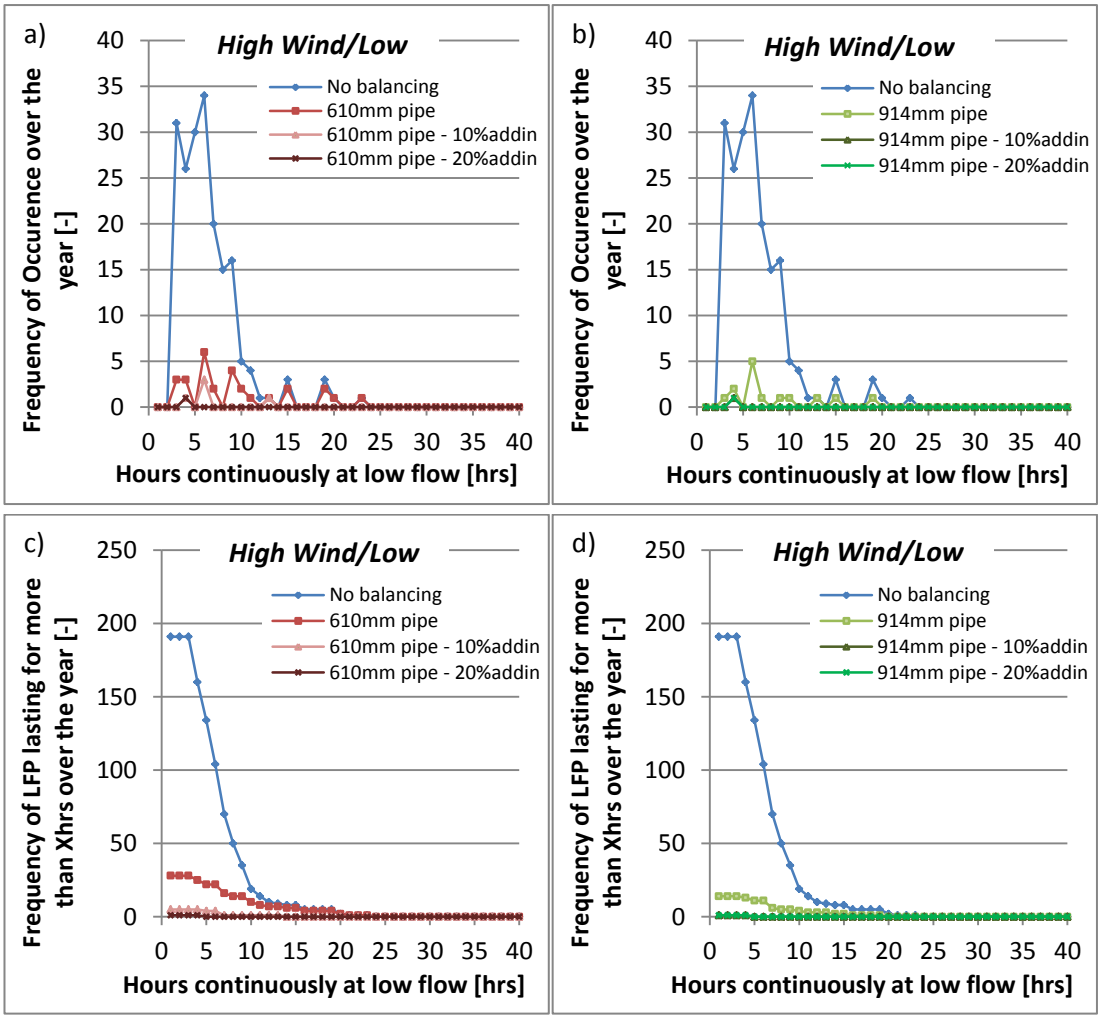

Figure 6.22 (top): Duration and frequency of low flow periods (LFPs) at wellhead in 'High Wind/Low Emission Intensity' UCED scenario if no flow balancing is considered (blue), if the 610mm OD pipelines are deployed for flow balancing (red - left), and if the 914mm OD pipelines are deployed for flow balancing (green - right) for different levels of additional inflows during LFPs (see legend). LFPs are defined as flows below 50% of nominal flow.

Figure 6.23 (bottom): Cumulative number of low flow periods (LFPs) at the wellhead lasting for longer than X hours (see x-axis) in the 'High Wind/Low Emission Intensity' UCED scenario if no flow balancing is considered (blue), if the 610mm OD pipelines are deployed for flow balancing (red - left), and if the 914mm OD pipelines are deployed for flow balancing (green - right) for different levels of additional inflows during LFPs (see legend). LFPs are defined as flows below 50% of nominal flow.

Figure 6.22 and Figure 6.23 illustrate the results when the same analysis is performed for the 'High Wind/Low Emission Intensity' scenario. When solely exploiting the balancing

capabilities of the 610mm or 914mm OD pipelines, respectively, without procuring additional inflows during critical periods, the number of LFPs the injection wells face can be reduced from 191 to 28 and 14, respectively, compared to the counterfactual case with no flow balancing. With additional inflows of 10% and 20% of nominal flow during low inflow periods, respectively, and the 610mm OD pipelines available for balancing, this number can further be reduced to 5 and 1. If the larger 914mm OD pipeline is available for balancing the number of LFPs at the injection wells can be reduced to 1 regardless of the evaluated additional inflow scenario during critical periods. It should be noted that the remaining 1 LFP that cannot be avoided is an effect of the initial conditions (i.e. starting working inventory is effectively zero, and the starting point in the considered reference year that coincides with a LFP). Importantly it can, therefore, be concluded that even in the worst case variability scenario all LFPs at the injection well level can effectively be avoided when exploiting the buffering capabilities of pipelines while additionally providing them with additional inflows of at most 20% of nominal flow during critical periods.

Overall, sensitivity case 2 shows that boosting inflows into the pipeline during LFPs by only around 10-20% of nominal flow can very strongly contribute to reducing the annual number of LFPs at the injection and storage level. When LFPs are defined as times of flow rates below 30% of the nominal amount the combination of using the buffer capabilities of pipelines and boosting additional inflows during critical periods can effectively eliminate LFPs at the injection wells even in the worst case variability scenario considered in this study. When defining LFPs as times of flow rates below 50% of nominal flow the same combination can eliminate the number of LFPs at the injection wells only in the 'Basecase' UCED scenario. In the 'High Wind/Low Emission Intensity' scenario the number of LFPs at the injection wells can be reduced by 90-97% compared to the counterfactual case when no flow balancing or similar options are utilised – this compares to reductions of 32-66% achievable when only pipelines are deployed for flow balancing without any additional inflows during LFPs.

6.5.3. Capture plant bypass

The option of operators of CCS power stations to turn off the capture unit independently from the power unit can have significant effects on the frequency and duration of LFPs. This option can be used for example for boosting the power output at times of high electricity prices by recovering a majority of the energy penalty associated with the CO_2 capture process. For the power plant operator it would economically make sense to use this option if the revenues from the sale of the additionally produced power offsets the increased carbon emission costs that are incurred as a direct consequence of not capturing some of the produced CO_2 and instead releasing it into the atmosphere (see also Chapter 3, section 3.6.7.3). This section explores this effect by evaluating how the number of LFPs at the injection and storage level over the reference year in the 'Basecase' UCED scenario changes

when the option for bypass is allowed. Similarly to section 3.6.7.3 the analysis is performed for different CO_2 prices, since they have been found to be a key influencing factor when deciding whether it is economical to shut in the capture unit. The analysis presented examines changes in the results when bypass is allowed at carbon prices of 50£/tCO_2 and 30£/tCO_2, respectively. At baseline carbon prices of 101.5£/tCO_2 (see Chapter 3) it was found that allowing for the option of bypass has only negligible effects on the duration and frequency of LFPs. Consequently this case is omitted when presenting the analysis.

6.5.3.1. 50% minimum flow

Figure 6.24 and Figure 6.25 illustrate the duration and frequency of LFPs at the injection wells in the 'Basecase' UCED scenario if (i) no flow balancing is considered and the option for bypass is not allowed (blue curves); (ii) if no flow balancing is considered and the option for bypass is allowed at CO_2 prices of 50£/tCO_2 (black) and 30£/tCO_2 (orange); (iii) if flow balancing is deployed and the option for bypass is not allowed (red or green); and (iv) if flow balancing is deployed and the option for bypass is allowed at carbon prices of 50£/tCO_2 (grey) and 30£/tCO_2 (yellow). The left diagrams show the respective graphs for when the 610mm OD reference pipeline is available for balancing, and the right diagrams show the equivalent graphs for when the larger 914mm OD pipelines are available for balancing. Whilst the top diagrams show the frequency of occurrence as a function of the duration of the LFP, the lower diagrams display the cumulative number of LFPs that extend for more than X hrs (as defined on x-axis). LFPs are defined as any periods when flow falls below 50% of the nominal rate in this subsection. For illustrative reasons and for decongesting the diagrams, graphs that have been previously shown are presented without markers (blue, red and green graphs in the diagrams).

It can be seen that allowing for the option for bypass increases the number of LFPs from 202 to 260 (by around 29%) if carbon prices are at 50£/tCO_2. However, if carbon prices are at 30£/tCO_2 the number of LFPs over the reference year increases dramatically from 202 to 507 (151% increase) compared to the counterfactual case when bypass is not allowed. If the 610mm OD pipelines are deployed for flow balancing and the option for bypass is allowed the residual number of LFPs at the injection wells increase to 64 at carbon prices of 50£/tCO_2 compared to the counterfactual case when the option for bypass is not allowed (32) (100% increase). At carbon prices of £30£/tCO_2 this increase rockets upwards to 438% (from 32 to 172). The deployment of the larger 914mm OD pipelines allows keeping the number of LFPs the injection wells face at low levels (11) even when allowing for capture plant bypass, at least at carbon prices of £50t/CO_2. At reduced carbon prices of 30£/tCO_2 this number, however, also increases significantly (to 80).

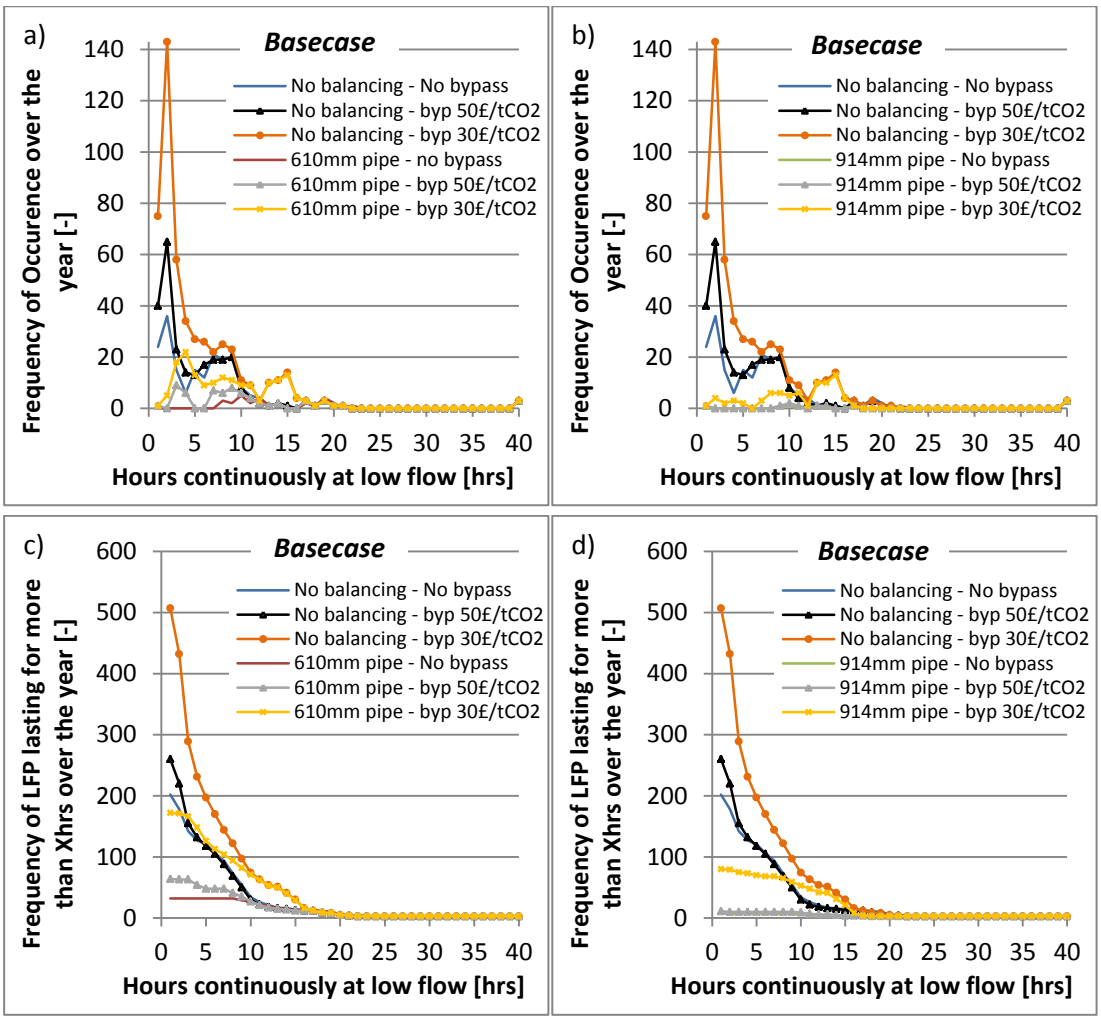

Figure 6.24 (top): Duration and frequency of low flow periods (LFPs) at wellhead in 'Basecase' UCED scenario if no flow balancing is considered and bypass is not allowed (blue), if no balancing is considered and bypass is allowed at carbon prices of 50£/tCO$_2$ (black) and 30£/tCO$_2$ (orange), if pipelines of 610mm and 914mm OD are deployed for flow balancing and bypass is not allowed (red and blue), and if pipelines of 610mm and 914mm OD are deployed for flow balancing and bypass is allowed for carbon prices of 50£/tCO$_2$ (grey) and 30£/tCO$_2$ (yellow). LFPs are defined as flows below 50% of nominal flow.

Figure 6.25 (bottom): Cumulative number of low flow periods (LFPs) at the wellhead lasting for longer than X hours (see x-axis) in the 'Basecase' UCED scenario if no flow balancing is considered and bypass is not allowed (blue), if no balancing is considered and bypass is allowed at carbon prices of 50£/tCO$_2$ (black) and 30£/tCO$_2$ (orange), if pipelines of 610mm and 914mm OD are deployed for flow balancing and bypass is not allowed (red and blue), and if pipelines of 610mm and 914mm OD are deployed for flow balancing and bypass is allowed for carbon prices of 50£/tCO$_2$ (grey) and 30£/tCO$_2$ (yellow). LFPs are defined as flows below 50% of nominal flow. LFP is defined as flows below 50% of nominal flow.

6.5.3.2. 30% minimum flow

Figure 6.26 and Figure 6.27 illustrate the equivalent analysis as in the previous subsection when LFPs are defined as periods of flows below 30% of the nominal rate.

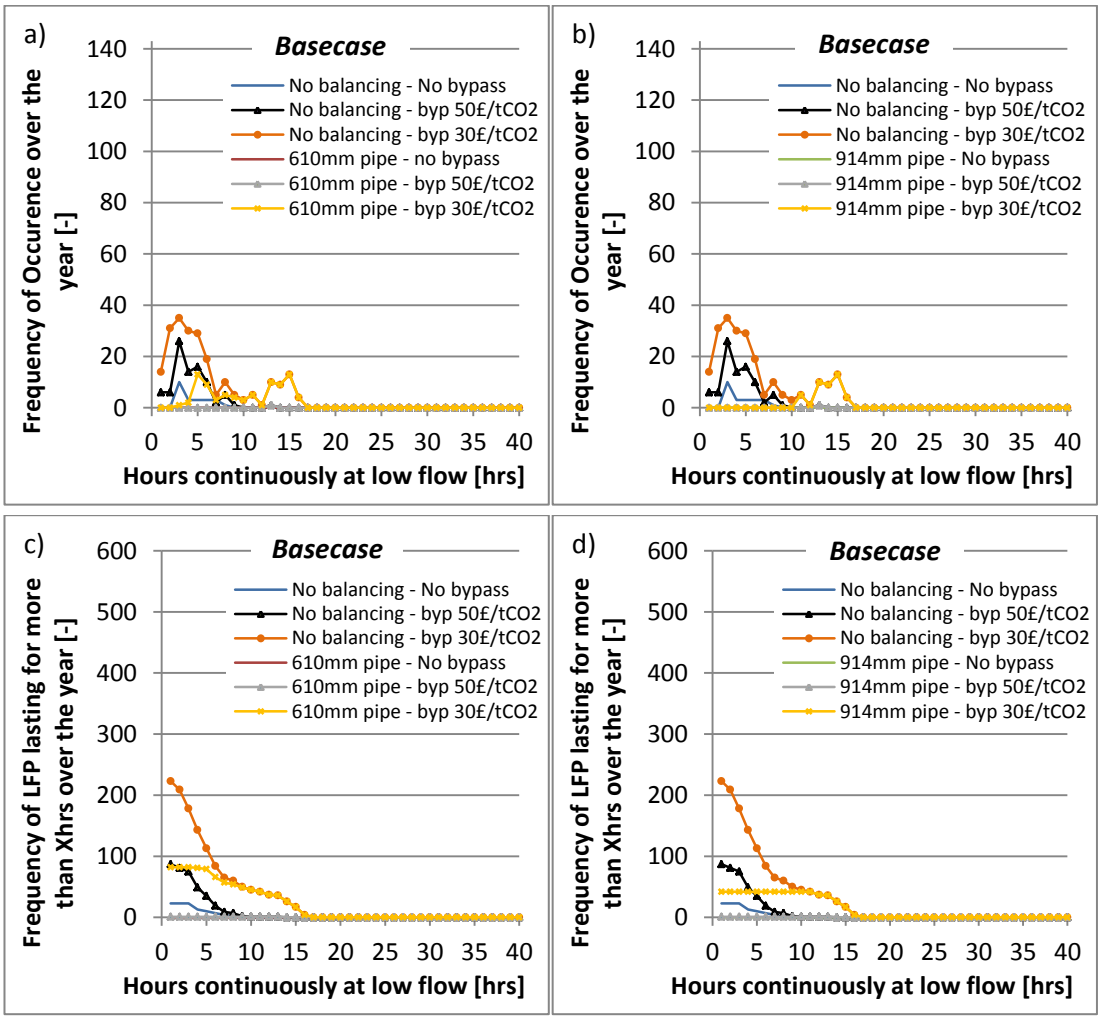

Figure 6.26 (top): Duration and frequency of low flow periods (LFPs) at wellhead in 'Basecase' UCED scenario if no flow balancing is considered and bypass is not allowed (blue), if no balancing is considered and bypass is allowed at carbon prices of 50£/tCO$_2$ (black) and 30£/tCO$_2$ (orange), if pipelines of 610mm and 914mm OD are deployed for flow balancing and bypass is not allowed (red and blue), and if pipelines of 610mm and 914mm OD are deployed for flow balancing and bypass is allowed for carbon prices of 50£/tCO$_2$ (grey) and 30£/tCO$_2$ (yellow). LFPs are defined as flows below 30% of nominal flow.

Figure 6.27 (bottom): Cumulative number of low flow periods (LFPs) at the wellhead lasting for longer than X hours (see x-axis) in the 'Basecase' UCED scenario if no flow balancing is considered and bypass is not allowed (blue), if no balancing is considered and bypass is allowed at carbon prices of 50£/tCO$_2$ (black) and 30£/tCO$_2$ (orange), if pipelines of 610mm and 914mm OD are deployed for flow balancing and bypass is not allowed (red and blue), and if pipelines of 610mm and 914mm OD are deployed for flow balancing and bypass is allowed for carbon prices of 50£/tCO$_2$ (grey) and 30£/tCO$_2$ (yellow). LFP is defined as flows below 50% of nominal flow. LFPs are defined as flows below 30% of nominal flow.

Allowing for the option for bypass increases the number of LFPs (with no balancing available) even stronger than in the previous section from 23 to 87 (by 278%) at carbon prices of 50£/tCO_2, and to 223 (870% increase) at carbon prices of 30£/tCO_2. Deploying either pipeline of 610mm or 914mm OD, nevertheless, allows bridging all LFPs at least at carbon prices of 50£/tCO_2 when bypass is allowed. At carbon prices of 30£/tCO_2, deploying the reference pipelines of 610mm or 914mm OD for balancing can assist in reducing the number of LFPs at the injection and storage level, however, around 82 and 42 of these low flow events remain, respectively, over the year.

Overall, the analysis in this section shows that when allowing for the option to bypass the number of LFPs feeding into the pipelines rises significantly, however, only at relatively low carbon prices. Whilst no significant effect could be observed when the option for bypass is allowed at baseline CO_2 prices of 101.5£/tCO_2, the number of LFPs feeding into the pipeline increases by 30-100% at carbon prices of 50£/tCO_2 and by 438-870% at carbon prices of 30£/tCO_2, dependent on the definition of a LFP. Although the flow balancing capabilities of the 610mm or 914mm OD pipelines can contribute to reducing the number of LFPs at the downstream injection and storage level from a comparatively high (or very high) level when bypass is allowed, the numbers stay substantial, and in some scenarios (i.e. at CO_2 prices of 30£/tCO_2) they stay higher than when the option for bypass is not allowed even when no flow balancing is carried out. It can, therefore, be concluded that when assessing whether the option for capture plant bypass should be allowed considerations should be given to the negative effects the induced variability of CO_2 flows can have on the downstream CO_2 T&S infrastructure, particularly when CO_2 prices are relatively low (e.g. 50£/tCO_2 and below).

6.6. Cost estimation of oversizing pipelines

Whilst this chapter does not focus on techno-economics of effectively designed CO_2 T&S systems it is helpful for appraising the economic viability of the option for oversizing pipelines to put the costs associated with it into context with the value of the components that would be protected by it, i.e. the injection wells. A brief and illustrative example cost calculation is hence provided in the following. The example calculation is based on cost models and cost numbers available in the literature, and it demonstrates that the costs of oversizing pipelines is reasonably small compared to the value (i.e. costs in this context) of the involved injection wells that would benefit from smoothed out flows upstream in the CO_2 transportation system.

There are several models for estimating the costs of CO_2 transportation pipelines available in the literature. They can be classified into five categories (Mechleri et al. 2017a): linear models (Heddle et al. 2003, Van den Broek et al. 2010, Element Energy 2010), models based on the weight of the pipeline (Gao et al. 2011, Piessens et al. 2008), quadratic equations

(IEAGHG 2002, Parker 2004), models based on flowrates (McCollum and Ogden 2006, Chandel et al. 2010, Knoope et al. 2013), and the CMU model (McCoy and Rubin 2008). For the cost estimation in this section the quadratic cost model developed by IEAGHG (2005) is used, since it allows offshore pipeline cost estimation, is simple, yet still regularly used in the CCS literature (Mechleri et al. 2017a, Ghazi and Race 2012, Liu and Gallagher 2011). According to IEAGHG (2005), capital costs for offshore pipelines can be expressed as:

$$C_{offshore}^{CAPEX} = 10^6 * [(0.4048 * L_{offshore} + 4.6946) \quad (11)$$
$$(0.00153 * L_{offshore} + 0.0113) * D_o$$
$$+ (0.000511 * L_{offshore} + 0.00024) * D_o^2$$

Where $L_{offshore}$ *is the length of the pipeline in km*
D_o *is the outer diameter of the pipeline in inches.*

Considering an average annual inflation of 1.7% in the EU between 2005 and 2019 (TradingEconomics 2019) and an exchange rate of 1.15€/£ in 2019 (Bloomberg, 2019a) the reference pipeline of 100km length and 610mm (24 inch) outer diameter in this chapter would have an approximate capital cost of 78.0M£ in 2019. Pipelines of an equivalent length and outer diameters of 762mm (30 inch) and 914mm (36 inch) would come at around 95.2M£ and 116.5M£. This corresponds to cost increases of around 17.2M£ (+22%) and 38.5M£ (+50%), respectively, for oversizing the reference pipeline of 100km. It should be noted that as an additional merit of oversizing the reference pipeline the economic flow capacities in this example would increase by a factor of 2.0-2.8x, respectively, from 13MTPA to 25.5MTPA and 36.5MTPA (see also section 5.4 for economic flow capacity calculations in this study). Overrsizing the pipelines could, therefore, simultaneously be seen an investment into future proofing of the transportation system.

Whilst pipelines can be oversized by increasing their diameter another effective way of increasing their linepacking capability is to increase their maximum operating pressure (MAOP). This can for example be achieved by increasing the wall thickness of the pipe (see also section 5.4). Since small deviations in wall thickness have only a relatively small effect on pipeline capital costs its impact is not specifically considered in equation 11. Yet, Gao et al. (2011) and Haumann et al. (2012) suggest material costs correspond to around 30% of pipeline CAPEX. Increasing the MAOP of the reference pipeline of 100km and 610mm outer diameter from '150'bar to '200'bar by increasing the wall thickness from 14.2mm to 20mm (41% increase in wall thickness - see Table 5.4) would, hence, increase pipeline capital costs by approx. (78.0M£ x 30% x 41% =) 9.6M£. Equivalent cost increases for pipeline of 100km length and 762m (30 inch) and 914mm (36 inch) outer diameter correspond to 7.1M£ and 11.5M£, respectively.

Higher operating pressures could also imply somewhat increased capital costs for compression and pumping stations. Nevertheless, it is assumed similar to IEAGHG

(2005) that these costs are largely independent of the pressure levels. Annual operating costs and maintenance costs are often assumed at 3% of capital costs (IEAGHG 2005, Mechleri et al. 2017a). The impact of operating at a somewhat increased pressure level (e.g. from 150bar to 200bar) whenever needed for the purpose of linepacking and depacking operation can consequently be expected to be relatively minor, particularly when discounted over the project lifetime.

Costs of CO_2 injection wells are highly variable and depend on a number of factors: drilling depth, well deviation/inclination, type of rock, type of rig used and its hire dayrate, materials and consumable, logistics support, project management and engineering (IEAGHG 2009). Particularly the first three factors can have a large impact on the drilling time which directly influences the required rig hire time, which in turn is a substantial cost driver cost driver at hire dayrates of around 155,000-300,000£/day (Capture Power Limited 2016a, EON 2012b). To illustrate the significant variations in well capital costs, IEAGHG (2009) presents example cost data ranging from 5.6M$-30.8M$ for relatively shallow reservoir wells to very deep reservoir wells, corresponding to a values of approx. 4.6-25.3M£ in 2019 (Bloomberg 2019b, Bank of England 2019). These cost numbers are also in the range of what other studies published by IEAGHG (2011b) suggest. They are also in line with the 10-20M£ estimated as capital cost per well by the Kingsnorth UK CCS demonstration project team (EON 2012b).

Considering a flow rate of around 10-13MTPA the reference trunk pipelines considered throughout this chapter would feed into a number of wells. Typically 1-2MTPA are considered as maximum flow rates through CO_2 injection wells (Kolster et al. 2018, Capture Power Limited 2016a). However, assuming a flow of 1.25MTPA per well as suggested by L.E.K.Consulting (2009) the reference pipelines considered in this chapter with a flow of 10.5-13MTPA would feed into approx. 8-10 wells. At a cost estimate of 10M£/well this would consequently mean a value of around 80-100M£ could at least partially be protected by: (i) oversizing the pipelines by increasing the MAOP from '150'bar to '200'bar for a cost increase of around 9.6-11.5M£ (9.9-12.3% of pipeline cost); or by (ii) oversizing the pipelines in terms of diameter with a cost increase of 17.2-38.5M£ (22-50% of pipeline cost) to increase the diameter from 610mm to 762mm and 914mm, respectively. As an additional merit of option (ii) the economic flow rate capacity of the pipeline in this example increases by a factor of 2.0-2.8x, which can also be seen as an investment into future proofing the system for higher future flow rates.

As a caveat it should be noted in this example calculation that the reductions in insurance costs - which can constitute a significant cost contribution to CCS projects (Spitz 2016) – achievable with operating the wells in a less flexible manner by smoothing out flows upstream in the system in oversized pipelines are not yet considered.

The short and illustrative example calculation shows that whilst in the end this has to be evaluated on a case by case basis the cost of oversizing the pipelines in order to smooth out flows upstream in the transportation system could be relatively small compared to the value of the wells that could be protected in this way.

6.7. Conclusions

This chapter has evaluated to what extent the linepacking and depacking capabilities of pipelines can be used to reduce the number of LFPs at the downstream injection and storage level. In this way the chapter has quantified the extent to which dense phase CO_2 transportation pipelines can provide capacity for flexibility and redundancy in the CCS system, as recently recommended by ZEP (2017), which can accommodate volatility in CO_2 supply and demand and, hence, mitigate integrity issues associated with variable flow rates at the injection and storage level.

CO_2 flows from three GB electricity system scenarios have been considered that differ in the average carbon intensity of the produced power (60g/kWh and 100g/kWh), and the level of wind deployment (30GW and 45GW) and CCS deployment (7-14GW). The selected electricity system scenarios were investigated conjointly with two realistic pipeline alternatives, which differ in the degree of oversizing for the flow transported. The pipelines that were considered had following design characteristics: Outer diameters of 610mm and 914mm, respectively, a length of 100km, and MAOPs of around 200bar. By analysing a range of core scenarios as well as a number of sensitivity cases the following conclusions could be drawn.

General:

- By making available flow balancing capability via oversizing of pipelines the number of LFPs at the downstream injection and storage level can be reduced substantially. In the 'Basecase' UCED scenario the annual number of LFPs at the injection level (LFPs defined as periods of flow below 50% of the design flow) can be reduced by 84% (from 202 to 32) and 97% (from 202 to 7) when deploying the reference pipeline with 610mm and 914mm OD, respectively, for flow balancing. This number somewhat drops to 44% (from 248 to 138) and 73% (from 248 to 68) for CO_2 flow profiles generated in the 'High Wind/Low Emission Intensity' UCED scenario.
- It is more challenging to reduce the number of LFPs in low emission scenarios. This is due to the lower relative flow rates frequently feeding into the pipeline during LFPs (due to the larger CCS fleets, many of which will shut down during periods of low net demand, as discussed in Chapter 3). This leads to a quicker depletion of the pipeline working inventory. As a consequence the depacking process cannot be used to bridge as many and long LFPs.

- When LFPs are defined as times of flow levels below 30% of the nominal rate the deployment of either the 610mm or 914mm OD reference pipelines can reduce the occurrence of such events at the injection and storage level to very few times over the year, if not to zero (i.e. from 23 to 0 in the 'Basecase'; from 143 to 6-10 in the Low EI/medium wind case; and from 191 to 14-28 in the 'High Wind/Low Emission Intensity' scenario, dependent on the deployed pipeline type).
- Consequently, when LFPs are defined as any times of flow levels below 30% of the nominal rate the larger 914mm OD pipelines perform only marginally better than the 610mm OD pipelines even though they are strongly oversized (due to the 610mm pipelines already being able to bridge almost all LFPs).
- In no evaluated core UCED scenario captured CO_2 flows fall below 10% of nominal flow. Consequently, no balancing capabilities would be required even if this was the minimum required flow level that needed to be sustained at the injection wells.

Sensitivity cases:

- When LFPs are defined as a relatively high percentage of nominal flow (i.e. 50%) the frequency and durations of these periods do not change much even when the minimum thermal generation level (i.e. inertial requirement from thermal power station) in the electricity system is reduced. However, fewer of them can be bridged with the balancing capabilities of the pipelines (70-92% compared to 84-97% with baseline minimum thermal generation limit), which is a consequence of the lower levels of inflows during many LFPs (i.e. due to reduced minimum thermal generation constraint) that lead to quicker depletion of pipeline working inventories.
- When LFPs are defined as relatively low percentages of the nominal flow (i.e. 30%) their frequency and number increases significantly at reduced minimum thermal generation limits. This is an effect of CCS power stations being able to shut in/reduce their load to a greater extent. Whilst the larger 914mm pipelines are still able to bridge almost all LFPs even at reduced inertial requirement, this is not achievable with the 610mm reference pipelines.
- Boosting inflows into the pipeline during LFPs by only around 10-20% of nominal flow can very strongly contribute to reducing the number of LFPs at the downstream injection and storage level: When LFPs are defined as times of flow rates below 30% of the nominal amount the combination of using the buffering capabilities of pipelines and boosting additional inflows during these critical periods can effectively eliminate LFPs at the injection level even in the worst case CO_2 flow variability energy system scenario considered in this study.
- When defining LFPs as times of flow rates below 50% of nominal flow the combination of using the buffering capabilities of pipelines and boosting additional inflows during critical periods can eliminate the number of LFPs at the injection wells only in the 'Basecase' UCED scenario. In the 'High Wind/Low Emission Intensity' scenario the number of LFPs at injection can be reduced by 90-97%

compared to the counterfactual case when no flow balancing or other options are utilised – this compares to reductions of 32-66% achievable when only pipelines are deployed for flow balancing without any additional inflows during LFPs.

- When allowing for the option to bypass at the capture plant level the number of LFPs feeding into the pipelines rises significantly, however, only at relatively low carbon prices. Whilst no significant effect could be observed when the option for bypass is allowed at the baseline CO_2 prices of 101.5£/tCO_2, the number of LFPs feeding into the pipeline increases by 30-100% at carbon prices of 50£/tCO_2 and by 438-870% at carbon prices of 30£/tCO_2, dependent on the definition of a LFP.
- Although the flow balancing capabilities of the 610mm and 914mm OD reference pipelines can contribute to reducing the number of LFPs at the downstream injection and storage level from a comparatively high/very high level when bypass is allowed, the numbers stay substantial, and in some scenarios (i.e. at CO_2 prices of 30£/tCO_2) stay higher than when the option for bypass is not allowed even if no flow balancing was carried out. Therefore, when assessing whether the option for capture plant bypass should be allowed considerations should be given to the negative effects of the induced variability of CO_2 flows on the downstream CO_2 T&S infrastructure, particularly at relatively low carbon prices (e.g. 50£/tCO_2 and below).

7. Solvent Storage at Natural Gas Fired PCC-CCS power stations

7.1. Introduction

The last chapters have quantified the variability of CO_2 flows that can be expected in future CO_2 T&S systems, and the contribution linepacking of dense phase CO_2 pipelines can make to avoiding critical low flow periods at the injection and storage level. It was demonstrated that in particular oversizing pipelines provides a powerful tool for reducing the number of LFPs at injection level to very low levels and across all considered energy system scenarios. Nevertheless, if oversized pipelines are not available (e.g. gradual increases in flow rates along with CCS roll out can reduce the relative oversizing of the pipeline system), or if CO_2 flow variability in pipelines is larger than in the evaluated scenarios, additional ways of mitigating this variability need to be considered. A sensitivity case in section 6.5.2 has demonstrated how additional inflows during periods of low CO_2 production are another very effective method for reducing the annual number of LFPs that injection wells face. These additional inflows could, for example, be procured from PCC-NGCC power stations using solvent storage in order to sustain high levels of exported CO_2 to the pipelines even at times of low electricity demand.

Whilst interim CO_2 storage facilities would be an alternative for providing this service the option for solvent storage could be economically particularly attractive through enabling the power plant operator to achieve additional revenues from power or ancillary service markets. Several studies indicate that the additional revenues achievable from increased sale of power at times of high electricity prices when delaying the energy intensive step of solvent regeneration via solvent storage, can compensate for the added investment costs required to make this option available (i.e. cost for solvent storage tanks and additional inventory; Versteeg et al. 2013, Chalmers 2010a, Cohen et al. 2011, Mechleri et al. 2017b). Hence, even if overall no significant additional profits could be achieved with the option of solvent storage, as a majority of the literature suggests, it could effectively constitute a low or net zero cost option for mitigating CO_2 flow rate variability in the downstream T&S system. A closer review of the range of techno-economic studies that exist in the literature is provided in the following section 7.2.

In general, techno-economic studies in the literature assessing the profitability of solvent storage use strongly simplifying assumptions when modelling underlying technical effects. Sanchez Fernandez et al. (2016) recently notes that a reason for the ambiguous and, at times, contradictory conclusions of many of these techno-economic studies examining solvent storage might be the complexity of the underlying technical system and the reliance on many strongly simplifying assumptions. Indeed it appears that whilst several techno-economic studies examine solvent storage at natural gas fired CCS power stations (Oates et al. 2014, Delarue et al. 2012, Versteeg et al. 2013), there is no detailed technical assessment of the part-load performance of these plants under the relevant operating conditions available in the literature.

This study intends to address this gap in the literature by carrying out a rigorous technical assessment of the performance of a natural gas fired CCS power station under solvent storage and delayed regeneration operation. By presenting the first detailed technical study of solvent storage at a natural gas fired power station fully integrated with post-combustion MEA based capture and compression, this process modelling work lays the foundation for future studies exploring in more detail the contribution that solvent storage can make to cost-effectively deliver a CO_2 flow balancing method for downstream T&S systems. Further, the study contributes to the technical and techno-economic solvent storage literature by providing it with more rigorous input data than is currently available.

As such, this study examines the behaviour of the power cycle as well as the capture plant at full load, as well as at part load, during solvent storage operation, and during regeneration of previously stored rich solvent. In contrast to previous literature the operating limits are described in detail. Two different part load power cycle and capture unit control strategies are assessed during additional regeneration of stored solvent using alternative steam extraction strategies: (1) floating IP/LP crossover pressure; and (2) throttled IP/LP crossover. Steam is extracted from the steam cycle - specifically from the crossover line between the IP and the LP steam turbine - and diverted to the capture unit to provide heat necessary for stripping off relatively high purity CO_2 from the solvent. Whilst in the floating IP/LP crossover line extraction strategy steam is diverted away from the steam cycle without any pressure control a valve is inserted before the LP turbine in the throttled crossover extraction strategy. This valve is used to control the pressure in the extraction line allowing sustaining the steam pressure in the capture unit and specifically in the reboiler at design conditions, which positively impacts the heat of regeneration in the desorber particularly at off design conditions. Nevertheless, the improved and energetically more favourable thermodynamic conditions in the desorber at off design conditions in this strategy come at the expense of throttling losses impacting the overall performance of the power station, the effect of which is presented for the first time in this study. In contrast, the floating steam extraction strategy avoids incurring throttling losses in the crossover line (between the IP and LP turbine) which, however, leads to lower reboiler steam pressures and hence energetically suboptimal conditions for solvent regeneration.

As a further addition to the literature a variable speed integrally geared centrifugal compressor model is deployed, able to predict the off design performance and operating limits of the compression unit. This is necessary to avoid simplified modelling of the compressor system that is unable to accurately assess key operational issues occurring during off design operation. As a consequence of the reduction of compressor suction pressures during additional regeneration of previously stored rich solvent, the inclusion of a robust compressor model is essential to avoid choking conditions at the compressor threatening overall system integrity even at reduced mass flow rates. Choking refers to a dangerous and potentially harmful operating point of the compressor characterised by a volumetric overflow making further head (i.e. pressure) increases over the compressor stages impossible (Luedtke 2004).

Finally, this chapter demonstrates the extent to which solvent storage can be used for decoupling electricity and CO_2 production over short periods of time for boosting CO_2 flows during periods of low electricity production. This can assist in avoiding critical periods of low flow at the downstream injection and storage level, hence mitigating or avoiding associated integrity risks as outlined in Chapter 2 and other literature (Spitz et al. 2017, Jensen et al. 2014, ZEP 2017, Lund et al. 2016, Shell 2015a).

To facilitate the adoption of the modelling results in future techno-economic assessments, as well as energy system modelling or CO_2 transportation network studies, correlations have been developed for key performance parameters of the CCS power station at varying load and operating points.

In contrast to the previous chapters investigating linepacking and line-depacking at dense phase CO_2 pipelines it is highlighted that the work presented in the current chapter is not directly integrated and soft linked with the results obtained about CO_2 flow variability from the power sector from chapter 3. Soft-linking the models for a detailed quantitative assessment of the potential of solvent storage to mitigate flow variability in the downstream T&S network is considered future work, however, goes beyond the scope of the current thesis.

The present chapter is structured as follows: Section 7.2 starts off with giving an overview over the existing literature about solvent storage. Subsequently section 7.3 provides a description of the model developed in this work. Section 7.4 presents the results. Section 7.5 develops correlations for key power station performance parameters for facilitation the adoption of the process modelling results in wider energy system or CO_2 T&S system simulations. Section 7.6 concludes.

It should be noted that the work discussed in this chapter has previously been presented in a paper in the International Journal for Greenhouse Gas control (Spitz et al. 2019).

7.2. Literature review on solvent storage

Appreciating the need for flexible operation of CCS power stations in future low carbon energy systems, several studies in the literature have examined the capabilities and optimal strategies to operate post-combustion CO_2 capture (PCC) units flexibly. In general, these studies have considered PCC integrated with a power cycle as a means of improving the economic performance of the overall power station in a wider electricity market characterised by variable electricity prices. Four options are generally considered:

1) Bypass: The option for bypass (sometimes referred to as exhaust gas venting) involves turning off the CO_2 capture plant independently from the power cycle in order to recover a majority of the electricity penalty associated with the CO_2 capture process. This option could be economically attractive during times of high electricity prices and relatively low CO_2 prices when the increased revenues from

the sale of additional power can offset increased payments for higher CO_2 emissions to the atmosphere (Gibbins and Crane 2004, Chalmers et al. 2009b, Delarue et al. 2012).

2) Solvent storage: Similar to the previous option a majority of the energy penalty associated with CO_2 capture can be recovered if the solvent that is used for absorption of CO_2 from the flue gases of the power plant in the absorber column is not immediately regenerated in the desorber. A schematic diagram of this process is provided in Figure 7.1. Instead of regenerating the solvent rich in CO_2 once it leaves the absorber directly in the desorber it is sent to a 'rich solvent storage tank' where it is stored for an as of yet undefined time. Whilst zero solvent is regenerated the CO_2 capture process is maintained by feeding previously stored lean solvent from the 'lean solvent storage tank' to the absorber. By avoiding regeneration of rich solvent in the desorber a large fraction of the energy penalty associated with CO_2 capture can be temporarily recovered boosting output of the CCS power station and revenues for example at times of high electricity prices. This operation can be sustained as long as the inventory of both the lean and rich solvent storage tanks allow. Only at times of reduced electricity prices the power plant operator would usually economically choose to part load the power station and reverse the process by regenerating rich solvent from the storage tank with the freed capacity in the desorber column alongside rich solvent from ongoing part load operation. During the reversed process the lean solvent storage tank would be filled. Due to an increased solvent regeneration energy penalty the power station would, however, only export less power. Nevertheless, compared to the regular and instantaneous regeneration of rich solvent from the absorber the penalty of the overall process of delaying regeneration and and performing it at a later point in time is small, in particular in the face of significant operating profits that can be achieved in electricity markets with large electricity price differentials (Gibbins and Crane 2004, Lucquiaud et al. 2008, Chalmers et al. 2009b, Cohen et al. 2012).
3) Variable capture level: The CO_2 capture level and hence the incurred energy penalty can be traded off and optimised as a function of electricity prices as well as any residual CO_2 emission payments (Errey et al. 2014, Rao and Rubin 2006).
4) Variable solvent regeneration (VSR): Alternatively to the previous options (or in complement with option 2 or 3) this option consists of allowing CO_2 to accumulate in the working solvent during times of high electricity prices, with subsequent regeneration of the solvent at times of low electricity prices (Mac Dowell and Shah 2014 & 2015, Mechleri et al. 2017a).

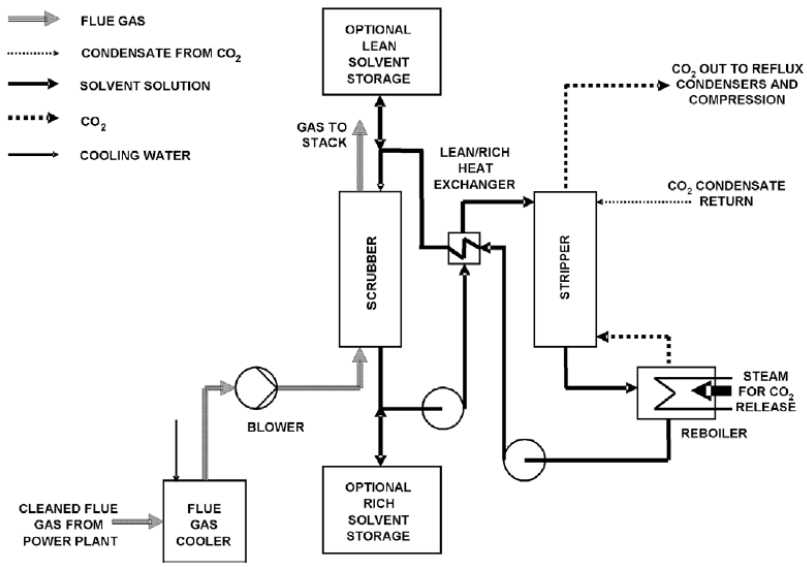

Figure 7.1: Schematic diagram of post-combustion capture plant with optional solvent storage tanks (Chalmers and Gibbins 2007).

There are several techno-economic and technical studies investigating the effects of the described options on either the profitability of the power plant, or the wider power system. For example, building on initial pioneering work from Gibbins and Crane (2004), Chalmers et al. (2009a, 2009b) examine the profitable price regimes under which the options for bypass and solvent storage can bring additional value. The authors find that bypass is economically valuable at electricity prices (in £/MWh) 2-3 times higher than the cost of CO_2 emitted (in £/tCO_2), and that solvent storage substantially reduces the CO_2 price at which bypass is economically attractive. Further, the authors find that the additional revenues that can be achieved with either option (e.g. over a day) are a strong function of the daily electricity price profile and, in particular, its 'peakiness'.

Building on this finding, Patiño-Echeverri and Hoppock (2012) investigate the electricity price differentials at which solvent storage could be economically valuable. They find that the required price differentials are a function of the cycling period, as well as the storage tank sizes of the solvent, the capacity factor of the power plant and whether the plant is new built or a retrofit. Depending on various input assumptions the required price differentials are determined to be in the large range of $40-141/MWh for daily cycling and $92-677/MWh for weekly cycling.

Similarly, Delarue et al. (2012) explore the market opportunities and electricity and CO_2 price regions in which flexible capture (i.e. bypass and solvent storage) can be profitable. Van Peteghem and Delarue (2014) develop an analytical optimisation framework assessing simplified block shaped (peak and off-peak) electricity price regimes under which solvent storage can be economically valuable. The study concludes that the required price ranges vary, and that they are most strongly influenced by the CO_2 emission certificate costs and investment costs of the solvent storage infrastructure.

Versteeg et al. (2013), Husebye et al. (2011), and De Kler et al. (2013) model the optimal operation of the power station and PCC unit under historical price patterns. Although the applicability of historical price patterns is uncertain given the large expected changes in future energy systems, the studies deliver some interesting results. Versteeg et al. (2013) conclude that if there is perfect foresight solvent storage can provide additional value for time periods of up to 3hrs at carbon prices of up to US$40/tCO$_2$. With imperfect foresight the study finds that solvent storage can be valuable for up to 8hrs for carbon prices up to $60/tCO$_2$, however, only when used in combination with an undersized regeneration unit. Husebye et al. (2011) demonstrate that flexible operation of the PCC unit can lead to increased profits that, however, are strongly correlated with the electricity price volatility. De Kler et al. (2013) show that flexible operation of the PCC unit, in particular varying the capture level, significantly improves the NPV value and business case of the overall power generation unit.

In a detailed study utilising a rule based optimisation model Cohen et al. (2011) assess the optimal behaviour of a coal fired power station by adjusting the operation of its PCC unit in response to price signals to the 2008 ERCOT (Electric Reliability Council of Texas) power system under varying degrees of foreknowledge. The authors conclude that bypass is unprofitable at carbon prices higher than US$70/tCO$_2$, while solvent storage is able to achieve additional operating profits of 9-29% regardless of the CO$_2$ price. Cohen et al. (2011) determines only relatively small optimal solvent storage tank capacities, sustaining operation in solvent storage mode at full load for 15-30min. Similarly Brasington (2012) finds that the storage tank sizes with potential to increase the economic profit for power plant operators are likely to be relatively small (i.e. for operation in full load solvent storage mode for less than 30min), when considering the additional operational complexities and investment costs.

In a follow up study considering possible future electricity price developments over time frames of 20 years Cohen et al. (2012) confirm many of their previous findings (i.e. solvent storage can allow for greater operating profits than inflexible capture or a bypass-only flexible capture facility). The authors note, however, that these benefits are sensitive to the economic assumptions and could be offset by the additional costs for the required solvent storage tanks and inventory.

Building on previous work Oates et al. (2014) optimise the solvent storage tank sizes and the size of the regeneration unit for a coal and natural gas fired CCS power station in the PJM (Pennsylvania, Jersey, Maryland Power Pool) system. They find that when flexible CCS was optimal, it was built with maximum storage size capacities. The potential benefit in the study would be largely driven by the cost savings from allowing the regenerator to be undersized.

Mechleri et al. (2017a) comes to a similar conclusion when assessing optimal solvent storage tank sizes under predefined electricity price patterns, even when not considering the possibility of reduced regenerator sizes. In a study benchmarking the profitability of all four previously discussed options for enhancing the flexibility of PCC units (see introduction

of this chapter) the authors find that even though additional profits are achievable via solvent storage they are sensitive to the targeted investment payback periods, the possible economic gains achievable via solvent storage overall increase with deployed tank sizes.

Sanchez Fernandez et al. (2016) recently notes that a reason for the ambiguous and, at times, contradictory conclusions of many of the techno-economic studies examining solvent storage might be the complexity of the underlying technical system and the reliance on many strongly simplifying assumptions. The authors note that particularly assumptions about the part-load performance and the capabilities of the power and capture unit when operated in the solvent storage and delayed regeneration modes would have a large influence on the outcomes of the techno-economic flexibility studies. Several techno-economic studies in the literature examine solvent storage at natural gas fired CCS power stations (Oates et al. 2014, Delarue et al. 2012, Versteeg et al. 2013) and there currently appears to be no detailed technical assessment of the part-load performance of these plants under the relevant operating conditions available in the literature.

This study intends to address this gap in the literature by carrying out a rigorous technical assessment of the performance of a natural gas fired CCS power station under solvent storage and delayed regeneration operation.

7.3. Model description

A model developed in gCCS (process modelling add-on built on the wider gPROMS modelling platform) demonstrates the part load behaviour and control strategies of a NGCC-CCS power station using solvent storage and delayed regeneration. The integrated power cycle and CO_2 capture unit design is based on and has been validated against a design examined by IEAGHG (2012). Due to missing information about the part-load performance of the gas turbines (GTs) these are modelled in the state of the art GT modelling software Thermoflow GT Master. To match the inlet and outlet process conditions of the IEAGHG (2012) reference plant as closely as possible the H-class GT model GE 9F.05 has been selected. Similarly, due to incomplete information about the capture plant, the design process conditions as well as the methodology for sizing the absorber and desorber columns follows (Herraiz et al. 2018) and Oexmann (2011). The desorber pressure and L/G ratio at a design capture rate of 90% was optimised in order to minimise reboiler duty (Freguia and Rochelle 2003). Since the parasitic energy penalty imposed by carbon capture is dominated by the reboiler duty, which itself is much more sensitive to the desorber pressure than the power consumption of the compression unit, this corresponds approximately to the point of maximum power output of the overall CCS power station (Sanchez Fernandez et al. 2016). Other process parameters such as reboiler and condenser temperatures and pressures were adopted from the literature from other studies presenting optimised 30wt% MEA solvent based post combustion CO_2 capture units (Herraiz et al. 2018, Gonzales Diaz 2016). A summary of the most relevant process conditions and design parameters for the power cycle and capture plant is provided in

Table 7.1. The values have been benchmarked and are in line with other sources in the literature (Rezazadeh et al. 2015, Jordal et al. 2012, Sanchez Fernandez et al. 2016).

Table 7.1: Full load configuration and design parameters for power cycle and capture unit.

GT model	GE 9F.05
Air inlet temperature	15°C
Preheated fuel temperature	117°C
Fuel composition	*see Appendix
HP inlet design pressure	170.0bar
IP inlet design pressure	40.0bar
LP inlet design pressure	3.75bar
Condenser design pressure	0.029bar
Flue gas temperature to absorber	40°C
Absorber packing height	13.0m
Absorber diameter	19.7m
Absorber design flooding fraction	75.0%
Lean solvent temperature to absorber	40°C
Desorber packing height	9.0m
Desorber diameter	8.0m
Desorber design pressure	1.9bar
Desorber design flooding fraction	75.0%
Reboiler design steam pressure	3.0bar
Reboiler design temperature	120°C
Reboiler heat transfer coefficient	1.36kW/(m^2K)
Reboiler duty	3.40 MJ/kg_{CO2}
Rich loading	0.474 mol_{CO2}/mol_{MEA}
Lean loading	0.264 mol_{CO2}/mol_{MEA}
L/G ratio ($kg_{solvent}$/$kg_{fluegas}$)	1.29
Overhead condenser temperature	40°C
CO_2 capture rate	90%

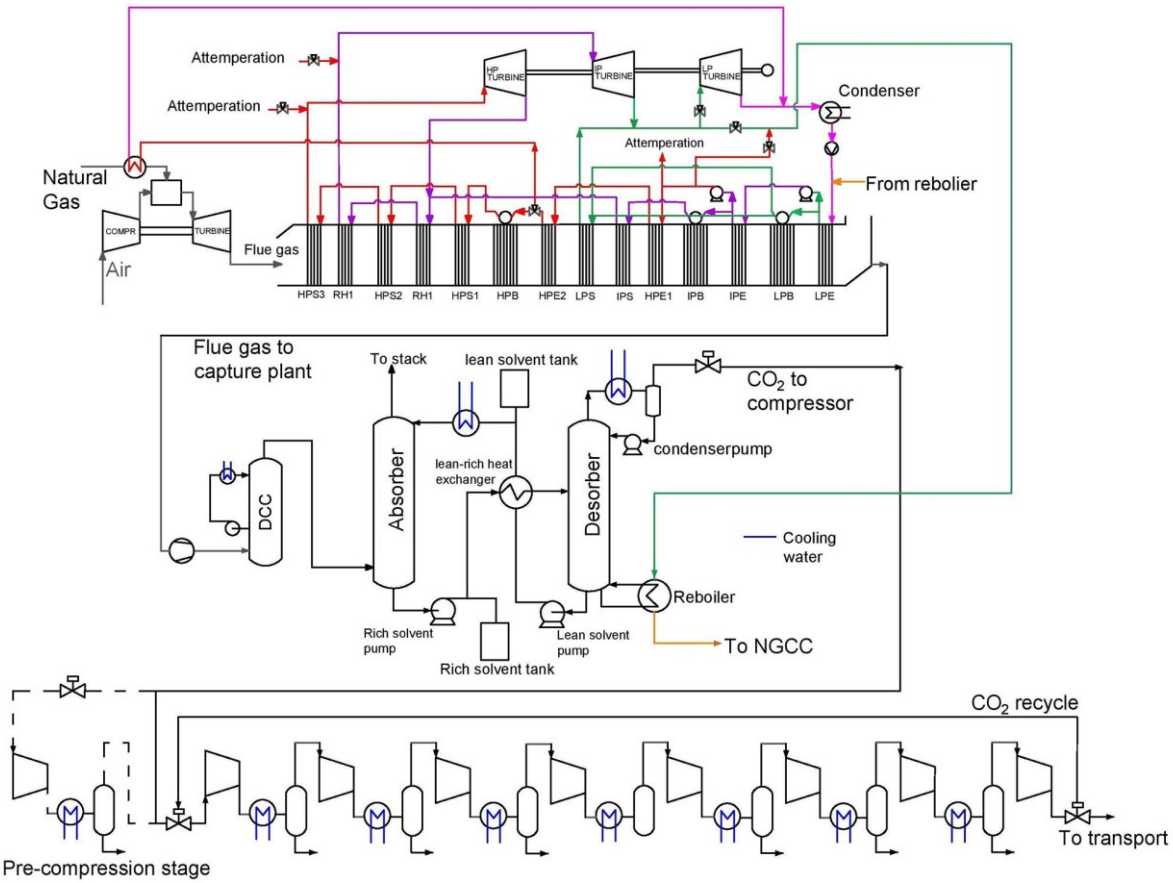

Figure 7.2: Schematic process diagram of the integrated power cycle, capture unit and compression system of the modelled NGCC-CCS power station. Similarly to IEAGHG (2012) the configuration considered consists of two parallel GT, HRSG, PCC and compression unit trains. Only the steam turbines are shared between both trains. For illustrative reasons parallel trains are not shown in the diagram.

An eight stage variable speed integrally geared compressor system design has been chosen due to relatively high part-load efficiencies (Liebenthal and Kather 2011, Modekurti et al. 2017, Bovon and Habel 2007), and due to the wide operating range advantageous for solvent storage and delayed regeneration. A full schematic overview of the modelled flowsheet is presented in Figure 7.2.

7.3.1. Part load strategy

Power cycle:

The GT part load performance is modelled with the state-of-the-art gas turbine simulator Thermoflow GT Master. The software takes into account optimal air-fuel ratios at different

load points, as well as the inefficiencies when deviating from design flow conditions due to suboptimal velocity triangles at the blades.

The steam cycle is modelled in a sliding pressure part load operating strategy in order to avoid inefficient throttling losses (Kehlhofer et al. 2009, Gonzales Diaz 2016, Sanchez Fernandez et al. 2016). The reduced pressure levels (HP, IP and LP) in the steam cycle at part load are a direct effect of the lower steam flow rates and the fact that the steam turbine swallowing capacities remain constant (i.e. Stodola Law). Standard heat transfer and pressure drop correlations are adopted similar to Kehlhofer et al. (2009) and Gonzales Diaz (2016). Due to rising GT outlet temperatures at part load (lower isentropic efficiency) the HP and IP flow temperature is controlled via attemperation to the maximum design levels of the steam turbines (601°C). Steam turbine isentropic efficiencies are assumed to be constant at part load (Sanchez Fernandez et al. 2016, Apan-Ortiz et al. 2018).

At regular part load operation (i.e. no additional regeneration of stored rich solvent) a floating crossover pressure steam extraction strategy is used. In line with Gonzales Diaz (2016) and Sanchez Fernandez et al. (2016), this strategy is modelled to be the more efficient, due to the avoidance of throttling losses at the inlet of the low pressure turbine cylinder.

At additional regeneration of stored rich solvent at part load, two crossover line extraction strategies are explored for supplying sufficient amounts of steam to the PCC capture unit: (1) floating crossover pressure extraction; and (2) throttled LP turbine crossover line extraction. Whilst in the floating IP/LP crossover line extraction strategy steam is diverted away from the steam cycle without any pressure control a valve is inserted before the LP turbine in the crossover line in the throttled steam extraction strategy. This valve is used to manipulate the pressure in the extraction line and by extension allows maintaining the steam pressure in the reboiler at design conditions which positively impacts the reboiler duty particularly at off-design operation. The improved and energetically more favourable thermodynamic conditions in the desorber at off design conditions in this strategy, however, come at the expense of throttling losses impacting power plant performance which are avoided in the floating IP/LP crossover line steam extraction strategy.

A summary of the adopted power and capture plant control strategies can be found in Table 7.2.

Capture plant:

Two strategies are generally considered in the literature for efficiently controlling the capture plant at part load: (i) Constant liquid-to-gas ratio in the absorber while maintaining the temperature and pressure conditions in the desorber column; and (ii) constant solvent flow rate with a varying degree of solvent regeneration in the desorber to maintain the capture rate (Kvamsdal et al. 2009, Van De Haar 2013, Van der Wijk et al. 2014, Mechleri et al. 2014). The studies in the literature proposing these part load operating strategies,

however, do not consider the effects on the operation of the capture unit at part load of the requirements of an integrated steam cycle. Sanchez Fernandez et al. (2016) demonstrates in an integrated assessment of the power cycle and capture unit that both suggested strategies need to be modified in order to take into account the decreasing crossover steam extraction pressure of the steam cycle at part load operation. Sanchez Fernandez et al. (2016), hence, proposes two modified capture plant part load strategies: (A) Constant desorber pressure: This strategy consists of maintaining the desorber pressure at the design value and varying the solvent flow in order to maintain the capture level; and (B) Constant L/G ratio and decreasing of desorber pressure: This strategy refers to maintaining the L/G ratio in the absorber by adjusting the solvent flow at lower loads. In contrast to strategies previously suggested, the desorber pressure is decreased for maintaining a constant lean loading.

Table 7.2: Control strategies of power cycle and capture unit at different operational modes.

	Regular Part load	**Additional regeneration of stored rich solvent: Strategy 1 (floating)**	**Additional regeneration of stored rich solvent: Strategy 2 (throttled LP)**	**Solvent Storage (/bypass) (at full load for max. electricity output)**
GT control	Optimal fuel and air supply determined by Thermoflow	Optimal fuel and air supply determined by Thermoflow	Optimal fuel and air supply determined by Thermoflow	Optimal fuel and air supply determined by Thermoflow
Crossover line pressure control	Uncontrolled (i.e. floating) extraction	Uncontrolled (i.e. floating) extraction	Throttled LP to maintain steam pressure in reboiler at design value (3bar)	No steam extraction. All generated steam is used for power production.
Reboiler temperature control	Determined by steam pressure (i.e. saturation temperature) and heat requirement by capture plant	Determined by steam pressure (i.e. saturation temperature) and heat requirement by capture plant	Implicitly controlled at design value (120°C)	/
Desorber pressure control	Optimal desorber pressure for minimising reboiler duty	Set to control lean loading at design value	Set to control lean loading at design value	/
Compression unit control	Variable speed drive, recycling, shutting in of one train at 40%GT load	Variable speed drive, recycling, use of a pre-compression stage	Variable speed drive, (Implicitly controlled to close to design conditions by capture unit control strategy)	/

It is worth noting that the two strategies proposed in Sanchez Fernandez et al. (2016) are based on the use of an equilibrium model to represent the desorber. Both strategies proposed by Sanchez Fernandez et al. (2016) were found to be suboptimal with the rate based desorber model deployed in this study due to non-optimal lean loadings resulting in unnecessarily high reboiler duties at part load. One of the novel contributions of this chapter is the inclusion of a rate based desorber model to represent more rigorously and more accurately the desorber and CO_2 compression unit operation.

The approach taken in this study for optimally controlling the capture plant at regular part load operation (i.e. no additional regeneration of stored rich solvent) is consequently based on Oh and Kim (2018) and Roeder and Kather (2014). Effectively, reboiler temperature is governed by decreasing steam pressures and saturation temperatures at part load on the steam side of the reboiler and by the heat requirements on the solvent side of the reboiler. For any reboiler temperature the desorber pressure (and consequently lean loading) is optimised leading to the lowest achievable reboiler duty. It has previously been shown by several authors (Freguia and Rochelle 2003, Oh and Kim 2018) that the desorber pressure for a given temperature – and by extension the lean loading - is a compromise between

- minimising the latent heat used for the evaporation of water in the solvent - lower at higher desorber pressures and higher lean loadings -, and
- minimising the sensible heat utilised for heating up the solvent - lower at lower desorber pressures and lower lean loadings.

The detailed power and capture plant control strategy at additional regeneration of previously stored rich solvent is, to the knowledge of the authors, not described in any of the previous studies in the literature. The control strategy adopted within this study consists of maintaining the lean loading of the regenerated solvent at the design value (i.e. at full load). This is to ensure that when solvent storage is used the absorber has access to solvent with design working capacity enabling 90% capture without increasing the solvent flow rate over the design value. This also ensures that the design flooding limit to the operation of the packed columns is not exceeded. In this case, 75% of the flooding velocity is implemented to avoid the occurrence of excessive pressure drop in the absorber, as well as an acceptable safety margin to avoid flooding conditions.

The possibility of overstripping the solvent is acknowledged, however, not considered within the present study. Overstripping refers to regenerating solvent to lower lean loading levels than at design conditions. This can be done for increasing the working capacity of the stored solvent which reduces the required solvent storage tank sizes, and hence the required inventories of additional solvent – both factors have been identified as primary cost drivers when implementing the option for solvent storage (Mac Dowell and Shah 2015).

Finally, there are several technical limitations that need to be taken into account when aiming at regenerating maximum amounts of previously stored rich solvent as quickly as possible:

1) LP steam turbine: A minimum level of steam flow must be maintained through the LP turbine to avoid overheating of the turbine casing (Sanchez Fernandez et al. 2016). This flow is set at 10% of the design steam flow based on Cotton (1994).
2) Desorber flooding level: Increasing the solvent flow through the desorber or reducing the desorber pressure has the effect of decreasing its margin to flooding conditions. A numerical constraint has been set to limit the maximum flooding approach to the design level of a 75% approach to flooding.
3) Desorber pressure: When increasing the amount of solvent regenerated in the desorber, higher steam extraction rates can lead to reduced steam pressures and consequently solvent temperatures in the reboiler in the floating extraction operating strategy. To maintain the lean loading to the desired value, the desorber pressure is reduced. A minimum operating desorber pressure of 1.01bara is assumed to avoid operating under a vacuum and protect the desorber packed column structural integrity.
4) CO_2 compressor: the operation is constrained within the range of operating speeds and volumetric flow rates avoiding surge and choke conditions.

Compressor unit:

The part load performance of the variable speed integrally geared compressor system is modelled according to the methodology described in Modekurti et al. (2017) and Liese and Zitney (2017). In the absence of directly available and reliable CO_2 compressor performance maps in the publically accessible literature, it is an accurate method for assessing the off design behaviour of the compression unit. The methodology is based on single stage dimensionless performance maps based on exit flow coefficients. In contrast to holistic multistage compressor maps, or single stage dimensionless maps based on inlet flow coefficients, these maps can be assumed to be invariant to the specific inlet flow conditions (or even to different gases; Luedtke 2004). This approach is appropriate since the inlet flow conditions at part load and under delayed regeneration of stored solvent deviate substantially.

An eight stage integrally geared compressor design was chosen following the methodology outlined in Modekurti et al. (2017) and Liese and Zitney (2017). It is worth noting that with eight stages of compression instead of the six stages frequently considered in the CCS literature, the tip speed of the impellers reduces to Mach numbers below 1. Although a higher number of compression stages decreases pressure increases over the individual impeller stages, this ensures the applicability of the methodology over the wide operating envelope necessary for additional solvent regeneration. Luedtke (2004) shows that, for Mach numbers higher than 1, dimensionless single stage performance maps based on exit flow coefficients become dependent on specific inlet flow conditions. Modelling configurations with six compressors would require the use of CO_2 compressor performance maps not available in the public domain literature.

In practise, eight compression stages might come at higher investment costs. Operational costs can, however, decrease if intercooling between all stages is considered (as in the present study). This marginal trade-off is considered to be reasonable within the scope of this study, since the evaluation of CO_2 compressor behaviour at part load in an integrated capture/power plant model with solvent storage operation is more accurate than the current literature. The design parameters of the individual compressor stages are presented in Table 7.3.

Compressor choke at maximum solvent regeneration

It is worth noting that a pre-compression stage, upstream of the main compressor system, is added together with a separate drive and intercooling stage for the implementation of the floating pressure strategy. This is necessary to avoid choking of the compressor caused by high volumetric flow rates at maximum regeneration of stored rich solvent. The pre-compression stage reduces volumetric flow rates, whenever necessary, in order to avoid volumetric overload of the main compressor by increasing its inlet suction pressure.

Under the alternative steam extraction strategy consisting of throttling the LP turbine, maximum solvent regeneration occurs without the need for a pre-compression stage.

Compressor surge

A surge flow coefficient criterion of $\varphi_{surge} = 0.72 \times \varphi_{design}$ is assumed, with φ representing the inlet flow coefficient (Liese and Zitney 2017). Surge refers to a damaging operating condition of the compressor caused by too low volumetric flow rates leading to instable and even reversed flow. It must be avoided to ensure the integrity of the machine. Partial recycling of flow ensures that the inlet flow coefficient never drops below 72% of the design value. To minimise compression work one compressor train is shut down at 40% GT load in line with IEAGHG (2012), with the remaining online compressor processing the combined flow of both capture units.

Table 7.3: Compressor system design and specified parameters.

Configuration	Integrally geared bullgear configuration
Number of stages	8
Design inlet pressure [bar]	1.9
Design outlet pressure [bar]	110
Outlet pressures of impeller 1-8 [bar]	3.35, 6.29, 11.7, 22.0, 37.8, 62.5, 85.5, 110
Design RPMs of impeller 1-8 [x1000]	7.5/7.5/11.1/11.1/19.7/19.7/20.0/20.0
Diameter of impeller 1-8 [m]	0.67/0.67/0.45/0.44/0.24/0.22/0.15/0.10
Design inlet flow coefficient of impeller 1-8	0.136/0.076/0.09/0.049/0.09/0.0625/0.09/0.11
Primary control strategy	Variable Speed Drive
Secondary control strategies	Recycling to avoid surge at low flows/ Shutting off one train
Max speed	105%
Intercooling	Between all stages to 40°C
Pre-compression stage operating strategy	Only active when reduced desorber pressure leads to volumetric overflow of stages and choking of main compressor
Pre-compression stage design	Inlet pressure: 1bar; Outlet pressure: 1.85bar; RPM: 4650; Diameter: 1.08m; Flow coefficient: 0.09

7.4. Results

This section begins with an assessment of the overall power station performance parameters under the different operating strategies considered, followed by a detailed examination of the behaviour of the capture unit and compression system.

7.4.1. Overall power station performance

Figure 7.3 and Figure 7.4 present the net electrical LHV (lower heating value) efficiency at different full load and part load strategies, as well as the overall electrical output of the power station. Figure 7.3 demonstrates how the LHV efficiency of the power station approaches 60% (59.5%) at full load bypass operation, reflecting a state-of-the-art modern design. An aggregated full load penalty of 7.0 percentage points is associated with baseline capture of 90% of the produced CO_2. When operating in solvent storage mode approximately 5.5 percentage points can be recovered. The residual penalty consists predominantly of fan power required to push flue gas through the direct contact cooler, absorber and stack and the solvent storage pumps. In the bypass operating mode, the solvent storage mode and the regular part load operating mode the decrease in efficiency is predominantly an effect of the decreasing efficiencies of the GTs at part-load. The effect is amplified when additionally regenerating previously stored solvent at part load (green and red curves) due to the negative effect this has on the overall electrical output of the plant. Efficiencies reach a minimum of 40.4% at minimum stable GT load under the throttled LP turbine extraction strategy – however, with the benefit of regenerating large quantities of stored solvent. This compares to 46.7% at regular part load operation and 40% GT load.

Figure 7.4 shows that via the option for solvent storage and delayed regeneration the operating range of the NGCC-CCS power station in terms of electrical output can be extended from 391-806MW to 339-891MW. This represents a 10% decrease and increase of the minimum stable power generation limit and the maximum export limit, respectively. Reducing the minimum stable output helps CCS power stations to avoid the high cycling costs resulting from shut-ins for short periods of time during periods of low net demand and excess power supply to the network. Further, power output ramp rates can be increased by quickly diverting steam from/to the capture unit, in addition to adjusting the output of the GT (Lucquiaud et al. 2014). Both options can prove particularly valuable in future low carbon power systems dominated by variable intermittent energy supply by improving the flexibility and operating range of CCS generators. Reducing the minimum thermal generation limit was found to be particularly valuable to the overall system by IEAGHG (2017). Both options also enable plants to provide significantly higher levels of fast acting spinning reserve for balancing power systems while simultaneously providing substantial levels of synchronised inertia.

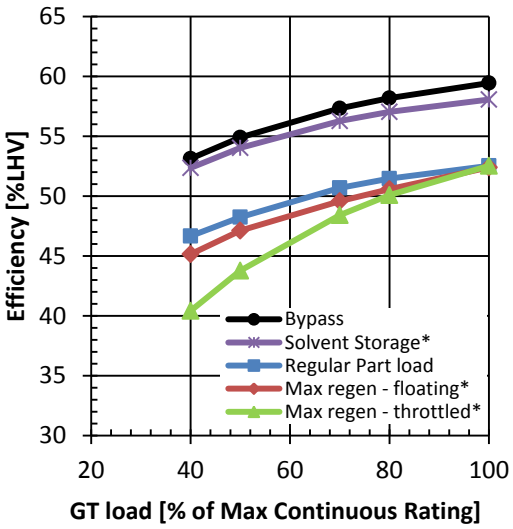

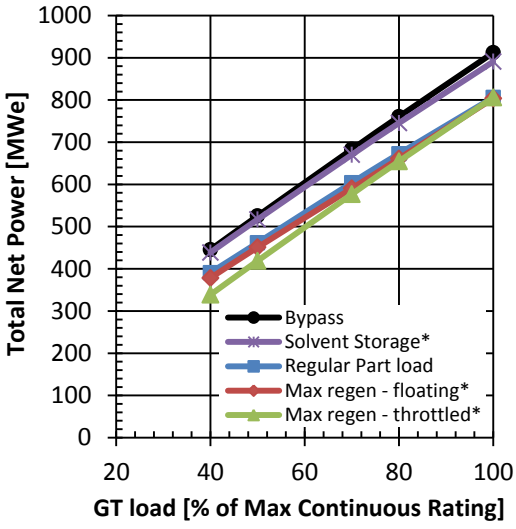

Figure 7.3 (left): Net LHV efficiency of NGCC-CCS power station as a function of GT load and operating strategy of the PCC unit and steam cycle (see legend).

Figure 7.4 (right): Net total power output as a function of GT load and operating strategy of the PCC unit and steam cycle (see legend).

* The duration of continuous operation with solvent storage and maximum regeneration is dictated by the inventory of the solvent storage tanks. The CCS power plant would return to operation at 'regular part-load' once that duration is exceeded.

As a caveat it should be noted that operating in solvent storage mode can only be sustained for a time dictated by the size and inventory of the solvent storage tanks. For example, for 1hr of solvent storage at full load, tank sizes to handle an additional solvent inventory of approx. 6200m^3 would be necessary for the considered power station with a nameplate capacity of 806MW, if no overstripping of solvent was performed. For plants of different capacities the solvent inventory would vary roughly linearly as a first approximation. If solvent overstripping was considered tank sizes could potentially be reduced by 30% (i.e. if lean loading of 0.2mol/mol were achieved instead of 0.264mol/mol in this study), however, this would need to be traded off with a higher energy penalty for regeneration. In contrast, bypass operation can be sustained indefinitely.

7.4.2. Integrated power and capture unit behaviour

Reboiler and Desorber column operation at part load

Figure 7.5 and Figure 7.6 illustrate the reboiler steam pressure and reboiler solvent temperature at regular part load (blue), and at maximum regeneration of stored rich solvent under both considered steam extraction strategies (green and red). The decreasing steam pressures at regular part load operation are an effect of a reduced flow through the steam turbines. With reduced mass flow, dropping condenser pressures as a consequence of the lower condensing steam flow and the swallowing capacity of the steam turbines

remaining unchanged, the inlet and outlet pressures of the steam turbines drop. The lower steam extraction flows at part load generally have a positive impact on the crossover pressure and on the pressure drop in the extraction line from the power cycle to the capture unit. Nevertheless, the lower densities and consequently higher velocities of the steam in the extraction line at least partially negate this positive effect by leading to increased pressure drops in the extraction line. Due to the large and direct effect of the pressure drop in the extraction line on the reboiler and consequently capture plant operation, it is of fundamental importance to consider the impact of varying steam densities in studies modelling the performance of power cycles integrated with PCC.

At maximum regeneration of stored solvent under the floating crossover pressure steam extraction strategy the increased amounts of extracted steam for additional regeneration results in a strong reduction in the reboiler steam pressure (red line) between GT loads of 100% to 70%. The effect is amplified by the strongly increased pressure drops in the extraction line due to both higher flow rates and reduced densities leading to increased velocities (see also Table C.3 in Appendix for extraction line pressure drops). At low loads reboiler steam pressure drops get more moderate. This can be attributed to the lower extracted steam flows limiting the pressure drop in the extraction line, as well as the small amount of capture plant capacity that is freed for additional regeneration of stored rich solvent. In contrast, when operating under the throttled LP pressure extraction strategy at maximum regeneration of stored rich solvent steam pressures in the reboiler are controlled to be constant (green curve, Figure 7.5).

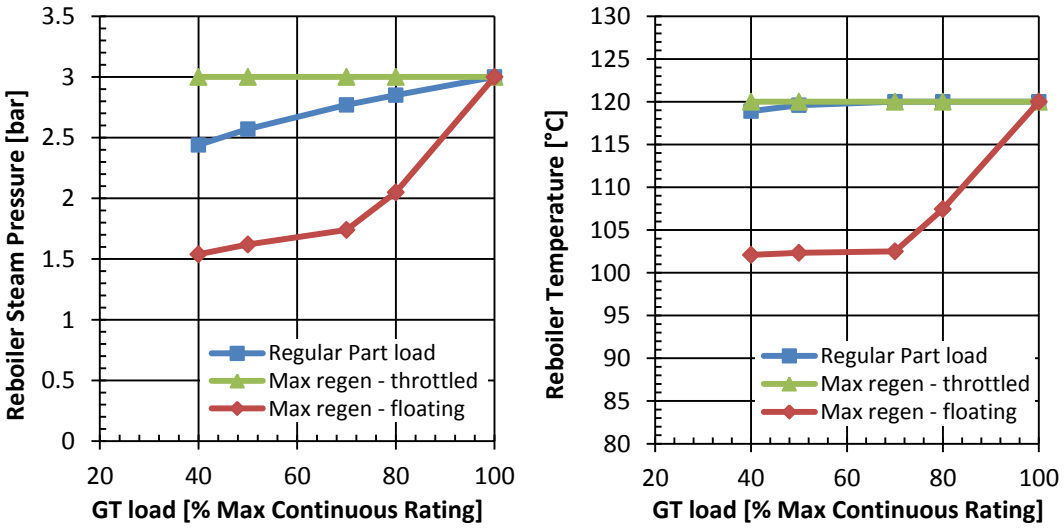

Figure 7.5 (right): Reboiler steam pressure as a function of GT load and operating strategy of the PCC unit and steam cycle (see legend).
Figure 7.6 (left): Reboiler Temperature as a function of GT load and operating strategy of the PCC unit and steam cycle (see legend).

Following the reductions of the reboiler steam pressure and saturation temperature, the reboiler solvent temperatures drop at part load (Figure 7.6). At regular part load the

reduction in temperatures is moderate, as the reduced pinch temperature in the reboiler can nearly be compensated by the lower heat (transfer) requirement by the capture unit. Consequently the reboiler temperature drops only to 119.6°C and 118.9°C at GT loads of 50% and 40%, respectively.

In contrast, at maximum regeneration of stored rich solvent under the floating crossover pressure extraction strategy the reboiler temperature drops substantially to around 102.4°C at 70% GT load, where it remains even at lower GT loads. The initial quick reduction when going into part load is a combined effect of both strongly reduced steam side pressures and temperatures, and of the increased heat transfer requirements in the reboiler due to additional flow for regeneration of stored solvent. The latter requires significantly higher pinch temperatures compared to the counterfactual regular part load operation which indirectly leads to lower solvent side reboiler temperatures. Below 70% GT load the reboiler temperature stabilises. This is an effect of the desorber pressure reaching atmospheric pressure and cannot be reduced any further, as previously explained. Controlling the lean loading at a constant desorber pressure implicitly fixes the reboiler temperature, which limits any amount of additional stored solvent that can be regenerated. At maximum regeneration of stored rich solvent under the throttled steam extraction strategy controlling the steam pressure in the reboiler and the lean solvent loading at design conditions similarly implicitly fixes the reboiler solvent side temperature at 120°C. Consequently the heat transfer achievable in the reboiler and the flooding limit in the desorber constrain the volumes of additional stored solvent that can be regenerated under this strategy.

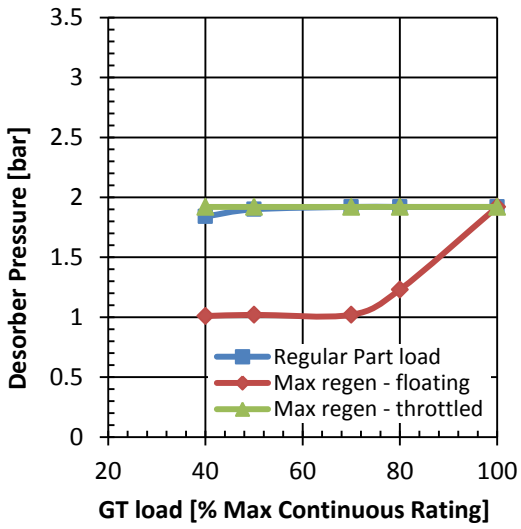

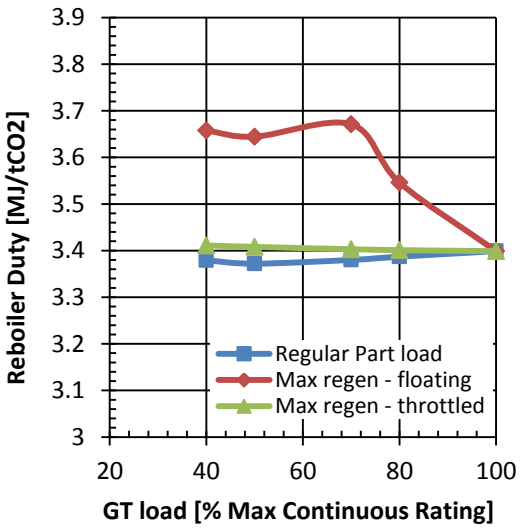

Figure 7.7: Desorber pressure as a function of GT load and operating strategy of the PCC unit and steam cycle (see legend).

Figure 7.8: Reboiler Duty as a function of GT load and operating strategy of the PCC unit and steam cycle (see legend).

Figure 7.7 illustrates the desorber pressure. The graphs show a strong resemblance to the reboiler temperature trends. At regular part load operation the desorber pressure is optimised according to the reboiler temperature to minimise the reboiler duty. As such, it only deviates marginally at low loads from the design value of 1.92bar to 1.84bar at 40% GT load (Figure 7.7).

At maximum regeneration of stored rich solvent under the floating crossover steam extraction strategy, the desorber pressure drops rapidly at lower loads to compensate for the falling reboiler temperatures and in order to maintain lean loadings at design conditions (i.e. lower desorber pressure means more CO_2 is stripped off the solvent even at reduced temperatures). At around 70% GT load desorber pressure reaches atmospheric pressures, setting the constraint for any further additional regeneration of stored rich solvent. Under the throttled crossover pressure steam extraction strategy the desorber pressure stays at design conditions in line with reboiler temperatures and lean loadings.

Figure 7.8 illustrates the resulting reboiler duty. At regular part load operation reboiler duty initially drops marginally when going into part load, before the trend is reversed at around 50% GT load. The initial drop results from the improved heat recycling in the lean/rich solvent heat exchanger as a consequence of the lower flow rates and subsequently higher residence times. Sanchez Fernandez et al. (2016) suggested the lower reboiler duty at part load could be an effect of longer residence times of the solvent/flue gases in the absorber and desorber columns leading to better heat and mass transfer. This effect could not be observed in the current study, which indicates that this may be determined by the sizing of the absorber. As a consequence of the decreasing reboiler temperatures the reboiler duty starts to increase below relative GT loads lower of around 50%.

At maximum regeneration of stored rich solvent under the floating crossover pressure steam extraction strategy, the reboiler duty increases sharply when going into part load. Again, this is predominantly a consequence of the decreasing reboiler temperature and pressure. The effect is, nevertheless, amplified by lower levels of thermal energy recycling possible in the lean/rich solvent crossover heat exchanger. This is caused by the lower temperatures of lean solvent exiting the desorber that undermine driving force and temperature pinch in the heat exchanger. Once the reboiler temperature stabilises at around 102.4°C, so does the reboiler duty. The slight drop in the reboiler duty at 50% GT load is an effect of the longer residence times of the solvent in the heat exchanger that, given the stabilised pinch temperature in the lean/rich crossover heat exchanger, lead to higher specific heat transfers. Due to progressively falling heat transfer coefficients at low flow rates this trend is again reversed at 40% GT load causing slight increases in reboiler duty. At maximum regeneration of stored rich solvent under the throttled crossover pressure extraction strategy reboiler duty stays very close to design conditions across all loads following the desorber conditions.

Solvent loadings and L/G ratio

Figure 7.9 and Figure 7.10 display rich and lean loadings of the solvent as well as the liquid-to-gas ratio in the absorber column under the different part load strategies. At maximum regeneration of stored rich solvent lean loading stays constant as part of the capture plant control strategy. Only the lean loadings at regular part load operation at 40% and 50% GT load drop slightly compared to the design value. This is line with Roeder and Kather (2014) and Oh and Kim (2018) and a consequence of the changing reboiler and desorber conditions. Rich loading across all GT loads and part load strategies remains unchanged. This suggests a sufficiently sized absorber for the mass transfer to happen efficiently, with the fluids reaching near equilibrium conditions at the outlet.

Figure 7.10 indicates falling L/G ratios across all evaluated part load operating strategies. With rich and lean loading being constant for both additional regeneration strategies this is an effect of the decreasing CO_2 concentrations and flow rates of flue gases at part load. The disproportionally faster reduction in L/G ratio at regular part load operation between 40-50% GT load can be traced back to be a result of the reduced optimal lean loadings.

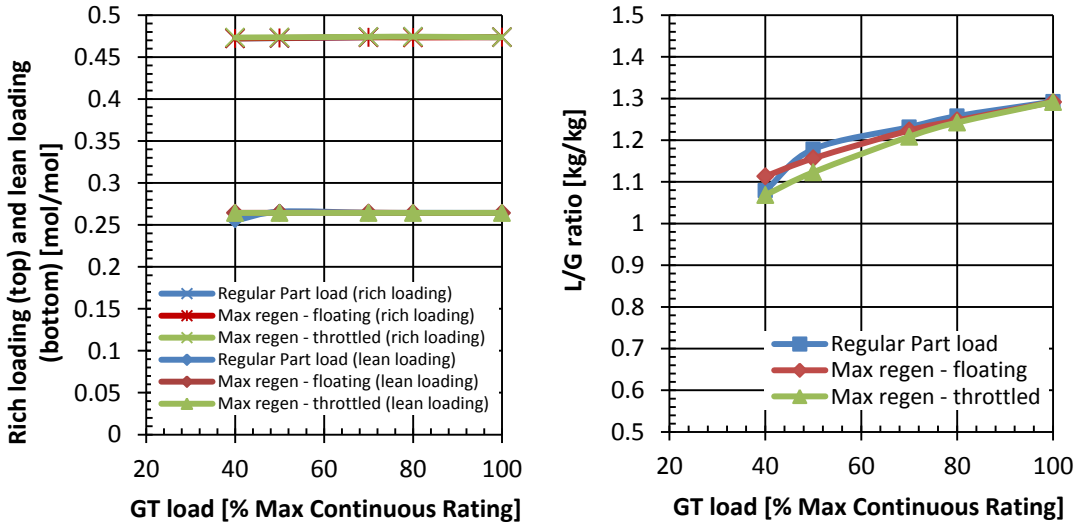

Figure 7.9 (left): Lean and rich loading as a function of GT load and operating strategy of the PCC unit and steam cycle (see legend).
Figure 7.10 (right): L/G ratio as a function of GT load and operating strategy of the PCC unit and steam cycle (see legend).

Regenerated amounts of CO_2

Figure 7.11 presents the maximum volumes of CO_2 that can be regenerated from previously stored rich solvent at different GT load point. Significantly higher levels of CO_2 can be regenerated under the throttled LP extraction strategy. The levels increase linearly towards

lower GT loads. In contrast, under the floating crossover pressure extraction strategy the volume stays relatively constant, rising only slightly towards lower GT loads. At 40% GT load an additional 8.1kg/s of CO_2 can be regenerated from stored rich solvent under the floating crossover pressure extraction strategy, representing around 18.7% of the CO_2 that needs to be regenerated from on-going operation. In contrast an extra 34.8kg/s of CO_2 can be regenerated from stored rich solvent at the same GT load point under the throttled LP crossover extraction strategy. While the limit to additional regeneration under the floating crossover extraction strategy is found to be the minimum desorber pressure, driven by the low steam pressure and high required temperature pinch in the reboiler, additional regeneration is constrained by the flooding level in the desorber at 80% GT load. This is also the case for the throttled LP extraction strategy. Table 7.4 summarises the constraints to maximum solvent regeneration at different loads.

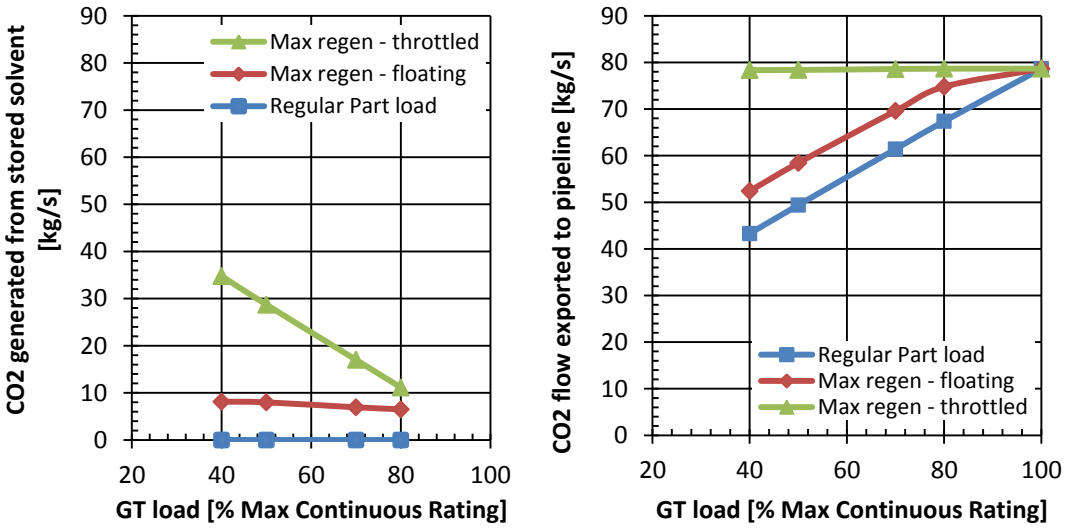

Figure 7.11 (left): Maximum amounts of CO_2 that can be produced from the regeneration of stored rich solvent at different GT loads and operating strategies of the PCC unit and steam cycle (see legend).

Figure 7.12 (right): Amount of CO_2 exported to pipeline as a function of GT load and operating strategy of the PCC unit and steam cycle (see legend).

When examining the CO_2 flows produced by regenerating stored rich solvent and by ongoing capture plant operation it can be seen that, across all GT loads, the maximum volumes of CO_2 exported to T&S can be maintained, at least for a certain duration, under the throttled LP crossover extraction strategy (see Figure 7.12). This is an important finding as it shows the extent to which electricity production can be decoupled from production of CO_2 when utilising the option for solvent storage. Particularly the injection wells can benefit from a minimum level of CO_2 flow during times of low CO_2 supply (e.g. during periods of low net demand when a majority of CCS power stations shut in and stop producing CO_2) as it can mitigate or avoid integrity risks associated with two phase flow occurring over the wellhead due to low backpressures from injection (Capture Power Limited 2016, Spitz et al. 2017, Spitz 2016, Jensen et al. 2014). Further, maintaining a minimum flow into the

reservoirs can avoid increased levels of residual trapping or formation of halites taking place in the near wellbore region of saline aquifers that over time can significantly hamper the store's injectivity as previously outlined in Chapter 2. Under the floating crossover extraction strategy, part load CO_2 flows that can be exported are 11-21% higher when additionally regenerating previously stored solvent.

Table 7.4: Technical constraints to maximum additional solvent regeneration.

GT load	Floating steam extraction	Throttled steam extraction
100%	Desorber capacity*	Desorber capacity*
80%	Desorber capacity*	Desorber capacity*
70%	Desorber min. pressure**	Desorber capacity*
50%	Desorber min. pressure**	Desorber capacity*
40%	Desorber min. pressure**	Desorber capacity*

*Maximum approach to flooding of 75% is reached and no more solvent can be regenerated in the desorber
**It should be noted that the reboiler could be oversized in order to achieve higher solvent side temperatures even in the face of dropping steam side pressures at part load. This would lead to higher desorber pressures when controlling lean loading as constant, mitigating the minimum desorber pressure constraint. However, reboiler oversizing is not considered further within this study.

Regeneration time for 1hr of solvent storage (at full load) and Electricity Output Penalty

The time necessary to regenerate stored rich solvent can be decisive for the economic viability of the option of solvent storage. For example, if it takes an entire night at fluctuating and not always ideal electricity prices to regenerate the accumulated volumes of stored rich solvent from 1hr of solvent storage operation the power plant operator might incur large economic losses. According to Chalmers (2010) ideal prices for regenerating stored solvent are high enough to cover the SRMC of the plant, but not any higher, as otherwise this incurs opportunity costs by not selling maximum amounts of energy in the form of electricity, but instead using some of the energy to regenerate stored rich solvent. In contrast, if the stored rich solvent can be regenerated relatively quickly when electricity prices are favourable, this can have substantial economic benefits. Further, the economic viability of solvent storage would be substantially less dependent on the variability of the electricity prices during the delayed regeneration process.

Figure 7.13 illustrates the time necessary to regenerate the amounts of solvent stored when operating 1hr at full load conditions in the solvent storage mode. In line with previous findings it shows that stored solvent can be regenerated significantly faster under the floating crossover pressure extraction strategy. At 40% GT loads the time it takes to regenerate rich solvent from 1hr of full load solvent storage operation is 2.1hrs compared with 8.7hrs when operating under the floating crossover extraction strategy.

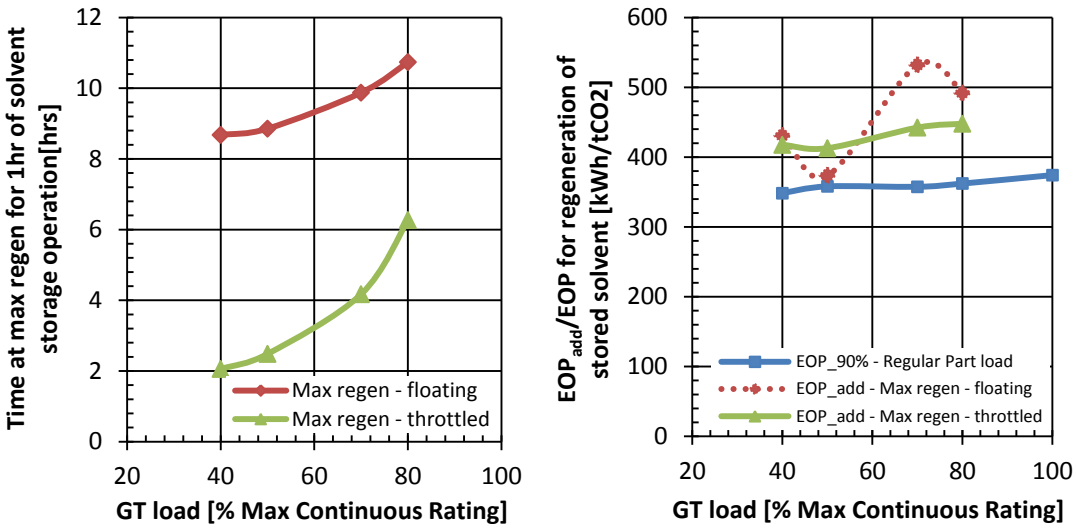

Figure 7.13 (left): Time spend (in hours) regenerating maximum amounts of stored rich solvent at different GT loads and operating strategies of the PCC unit and steam cycle for every hour previously operated in the solvent storage (i.e. bypass) mode at full load.

Figure 7.14 (right): Additional EOP (Electricity Output Penalty) for the regeneration of CO_2 from stored solvent at different GT loads and operating strategies of the PCC unit and steam cycle (green and red curves, see legend). For benchmarking purposes the EOP associated with regular 90% capture operation (i.e. no additional regeneration of stored solvent) has been plotted as well (blue curve).

When intending to provide more (or less) solvent storage capacity the required amount of additional solvent as well as the rich and lean solvent tank capacity can be calculated as a first approximation according to:

$$Inventory = 6{,}200\ tonnes/h * time_{intended} \quad (12)$$

Where *Inventory is the additional inventory of solvent required, as well as the required capacity of the rich and lean solvent storage tanks*

$t_{intended}$ is the time of solvent storage operation at full load that the operator of the power station intends to make available

For every hour of solvent storage operation at full load, and depending on the load and regeneration strategy, the time it takes to regenerate the accumulated solvent can be extracted from Figure 7.13. It shall be noted that stored solvent can only be regenerated when this has previously been accumulated by solvent storage operation.

Finally, the electricity output penalty (EOP) associated with the additional regeneration of stored solvent under both considered steam extraction strategies is assessed. The electricity output penalty metric used in (Lucquiaud and Gibbins 2011a) measures the reduction in power output of the overall power station on the basis of tonnes of CO_2 captured. It allows for penalties associated with CO_2 capture in the capture unit, the compression unit and the power cycle to be aggregated and then compared on an equal

basis across power stations. The EOP is also largely independent of the power cycle thermal efficiency (Lucquiaud and Gibbins 2011b). It is defined as:

$$EOP = \frac{P_{without\ CO2\ capture} - P_{90\%\ CO2\ capture}}{m_{CO2\ 90\%\ capture}} \quad (13)$$

Where $P_{without\ CO2\ capture}$ *is electricity output of the power station if the capture unit is off*
$P_{90\%\ CO2\ capture}$ *is electricity output of the power station at 90% CO_2 capture operation*
$m_{CO2\ 90\%\ capture}$ *is the mass flow of captured CO_2.*

For the purpose of illustrating the penalty the additional regeneration of previously stored rich solvent imposes on the overall power station on a per-ton-of-additional-CO_2-regenerated basis the additional EOP, or EOP_{add}, is introduced in formula 14.

$$EOP_{add} = \frac{P_{90\%\ CO2\ capture} - P_{\max\ regen}}{m_{CO2\ max.regen.} - m_{CO2\ 90\%\ capture}} \quad (14)$$

Where $P_{90\%\ CO2\ capture}$ *is electricity output of the power station at 90% CO_2 capture operation*
$P_{max\ regen}$ *is electricity output during additional regeneration of previously stored rich solvent*
$m_{CO2\ 90\%\ capture}$ *is the mass flow of captured CO_2 at regular 90% capture operation*
$m_{CO2\ max\ regen}$ *is the mass flow of regenerated CO_2 during additional regeneration of stored rich solvent.*

Whilst the EOP hence indicates the energy penalty associated with carbon capture on a per-ton-of-CO_2 basis during regular 90% capture operation, EOP_{add} informs about the total additional penalty associated with regeneration of previously stored rich solvent on the basis of the amount of CO_2 regenerated from this previously stored rich solvent. Both the EOP and the EOP_{add} are plotted in Figure 7.14.

The figure shows how EOP_{add} varies between 374-532kWh/tCO_2 (red dotted and green line). This compares to an EOP of approx. 380kWh/tCO_2 at regular 90% capture operation at full load. For the purpose of benchmarking values the $EOP_{90\%}$ associated with regular capture operation at full load and part load operation has been plotted. It can be seen that the EOP_{add} is around 4-49% higher than $EOP_{90\%}$ for regular capture under the floating extraction strategy, and 15-24% higher when accepting LP turbine throttling losses in order to maintain the crossover pressure.

Under the throttled LP pressure steam extraction strategy EOP_{add} decreases slightly towards GT loads. A minimum is reached at 50% GT load before it marginally starts increasing again. With the reboiler duty being nearly constant across the loads the slight decrease in EOP_{add} is found to be an effect of the improved efficiencies of the compressor station when operating at or close to its design conditions compared to the counterfactual reference case of regular part load operation. Similarly, the slight increase of the additional EOP at

40%GT load is an effect of this advantage being negated by the improved efficiencies of the compressor at regular part load conditions when one compressor train shuts down.

EOP_{add} varies significantly more under the floating crossover pressure extraction strategy. The rise in EOP_{add} at 70% load under the floating steam pressure extraction strategy is an effect of the strongly increased reboiler and of the compression duty to be provided for by the power cycle for the entirety of the regenerated solvent, even though only the additionally regenerated solvent is accountable for it. The subsequent drop in EOP_{add} is related to the higher volumes of additionally regenerated stored solvent that the higher reboiler and compression duty can be depreciated over. The final increase in EOP_{add} is an effect of the part load efficiency losses of the compression unit, as well as a small amount of recycling of CO_2 to avoid surge conditions in the compressor. Due to the small number of explicitly modelled load points and the competing trends strongly affecting EOP_{add} under the floating steam extraction strategy the exact course of the (red) curve is uncertain. Hence, for illustrative reasons, the curve has been approximated by a dotted line only.

7.4.3. Compressor system behaviour

Inlet volumetric flow and design pressure trajectory

Figure 7.15 displays the compression unit suction volumetric flow rates under all considered part load strategies. While the volumetric flow rates at regular part load or at maximum regeneration of stored solvent under the throttled LP crossover line steam extraction strategy are always lower or at design conditions, volumetric flow rates increase substantially at maximum regeneration of stored solvent under the floating steam extraction pressure strategy (i.e. lower desorber pressure, see Figure 7.7). The high volumetric flow rates combined with a required pressure ratio of 190% of the nominal level leads to choking conditions in the first stages of the compressor, making it impossible for the baseline compression system to achieve the required outlet pressures of 110bar. Even at maximum rotational shaft speed (105% of design; American Petroleum Institute 2002) exceeding the choke limit of the compressor cannot be avoided.

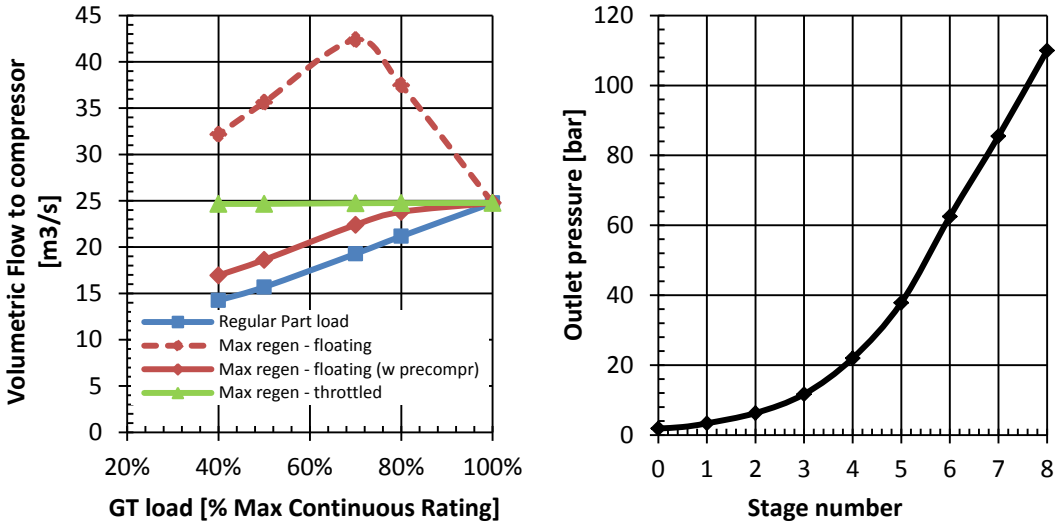

Figure 7.15 (left): Volumetric flow of CO_2 to the compressor at different GT loads and operating strategies of the PCC unit and steam cycle (see legend). To reduce the excessive volumetric flow rates in the ‚Max regen – floating' operating strategy (red line) a pre-compression stage has been inserted (red dotted line) enabling the main compressor to cope with the flow.
Figure 7.16 (right): Design pressure trajectory over individual compression stages.

To enable the compressor unit to cope with the high volumetric flow rates the addition of a pre-compression stage is necessary under the floating crossover pressure extraction strategy (see section 7.3). The purpose of this pre-compression step is to reduce the volumetric flow rates under the given additional regeneration strategy by increasing the pressure of the flow from 1bar to 1.85bar. The main compressor is then able to take the flow to the required outlet pressure of 110bar, across all GT load levels, and following approximately the design pressure trajectory presented in Figure 7.16. Figure 7.15 illustrates the reduction of volumetric flow rates achieved by the pre-compression stage (red dotted line versus solid red line). It is recognised that in practice the outlet pressure of the pre-compression stage can be optimised when traded off with the pressure increases achieved by the main compressor. It is further pointed out that the additional complexities associated with handling increased volumetric flow rates at the compression station are likely to make the utilisation of the floating crossover pressure extraction strategy unattractive for additional solvent regeneration.

Compression duty

Finally, Figure 7.17 shows the compression duty under all considered part load strategies. The diagram shows that, at regular part load, compression duty falls nearly linearly from 100-70% GT load. At 50% GT load the high necessary pressure increases prevent substantial rotational speed reductions of the compressor for avoiding surge conditions. Due to the relatively low flow, recycling of 11.3% of the flow is still required, which produces a relative

rise in the curve. At 40% GT load one compressor is shut in, avoiding recycling and part load efficiency losses, to make significant power savings.

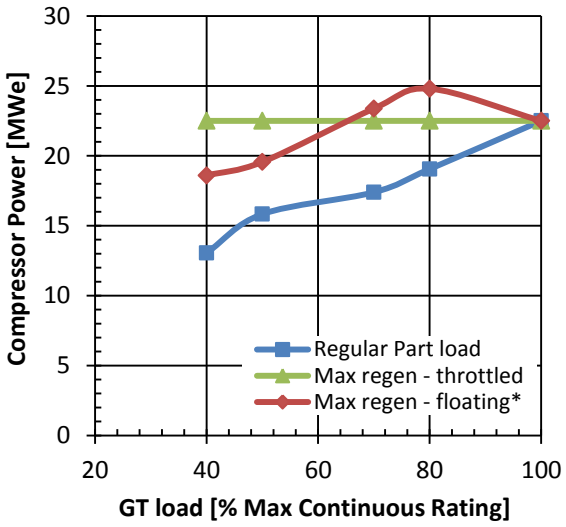

Figure 7.17: Total electrical power required for the compression of captured and exported CO_2 at different GT loads and operating strategies of the PCC unit and steam cycle (see legend).

*The compression duty required by the 'Max regen – floating' operating strategy includes work required by the pre-compression stage.

At maximum regeneration under the floating pressure strategy compressor power requirements increase at 80%GT load. This is an effect of the slightly reduced mass flow of CO_2 not compensating for the strongly increased compression ratio caused by lower desorber pressure. Power requirements start declining below 80% GT load due to lower CO_2 mass flows as well as stabilised required pressure ratios. The small observed relative increase in the curve at 40% GT load is the result of recycling of 6.5% of the flow in order to avoid surge conditions in the last stages of the compressor. At maximum regeneration under the throttled strategy compressor duty stays constant, as a consequence of the compression system operating very close to its design conditions across all GT load levels.

7.5. Correlations for the prediction of plant performance for electricity system modelling

Correlations fitted to key performance parameters at varying load and operating conditions derived from the rigorous models presented in this article can be useful for representing CCS power plant performance in wider electricity system or CO_2 networks models. The LHV efficiency, the electrical power output, and the CO_2 flows exported from the power station can be approximated at a relatively high degree of accuracy by 3rd order polynomials. The polynomials are valid over the full stable load range of the power station - i.e. 100-40%GT

load. For the calculated coefficients of the polynomials the reader is referred to Table C.2 in the appendix.

A further key performance parameter essential for energy system modelling is the time necessary to regenerate stored solvent at varying operating conditions.

It can be represented by an exponential function of the following form, in order to predict the duration necessary for regenerating stored solvent from 1hr of solvent storage operation at full load under the throttled steam extraction strategy (mean squared error=1):

$$y = 128.43 \ * (100 - x)^{-1.009}$$

where y is the time in hours to regenerate stored solvent from 1hr of solvent storage operation at full load, and x is the GT load in % during additional regeneration.

The function is valid over the full stable load range of the power station.

Due to several complex nonlinearities no such function could be found for similarly describing the corresponding curve under the floating pressure steam extraction strategy with sufficient accuracy. Energy system modellers are hence advised to take the throttled steam extraction strategy for additional regeneration of stored solvent as a reference case. It is consistent with the findings of the engineering analysis in this paper showing that additional complexities within the compression stages to handle excessive volumetric flow rates during additional regeneration makes this strategy less likely to be used.

7.6. Conclusions

This chapter examines the full load and part load performance of a NGCC-CCS power station with a particular focus on the operation of the plant during solvent storage and delayed regeneration. The GT and power cycle are integrated with the capture unit and compression system in a rigorous model to understand the behaviour and operational limits of the individual systems. Five key observations can be made on the modelling results.

First, it has been found that the strategies most widely suggested in the literature for part load operation of the capture unit are either infeasible when integrated with a NGCC power cycle, or lead to sub-optimal results. A modified strategy was hence adopted, consisting of choosing the optimal reboiler duty by varying the desorber pressure and hence lean loading, in response to changes in the reboiler temperature that in turn are governed by the falling steam pressures in the reboiler (i.e. saturation temperature), the heat transfer capacity of the reboiler and the heat requirements of the capture unit.

Second, no part load strategy for the additional regeneration of previously stored solvent could be identified in the literature. The strategy adopted in this study consists of constraining the lean loading of the regenerated solvent to design levels. This ensures that the flooding limit in the absorber is not exceeded when using the solvent at full load during solvent storage operation. Two alternative steam extraction strategies were considered: (1) floating crossover pressure; and (2) throttled LP crossover pressure. Whilst the throttled steam extracton strategy allows controlling the steam pressure in the reboiler and by extension sustaining optimal thermodynamic conditions in the reboiler even at off design conditions the floating steam extraction strategy benefits from avoiding the inefficiencies associated with the throttling process. Despite the fact that a floating crossover pressure strategy offers good performance at part-load with 90% capture, the additional complexities associated with handling increased volumetric flow rates at the compression station could, however, make this strategy unattractive for additional solvent regeneration. A further disadvantage of the floating steam extraction strategy is the relatively high EOP associated with additional regeneration of previously stored rich solvent at load levels around 70-80% load due to non optimal steam conditions and reduced steam side pressures in the reboiler.

Third, the power export envelope of a NGCC-CCS power station can be extended significantly from 389-803MW to 339-891MW via the option for solvent storage. This can be particularly valuable for balancing future low carbon electricity systems dominated by variable renewable power supply either through providing faster as well as larger amounts of spinning reserve or by supplying substantial levels of synchronised inertia at a reduced power footprint on the overall system.

Fourth, another important consideration, particularly in the overall context of this thesis, is the extent to which the electricity production can be decoupled from the flows of exported CO_2. It has been demonstrated that nominal amounts of CO_2 (i.e. 79kg/s corresponding to 2.45MTPA) can be exported to the downstream CO_2 T&S system even at low or minimum electricity output when exploiting the option for solvent storage. As a caveat it should be noted that exporting nominal flow rates of CO_2 even at minimum stable load is, however, only possible under the throttled crossover steam extraction strategy since it enables optimal conditions in the reboiler even at off design conditions. Flows of 2.45MTPA represent around 19% of the design flow capacity of a 610mm OD pipeline, and around 7% of the economic flow capacity of the 914mmOD pipeline. When simultaneously exploiting the balancing capabilities of a 100km 610mm OD (914mm OD) dense phase CO_2 pipeline, it has been demonstrated in Chapter 6, that procuring additional pipeline inflows, for example via solvent storage, sized to deliver at least 10% of nominal pipeline flow during periods of low inflows, can reduce the number of these critical events at the injection and storage level from 202 per year to 2 (2), representing an overall 99% reduction for the reference electricity system scenario. This compares to reductions of 90% (97%) being achievable when exploiting the linepacking capabilities of pipelines only.

In the overall context of this thesis it can, therefore, be concluded that solvent storage can deliver an important contribution not only to the electricity system but also to operators of future downstream CO_2 T&S networks, by reducing the flow variability feeding into the system mitigating many of the associated risks, particularly for injection wells. With an additional solvent inventory of the solvent storage tanks of 6,200m^3 the examined CCS power station can operate 1hr at full load in the solvent storage mode. This corresponds similarly to the additional amount of inventory required for the plant to export nominal amounts of CO_2 for up to 2.1hrs, whilst effectively operating below the minimum stable generation limit. A higher additional inventory is required, or the option of solvent storage at several NGCC-CCS power stations, if CO_2 pipeline inflow boosts over longer time periods were necessary**.**

Further, the electricity output penalty (EOP) imposed by the additional regeneration of stored solvent is in a similar range for both strategies. While it stays relatively constant across all GT loads under the throttled crossover pressure strategy from 420-450kWh/tCO2, it varies, nevertheless, substantially under the floating extraction pressure strategy from 375-530kWh/tCO2. It is worth noting that on average the EOP for additional regeneration of stored solvent is around 20% higher on a per-tonne-of-CO_2 basis than for regeneration of solvent at design conditions. Both strategies differ notably when it comes to the minimum duration for additional solvent regeneration. Depending on GT load, stored solvent can be regenerated 2.5-4.5 times faster under the throttled crossover pressure extraction strategy compared to the floating extraction strategy, and as fast as 2.1 hours for 1hr of interim solvent storage. The time necessary to regenerate previously stored solvent, which the power plant operator would economically commit to only at periods of advantageously low electricity prices, can have substantial economic implications when it comes to the profitability of the option for solvent storage.

Finally, the compressor system is evaluated under both delayed solvent regeneration strategies. In contrast to previous studies, it is demonstrated that the baseline compressor station is unable to cope with the high volumetric flow rates caused by decreasing desorber pressures at maximum regeneration of stored solvent under the floating crossover pressure extraction strategy. This is an important finding since it shows that delayed solvent regeneration under the floating steam extraction strategy would be technically infeasible without additional investment into a pre-compression stage. No issues are identified with a throttled crossover pressure steam extraction strategy. It should be noted that in practice both evaluated steam extraction strategies two strategies are not mutually exclusive and could be used in combination.

The results from this study provide future techno-economic studies on solvent storage in NGCC-CCS power stations with a more technically rigorous basis than has previously been available in the literature. Further research could explore several modifications of solvent storage, including oversizing of the desorber and reboiler for faster and more energy efficient regeneration of previously stored rich solvent, as well as the possibility for overstripping of the solvent in order to reduce the required inventories and sizes of solvent

storage tanks that constitute the dominant cost driver (i.e. for adding the solvent storage capability). To assist with the utilisation of the simulation results in wider energy system models a set of correlations is developed for key performance parameters at various load and operating conditions.

A particularly interesting area for future work in the context in this thesis is the assessment of the extent to which solvent storage can be used to smoothen out CO_2 flows through the downstream T&S network, and at what costs. In the light of alternative options to mitigate issues associated with variable flow rates in the downstream T&S system (e.g. linepacking, CO_2 interim storage, making wells more flexible, etc.; Spitz et al. 2018) a techno-economic comparison with other options discussed in Chapter 4 would be highly valuable. In contrast to alternative options it is expected that solvent storage can contribute to offsetting some or all of the costs associated with CO_2 smoothing by allowing for additional revenue from electricity arbitrage in the electricity market (Oates et al. 2014, Van der Wijk et al. 2014, Mechleri et al. 2017a, Cohen et al. 2011, Versteeg et al. 2013, Chalmers 2010b).

8. Conclusions and Recommendations

8.1. Conclusions

This thesis aims at improving the understanding of the operational flexibility that can be expected to be required of future CCS process chains, as well as the associated challenges. The thesis further explores operational and design options available for mitigating the identified integrity issues associated with time varying CO_2 flow rates, particularly at the injection and storage level of the CCS process chain.

A focus is placed on CCS deployment in GB low carbon electricity systems. Using a combination of unit commitment economic dispatch models of power stations, including wind, solar, nuclear and combined cycle gas turbines with CO_2 capture, with hydraulic models of dense phase CO_2 pipelines, a method to characterise the magnitude and frequency of the variability of flow changes in CO_2 transport networks and at injection wells is presented for the first time. The key findings and conclusions of this thesis are laid out over the following paragraphs. For a number of more detailed conclusions and findings the reader is referred to the respective individual chapters.

Issues associated with flexible operation of CCS infrastructure

No significant integrity concerns could be identified relating to the capture plants' and transportation pipelines' abilities to follow the load profiles expected of the underlying CO_2 producing processes (e.g. power, cement, steel, other industrial plants). Importantly, however, there are several potentially harmful effects to consider at the injection and storage level. The repeated cycling of injection wells, particularly when transitioning or operating at two-phase flow conditions, can lead to deleterious effects such as cyclic thermal stresses, cracking of cement and wellbore materials, clathrate hydrate formation, hydrogen induced embrittlement of well materials, and harmful oscillation and vibrations that over time compromise the integrity of the wells and reduce their lifetime. At the storage level repeated cyclical flow profiles can lead to an impaired injectivity due to increased levels of residual trapping or halite precipitation in saline aquifers blocking flow pathways. Although no clear 'show stoppers' exist prohibiting flexible operation in general, it becomes clear that some of the risks and uncertainties (and ultimately costs) can be avoided if the requirements for flexible operation of injection wells are better understood, and if measures are taken to mitigate either the causes or the symptoms of the mentioned deleterious effects.

CO_2 flow profiles from GB low carbon electricity system

For the first time a detailed characterisation of CO_2 flow profiles from low carbon electricity systems feeding into downstream T&S networks is provided in Chapter 3. A GB future electricity system analysis is carried out, representing the most challenging CO_2 flow variability scenarios to T&S network operations, since CO_2 flows captured from other type large point emitters can generally be expected to be more stable. The GB system is particularly interesting as a case study due to its island characteristics with high penetrations of VRE (i.e. promoting variable operation of CCS power stations), excellent renewable resource data availability, and relatively high likelihood of CCS deployment. Further, the likelihood of CO_2 injection into depleted hydrocarbon fields for geological storage is high. This generally promotes two-phase flow which leads to the mentioned integrity hampering effects at injection wells that are associated with variable and low flow rates. The results demonstrate that over the entire year, and across all investigated scenarios, the variability of CO_2 flows exported from NGCC-CCS power stations to downstream transportation networks is substantial.

In the base-line investigated scenario it is found that 21% of the yearly net CO_2 flow rate changes over 6h-periods are greater than 30% of the nominal flow, and 12% of the changes are greater than 50% of the nominal flow. Further, the results show that in general CCS power stations experience more load changes over 6-hour periods, and changes of greater amplitudes, under low emissions intensity scenarios, due to the greater number of CCS plants required to achieve these targets, some of which will need to load follow. This is a particularly relevant finding given the strong efforts of the GB and other jurisdictions to achieve a nearly complete decarbonisation of their power systems over the next decades. Looking at the annual number of critical low flow periods (LFPs) it was found that dependent on the target CO_2 emission intensity scenarios (100gCO_2/kWh and 60gCO_2/kWh average yearly emission intensity, respectively) around 200-250 of these events can be expected over the year when defined as periods with flows less than 50% of the nominal amount, and 23-191 can be expected when these are defined as periods with flows below than 30% of the nominal amount. No periods exist with flows below 10% of the nominal flow, as a consequence of the minimum thermal generation constraint of 15GW in the electricity system. Finally, the frequency of CCS plants starting-up (and shutting-down) creating step changes in CO_2 flow is a very strong function of the target emission intensity, and to a much lesser extent of the installed wind capacity scenario.

Options to mitigate integrity hampering effects associated with flexible operation

Options to mitigate the issues associated with the frequent and irregular flow rate fluctuations at the injection and storage level can be classified according to where they would act in the T&S system. At the injection well level, operational options exist to avoid hydrate formation and to boost pressure levels to mitigate the occurrence of two-phase flow. Nevertheless, these are expensive for regular or continuous operation. In networks of

a certain size with several injection wells being present, the system operator could choose to distribute the cycling and ramping load across the wells and operate them according to their individual specific needs. As such, the operator could choose to react to periods of low CO_2 flows by shutting in as many wells as required for ensuring sufficient flow in the remaining online wells, to allow these to operate within their preferred operating envelope, and at sufficiently high flow rates to avoid two-phase flow.

Given the high frequency and amplitudes of CO_2 flow rate fluctuations expected from the power sector, as determined in Chapter 3, the number of shut-ins per well and the associated thermal stresses are, however, likely to stay significant, particularly since any shut-down and subsequent start-up of a well is associated with two transitions through the low flow region of the well, as well as one period of zero injection that comes with own challenges for the storage site (see reduction of injectivity in aquifers due to increased residual trapping, see section 2.2.4).

Several well design options could, however, enable avoiding two-phase flow and the associated issues. Due to increased technical complexity in the subsurface and the consequently higher likelihood of failure, flexible well design options come with a substantially increased risk and insurance premium and have, hence, been avoided so far in CCS projects.

Options for balancing CO_2 flows upstream in the system can reduce the variability of CO_2 faced by injection wells and storage sites directly mitigating any associated issues. Although interim CO_2 storage capability could be made available in the form of buffer tanks or geological storage within the transportation network or boundaries of the CCS power plant, two options were identified as potentially particularly cost economic: Linepacking of dense phase CO_2 pipelines, and solvent storage at PCC-NGCC power stations.

Balancing capabilities of dense phase CO_2 pipelines

The potential of dense phase CO_2 pipelines to be used as buffer stores via linepacking and depacking, i.e. the ability of the pipeline to sustain a minimum outflow even at times of low inflows, can avoid critical periods of low flow at the injection level, which present the greatest risk of two-phase flow and associated deleterious effects. If linepacking is considered in the design phase of the pipeline networks, substantial line-depacking times of up to 7-36hrs can be achieved even for individual pipelines of 50-150km length. The most influential factors determining the achievable line-depacking times in the order of sensitivity are:

- The outflow & inflow flow regime during the depacking process,
- The length of the pipeline,
- The flow capacity utilisation of the pipeline at nominal operation,
- The maximum operating pressure,
- The pipeline diameter.

Line-depacking times of offshore pipelines are insensitive to the absolute levels of inflows and outflows during the depacking process. Line-depacking times are, however, very strongly dependent on the absolute difference between inflows and outflows during the pipeline depacking process.

Building on this finding Chapter 6 develops a simplified buffer storage model representative of long distance CO_2 trunklines typically considered in the GB context, for exploring the number of critical LFPs that can be avoided at the injection and storage level when exploiting the balancing capabilities of pipelines. A number of energy system scenarios from Chapter 3 are soft-linked with the pipeline buffer model to provide a representative set of CO_2 pipeline inflow scenarios. The results demonstrate that it is possible to reduce the number of occurrences of periods of low flow at the injection level by increasing the required diameter or max. operating pressure of dense phase CO_2 pipelines, and by extension their linepacking capabilities. For an offshore pipeline of 100 km and 610mm (914mm) outer diameter, the number of LFPs at the well is reduced from 202 to 32 per year (7) in the reference electricity system scenario of this study with 7.0GW of CCS capacity installed. For the 'High Wind/Low Emission Intensity' GB power system scenario with 8.8GW of CCS capacity installed the number of LFPs at the injection level can be decreased from 248 to 138 (68) with a 100km and 610mm (914mm) diameter pipeline. Increasing the buffering capabilities of pipelines can, hence, greatly reduce the need to operate injection wells flexibly with a positive effect on their long term integrity.

Solvent storage as a method for balancing CO_2 flow variability

Using solvent storage in combined cycle gas turbines with post-combustion CO_2 capture can assist in balancing flow variability, reducing further the need for injection wells to operate flexibly. Yet, no study could be identified in the literature rigorously evaluating the technical implications of solvent storage at natural gas fired power plants, its energy effectiveness, and the extent to which it allows decoupling of electricity and CO_2 production.

Rigorous modelling of an 800MW state-of-the-art CCS power stations shows that a controlled steam extraction strategy by throttling the low pressure turbine of the combined cycle is the preferred strategy - over a floating crossover pressure steam extraction strategy - for the time-shifted CO_2 release via delayed solvent regeneration. By decoupling electricity and CO_2 production nominal amounts of CO_2 (around 2.45MTPA) can be exported to the downstream CO_2 T&S system even at low or minimum electricity output when exploiting the option for solvent storage. Flows of 2.45MTPA represent around 19% of the design flow capacity of a 610mm outer diameter pipeline, and around 7% of the economic flow capacity of the 914mm outer diameter pipeline.

Smoothing of flows with solvent storage, sized to deliver at least 10% of nominal pipeline flow, further reduces the number of annual occurrences of critical low flow periods at injection wells to 2 (2) for the reference electricity system scenario, representing an overall

reduction of more than 99%. In the 'High Wind/Low Emission Intensity' scenario an equivalent reduction to 72 (32) residual LFPs could be achieved, representing a reduction of 71% (87%) of the number of low flow periods compared to the unbalanced counterfactual scenario.

This shows clearly that solvent storage can provide an important contribution to balancing both electricity networks and CO_2 T&S networks. It can balance flow variability feeding into the system, mitigating many of the integrity risks particularly at the injection and storage level. With an additional inventory of the solvent storage tanks of 6,200m^3 the investigated 800MW CCS power station can operate 1hr at full load in the solvent storage mode. This corresponds similarly to the additional amount of inventory required for the plant to be able to export nominal amounts of CO_2 for up to 2.1hrs, whilst effectively operating below the minimum stable generation limit of the base power station. A higher additional inventory is required, or the option of solvent storage at several NGCC-CCS power stations, if CO_2 pipeline inflow boosts over longer time periods are necessary.

Overall, this study highlights the substantial variability of CO_2 flows that can be expected in future CCS networks. Nevertheless, it demonstrates that powerful options exist to mitigate CO_2 flow variability and reduce the annual number of critical low flow periods at the injection well level to very low numbers, if not to zero. Ways, hence, exist to mitigate or entirely avoid the integrity risks that frequent and irregular changes in the production levels of CO_2 flows imply to the downstream injection and storage infrastructure. A key take away message for policy makers and other stakeholders is that these options will, however, need to be considered at the design stage of the network. Although the options discussed in most detail in this work, namely linepacking and solvent storage, will come at a small relative cost premium, this is likely to be small compared to the risk and expensive follow up costs should lifetimes of injection wells be compromised.

8.2. Future work

There are several ways to further improve the understanding of the operating flexibility required of future CCS networks, and the associated challenges. Some of the areas in which future work is considered to be particularly relevant in the overall context of this thesis are summarised in the following:

- An elaborate study investigating and quantifying in more detail how many cycles CO_2 injection wells are able to sustain without compromising on their integrity would be very valuable. The assessment could build on the modelling work of Lund et al. (2015), Roy et al. (2016) and Torsæter et al. (2017) and examine the long term integrity effects on well materials caused by temperature and pressure variations

over several tens and hundreds of cycles. Ideally the study should be complemented by experimental work improving credibility and quality of the findings. Together this could substantially reduce the uncertainty regarding the level of effort that needs to be undertaken to mitigate and/or avoid flexible operation of injection wells.

- A detailed analysis of the degree to which cyclical operation of saline injection sites reduces the injectivity of the wellbores would be highly relevant. It could quantitatively inform CCS system designers about the level of redundancy that needs to be planned into CCS systems since injectivity issues can significantly threaten the economic and technical success of CCS projects at later points in time. Edlmann et al. (2019) provides the first study to investigate this topic in detail. The authors demonstrate how standard reservoir modelling software is unable to accurately quantify the experimentally validated effects of increased levels of residual trapping caused by alternating invasion of CO_2 and brine into the near wellbore region. Further work is, hence, required to improve the accuracy of modelling tools, and to expand analysis quantifying also injectivity reductions at different reservoir and test conditions (e.g.: type or rock, flow patterns, number of cycles, temperature profiles, etc.).
- A detailed cost comparison between options to mitigate or solve integrity issues associated with variable flow at the injection and storage level is required. Options that should be considered are operating and design options specifically at the injection well and storage site level, as well as options available for balancing CO_2 flow variability upstream in the system directly mitigating any downstream associated issues. The work would inform CCS system designers about the most cost-effective way to hedge against negative and lifetime hampering effects induced by frequent and irregular CO_2 flow rate variations that to date are not fully understood.
- The present thesis has explicitly focused on CO_2 flows from low carbon electricity systems. Expanding the analysis to other types of CO_2 sources such as cement, steel, or chemical plants and refineries would be highly relevant to better understand and prepare for CO_2 flow profiles that need to be accommodated by injection wells and storage sites. It is only when the requirement for operating flexibility is better understood, that the implications and the potentially additional costs associated with managing the operational issues that flexible operation imply can be minimised. Particularly decarbonisation of the heat sector via hydrogen as a zero carbon energy vector - which is expected to be produced predominantly via steam or autothermal reforming of methane with CCS add-on - has the potential to significantly influence feed-flow patterns and hence required CO_2 T&S network designs. The huge daily and seasonal variations of heat demand present, nevertheless, a challenge to the supply of H_2. This can be addressed either with oversizing of hydrogen production facilities which would, consequently, frequently run at low capacity factors, or by installing large scale hydrogen storage facilities (e.g. geological). For an efficient and cost-effective design of CO_2 T&S infrastructure

the implication of either strategy (or a hybrid strategy) on the produced CO_2 flow profiles still needs to be better understood.

- The present thesis has carried out a relatively high level analysis of representative CCS network scenarios in the GB context. A future study should draw up and investigate more realistic CCS network scenarios considering, for instance, geographical distributions of individual CO_2 sources and storage sites. It would be particularly relevant to consider into more detail specific geological reservoir parameters to back-calculate critical flow level thresholds below which two-phase flow occurs. Possibly a cost-effective CCS network can be designed with a portfolio of storage site that minimises the potential for two-phase flow even at low CO_2 flow rates (e.g. by relying predominantly on aquifers in contrast to depleted hydrocarbon fields). In general, taking into account more details of the characteristics of CO_2 sources and sinks will allow more accurate quantification of the extent to which injection wells and storage sites need to sustain potentially harmful flexible operation - i.e. after flow balancing options are taken into account - than could be provided in the present study.
- A quantitative analysis of the costs and economic benefits of solvent storage as a way of balancing CO_2 flow rates feeding into the downstream T&S infrastructure would be useful. The assessment could compare the cost of making available the option for solvent storage with the additional revenues that could be achieved from additional sale of power during times of high electricity prices. In this way the study could provide CCS system designers with evidence about the relevance or importance of solvent storage, the extent to which it can balance CO_2 flows in CCS networks, and whether it is overall a net positive or net negative cost option.
- Finally, extending the current study and methodology to other countries with different renewable resource availability, different expected renewable power and CCS deployment levels, and different T&S network scenarios would allow benefitting to a greater extent from the findings of this study also in the context of CCS outside of GB.

9. References

Abdilahi, A.M., Mustafa, M.W., Abujarad, S.Y., Mustapha, M., 2018. Harnessing flexibility potential of flexible carbon capture power plants for future low carbon power systems. *Review. Renew. Sustain. Energy Rev.*, 81, 3101–3110.

ADM, 2017. ADM Begins Operations for Second Carbon Capture and Storage Project. Available at: - *https://www.adm.com/news/news-releases/adm-begins-operations-for-second-carbon-capture-and-storage-project-1*. (Accessed on 25.07.2018).

Advanced Resources International, 2011. GLOBAL TECHNOLOGY ROADMAP FOR CCS IN INDUSTRY - Sectoral Assessment CO_2 Enhanced Oil Recovery.

Aghajani, H., Race, J.M., Wetenhall, B., Sanchez Fernandez, E., Lucquiaud, M., Chalmers, H., 2017. On the potential for interim storage in dense phase CO_2 pipelines. *Int. J. Greenh. Gas Control,* 66, 276–287.

Albawi, a., De Andrade, J., Torsæter, M., Opedal, N., Stroisz, a., Vrålstad, T., 2014. Experimental Set-Up for Testing Cement Sheath Integrity in Arctic Wells. In *OTC Arct. Technol. Conf., 10-12 February, Houston, USA.*

Al-Khelaiwi, F., 2013. *A Comprehensive Approach to the Design of Advanced Well Completions*. Dr. Philos. Diss. Heriott Watt Univ. Edinburgh, UK.

Alleman, D., 2016. A LOOK AT UNDERGROUND NATURAL GAS STORAGE OPERATION AND REGULATION IN THE UNITED STATES. Available at: - *https://www.google.com/url?sa=t&rct=j&q=&esrc=s&source=web&cd=2&cad=rja&uact=8&ved=2ahUKEwie65X2jandAhUjK8AKHQ4kDKYQFjABegQICRAC&url=https%3A%2F%2Fdsp*. (Accessed on 22.07.2018).

Allen, M.R., Frame, D.J., Huntingford, C., Jones, C.D., Lowe, J. a., Meinshausen, M., Meinshausen, N., 2009. Warming caused by cumulative carbon emissions towards the trillionth tonne. *Nature*, 458, 1163–1166.

Allen, M., 2016. The carbon price trap How hot will it get in a world run by economists? In *UKCCSRC Winter School, 15-18 February, Sheffield, UK.*

Al-Mahasneh, A.J., Anavatti, S.G., Garratt, M. a., 2018. Review of Applications of Generalized Regression Neural Networks in Identification and Control of Dynamic Systems.

Al-Mamoori, A., Krishnamurthy, A., Rownaghi, A. a., Rezaei, F., 2017. Carbon Capture and Utilization Update. *Energy Technol.*, 5, 834–849.

American Electric Power, 2011. CO_2 COMPRESSION REPORT - Mountaineer CCS II Project Phase 1.

American Petroleum Institute, 2002. Axial and Centrifugal Compressors and Expander-compressors for Petroleum, Chemical and Gas Industry Services, API 617.

Andrew, R.M., 2018. Global CO_2 emissions from cement production. *Earth Syst. Sci. Data*, 10, 1–52.

Apan-Ortiz, J.I., Sanchez-Fernández, E., González-Díaz, A., 2018. Use of steam jet booster as an integration strategy to operate a natural gas combined cycle with post-combustion CO_2 capture at part-load. *Energy*, In press.

Aquistore, 2015. Leading the World in Deep Saline CO_2 Geological Storage. Available at: - *http://aquistore.ca/*. (Accessed on 20.04.2019).

Aursand, P., Hammer, M., Lavrov, A., Lund, H., Munkejord, S.T., Torsæter, M., 2017. Well integrity for CO_2 injection from ships: Simulation of the effect of flow and material parameters on thermal stresses. *Int. J. Greenh. Gas Control*, 62, 130–141.

Aursand, P., Hammer, M., Munkejord, S.T., Wilhelmsen, Ø., 2013. Pipeline transport of CO_2 mixtures: Models for transient simulation. *Int. J. Greenh. Gas Control,* 15, 174–185.

Bank of England, 2019. Inflation calculator. Available at: - *https://www.bankofengland.co.uk/monetary-policy/inflation/inflation-calculator*. (Accessed on 03.05.2018).

Bannach, A., Hauer, R., Streibel, M., Kühn, M., Stienstra, G., 2015. Stable Large-scale CO_2 Storage in Defiance of an Energy System Based on Renewable Energy - Modelling the Impact of Varying CO_2 Injection Rates on Reservoir Behavior. *Energy Procedia*, 76, 573–581.

Behbahani-Nejad, M., Bagheri, a., 2008. A MATLAB Simulink Library for Transient Flow Simulation of Gas Networks. *Proc. World Acad. Sci. Eng. Technol.*, 33, 153–159.

Bellarby, J., 2009. *Well Completion Design*. Elsevier: Amsterdam, 2009.

Bellona, 2007. Carbon Dioxide Storage: Geological Security and Environmental Issues - Case Study on the Sleipner Gas field in Norway.

Bhardwaj, A., Kamboj, V.K., Shuklam, V.K., Singh, B., Khurana, P., 2012. Unit commitment in electrical power system - A literature review. In *IEEE Int. Power Eng. Optim. Conf., 6-7 June, Melaka, Malaysia.*

Bilio, M., Brown, S., Fairwheather, M., Mahgerefteh, H., 2009. CO_2 pipelines material and safety considerations. *IChemE Symp. Ser. HAZARDS XXI Process Saf. Environ. Prot.*, 155, 423–429.

Bloomberg, 2019a. GBP to EUR Exchange Rate - Bloomberg Markets. Available at: - *https://www.bloomberg.com/quote/GBPEUR:CUR*. (Accessed on 02.05.2019).

Bloomberg, 2019b. GBP to USD Exchange Rate - Bloomberg Markets. Available at: - *https://www.bloomberg.com/quote/GBPEUR:CUR*. (Accessed on 02.05.2019).

Bloomberg New Energy Finance, 2018. Clean Energy Investment Trends 2017.

Bonneville, A., Nguyen, B.N., Stewart, M., Hou, Z.J., Murray, C., Gilmore, T., 2014. Geomechanical evaluation of thermal impact of injected CO_2 temperature on a geological reservoir: Application to the future gen 2.0 site. *Energy Procedia*, 63, 3298–3304.

Bouillot, B., Herri, J.M., 2016. Framework for clathrate hydrate flash calculations and implications on the crystal structure and final equilibrium of mixed hydrates. *Fluid Phase Equilib.*, 413, 184–195.

Bovon, P.L., Habel, R., 2007. CO_2 Compression Challenges. In Proc. *ASME Turbo Expo, May 14–17, Montreal, Canada.*

Boyce, M.P., 1997. *Transport and storage of fluids*. In Perry, R.H., Green, D.W., Maloney, J.O. (Eds.), Perry's Chemical Engineers' Handbook., 7th ed., McGraw-Hill: New York, USA.

Brasington, R.D., 2012. *Integration and operation of post-combustion capture system on coal-fired power generation: load following and peak power*. Bachelor Sci. Diss. Univ. Pittsburgh, Pittsburgh, USA.

Brooks, H., Tucker, N., 2015. Electrospinning predictions using artificial neural networks. *Polymer,* 58, 22–29.

Brouwer, A.S., Van Den Broek, M., Seebregts, A., Faaij, A., 2014. Impacts of large-scale Intermittent Renewable Energy Sources on electricity systems, and how these can be modeled. *Renew. Sustain. Energy Rev.*, 33, 443–466.

Brouwer, A.S., van den Broek, M., Seebregts, A., Faaij, A., 2015. Operational flexibility and economics of power plants in future low-carbon power systems. *Appl. Energy*, 156, 107–128.

Brown, S., Mahgerefteh, H., Martynov, S., Sundara, V., Dowell, N. Mac, 2015. A multi-source flow model for CCS pipeline transportation networks. *Int. J. Greenh. Gas Control*, 43, 108–114.

Brownsort, P., 2015. Ship transport of CO_2 for Enhanced Oil Recovery – Literature Survey.

Bruce, A.R.W., Harrison, G.P., Gibbins, J., Chalmers, H., 2014. Assessing operating regimes of CCS power plants in high wind and energy storage scenarios. *Energy Procedia*, 63, 7529–7540.

Bruce, A.R.W., 2015. *Impacts of variable renewable generation on thermal power plant operating regimes*. Dr. Philos. Diss. Univ. Edinburgh, Edinburgh.

Bruce, A.R.W., Gibbins, J., Harrison, G.P., Chalmers, H., 2016. Operational flexibility of future generation portfolios using high spatial- and temporal resolution wind data Operational flexibility of future g and temporal- resolution windeneration portfolios using high spatial- data. *IEEE Trans. Sustain. Energy*, 7, 697–707.

Bruno, M.S., Couture, J., Young, J.T., 2011. Concentrate and Brine Management Through Deep Well Injection. In *Water Reuse Symp., September, Phoenix, Arizona, USA.*

BS EN10208-2, 2009. BS EN 10208-2, Steel pipes for pipelines forcombustible fluids. Technical delivery conditions. Pipes ofrequirement class B British Standards Institute, London, UK.

Busby, J., 2015. UK shallow ground temperatures for ground coupled heat exchangers. *Q. J. Eng. Geol. Hydrogeol.*, 77.

Cany, C., Mansilla, C., da Costa, P., Mathonnière, G., Duquesnoy, T., Baschwitz, A., 2016. Nuclear and intermittent renewables: Two compatible supply options? The case of the French power mix. *Energy Policy*, 95, 135–146.

Cany, C., Mansilla, C., Mathonnière, G., da Costa, P., 2018. Nuclear power supply: Going against the misconceptions. Evidence of nuclear flexibility from the French experience. *Energy*, 151, 289–296.

Capture Power Limited, 2015. K02 - Full Chain Basis of Design.

Capture Power Limited, 2016a. K33 - Pipeline Infrastructure and Design Confirming the Engineering Design Rationale Technical Transport.

Capture Power Limited, 2016b. K38 - Subsurface Well Report - White Rose CCS Demonstration project.

Capture Power Ltd., 2015a. K34 - Flow Assurance Report.

Capture Power Ltd., 2015b. K27 - Oxy Power Plant Process Description.

Capture Power Ltd., 2015c. K30 - Storage Process Description.

Carroll, S., Carey, J.W., Dzombak, D., Huerta, N.J., Li, L., Richard, T., Um, W., Walsh, S.D.C., Zhang, L., 2016. Review: Role of chemistry , mechanics, and transport on well integrity in CO_2 storage environments. *Int. J. Greenh. Gas Control*, 49, 149–160.

CCC, 2015. The Fifth Carbon Budget: The next step towards a low-carbon economy. Available at: - *https://www.theccc.org.uk/publication/the-fifth-carbon-budget-the-next-step-towards-a-low-carbon-economy*. (Accessed: 24.07.2018).

CCC, 2016. Next steps for UK heat policy.

CCC, 2018. Hydrogen in a low-carbon economy.

Ceccarelli, N., Van Leeuwen, M., Wolf, T., Van Leeuwen, P., Van Der Vaart, R., Maas, W., Ramos, A., 2014. Flexibility of low-CO_2 gas power plants: Integration of the CO_2 capture unit with CCGT operation. *Energy Procedia*, 63, 1703–1726.

Celikoglu, H.B., 2006. Application of radial basis function and generalized regression neural networks in non-linear utility function specification for travel mode choice modelling. *Math. Comput. Model.*, 44, 640–658.

Chalmers, H., Gibbins, J., 2007. Initial evaluation of the impact of post-combustion capture of carbon dioxide on supercritical pulverised coal power plant part load performance. *Fuel*, 86, 2109–2123.

Chalmers, H., Leach, M., Lucquiaud, M., Gibbins, J., 2009a. Valuing flexible operation of power plants with CO_2 capture. *Energy Procedia*, 1, 4289–4296.

Chalmers, H., Lucquiaud, M., Gibbins, J., Leach, M., 2009b. Flexible Operation of Coal Fired Power Plants with Postcombustion Capture of Carbon Dioxide. *J. Environ. Eng.*, 135, 449–458.

Chalmers, H., 2010a. Flexible operation of coal-fired power plant with CO_2 capture. IEA Clean Coal Centre, 2010.

Chalmers, H., 2010b. *Flexible operation of coal-fired power plants with post-combustion capture of carbon dioxide*. Dr. Philos. Diss. Surrey, Surrey.

Chandel, M.K., Pratson, L.F., Williams, E., 2010. Potential economies of scale in CO_2 transport through use of a trunk pipeline. *Energy Convers. Manag.*, 51, 2825–2834.

Chapman, K., Krishniswami, P., Wallentine, V., Abbaspour, M., Ranganathan, R., Addanki, R., Sengupta, J., Chen, L., 2005. Virtual Pipeline System Testbed to Optimize the U.S. Natural Gas Transmission Pipeline System. Available at: - *https://www.osti.gov/biblio/861668*. (Accessed on 07.01.2019).

Chaudry, M., Abeysekera, M., Hosseini, S.H.R., Jenkins, N., Wu, J., 2015. Uncertainties in decarbonising heat in the UK. *Energy Policy*, 87, 623–640.

Cohen, S.M., Rochelle, G.T., Webber, M.E., 2011. Optimal operation of flexible post-combustion CO_2 capture in response to volatile electricity prices. *Energy Procedia*, 4, 2604–2611.

Cohen, S.M., Rochelle, G.T., Webber, M.E., 2012. Optimizing post-combustion CO_2 capture in response to volatile electricity prices. *Int. J. Greenh. Gas Control*, 8, 180–195.

Cole, I.S., Corrigan, P., Sim, S., Birbilis, N., 2011. Corrosion of pipelines used for CO_2 transport in CCS: Is it a real problem? *Int. J. Greenh. Gas Control*, 5, 749–756.

Conejo, A.J., Carrión, M., Morales, J.M., 2010. *Decision Making Under Uncertainty in Electricity Markets*. Springer-Verlag: Berlin Heidelberg.

Cotton, K.C., 1994. *Evaluating and Improving Steam Turbine Performance*, 2nd ed. Cotton Fact.

Cybenko, G., 1989. Mathematics of Control, Signals, and Systems Approximation by Superpositions of a Sigmoidal Function. *Math. Control Signals Syst.*, 2, 303–314.

Daly, P., Flynn, D., Cunniffe, N., 2015. Inertia considerations within unit commitment and economic dispatch for systems with high non-synchronous penetrations. IEEE Eindhoven PowerTech, PowerTech 2015.

Davidson, R., 2011. Pre-combustion capture of CO_2 in IGCC plants.

De Andrade, J., Torsaeter, M., Todorovic, J., Opedal, N., Stroisz, A., Vrålstad, T., 2014. Influence of casing centralization on cement sheath integrity during thermal cycling. In *IADC/SPE Drilling Conference and Exhibition, 4-6 March, Forth Worth, Texas, USA, 2014,* 2, 870–879.

De Kler, R.C.F., Verbaan, M., Goetheer, E.L.V., 2013. Reducing the cost of post combustion capture technology for pulverized coal power plants by flexible operation. *Energy Procedia*, 37, 2703–2714.

Delarue, E., Martens, P., D'haeseleer, W., 2012. Market opportunities for power plants with post-combustion carbon capture. *Int. J. Greenh. Gas Control*, 6, 12–20.

Denholm, P., O'Connell, M., Brinkman, G., Jorgenson, J., 2015. Overgeneration from Solar Energy in California. A Field Guide to the Duck Chart.

Domenichini, R., Mancuso, L., Ferrari, N., Davison, J., 2013. Operating flexibility of power plants with carbon capture and storage (CCS). *Energy Procedia*, 37, 2727–2737.

Drilling Contractor, 2011. Merged multilaterals system cuts time, risk. Available at: - *http://www.drillingcontractor.org/merged-multilaterals-system-cuts-time-risk-9935.* (Accessed on: 26.05.2016).

EBTF, 2011. European best practice guidelines for assessment of CO_2 capture technologies. In: CESAR-project 7th FrameWork Programme.

Edlmann, K., Hinchliffe, S., Heinemann, N., Johnson, G., Ennis-King, J., McDermott, C.I., 2019. Cyclic CO_2 – H_2O injection and residual trapping: implications for CO_2 injection efficiency and storage security. *Int. J. Greenh. Gas Control*, 80, 1–9.

EIA, 2011. Electricity demand changes in predictable patterns. Available at: - *https://www.eia.gov/todayinenergy/detail.php?id=4190.* (Accessed on 11.09.2018).

EIA, 2017. Underground natural gas working storage capacity. Available at: - *https://www.eia.gov/naturalgas/storagecapacity/#tabs-map3.* (Accessed on 07.09.2018).

EIA, 2018. Levelized Cost and Levelized Avoided Cost of New Generation Resources in the Annual Energy Outlook 2018.

EirGrid and SONI, 2015. Annual Renewable Energy Constraint and Curtailment Report 2015.

Element Energy, 2010. CO_2 pipline infrastructure: An analysis of global challenges and opportunities.

Element Energy, 2013. Infrastructure in a low-carbon energy system to 2030: Carbon capture and storage.

Energy Research Partnership, 2015. Managing Flexibility Whilst Decarbonising the GB Electricity System.

Energy Technologies Institute, 2014. Helping to accelerate the implementation of CCS in the UK.

English, N.J., MacElroy, J.M.D., 2015. Perspectives on molecular simulation of clathrate hydrates: Progress, prospects and challenges. *Chem. Eng. Sci.*, 121, 133–156.

EON, 2011. Kingsnorth carbon dioxide capture and storage demonstration project - Key knowledge reference book.

EON, 2012a. Establish CO_2 Supply Properties. Available at: - *webarchive.nationalarchives.gov.uk/20121217150422/http://decc.gov.uk/Media/viewfile.ashx?FilePath=11/ccs/chapter7/7.7-establish-co2- supply-properties.pdf&filetype=4.* (Accessed on 26.05.2016).

EON, 2012b. Post-FEED Project Cost Estimates. Kingsnorth Carbon Capture & Storage Demonstration Project, 2010. Available at: - *http://webarchive.nationalarchives.gov.uk/20121217150422/http://decc.gov.uk/en/content/cms/emissions/ccs/ukccscomm_prog/feed/e_on_fe ed_/pro*. (Accessed on 29.08.2018).

Equinor, 2018. Carbon Storage. Available at: - *https://www.equinor.com/en/how-and-why/climate-change/carbon-storage.html*. (Accessed on 25.07.2018).

Errey, O., Chalmers, H., Lucquiaud, M., Gibbins, J., 2014. Valuing responsive operation of post-combustion CCS power plants in low carbon electricity markets. *Energy Procedia*, 63, 7471–7484.

ETI, 2014. A Picture of CO_2 Storage in the UK - Learnings from the ETI ' s UKSAP and derived projects.

ETI, 2015. Carbon capture and storage: Building the UK carbon capture and storage sector by 2030 - Scenarios and actions.

European Commission, 2018. Novel carbon capture and utilisation technologies. Available at: - *https://ec.europa.eu/research/sam/index.cfm?pg=ccu.* (Accessed on 11.10.2018).

Fajardy, M., Mac Dowell, N., 2018. The energy return on investment of BECCS: Is BECCS a threat to energy security? *Energy Environ. Sci.*, 11, 1581–1594.

Farhat, K., Benson, S.M., 2013. A technical assessment of CO_2 Interim Storage in deep saline aquifers. *Int. J. Greenh. Gas Control*, 15, 200–212.

Farhat, K., Brandt, A., Benson, S.M., 2011. CO_2 interim storage: Technical characteristics and potential role in CO_2 market development. *Energy Procedia*, 4, 2628–2636.

Fombad, M.W., 2016. *A TECHNOLOGY PERSPECTIVE AND OPTIMIZED WORKFLOW TO INTELLIGENT WELL APPLICATIONS*. MSc Diss. Texas A&M Univ. Texas, USA.

Frangioni, A., Gentile, C., Lacalandra, F., 2008. Solving unit commitment problems with general ramp constraints. *Int. J. Electr. Power Energy Syst.*, 30, 316–326.

Freguia, S., Rochelle, G.T., 2003. Modeling of CO_2 capture by aqueous monoethanolamine. *AIChE J.*, 49, 1676–1686.

Fridahl, M., Lehtveer, M., 2018. Bioenergy with carbon capture and storage (BECCS): Global potential, investment preferences, and deployment barriers. *Energy Res. Soc. Sci. 42*, 155–165.

Gao, L., Fang, M., Li, H., Hetland, J., 2011. Cost analysis of CO_2 transportation: Case study in China. *Energy Procedia*, 4, 5974–5981.

Gas Turbine World, 2013. *2013 GTW Handbook*. Pequot Publishing: Southport, North Carolina, USA.

Gassnova, 2017. FULL SCALE CCS INNORWAY. Available at: - *https://www.cslforum.org/cslf/sites/default/files/documents/AbuDhabi2017/AbuDhabi17-TW-Haugan-Session4.pdf*. (Accessed on 30.07.2018).

GCCSI, 2011a. Accelerating the Uptake of CCS: Industrial Use of Captured Carbon Dioxide.

GCCSI, 2011b. Knowledge sharing report - CO_2 liquid logistics shipping concept: business model, Available at: - *http://www.globalccsinstitute.com/publications/co2-liquid-logistics-shipping-concept-llsc-%E2%80%93-business-model-report*. (Accessed on 30.07.2012).

GCCSI, 2013. The global status of CCS.

GCCSI, 2017. The global status of CCS.

Ghazi, N., Race, J.M., 2012. TECHNO-ECONOMIC MODELLING AND ANALYSIS OF CO_2 PIPELINES. In *Proceedings of the 2012 9th International Pipeline Conference. September 24-28, 2012, Calgary, Alberta, Canada.*

Gibbins, J.R., Crane, R.I., 2004. Scope for reductions in the cost of CO_2 capture using flue gas scrubbing with amine solvents. *Proc. Inst. Mech. Eng. Part A J. Power Energy*, 218, 231–239.

Global Carbon Project, 2017. Global Carbon Budget 2017. *Available at: - http://www.globalcarbonproject.org/carbonbudget/index.htm*. (Accessed 24.07.2018).

Gonzales Diaz, A., 2016. *SEQUENTIAL SUPPLEMENTARY FIRING IN NATURAL GAS COMBINED CYCLE PLANTS WITH CARBON CAPTURE FOR ENHANCED OIL RECOVERY*. Dr. Philos. Diss. Univ. Edinburgh, Edinburgh.

González-Díaz, M.O., González-Díaz, A., Lucquiaud, M., González-Santaló, J.M., Méndez-Aranda, Á., Alcaráz-Calderón, A.M., 2017. Effect of the ambient conditions on gas turbine combined cycle power plants with post-combustion CO_2 capture. *Energy*, 134, 221–233.

Goodarzi, S., Settari, A., Zoback, M.D., Keith, D.W., 2015. Optimization of a CO_2 storage project based on thermal, geomechanical and induced fracturing effects. *J. Pet. Sci. Eng.,* 134, 49–59.

Grainger, J.J., Stevenson, W.D., 1994. *Power System Analysis*. MacGraw-Hill: New York, USA, 1994.

Greenwood, D.M., Lim, K.Y., Patsios, C., Lyons, P.F., Lim, Y.S., Taylor, P.C., 2017. Frequency response services designed for energy storage. *Appl. Energy*, 203, 115–127.

Gupta, M., Coyle, I., Thambimuthu, K., 2003. CO_2 Capture Technologies and Opportunities in Canada.

Halliburton, 2014. Intelligent Completions. Available at: - *www.halliburton.com/public/cps/contents/Books_and_Catalogs/web/CPSCatalog/03_Intelligent_Completions.pdf*. (Accessed on 26.05.2016).

Han, X.S., Gooi, H.B., 2007. Effective economic dispatch model and algorithm. *Int. J. Electr. Power Energy Syst.*, 29, 113–120.

Happ, H.H., 1977. OPTIMAL POWER DISPATCH -A COMPREHENSIVE SURVEY. *IEEE Trans. Power Appar. Syst.*, 841–854.

Haumann, D., Göttlicher, G., Osmancevic, E., Kuhn, T., Konrad, C., Strittmatter, J., 2012. CO_2 Pipeline Transport from Germany to Algeria. In *7th Pipeline Technology Conference 2012, 28-30 March, Hanover, Germany.*

Hawkins, S., 2012. *A High Resolution Reanalysis of Wind Speeds over the British Isles for Wind Energy Integration*. Dr. Philos. Diss. Univ. Edinburgh, Edinburgh.

Heddle, G., Herzog, H., Klett, M., 2003. The Economics of CO_2 storage. Laboratory for Energy and the Environment, Massachusetts Institute of Technology.

Herraiz, L., Fernández, E.S., Palfi, E., Lucquiaud, M., 2018. Selective exhaust gas recirculation in combined cycle gas turbine power plants with post-combustion CO_2 capture. *Int. J. Greenh. Gas Control*, 71, 303–321.

Heuberger, C.F., Staffell, I., Shah, N., Dowell, N. Mac, 2017. A systems approach to quantifying the value of power generation and energy storage technologies in future electricity networks. *Comput. Chem. Eng.*, 107, 247–256.

Hobbs, B.F., Rothkopf, M.H., O'Neill, R.P., Hung-po Chao, 2001. *The Next Generation of Electric Power Unit Commitment Models*, Kluwer Academic Publishers: New York.

Holttinen, H., Meibom, P., Orths, A., Lange, B., O'Malley, M., Olav Tande, J., Estanqueiro, A., Gomez, E., Söder, L., Strbac, G., Smith, J.C., Van Hulle, F., 2014. Impacts of large amounts of wind power on design and operation of power systems, results of IEA collaboration. *Wind Energy*, 17, 657–669.

Husebye, J., Anantharaman, R., Fleten, S.E., 2011. Techno-economic assessment of flexible solvent regeneration & storage for base load coal-fired power generation with post combustion CO_2 capture. *Energy Procedia*, 4, 2612–2619.

Hussain, B., 2017. *DYNAMIC SIMULATIONS OF CARBON DIOXIDE PIPELINE TRANSPORTATION FOR THE PURPOSE OF CARBON CAPTURE AND STORAGE*. Dr. Philos. Diss. Univ. Birmingham, Birmingham.

IAEA, 2014. Non-baseload Operation in Nuclear Power Plants: Load Following and Frequency Control Modes of Flexible Operation. Available at: - *https://www-pub.iaea.org/books/iaeabooks/11104/Non-baseload-Operation-in-Nuclear-Power-Plants-Load-Following-and-Frequency-Co.* (Accessed on 02.08.2018).

IEA, 2015. Energy Technology Perspectives 2015.

IEA, 2016a. CO_2 emissions from fuel combustion.

IEA, 2016b. World Energy Outlook 2016.

IEA, 2017a. Energy Technology Perspectives 2017.

IEA, 2017b. World Energy Investment 2017.

IEA, 2017c. Renewables 2017.

IEAGHG, 2002. Transmission of CO_2 and Energy, PH4/6, March, 2002.

IEAGHG, 2005. Building the Cost Curves for CC2 Storage: European Sector, 2005/02, February, 2005.

IEAGHG, 2009. CO_2 Storage in Depleted Gas Fields, 2009/01, June, 2009.

IEAGHG, 2010. Development of a Global CO_2 Pipeline Infrastructure, 2010/13, August, 2010.

IEAGHG, 2011a. Rotating equipment for carbon dioxide capture and storage, 2011/07, September, 2011.

IEAGHG, 2011b. Global Storage Resources Gap Analysis for Policy Makers, 2011/10, September, 2011.

IEAGHG, 2012a. CO_2 Transport via Pipeline and Ship. Available at: - *https://ieaghg.org/docs/General_Docs/IEAGHG_Presentations/3._CO2_Transport_Overview_-_S._Santos_IEAGHG.pdf*. (Accessed on 30.07.2012).

IEAGHG, 2012b. OPERATING FLEXIBILITY OF POWER PLANTS WITH CCS, 2012/6, June, 2012.

IEAGHG, 2012c. CO_2 Capture at Gas Fired Power Plants, 2012/8, July, 2012. IEAGHG.

IEAGHG, 2013. UK FEED Studies 2011 – A Summary, 2013/12, October 2013.

IEAGHG, 2016. Operational Flexibility of CO_2 Transport and Storage, 2016/04, March, 2016.

IEAGHG, 2017. Valuing Flexibility in CCS Power Plants, 2017/09, December, 2017.

IEC, 2015. Strategic asset management of power networks.

IPCC, 2005. Carbon dioxide capture and storage.

IPCC, 2014. Climate Change 2014: Synthesis Report. Contribution of Working Groups I, II and III to the Fifth Assessment Report of the Intergovernmental Panel on Climate Change [Core Writing Team, R.K. Pachauri and L.A. Meyers (eds.)]. IPCC, Geneva, Switzerland.

Jackson, M.D., Addiego-Guevara, E. a., Giddins, M.A., 2008. Insurance Value of Intelligent Well Technology Against Reservoir Uncertainty. In *SPE/DOE Improved Oil Recovery Symposium, 19 – 23 April, Tulsa, Oklohoma, USA.*

Jakob, M., Hilaire, J., 2015. Climate science: Unburnable fossil-fuel reserves. *Nature*, 517, 150–152.

JapanCCS, 2018. Tomakomai CCS Demonstration Project. *Available at: - http://www.japanccs.com/en/business/demonstration*. (Accessed on 25.07.2018).

Jenkins, J.D., Zhou, Z., Ponciroli, R., Vilim, R.B., Ganda, F., de Sisternes, F., Botterud, a., 2018. The benefits of nuclear flexibility in power system operations with renewable energy. *Appl. Energy*, 222, 872–884.

Jensen, M.D., Schlasner, S.M., Sorensen, J. a., Hamling, J. a., 2014. Operational flexibility of CO_2 transport and storage. *Energy Procedia*, 63, 2715–2722.

Jordal, K., Ystad, P.A.M., Anantharaman, R., Chikukwa, A., Bolland, O., 2012. Design-point and part-load considerations for natural gas combined cycle plants with post combustion capture. *Int. J. Greenh. Gas Control*, 11, 271–282.

Kaufmann, R., Aavatsmark, I., Nøkleby, P.H., Aurdal, T. a., 2016. Using an aquifer as CO_2 buffer storage. *Int. J. Greenh. Gas Control*, 53, 106–116.

Keay, M., 2016. Electricity markets are broken – can they be fixed?. Available at: - *https://www.oxfordenergy.org/publications/electricity-markets-are-broken-can-they-be-fixed/*. (Accessed on 11.09.2018).

Kehlhofer, R., Rukes, B., Hannemann, F., Stirnimann, F., 2009. *Combined-Cycle Gas & Steam Turbine Power Plants*, 3rd ed., PennWell Books: Houston, USA.

Kirschen, D.S., Strbac, G., 2004. *Fundamentals of Power System Economics*, John Wiley & Sons: Chichester, England.

Kler, R. De, Neele, F., Nienoord, M., Brownsort, P., Koornneef, J., Belfroid, S., Peters, L., Wijhe, A. Van, Loeve, D., 2016. Transportation and unloading of CO_2 by ship - a comparative assessment. Available at: - *https://www.google.com/url?sa=t&rct=j&q=&esrc=s&source=web&cd=1&cad=rja&uact=8&ved=2ahUKEwj-77yGocncAhUG3xoKHTZTAzgQFjAAegQIARAC&url=https%3A%2F%2Fwww.co2-cato.org%2Fc*. (Accessed on 15.07.2018).

Knoope, M.M.J., Ramírez, A., Faaij, a. P.C., 2013. A state-of-the-art review of techno-economic models predicting the costs of CO_2 pipeline transport. *Int. J. Greenh. Gas Control*, 16, 241–270.

Knoope, M.M.J., Ramírez, A., Faaij, a. P.C., 2015. Investing in CO_2 transport infrastructure under uncertainty: A comparison between ships and pipelines. *Int. J. Greenh. Gas Control*, 41, 174–193.

Knudsen, J.N., Jensen, J.N., Power, D.E., 2009. Experience with the CASTOR / CESAR Pilot Plant. In *Workshop for Operating Flexibility of Power Plants with CCS, November, Imperial College, London, UK.*

Kolster, C., Agada, S., Mac Dowell, N., Krevor, S., 2018. The impact of time-varying CO_2 injection rate on large scale storage in the UK Bunter Sandstone. *Int. J. Greenh. Gas Control*, 68, 77–85.

Kvamsdal, H.M., Jakobsen, J.P., Hoff, K. a., 2009. Dynamic modeling and simulation of a CO_2 absorber column for post-combustion CO_2 capture. *Chem. Eng. Process. Process Intensif.*, 48, 135–144.

L.E.K.Consulting, 2009. An Ideal Portfolio of CCS Projects and Rationale for Supporting Projects.

Lamont, A.D., 2008. Assessing the long-term system value of intermittent electric generation technologies. *Energy Econ.*, 30, 1208–1231.

Lamont, A.D., 2013. Assessing the economic value and optimal structure of large-scale electricity storage. *Power Syst. IEEE Trans.,* 28, 911–921.

Larock, B.E., Jeppson, R.W., Watters, G.Z., 2000. *Hydraulics of Pipeline Systems*, CRC Press: New York.

Larsson, S., Fantazzini, D., Davidsson, S., Kullander, S., Höök, M., 2014. Reviewing electricity production cost assessments. *Renew. Sustain. Energy Rev.*, 30, 170–183.

LCICG, 2012. Carbon Innovation Coordination Group Technology Innovation Needs Assessment (TINA) Carbon Capture & Storage in the Power Sector. Summary report, 2012.

Leeson, D., Dowell, N. Mac, Shah, N., Petit, C., Fennell, P.S., 2017. A Techno-economic analysis and systematic review of carbon capture and storage (CCS) applied to the iron and steel, cement, oil refining and pulp and paper industries, as well as other high purity sources. *Int. J. Greenh. Gas Control*, 61, 71–84.

Lew, D., Brinkman, G., Ibanez, E., Florita, A., Heaney, M., Hodge, B., Hummon, M., King, J., 2013. The Western Wind and Solar Integration Study Phase 2. National Energy Technology Laboratory, Denver, Colorado, US.

Li, C.A., Johnson, R.B., Svoboda, A.J., 1997. A new unit commitment method. *IEEE Trans. Power Syst.*, 12, 113–119.

Li, X., Xu, R., Wei, L., Jiang, P., 2015. Modeling of wellbore dynamics of a CO_2 injector during transient well shut-in and start-up operations. *Int. J. Greenh. Gas Control*, 42, 602–614.

Liebenthal, U., Kather, A., 2011. Design and Off-Design Behaviour of a CO_2 Compressor for a Post-Combustion CO_2 Capture Process. In *5th International Conference on Clean Coal Technologies, 8-12 May, Saragoza, Spain.*

Liese, E., Zitney, S.E., 2017. The impeller exit flow coefficient as a performance map variable for predicting centrifugal compressor off-design operation applied to a supercritical CO_2 working fluid. *Proc. ASME Turbo Expo*, 9, 1–10.

Liu, H., Gallagher, K.S., 2011. Preparing to ramp up large-scale CCS demonstrations: An engineering-economic assessment of CO_2 pipeline transportation in China. *Int. J. Greenh. Gas Control*, 5, 798–804.

Livingstone, D.J., 2009. *Artificial Neural Networks*, Humana Press: Towata, USA.

Lockwood, T., 2017. A Compararitive Review of Next-generation Carbon Capture Technologies for Coal-fired Power Plant. *Energy Procedia*, 114, 2658–2670.

Lohrenz, J., Bray, B.G., Aime, M., Clark, C.R., 1964. Calculating Viscosity of Reservoir Fluids From Their Composition. *J. Pet. Technol.*, 16, 1171–1176.

Loisel, R., Alexeeva, V., Zucker, a., Shropshire, D., 2018. Load-following with nuclear power: Market effects and welfare implications. *Prog. Nucl. Energy*, 109, 280–292.

Lokhov, A., 2011. Technical and Economic Aspects of Load Following with Nuclear Power Plants. Available at: - *https://www.oecd-nea.org/ndd/reports/2011/load-following-npp.pdf*. (Accessed on 12.11.2018).

Lucquiaud, M., Chalmers, H., Gibbins, J., 2008. Potential for flexible operation of pulverised coal power plants with CO_2 capture. *Mater. Sci. Eng. Energy Syst.,* 2, 177–183.

Lucquiaud, M., Errey, O., Chalmers, H., Liang, X., Gibbins, J., Abu Zahra, M.R.M., 2011. Techno-economic assessment of future-proofing coal plants with post-combustion capture against technology developments. *Energy Procedia*, 4, 1909–1916.

Lucquiaud, M., Fernandez, E.S., Chalmers, H., Dowell, N. Mac, Gibbins, J., 2014. Enhanced operating flexibility and optimised off-design operation of coal plants with post-combustion capture. *Energy Procedia*, 63, 7494–7507.

Lucquiaud, M., Gibbins, J., 2011a. On the integration of CO_2 capture with coal-fired power plants: A methodology to assess and optimise solvent-based post-combustion capture systems. *Chem. Eng. Res. Des.*, 89, 1553–1571.

Lucquiaud, M., Gibbins, J., 2011b. Effective retrofitting of post-combustion CO_2 capture to coal-fired power plants and insensitivity of CO_2 abatement costs to base plant efficiency. *Int. J. Greenh. Gas Control*, 5, 427–438.

Luedtke, K.H., 2004. *Process Centrigual Compressors*. Springer-Verlag: Berlin Heidelberg.

Lund, H., Torsæter, M., Munkejord, S.T., 2015. Study of thermal variations in wells during CO_2 injection. In *Soc. Pet. Eng. - SPE Bergen One Day Semin. 2015, 327–337.*

Ma, J., Silva, V., Belhomme, R., Kirschen, D.S., Ochoa, L.F., 2013. Evaluating and Planning Flexibility in Sustainable Power Systems. *IEEE Trans. Sustain. Energy*, 4, 200–209.

Mac Dowell, N., Fennell, P.S., Shah, N., Maitland, G.C., 2017. The role of CO_2 capture and utilization in mitigating climate change. *Nat. Clim. Chang.*, 7, 243–249.

Mac Dowell, N., Shah, N., 2015. The multi-period optimisation of an amine-based CO_2 capture process integrated with a super-critical coal-fired power station for flexible operation. *Comput. Chem. Eng.*, 74, 169–183.

Mac Dowell, N., Staffell, I., 2016. The role of flexible CCS in the UK's future energy system. *Int. J. Greenh. Gas Control,* 48, 327–344.

Martynov, S., Mac Dowell, N., Brown, S., Mahgerefteh, H., 2015. Assessment of Integral Thermo-Hydraulic Models for Pipeline Transportation of Dense-Phase and Supercritical CO_2. *Ind. Eng. Chem. Res.*, 54, 8587–8599.

Masella, J.M., Tran, Q.H.H., Ferre, D., Pauchon, C., 1998. Transient simulation of two-phase flows in pipes. *Rev. L'Institut Français du Pétrole*, 53, 801–811.

Matthews, H.D., Gillett, N.P., Stott, P. a., Zickfeld, K., 2009. The proportionality of global warming to cumulative carbon emissions. *Nature*, 459, 829–832.

McCollum, D.L., Ogden, J.M., 2006. Techno-economic models for carbon dioxide compression, transport, and storage & correlations for estimating carbon dioxide

density and viscosity. Institute for Transportation Studies, University of California Davis, USA.

McCoy, S.T., Rubin, E.S., 2008. An engineering-economic model of pipeline transport of CO_2 with application to carbon capture and storage. *Int. J. Greenh. Gas Control*, 2, 219–229.

McCulloch, W.S., Pitts, W., 1990. A logical calculus nervous activity. *Bull. Math. Biol.*, 52, 99–115.

McNeil, C., 2014. AEP PVF Post-Injection Monitoring and Site Care Program. Thirteenth Annual Conference on Carbon Capture, Utilization & Storage. In *13th Annual Conference on Carbon Capture, Utilization & Storage, April 28-May 1, Pittsburgh, USA*.

McNeil, C., 2016. RE: CCUS presentation - Cycling flexibility of CO_2 injection wells (Issue of hydrate formation). Person communication to author via email 30.06.2016.

Mechleri, E., Brown, S., Fennell, P.S., Mac Dowell, N., 2017a. CO_2 capture and storage (CCS) cost reduction via infrastructure right-sizing. *Chem. Eng. Res. Des.*, 119, 130–139.

Mechleri, E., Fennell, P.S., Dowell, N.M., 2017b. Optimisation and evaluation of flexible operation strategies for coal- and gas-CCS power stations with a multi-period design approach. *Int. J. Greenh. Gas Control*, 59, 24–39.

Mechleri, E., Lawal, A., Ramos, A., Davison, J., Dowell, N. Mac, 2017c. Process control strategies for flexible operation of post-combustion CO_2 capture plants. *Int. J. Greenh. Gas Control*, 57, 14–25.

Mechleri, E.D., Biliyok, C., Thornhill, N.F., 2014. Dynamic simulation and control of post-combustion CO_2 capture with MEA in a gas fired power plant. *Computer Aided Chemical Engineering*, 619-624.

Mitchell, A.F., Skarsholt, L.T., 2008. Advanced Wells : How are they Being Used and are they Creating Value. In *SPE/DOE Improv. Oil Recover. Symp., 19-23 April, Tulsa, Oklahoma, USA.*

Modekurti, S., Eslick, J., Omell, B., Bhattacharyya, D., Miller, D.C., Zitney, S.E., 2017. Design, dynamic modeling, and control of a multistage CO 2 compression system. *Int. J. Greenh. Gas Control*, 62, 31–45.

Mohitpour, M., Golshan, H., Murray, A., 2003. *Pipeline Design & Construction: A Practical Approach*, 3rd Edition, ASME Press: New York, USA.

Mohitpour, M., Seevam, P., Botros, K.K., Rothwell, B., Ennis, C., 2012. *Pipeline Transportation of Carbon Dioxide Containing Impurities*, ASME: New York, USA.

Mohtadi-Bonab, M. a., Eskandari, M., Rahman, K.M.M., Ouellet, R., Szpunar, J. a., 2016. An extensive study of hydrogen-induced cracking susceptibility in an API X60 sour service pipeline steel. *Int. J. Hydrogen Energy*, 41, 4185–4197.

Morren, J., Pierik, J., de Haan, S.W.H., 2006. Inertial response of variable speed wind turbines. *Electr. Power Syst. Res.*, 76, 980–987.

Mossalam, A., Arafa, M., 2017. Using artificial neural networks (ANN) in projects monitoring dashboards' formulation. *HBRC J.*, 14, 385–392.

Munkejord, S.T., Bernstone, C., Clausen, S., de Koeijer, G., Molnvik, M.J., 2013. Combining thermodynamic and fluid flow modelling for flow assurance. *Energy Procedia,* 37, 2904–2913.

National Grid, 2011. Operating the Electricity Transmission Networks in 2020.

National Grid, 2013. 2013 Electricity Ten Year Statement.

National Grid, 2014. UK Future Energy Scenarios 2014.

National Grid, 2015a. Metered half-hourly electricity demand.

National Grid, 2015b. National Grid EMR Electricity Capacity Report.

National Grid, 2016a. Future Requirements for Balancing Services.

National Grid, 2016b. System Operability Framework 2016.

National Grid, 2016c. Future Energy Scenarios 2016.

National Grid, 2016d. National Grid EMR Electricity Capacity Report.

National Grid, 2016e. Winter Consultation.

National Grid, 2017a. Future Energy Scenarios 2017.

National Grid, 2017b. Gas Transportation Transmission Planning Code.

NETL, 2014. Near-Term Projections of CO_2 Utilization for Enhanced Oil Recovery. Available *at: - https://www.netl.doe.gov/research/energy-analysis/search-publications/vuedetails?id=632*. (Accessed on 08.08.2018).

NETL, 2017. What are the different storage types for geologic CO_2 storage? Available at: - *https://www.netl.doe.gov/research/coal/carbon-storage/carbon-storage-faqs/what-are-the-different-storage-types-for-geologic-co2-storage*. (Accessed on 31.07.2018)., US Department of Energy.

Nimtz, M., Klatt, M., Wiese, B., Kühn, M., Joachim Krautz, H., 2010. Modelling of the CO_2 process and transport chain in CCS systems - Examination of transport and storage processes. *Chemie der Erde*, 70, 185–192.

NIST, 2007. Thermophysical Properties of Hydrocarbon Mixtures Database (SUPERTRAPP), Version 3.2 ed. National Institute of Standards and Technology.

Norwegian Ministry of Petroleum and Energy, 2016. Feasibility study for full-scale CCS in Norway.

NRG Energy, 2018. Petra Nova. Available at: - *https://www.nrg.com/case-studies/petra-nova.html*. (Accessed on 25.07.2018).

Nygaard, R., Salehi, S., Weideman, B., Calpetra, R.L., 2014. Effect of Dynamic Loading on Wellbore Leakage for the Wabamun Area CO_2 Sequestration Project. In *Canadian Unconventional Resrouces Conference, 15-17 November, Calgary, Canada, SPE J., 69–82.*

O'Dwyer, C., Flynn, D., 2015. Using Energy Storage to Manage High Net Load Variability at Sub-Hourly Time-Scales. *IEEE Trans. Power Syst.*, 30, 2139–2148.

Oates, D.L., Versteeg, P., Hittinger, E., Jaramillo, P., 2014. Profitability of CCS with flue gas bypass and solvent storage. *Int. J. Greenh. Gas Control*, 27, 279–288.

Oexmann, J., 2011. *Post Combustion CO_2 Capture: Energetic Evaluation of Chemical Absorption Processes in Coal Fired Steam Power Plants*. Dr. Philos. Diss. Tech. Univ. Hamburg-Harburg, Hambg.

Ofgem, 2013. Electricity Capacity Assessment Report 2013.

Ofgem, 2014. National Electricity Transmission System Security and Quality of Supply Standard: Normal Infeed Loss Risk (GSR015).

Oh, S.Y., Kim, J.K., 2018. Operational optimization for part-load performance of amine-based post-combustion CO_2 capture processes. *Energy*, 146, 57–66.

Oldenburg, C.M., 2003. Carbon Dioxide as Cushion Gas for Natural Gas Storage. *Energy & Fuels*, 17, 240–246.

Onyebuchi, V.E., Kolios, A., Hanak, D.P., Biliyok, C., Manovic, V., 2018. A systematic review of key challenges of CO_2 transport via pipelines. *Renew. Sustain. Energy Rev.*, 81, 2563–2583.

Oxburgh, 2016. LOWEST COST DECARBONISATION FOR THE UK: THE CRITICAL ROLE OF CCS. Report to the Secretary of State for Business, Energy and Industrial Strategy from the Parliamentary Advisory Group on Carbon Capture and Storage (CCS).

Pale Blue Dot Energy, 2016. Progressing development of the UK's Strategic Carbon Dioxide Storage Resource: A Summary of Results from the Strategic UK CO_2 Storage Appraisal Project.

Palisade, 2018. Software Product Manuals and Documentation. Available at: - *https://www.palisade.com/support/manuals.asp*. (Accessed on 10.11.2018).

Palisade Corporation, 2015. NeuralTools - Neural Network Add-In for Microsoft Excel. Available at : - *https://www.palisade.com/support/manuals.asp*. (Accessed on 15.11.2018).

Palmintier, B., 2013. *Incorporating operational flexibility into electric generation planning*. Dr. Philos. Diss. Massachusetts Inst. Technol. Camebridge, USA.

Paris, K.A., 2015. *Transient simulation of gas networks for integration studies with the power grid*. Semester Proj. ETH Zuerich, Switz.

Parker, N., 2004. Using Natural Gas Transmission Pipeline Costs to Estimate Hydrogen Pipeline Costs. Institute of Transportation Studies, University of California, USA.

Patiño-Echeverri, D., Hoppock, D.C., 2012. Reducing the energy penalty costs of postcombustion CCS systems with amine-storage. *Environ. Sci. Technol.*, 46, 1243–1252.

Pedersen, K.S., Fredenslund, A., Christensen, P.L., Thomassen, P., 1984. Viscosity of crude oils. *Chem. Eng. Sci.*, 39, 1011–1016.

Pfenninger, S., Staffell, I., 2016. Long-term patterns of European PV output using 30 years of validated hourly reanalysis and satellite data. *Energy*, 114, 1251–1265.

Piessens, K., Laenen, B., Nijs, W., Matthieu, P., Baele, J.-M., Hendriks, C., Bertrand, E., Bierkens, J., Brandsma, R., Broothaers, M., De Visser, E., Dreesen, R., Hildenbrand, S., Lagrou, D., Vandeginste, V., Welke, 2008. Policy Support System for Carbon Capture and Storage, Science for a Sustainable Development.

Porter, R.T.J., Fairweather, M., Pourkashanian, M., Woolley, R.M., 2015. The range and level of impurities in CO_2 streams from different carbon capture sources. *Int. J. Greenh. Gas Control*, 36, 161–174.

Porter, R.T.J., Mahgerefteh, H., Brown, S., Martynov, S., Collard, A., Woolley, R.M., Fairweather, M., Falle, S. a. E.G., Wareing, C.J., Nikolaidis, I.K., Boulougouris, G.C., Peristeras, L.D., Tsangaris, D.M., Economou, I.G., Salvador, C., Zanganeh, K., Wigston, A., Najafali, J.N., Shafeen, A., Beigzadeh, A., Farret, R., Gombert, P., Hebrard, J., Proust, C., Ceroni, A., Flauw, Y., Zhang, Y., Chen, S., Yu, J., Talemi, R.H., Bensabat, J., Wolf, J.L., Rebscher, D., Niemi, A., Jung, B., Dowell, N. Mac, Shah, N., Kolster, C., Mechleri, E., Krevor, S., 2016. Techno-economic assessment of CO_2 quality effect on its storage and transport: CO_2 QUEST - An overview of aims, objectives and main findingsRichard. *Int. J. Greenh. Gas Control*, 54, 662–681.

Poyry, 2017. A Business Case for a UK Industrial CCS Support Mechanism. Available at: - *http://www.teessidecollective.co.uk/teesside-collective-report-a-business-case-for-a-uk-industrial-ccs-support-mechanism/.* (Accessed on 11.11.2018).

PSE, 2014. gCCS - a commercial system modelling environment for whole-chain CCS applications. Available at: - *https://www.eti.co.uk/library/gccs-a-commercial-system-modelling-environment-for-whole-chain-ccs-applications/*. (Accessed on: 25.11.2018).

PSE, 2018. gCCS whole-chain system modelling. Available at: - *https://www.psenterprise.com/products/gccs/wholechain*. (Accessed on 25.11.2018).

PSE, 2019. gSAFT advanced thermodynamics. Available at: - *https://www.psenterprise.com/products/gsaft*. (Accessed on 10.01.2019).

Pudjianto, D., Aunedi, M., Djapic, P., Strbac, G., 2014. Whole-systems assessment of the value of energy storage in low-carbon electricity systems. *IEEE Trans. Smart Grid*, 5, 1098–1109.

Pye, S., Anandarajah, G., Fais, B., McGlade, C., Strachan, N., 2015. Pathways to Deep Decarbonisation. SDSN & IDDRI, 2015.

Race, J., Wetenhall, B., Seevam, P.N., Downie, M.J., 2012. Towards a CO_2 Pipeline Specification: Defining Tolerance Limits for Impurities. In *3rd International Forum on Transportation of CO_2 by Pipeline, 20-21 June, Newcastle-upon-Tyre, UK.*

Race, J.M., Seevam, P.N., Downie, M.J., 2007. Challenges for Offshore Transport of Anthropogenic Carbon Dioxide. In *26th International Conference on Offshore Mechanics and Arctic Engineering, San Diego, California, USA.*

Ramamurthi, K., Sunil Kumar, S., 2003. Prediction of inception of thermal oscillations and their waveforms in flow of heated subcritical liquids. *Heat Mass Transf. und Stoffuebertragung*, 39, 359–366.

Rao, A.B., Rubin, E.S., 2006. Identifying cost-effective CO 2 control levels for amine-based CO 2 capture systems. *Ind. Eng. Chem. Res.*, 45, 2421–2429.

Rao, K.R., 2006. Companion Guide to the ASME Boiler & Pressure Vessel Code, Volume 2, Second Edition: Criteria and Commentary on Select Aspects of the Boiler & Pressure Vessel and Piping Codes, 2nd Revise. ed. American Society of Mechanical Engineers.

RenewableUK, 2017. RenewableUK Wind Energy Statistics. Available at: - *https://www.renewableuk.com/page/UKWEDhome*. (Accessed on 18.06.2017).

Rezazadeh, F., Gale, W.F., Hughes, K.J., Pourkashanian, M., 2015. Performance viability of a natural gas fired combined cycle power plant integrated with post-combustion CO_2 capture at part-load and temporary non-capture operations. *Int. J. Greenh. Gas Control*, 39, 397–406.

Ripmeester, J.A., Alavi, S., 2016. Some current challenges in clathrate hydrate science: nucleation, decomposition and the memory effect. *Curr. Opin. Solid State Mater. Sci.*, 344–351.

Robinson, M., 2003. Intelligent Well Completions. Available at: - *https://www.onepetro.org/search?q=technology+today+series+mike+robinson+intelligent+well+completions&peer_reviewed=&published_between=&from_year=&to_year=&rows=10.* (Accessed on 26.05.2016).

Roeder, V., Kather, A., 2014. Part Load Behaviour of Power Plants with a Retrofitted Post-combustion CO_2 Capture Process. *Energy Procedia*, 51, 207–216.

Romano, M.C., Anantharaman, R., Arasto, A., Ozcan, D.C., Ahn, H., Dijkstra, J.W., Carbo, M., Boavida, D., 2013. Application of advanced technologies for CO_2 capture from industrial sources. *Energy Procedia*, 37, 7176–7185.

Rosenblatt, F., 1958. The Perceptron: A Probabilistic Model for Information Storage and Organization in The Brain. *Psychol. Rev.*, 65, 65–386.

Roussanaly, S., Brunsvold, A.L., Hognes, E.S., 2014. Benchmarking of CO_2 transport technologies: Part II - Offshore pipeline and shipping to an offshore site. *Int. J. Greenh. Gas Control*, 28, 283–299.

Roy, P., Walsh, S.D.C., Morris, J.P., Iyer, J., Hao, Y., Carroll, S., Gawel, K., Todorovic, J., Torsæter, M., 2016. Studying the impact of thermal cycling on wellbore integrity during CO_2 injection. In *50th US Rock Mech. / Geomech. Symp. 2016*, 4, 3411–3422.

Ruden, T. a., Xu, Z.G., Selberg, M.H., Haugset, T., Langsholt, M., Liu, L., Amundsen, J., 2013. Simulating flow of CO_2 with impurities in OLGA; Dealing with narrow phase-envelopes and the critical point. *Energy Procedia*, 51, 344–352.

Sanchez Fernandez, E., Naylor, M., Lucquiaud, M., Wetenhall, B., Aghajani, H., Race, J., Chalmers, H., 2016. Impacts of geological store uncertainties on the design and operation of flexible CCS offshore pipeline infrastructure. *Int. J. Greenh. Gas Control*, 52, 139–154.

Sanchez Fernandez, E., Sanchez del Rio, M., Chalmers, H., Khakharia, P., Goetheer, E.L.V., Gibbins, J., Lucquiaud, M., 2016b. Operational flexibility options in power plants with integrated post-combustion capture. *Int. J. Greenh. Gas Control*, 48, 275–289.

Sankar, R., Knabe, S., 2010. Downhole Commingling Research. Available at: - *https://www.google.com/url?sa=t&rct=j&q=&esrc=s&source=web&cd=2&cad=rja&uact=8&ved=2ahUKEwih-fz_pKndAhWRHsAKHW6PCpgQFjABegQICRAC&url=https%3A%2F%2Fwww.bsee.gov%2Fsites%2Fbsee.gov%2Ffiles%2Ftap-technical-asses.* (Accessed on 02.03.2016).

SaskPower, 2018. Boundary Dam Power Station. Available at: - *https://www.saskpower.com/our-power-future/our-electricity/electrical-system/system-map/boundary-dam-power-station.* (Accessed 25.07.2018).

Schlumberger, 2018. OLGA single component. Available at: - *https://www.software.slb.com/products/olga/olga-pipeline-management/single-component.* (Accessed on 13.09.2018).

Schmidt, O., Hawkes, a., Gambhir, a., Staffell, I., 2017. The future cost of electrical energy storage based on experience rates. *Nat. Energy*, 6, 17110.

Scott, V., Gilfillan, S., Markusson, N., Chalmers, H., Haszeldine, R.S., 2013. Last chance for carbon capture and storage. *Nat. Clim. Chang.*, 3, 105–111.

Serpa, J., Morbee, J., Tzimas, E., 2011. Technical and economic characteristics of a CO_2 transmission pipeline infrastructure.

Sheble, G.B., Fahd, G.N., 1994. Unit commitment literature synopsis. *IEEE Trans. Power Syst.,* 9, 128–135.

Shell, 2015a. Peterhead CCS Project - Well Operation Guidelines.

Shell, 2015b. Peterhead CCS Project - Geomechanics Report.

Shell, 2015c. Knowledge share speed dating. In *European CCS Forum, 2nd September, Glasgow, UK.*

Shell, 2016. Peterhead CCS Project - Basis of Design for the CCS Chain. Available at: - *https://www.gov.uk/government/publications/carbon-capture-and-storage-knowledge-sharing-technical-full-chain*. (Accessed on 15.06.2017).

Silva, V.L., 2010. *Value of flexibility in systems with large wind penetration*. Dr. Philos. Diss. Imperial College London.

Simopoulos, D.N., Kavatza, S.D., Vournas, C.D., 2006. Reliability Constrained Unit Commitment Using Simulated Annealing. *IEEE Trans. Power Syst.*, 21, 1699–1706.

Skagestad, R., Eldrup, N., Richard, H., Belfroid, S., Mathisen, A., Lach, A., Haugen, H.A., Skagestad, R., Eldrup, N., Ri-, H., Belfroid, S., Mathi-, A., 2014. Ship transport of CO_2 - Status and Technology Gaps. Available at: - *https://www.google.com/url?sa=t&rct=j&q=&esrc=s&source=web&cd=4&cad=rja&uact=8&ved=2ahUKEwiB3PTtpd3cAhWExYUKHaDwAAMQFjADegQIBxAC&url=https%3A%2F%2Fwww.gassnova.no%2Fno%2FDocuments%2FShip*. (Accessed on 22.09.2018).

Sminchak, J., Zeller, E., Bhattacharya, I., 2014. Analysis of unusual scale build-up in a CO_2 injection well for a pilot scale CO_2 storage demonstration project. *Greenh. Gases Sci. Technol.,* 4, 357–366.

Spitz, T., 2016. Summary of Learnings. Secondment to FEED study team of White Rose CCS Demonstration project at National Grid Carbon Ltd.

Spitz, T., Avagyan, V., Ascui, F., Bruce, a. R.W., Chalmers, H., Lucquiaud, M., 2018. On the variability of CO_2 feed flows into CCS transportation and storage networks. *Int. J. Greenh. Gas Control*, 74, 296–311.

Spitz, T., Chalmers, H., Ascui, F., Lucquiaud, L., 2017. Operating Flexibility of CO_2 Injection Wells in Future Low Carbon Energy System. *Energy Procedia*, 114, 4797–4810.

Spitz, T., Gonzáles, A., Chalmers, H., Lucquiaud, M., 2019. Operating Flexibility of Natural Gas Combined Cycle Power plant integrated with Post-Combustion Capture. *Int. J. Greenh. Gas Control*, In Press.

Staffell, I., Green, R., 2016. Is There Still Merit in the Merit Order Stack? The Impact of Dynamic Constraints on Optimal Plant Mix. IEEE Trans. *Power Syst.*, 31, 43–53.

Stanojevic, V., 2011. Unit commitment by dynamic programming method. *https://uk.mathworks.com/matlabcentral/fileexchange/32073-unit-commitmentby-dynamic-programming-method.* (Accessed 18 June 2017).

Strbac, G., Aunedi, M., Pudjianto, D., Djapic, P., Teng, F., Sturt, A., Jackravut, D., Sansom, R., Yufit, V., Brandon, N., 2012. Strategic Assessment of the Role and Value of Energy Storage Systems in the UK Low Carbon Energy Future Report for Carbon Trust.

Strbac, G., Aunedi, M., Pudjianto, D., Teng, F., Djapic, P., Druce, R., Carmel, A., Borkowski, K., 2015. Value of Flexibility in a Decarbonised Grid and System Externalities of Low-Carbon Generation Technologies. Imp. Coll. London, NERA Econ. Consult.

Strbac, G., Pudjianto, D., Sansom, R., Djapic, P., Ameli, H., Shah, N., Hawkes, A., 2018. Analysis of Alternative UK Heat Decarbonisation Pathways For the Committee on Climate Change.

Summit Power, 2017. Clean Air, Clean Industry,Clean Growth: How Carbon Capture Will Boost the UK Economy.

Teng, F., Strbac, G., 2016. Assessment of the Role and Value of Frequency Response Support from Wind Plants. IEEE Trans. Sustain. *Energy*, 7, 586–595.

Tielens, P., Van Hertem, D., 2016. The relevance of inertia in power systems. Renew. Sustain. *Energy Rev.*, 55, 999–1009.

Tolvanen, H.J., 2007. Life cycle energy cost savings and pump selection. *World Pumps*, 34–37.

Torsæter, M., Todorovic, J., Lavrov, A., Gawel, K., Lund, H., Roy, P., Carroll, S., 2017. Avoiding Damage of CO_2 Injection Wells Caused by Temperature Variations. *Energy Procedia*, 114, 5275–5286.

TradingEconomics, 2019. European Union Inflation Rate. Available at: - *https://tradingeconomics.com/european-union/inflation-rate.* (Accessed on 02.05.20199).

Tran, T.H., French, S., Ashman, R., Kent, E., 2018. Linepack planning models for gas transmission network under uncertainty. *Eur. J. Oper. Res.*, 268, 688–702.

Trillionthtonne, 2018. TrillionthTonne. Available at: - *http://trillionthtonne.org/.* (Accessed 24.07.2018).

Ueckerdt, F., Hirth, L., Luderer, G., Edenhofer, O., 2013. System LCOE: What are the costs of variable renewables? *Energy*, 63, 61–75.

Uilhoorn, F.E., 2013. Evaluating the risk of hydrate formation in CO_2 pipelines under transient operation. *Int. J. Greenh. Gas Control,* 14, 177–182.

UK BEIS, 2016. Electricity Generation Costs.

UK BEIS, 2017a. Updated energy and emissions projections 2016.

UK BEIS, 2017b. Industrial Decarbonisation and Energy Efficiency Roadmap Action Plan - Cement Sector.

UK BEIS, 2018a. THE FUTURE FOR SMALL-SCALE LOW-CARBON GENERATION.

UK BEIS, 2018b. Solar photovoltaics deployment. Available at: - *https://www.gov.uk/government/statistics/solar-photovoltaics-deployment.* (Accessed on 11.09.2018).

UK BEIS, 2018c. The Clean Growth Strategy: Leading the way to a low carbon future.

UK CCUS Cost Challenge Taskforce, 2018. Delivering Clean Growth. Available at: - *https://www.gov.uk/government/publications/delivering-clean-growth-ccus-cost-challenge-taskforce-report*. (Accessed on 30.07.2018).

UK DECC, 2012. The Future of Heating: A strategic framework for low carbon heat in the UK.

UK DECC, 2016. Updated energy and emissions projections 2015.

UK MET Office, 2014. Marine & coastal projections images Figure 6.5: modelled near sea bed temperature. Available at: - *http://ukclimateprojections.metoffice.gov.uk/24034.* (Accessed on 13.09.2018).

UKERC, 2006. The Costs and Impacts of Intermittency: An assessment of the evidence on the costs and impacts of intermittent generation on the British electricity network.

UKERC, 2016. The costs and impacts of intermittency – 2016 update electricity generation technologies.

UNFCC, 2018. Paris Agreement - Status of Ratification. Available at: - *https://unfccc.int/process/the-paris-agreement/status-of-ratification.* (Accessed on 23.07.2018).

Van De Haar, A.M., 2013. *Analysis of the dynamic performance of a MEA-based carbon capture unit for coal-fired power plants*. Master Sci. Diss. Delft Univ. Technol. Delft.

Van den Broek, M., Ramirez, A., Groenenberg, H., Neele, F., Viebahn, P., Turkenburg, W., Faaij, A., 2010. Feasibility of storing CO_2 in the Utsira formation as part of a long term

Dutch CCS strategy - An evaluation based on a GIS/MARKAL toolbox. *Int. J. Greenh. Gas Control*, 4, 351–366.

Van der Harst, L., 2017. *Operational Flexibility of Dense Phase CO_2 Pipeline Transportation Systems using Interim Storage*. MSc Diss. Univ. Edinburgh, Edinburgh.

Van der Wijk, P.C., Brouwer, A.S., Van den Broek, M., Slot, T., Stienstra, G., Van der Veen, W., Faaij, A.P.C., 2014. Benefits of coal-fired power generation with flexible CCS in a future northwest European power system with large scale wind power. *Int. J. Greenh. Gas Control*, 28, 216–233.

Van Peteghem, T., Delarue, E., 2014. Opportunities for applying solvent storage to power plants with post-combustion carbon capture. *Int. J. Greenh. Gas Control*, 21, 203–213.

Vandeginste, V., Piessens, K., 2008. Pipeline design for a least-cost router application for CO_2 transport in the CO_2 sequestration cycle. *Int. J. Greenh. Gas Control*, 2, 571–581.

Vermeulen, T.N., 2011. Knowledge Sharing Report-CO_2 Liquid Logistics Shipping Concept (LLSC): Overall Supply Chain Optimization. Global CCS Institute.

Versteeg, P., Oates, D.L., Hittinger, E., Rubin, E.S., 2013. Cycling coal and natural gas-fired power plants with CCS. *Energy Procedia*, 37, 2676–2683.

Viana, A., Pedroso, J.P., 2013. A new MILP-based approach for unit commitment in power production planning. Int. J. Electr. *Power Energy Syst*., 44, 997–1005.

Vilarrasa, V., Laloui, L., 2016. Impacts of thermally induced stresses on fracture stability during geological storage of CO_2. *Energy Procedia*, 86, 411–419.

Villamor, L.V., 2017. *Combined impact of wind and solar on conventional generators in the UK electricity system*. MSc Diss. Univ. Edinburgh, Edinburgh.

Vouk, D., Malus, D., Halkijevic, I., 2011. Neural networks in economic analyses of wastewater systems. *Expert Syst. Appl.*, 38, 10031–10035.

Wang, S.J., Shahidehpour, S.M., Mokhtari, S., Irisarri, G.D., Kirschen, D.S., 1995. Short-term generation scheduling with transmission and environmental constraints using an augmented lagrangian relaxation. *IEEE Trans. Power Syst.,* 10, 1294–1301.

Wang, Y., Zhao, L., Otto, A., Robinius, M., Stolten, D., 2017. A Review of Post-combustion CO_2 Capture Technologies from Coal-fired Power Plants. *Energy Procedia*, 114, 650–665.

Wetenhall, B., Aghajani, H., Chalmers, H., Benson, S.D., Ferrari, M.C., Li, J., Race, J.M., Singh, P., Davison, J., 2014a. Impact of CO_2 impurity on CO_2 compression, liquefaction and transportation. *Energy Procedia*, 63, 2764–2778.

Wetenhall, B., Race, J., Downie, M., 2014b. The Effect of CO_2 Purity on the Development of Pipeline Networks for Carbon Capture and Storage Schemes. *Int. J. Greenh. Gas Control*, 30, 197–211.

Wetenhall, B., Race, J.M., Downie, M.J., 2014c. The Effect of CO_2 Purity on the Development of Pipeline Networks for Carbon Capture and Storage Schemes. *Int. J. Greenh. Gas Control*, 30, 197–211.

Wetenhall, B., Race, J., Aghajani, H., Fernandez, E.S., Naylor, M., Lucquiaud, M., Chalmers, H., 2017a. Considerations in the Development of Flexible CCS Networks. *Energy Procedia*, 114, 6800–6812.

Wetenhall, B., Race, J.M., Aghajani, H., Barnett, J., 2017b. The main factors affecting heat transfer along dense phase CO_2 pipelines. *Int. J. Greenh. Gas Control*, 63, 86–94.

Wiese, B., Nimtz, M., Klatt, M., Kühn, M., 2010. Sensitivities of injection rates for single well CO_2 injection into saline aquifers. *Chemie der Erde*, 70, 165–172.

Witkowski, A., Majkut, M., Rulik, S., 2014. Analysis of pipeline transportation systems for carbon dioxide sequestration. *Arch. Thermodyn.,* 35, 117–140.

Wood, A.J., Wollenberg, B.F., Sheblé, G.B., 2013. *Power generation, operation and control,* 3rd ed., John Wiley &Sons: Hoboken, New Jersey, USA.

World Resources Institute, 2018. The Carbon Budget. Available at: - *http://www.wri.org/ipcc-infographics.* (Accessed 24.07.2018).

Worldsteel Association, 2017. Steel and CO_2 – a global perspective. In *IEA Workshop, 20th November, Paris, France.*

Xia, X., Elaiw, a. M., 2010. Optimal dynamic economic dispatch of generation: A review. *Electr. Power Syst. Res.*, 80, 975–986.

Yen, S.K., Huang, I.B., 2003. Critical hydrogen concentration for hydrogen-induced blistering on AISI 430 stainless steel. Mater. *Chem. Phys.*, 80, 662–666.

ZEP, 2011. The Costs of CO_2 Capture, Transport and Storage. Available at: - *https://www.globalccsinstitute.com/publications/costs-co2-capture-transport-and-storage.* (Accessed on 30.07.2018).

ZEP, 2017. Future CCS Technologies.

ZeroCO2, 2018. Century Plant. Available at: - *http://www.zeroco2.no/projects/century-plant*. (Accessed on 25.07.208).

Zhang, J., Morris, a. J., 1998. A sequential learning approach for single hidden layer neural networks. Neural Networks 11, 65–80.

Zhang, Z.X., Wang, G.X., Massarotto, P., Rudolph, V., 2006. Optimization of pipeline transport for CO_2 sequestration. Energy Convers. Manag. 47, 702–715.

Zhao, Y., Zhao, H., 2017. Evaluating Toll Revenue Uncertainty Using Neural Network Models. Transp. Res. Procedia 25, 2949–2956.

Zhu, J., 2009. Opimization of Power System Operation.

Appendix A1

Power Generation Portfolios

Figure A.1: Power Generation types and capacities installed in all core UCED scenarios

15GW Wind & Low Emission Intensity (60g/kWh)	
Power Generation Type	Capacity
Nuclear	17.1GW
CCS	20.2GW
CCGT	12.0GW
OCGT	19.8GW
15GW Wind & Medium Emission Intensity (100g/kWh)	
Power Generation Type	Capacity
Nuclear	17.1GW
CCS	12.3GW
CCGT	21.0GW
OCGT	18.6GW
15GW Wind & High Emission Intensity (140g/kWh)	
Power Generation Type	Capacity
Nuclear	17.1GW
CCS	7.0GW
CCGT	26.0GW
OCGT	18.6GW
30GW Wind & Low Emission Intensity (60g/kWh)	
Power Generation Type	Capacity
Nuclear	17.1GW
CCS	14.0GW
CCGT	14.0GW
OCGT	19.8GW
30GW Wind & Medium Emission Intensity (100g/kWh)	
Power Generation Type	Capacity
Nuclear	17.1GW
CCS	7.0GW
CCGT	22.0GW
OCGT	19.2GW
30GW Wind & High Emission Intensity (140g/kWh)	
Power Generation Type	Capacity
Nuclear	17.1GW
CCS	0.9GW
CCGT	29.0GW
OCGT	18.6GW

UCED Scenario: 45GW Wind & Low Emission Intensity (60g/kWh)	
Power Generation Type	Capacity
Nuclear	17.1GW
CCS	8.8GW
CCGT	16.0GW
OCGT	19.8GW
UCED Scenario: 45GW Wind & Medium Emission Intensity (100g/kWh)	
Power Generation Type	Capacity
Nuclear	17.1GW
CCS	0.9GW
CCGT	25.0GW
OCGT	18.6GW
UCED Scenario: 45GW Wind & High Emission Intensity (140g/kWh)	
Power Generation Type	Capacity
Nuclear	17.1GW
CCS	0.0GW
CCGT	25.0GW
OCGT	19.2GW

Appendix A2

Thermal full load efficiencies

Due to the uncertainty regarding thermal efficiencies (LHV) of thermal generators in future decades, a sensitivity case was run to explore the influence of efficiencies on the CO_2 emission intensity of the power generation fleet (including wind power). The results for the base case UCED scenario show that the emission intensity is approximately inversely proportional to full load efficiencies of thermal power generators (Figure A.2). A reduction of all thermal full load efficiencies (LHV) of 1% leads to an increase in the annual average CO_2 emission intensity of around 1.7g/kWh compared to the base case. Similarly, the maximum and minimum CO_2 flow captured in the sensitivity case is inversely proportional to the LHV thermal efficiency. Whilst a maximum and minimum flow of 21.9MPTA and 3.6MPTA is captured at reduced thermal efficiency (-3%LHV efficiency compared to base case), these flows drop by 8-9% to 19.9MPTA and 3.3MTPA at the highest considered thermal efficiencies (+3% LHV efficiency compared to base case), respectively.

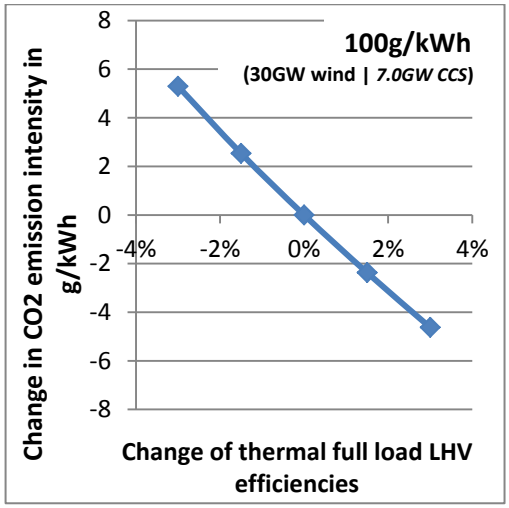

Figure A.2: Change in CO_2 emission intensity in base case ('medium' wind speeds, 30GW wind, 100g/kWh) with increased (+1.5%, +3.0%) and decreased (-1.5%, - 3.0%) full load LHV efficiencies of thermal generating plants.

Appendix A3

Spinning reserve requirement

A further important parameter is the amount of spinning reserve that is scheduled, hence a sensitivity study was performed based on the base case UCED scenario (30GW wind capacity, 100g/kWh emission intensity, 7GW CCS capacity) – see Figure A.3-Figure A.4. The results show that increasing the amount of scheduled spinning reserve by 0.25σ in order to secure the network against larger unanticipated changes of net demand, thus increasing security of supply, increases the CO_2 emission intensity of the power generation fleet by around 1.5g/kWh. The effect of a varied spinning reserve requirement on the FDCs can be seen in Figure A.4. Increasing spinning reserve requirement has the effect of reducing the time CCS plants can operate at full load, as more plants need to part-load in order to provide the required amount of reserve. The amount of the time the plants operate at part-load in turn increases. Conversely, the effect of reducing the amount of spinning reserve increases the amount of time CCS power plants can operate at full load, as the requirement for operating at lower loads for providing back-up reserve power is not as prominent.

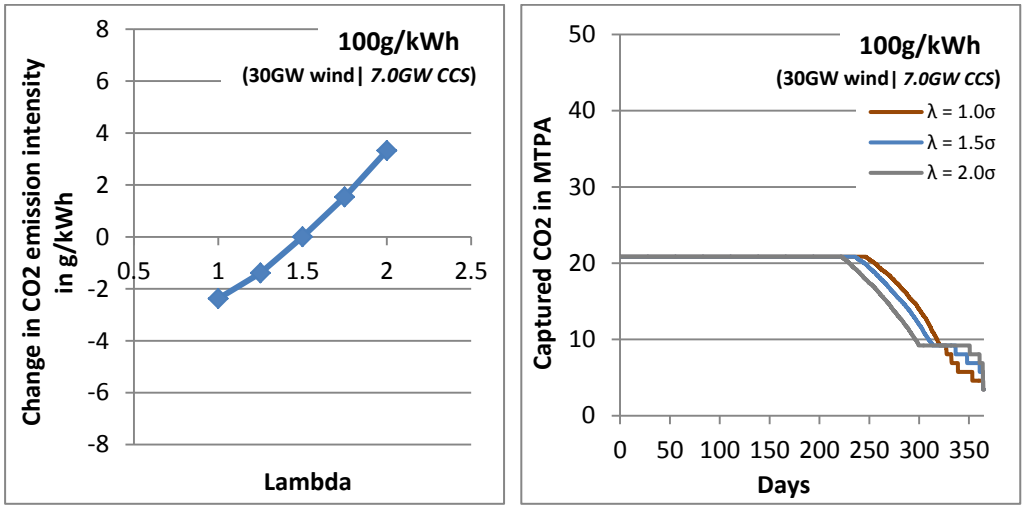

Figure A.3 (left): Change in CO_2 emission intensity in base case with increased (+0.25σ, +0.5σ) and decreased (-0.25σ, -0.5σ) spinning reserve requirements.

Figure A.4 (right): CO_2 capture duration profile for 30GW wind capacity in 100g/kWh emission intensity scenario for 'medium' wind speeds for different spinning reserve requirements: (i) λ = 1.0σ (brown) (ii) λ = 1.5σ (blue) and (iii) λ= 2.0σ (grey).

The analysis shows that the required amount of spinning reserve is an important parameter that can modify the dispatch behaviour of power plants, and significantly affect emission levels. A more detailed analysis is therefore recommended to explore the optimal amount and ways of providing spinning reserve for reducing both system costs and emissions.

In contrast to operating profiles, the amount of spinning reserve does not directly affect the minimum and maximum flow produced by the power stations in the sensitivity cases. This is, however, an effect of minimum flow being a 'stepwise' function of the number of CCS

power plants that are required to run at minimum load at the lowest annual net demand levels to satisfy reserve requirements. For the case considered here, the reduction/increase in reserve requirement across the sensitivity cases does not lead to an overstepping of a 'threshold', which would justify dispatching either more or less CCS plants at minimum net demand periods for satisfying reserve requirements at lowest cost.

Appendix B1

Validation of gCCS for line-packing purpose – Supplementary data

Table B.1-Table B.2 provide the fundamental modelling parameters and pipeline design specifications for benchmarking linepacking times obtained with the process simulation tool gCCS against the values presented in Aghajani et al. (2017) and calculated with competitor software OLGA.

Table B.1: Key parameters and initial conditions for the set of pipeline scenarios for which linepacking times have been determined by on Aghajani et al. (2017) and Van der Harst (2017) using the process flow simulation tools OLGA and gCCS, respectively.

Parameter	Value	Unit
Horizontal Distance	50, 100, 150	km
Roughness	0.0457	mm
Ambient Temperature	5	°C
Burial Depth	1.1	m
Inlet pressure	110	bar
Inlet Temperature	30	°C
Inlet Composition	Pure CO2	
Flowrate	Table B.2	kg/s
Outer Diameter	Table B.2	mm
Wall Thickness	Table B.2	mm
MAOP	Table B.2	bar
Surrounding Environment	OLGA: Sandy Soil gCCS: Water/Sandy Soil	
Heat Transfer Coefficients		
- Steel	OLGA: 60.55 | gCCS: Default	$W/m^2/K$
- Soil/Water	OLGA: 2.595 | gCCS: Default	$W/m^2/K$
Initial Conditions	Steady State	

Table B.2: Pipeline types for which linepacking times have been obtained by Aghajani et al. (2017) and Van der Harst (2017) using the process flow simulation tools OLGA and gCCS, respectively.

Pipeline No.	OD	wt	Length	Flow	MAOP	Pipeline No.	OD	wt	Length	Flow	MAOP
1	457	8	50	150	113.4	40	610	11	50	150	116.9
2	457	8	100	150	113.4	41	610	11	100	150	116.9
3	457	8	150	150	113.4	42	610	11	150	150	116.9
4	457	8.8	50	150	124.8	43	610	12.5	50	150	132.8
5	457	8.8	100	150	124.8	44	610	12.5	100	150	132.8
6	457	8.8	150	150	124.8	45	610	12.5	150	150	132.8
7	457	10	50	150	141.8	46	610	14.2	50	150	150.8
8	457	10	100	150	141.8	47	610	14.2	100	150	150.8
9	457	10	150	150	141.8	48	610	14.2	150	150	150.8
10	457	11	50	150	156.0	49	610	14.2	50	110	150.8
11	457	11	100	150	156.0	50	610	14.2	100	110	150.8
12	457	11	150	150	156.0	51	610	14.2	150	110	150.8
13	457	11	50	110	156.0	52	610	14.2	50	70	150.8
14	457	11	100	110	156.0	53	610	14.2	100	70	150.8
15	457	11	150	110	156.0	54	610	14.2	150	70	150.8

16	457	11	50	70	156.0	55	610	14.2	50	35	150.8
17	457	11	100	70	156.0	56	610	14.2	100	35	150.8
18	457	11	150	70	156.0	57	610	14.2	150	35	150.8
19	457	11	50	35	156.0	58	914	16	50	150	113.4
20	457	11	100	35	156.0	59	914	16	100	150	113.4
21	457	11	150	35	156.0	60	914	16	150	150	113.4
22	508	8.8	50	150	112.3	61	914	17.5	50	150	124.1
23	508	8.8	100	150	112.3	62	914	17.5	100	150	124.1
24	508	8.8	150	150	112.3	63	914	17.5	150	150	124.1
25	508	10	50	150	127.6	64	914	20	50	150	141.8
26	508	10	100	150	127.6	65	914	20	100	150	141.8
27	508	10	150	150	127.6	66	914	20	150	150	141.8
28	508	11	50	150	140.3	67	914	20	50	110	141.8
29	508	11	100	150	140.3	68	914	20	100	110	141.8
30	508	11	150	150	140.3	69	914	20	150	110	141.8
31	559	10	50	150	115.9	70	914	20	50	70	141.8
32	559	10	100	150	115.9	71	914	20	100	70	141.8
33	559	10	150	150	115.9	72	914	20	150	70	141.8
34	559	11	50	150	127.5	73	914	20	50	35	141.8
35	559	11	100	150	127.5	74	914	20	100	35	141.8
36	559	11	150	150	127.5	75	914	20	150	35	141.8
37	559	12.5	50	150	144.9						
38	559	12.5	100	150	144.9						
39	559	12.5	150	150	144.9						

Appendix B2

Pipeline simulation schedule for modelling the depacking process

Following up the discussions about the pipeline simulation methodology in section 5.7, Figure 1.1 presents the simulation schedule implemented in gCCS for carrying out the depacking simulation of the reference pipeline of 100km length, 610mm outer diameter, an MAOP of '150'*bar, and 100% flow capacity utilisation. The inflows|outflows during the depacking process are at 0%|50% of nominal flow (i.e. maximum flow - 13MTPA or 412.23kg/s). A copy of the model and case file for this specific simulation has been uploaded to the research archive of the University of Edinburgh, to facilitate building on the model in future studies, as well as for easier replication of the results.

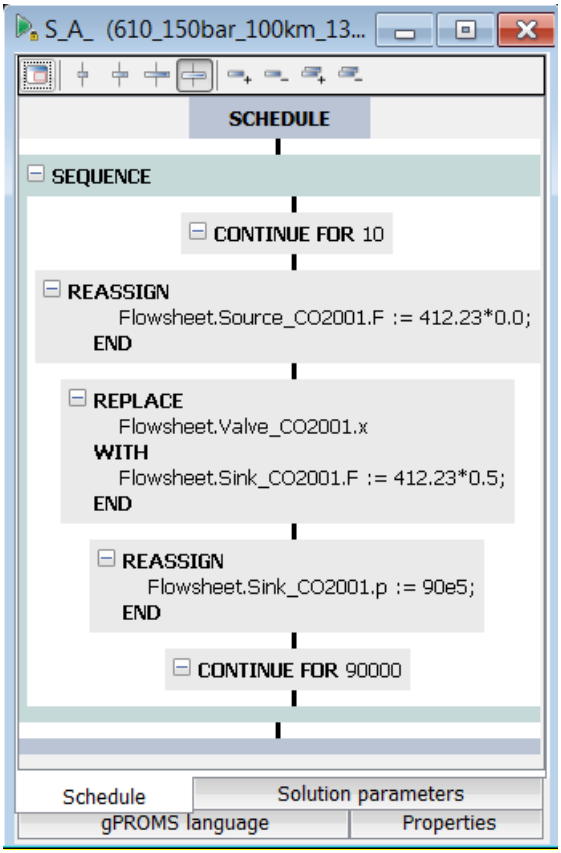

Figure B.1: Schedule of the pipeline simulation modellig the depacking process of the reference pipeline of 100km length, 610mm outer diameter, an MAOP of '150'*bar, and 100% flow capacity utilisation. Inflows|outflows during the depacking process are at 0%|50% of nominal (i.e. maximum) flow of 13MTPA or 412.23kg/s.

*The MAOPs presented in legend are only indicative - for actual MAOP see Table 5.4.

Appendix B3

Momentum equation dynamics on vs. off

In order to speed up simulation times the momentum equation is modelled as steady state across all core pipeline scenarios presented in section 5.8 (see also section 5.4 for asumption). To evaluate the accuracy of this simplification several scenarios were simulated for benchmarking purposes in a fully dynamic manner. The benchmark scenarios comprise pipelines of 508mm, 610mm, and 914mm outer diameter, a reference length of 100km, and a MAOP of around 150bar (dependent on available standard pipeline wall thickness MAOP just above 150bar), respectively. Similarly to the methodology outlined in section 5.4 the nominal flow rates for the respective pipeline diameters were taken as 8MTPA, 13MTPA, and 36.5MTPA. A depacking process was modelled with zero inflows into the pipe after valve shut-in, and 50% of nominal flow being sustained at the outlet of the pipeline until a minimum pressure of 90bar is reached. A valve shut in period of 5s is assumed (Aghajani et al. 2017). The maximum achievable pipe depacking time is reached once the pipeline outlet pressure falls to the minimum allowable pressure of 90bar. The pressure drops to 90bar at the outlet of the pipeline first. The outlet pressure is, hence, monitored.

Figure B.2 displays the outlet pressure of the reference pipelines (610mm OD, 100km, 13MTPA) over time after valve shut-in (at t=0s). The minimum allowable pressure is reached at the pipeline outlet at 3528s after valve closure when the pipeline is modelled in a fully dynamic mode (green curve), and after 3513s when modelling the momentum in steady state (blue curve). Similarly, determined depacking times of the other benchmark scenarios differ by only 1.1% when modelled fully dynamically, and when using a simplified momentum equation. For the purpose of this study it is, hence, concluded that it is reasonable to linearise the inertial term in the momentum equation by modelling it as steady state in order to drastically speed up simulation times (i.e. by a factor of roughly 70).

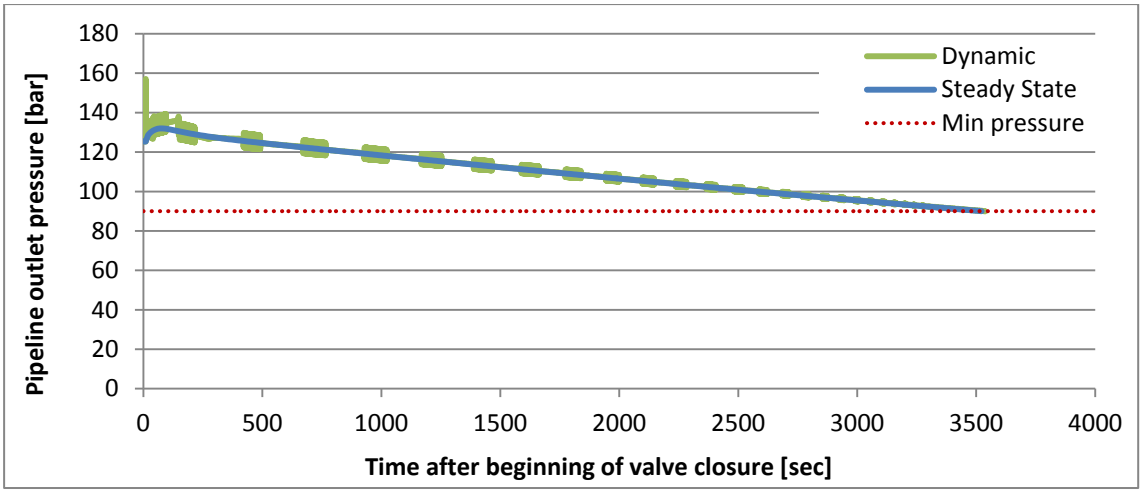

Figure B.2: Outlet pressure during line-depacking process with momentum equation in dynamics (green) and steady state (blue). Red line shows minimum permissible pipeline pressure.

It should be noted that the oscillations in the pipeline outlet pressure observed in the fully dynamic simulation of the reference pipe in Figure B.2 (green curve) are an effect of a not optimised control mechanism for the outflow control valve. The oscillations do not significantly impact the overall development of the pipeline outlet pressure during the depacking process.

Appendix B4

Numerical values for line-depacking times and working capacities as calculated in subsections 5.8.1-5.8.4

To facilitate adoption of the results for future studies the numerical values of the line-depacking times as calculated and presented in Chapter 5, subsections 5.8.1-5.8.3, are summarised in Table B.3-Table B.5. Similarly the numerical values of the working capacities as determined in section 5.8.4 are presented in Table B.6 - Table B.8.

Table B.3: Line-depacking times (in hours) for core pipeline scenarios as presented in subsection 5.8.1. Inflow|outflow scenario during depacking process is 0%|50% (top table), 10%|50% (middle table), and 20%|50% (bottom table) of nominal flow.

0%in| 50%out	**508mm 50km**	**508mm 100km**	**508mm 150km**	**610mm 50km**	**610mm 100km**	**610mm 150km**	**914mm 50km**	**914mm 100km**	**914mm 150km**
'150bar'*, 100% CU	0.70	1.34	1.80	0.50	0.98	1.29	0.35	0.81	1.14
'200bar'*, 100% CU	1.10	2.16	3.06	0.99	1.98	2.84	0.68	1.48	2.18
'150bar'*, 50% CU	1.61	3.26	4.82	1.24	2.53	3.75	1.00	2.17	3.28
'200bar'*, 50% CU	2.39	4.83	7.19	2.20	4.46	6.67	1.64	3.46	5.23
10%in| 50%out	**508mm 50km**	**508mm 100km**	**508mm 150km**	**610mm 50km**	**610mm 100km**	**610mm 150km**	**914mm 50km**	**914mm 100km**	**914mm 150km**
'150bar'*, 100% CU	0.89	1.69	2.26	0.66	1.24	1.62	0.49	1.05	1.46
'200bar'*, 100% CU	1.39	2.71	3.83	1.27	2.50	3.56	0.90	1.89	2.76
'150bar'*, 50% CU	2.03	4.09	6.04	1.57	3.19	4.71	1.30	2.76	4.14
'200bar'*, 50% CU	3.01	6.05	9.00	2.77	5.60	8.36	2.10	4.38	6.59
20%in| 50%out	**508mm 50km**	**508mm 100km**	**508mm 150km**	**610mm 50km**	**610mm 100km**	**610mm 150km**	**914mm 50km**	**914mm 100km**	**914mm 150km**
'150bar'*, 100% CU	1.22	2.27	3.01	0.91	1.68	2.17	0.72	1.46	1.99
'200bar'*, 100% CU	1.88	3.62	5.10	1.73	3.36	4.75	1.27	2.59	3.72
'150bar'*, 50% CU	2.74	5.47	8.06	2.13	4.28	6.30	1.80	3.74	5.58
'200bar'*, 50% CU	4.04	8.09	12.01	3.73	7.50	11.17	2.87	5.90	8.84

Table B.4: Line-depacking times (in hours) for core pipeline scenarios as presented in subsection 5.8.2. Inflow|outflow scenario during depacking process is 0%|30% (top table), 10%|30% (middle table), and 20%|30% (bottom table) of nominal flow.

0%in| 30%out	**508mm 50km**	**508mm 100km**	**508mm 150km**	**610mm 50km**	**610mm 100km**	**610mm 150km**	**914mm 50km**	**914mm 100km**	**914mm 150km**
'150bar'*, 100% CU	1.23	2.33	3.17	0.91	1.74	2.32	0.70	1.49	2.09
'200bar'*, 100% CU	1.89	3.70	5.27	1.73	3.42	4.91	1.25	2.62	3.83
'150bar'*, 50% CU	2.74	5.50	8.14	2.13	4.30	6.37	1.78	3.74	5.61
'200bar'*, 50% CU	4.04	8.12	12.09	3.73	7.53	11.25	2.85	5.90	8.88
10%in| 30%out	**508mm 50km**	**508mm 100km**	**508mm 150km**	**610mm 50km**	**610mm 100km**	**610mm 150km**	**914mm 50km**	**914mm 100km**	**914mm 150km**
'150bar'*, 100% CU	1.88	3.53	4.78	1.42	2.65	3.51	1.16	2.33	3.22
'200bar'*, 100% CU	2.88	5.58	7.92	2.65	5.18	7.40	1.99	4.03	5.83
'150bar'*, 50% CU	4.15	8.29	12.24	3.25	6.51	9.60	2.77	5.71	8.51
'200bar'*, 50% CU	6.10	12.21	18.17	5.65	11.34	16.91	4.38	8.96	13.41
20%in| 30%out	**508mm 50km**	**508mm 100km**	**508mm 150km**	**610mm 50km**	**610mm 100km**	**610mm 150km**	**914mm 50km**	**914mm 100km**	**914mm 150km**
'150bar'*, 100% CU	3.85	7.12	9.57	2.95	5.47	7.07	2.52	4.84	6.60
'200bar'*, 100% CU	5.84	11.21	15.86	5.42	10.44	14.85	4.19	8.24	11.82
'150bar'*, 50% CU	8.39	16.65	24.53	6.60	13.12	19.28	5.74	11.61	17.21
'200bar'*, 50% CU	12.29	24.50	36.39	11.41	22.79	33.92	8.98	18.12	27.02

Table B.5: Line-depacking times (in hours) for core pipeline scenarios as presented in subsection 5.8.3. Inflow|outflow scenario during depacking process is 0%|10% nominal flow.

0%in| 10%out	**508mm 50km**	**508mm 100km**	**508mm 150km**	**610mm 50km**	**610mm 100km**	**610mm 150km**	**914mm 50km**	**914mm 100km**	**914mm 150km**
'150bar'*, 100% CU	3.84	7.22	9.84	2.95	5.39	7.30	2.52	4.85	6.73
'200bar'*, 100% CU	5.84	11.31	16.14	5.40	10.52	15.09	4.19	8.25	11.95
'150bar'*, 50% CU	8.39	16.68	24.65	6.60	13.13	19.28	5.74	11.61	17.23
'200bar'*, 50% CU	12.29	24.53	36.51	11.41	22.81	34.01	8.98	18.08	27.04

Table B.6: Working capacities (in tons) for core pipeline scenarios as presented in subsection 5.8.4. Inflow|outflow scenario during depacking process is 0%|50% (top table), 10%|50% (middle table), and 20%|50% (bottom table) of nominal flow.

0%in| 50%out	**508mm 50km**	**508mm 100km**	**508mm 150km**	**610mm 50km**	**610mm 100km**	**610mm 150km**	**914mm 50km**	**914mm 100km**	**914mm 150km**
'150bar'*, 100% CU	319.4	611.1	822.7	371.8	723.9	956.4	727.4	1674.2	2366.9
'200bar'*, 100% CU	500.6	983.1	1395.7	735.4	1470.8	2106.7	1407.4	3077.5	4525.5
'150bar'*, 50% CU	367.7	742.7	1100.0	457.7	939.1	1391.4	1036.2	2254.1	3411.5
'200bar'*, 50% CU	545.3	1101.0	1640.5	813.5	1655.3	2476.1	1704.6	3603.6	5446.5
10%in| 50%out	**508mm 50km**	**508mm 100km**	**508mm 150km**	**610mm 50km**	**610mm 100km**	**610mm 150km**	**914mm 50km**	**914mm 100km**	**914mm 150km**
'150bar'*, 100% CU	326.8	615.9	823.4	387.8	736.2	962.4	810.2	1750.0	2430.6
'200bar'*, 100% CU	508.2	988.0	1396.3	751.9	1483.2	2112.6	1495.4	3153.2	4591.2
'150bar'*, 50% CU	371.6	746.0	1101.9	466.0	946.4	1397.1	1078.9	2295.4	3449.8
'200bar'*, 50% CU	549.3	1104.3	1642.7	822.2	1662.9	2482.1	1749.5	2646.1	5485.2
20%in| 50%out	**508mm 50km**	**508mm 100km**	**508mm 150km**	**610mm 50km**	**610mm 100km**	**610mm 150km**	**914mm 50km**	**914mm 100km**	**914mm 150km**
'150bar'*, 100% CU	334.0	620.2	822.8	403.8	747.7	966.7	895.8	1822.9	2489.6
'200bar'*, 100% CU	515.6	992.2	1395.4	768.4	1494.9	2116.6	1584.0	3232.7	4651.0
'150bar'*, 50% CU	375.2	749.1	1103.8	474.3	953.5	1402.5	1122.0	2335.1	3484.7
'200bar'*, 50% CU	553.2	1107.4	1644.6	830.7	1670.3	2487.4	1794.6	3688.4	5523.1

Table B.7: Working capacities (in tons) for core pipeline scenarios as presented in subsection 5.8.4. Inflow|outflow scenario during depacking process is 0%|30% (top table), 10%|30% (middle table), and 20%|30% (bottom table) of nominal flow.

0%in| 30%out	**508mm 50km**	**508mm 100km**	**508mm 150km**	**610mm 50km**	**610mm 100km**	**610mm 150km**	**914mm 50km**	**914mm 100km**	**914mm 150km**
'150bar'*, 100% CU	336.1	638.8	868.4	404.6	772.8	1031.4	875.7	1857.7	2611.5
'200bar'*, 100% CU	517.9	1011.8	1443.3	769.5	1521.8	2185.7	1563.5	3268.1	4777.8
'150bar'*, 50% CU	375.2	753.0	1114.7	472.7	958.1	1443.3	1108.2	2335.2	3507.3
'200bar'*, 50% CU	552.9	1111.6	1656.0	829.1	1675.3	2503.2	1780.0	3687.5	5447.0
10%in| 30%out	**508mm 50km**	**508mm 100km**	**508mm 150km**	**610mm 50km**	**610mm 100km**	**610mm 150km**	**914mm 50km**	**914mm 100km**	**914mm 150km**
'150bar'*, 100% CU	343.9	644.9	871.8	421.1	786.9	1041.5	961.3	1937.5	2680.6
'200bar'*, 100% CU	525.7	1017.9	1446.6	786.5	1536.2	2196.0	1653.5	2251.9	4851.9
'150bar'*, 50% CU	379.1	756.5	1117.5	481.2	965.9	1424.1	1151.2	2376.4	3546.5
'200bar'*, 50% CU	557.0	1115.2	1658.9	837.9	1683.3	2510.2	1825.1	3731.8	5588.2
20%in| 30%out	**508mm 50km**	**508mm 100km**	**508mm 150km**	**610mm 50km**	**610mm 100km**	**610mm 150km**	**914mm 50km**	**914mm 100km**	**914mm 150km**
'150bar'*, 100% CU	351.4	650.4	873.8	437.5	811.0	1049.5	1047.5	2016.2	2749.3
'200bar'*, 100% CU	533.4	1023.4	1448.5	803.5	1549.8	2204.1	1743.3	3434.0	4923.1
'150bar'*, 50% CU	383.1	760.0	1120.1	489.6	973.6	1430.4	1194.3	2418.1	3585.1
'200bar'*, 50% CU	561.0	1118.7	1661.4	846.6	1692.3	2516.7	1870.4	3775.1	5628.5

Table B.8: Working capacities (in tons) for core pipeline scenarios as presented in subsection 5.8.4. Inflow|outflow scenario during depacking process is 0%|10% nominal flow.

0%in| 10%out	**508mm 50km**	**508mm 100km**	**508mm 150km**	**610mm 50km**	**610mm 100km**	**610mm 150km**	**914mm 50km**	**914mm 100km**	**914mm 150km**
'150bar'*, 100% CU	351.1	659.3	898.2	427.5	800.1	1083.0	1047.5	2018.5	2801.3
'200bar'*, 100% CU	533.2	1032.9	1474.1	800.8	1561.7	2204.1	1743.3	3437.6	4978.4
'150bar'*, 50% CU	383.1	761.4	1125.4	489.6	974.5	1430.4	1194.3	2418.1	3589.5
'200bar'*, 50% CU	561.0	1120.2	1667.0	846.6	1692.3	2523.9	1870.4	3766.6	5633.3

Appendix B5

Additional information and predictive abilities of the artificial neural networks developed in section 5.8.5

Following the discussion in section **Error! Reference source not found.** presents additional nformation provided in the output reports by NeuralTools after generating ANN_{time} and $ANN_{working\_cap}$. Whilst NeuralTools does not provide prediction equations and biases the networks can be replicated by using the information provided in Figure B.3 together with the input training data presented in Table B.3 -Table B.8.

ANN_time	
Summary	
Net Information	
Name	Net Trained on Thomas
Configurations Included in Search	GRNN, MLFN 2 to 6 nodes
Best Configuration	MLFN Numeric Predictor (3 nodes)
Location	This Workbook
Independent Category Variables	1 (IN|OUT)
Independent Numeric Variables	4 (OD [mm], L [km], MAOP [bar], capacity [%])
Dependent Variable	Numeric Var. (t [hrs])
Training	
Number of Cases	214
Training Time	04:00:00
Number of Trials	97832492
Reason Stopped	Auto-Stopped
% Bad Predictions (30% Tolerance)	1.8692%
Root Mean Square Error	0.5434
Mean Absolute Error	0.3681
Std. Deviation of Abs. Error	0.3997
Testing	
Number of Cases	38
% Bad Predictions (30% Tolerance)	0.0000%
Root Mean Square Error	0.6655
Mean Absolute Error	0.4191
Std. Deviation of Abs. Error	0.5169
Data Set	
Name	Thomas
Number of Rows	252
Manual Case Tags	NO
Variable Impact Analysis	
IN|OUT	39.1020%
L [km]	23.3013%
capacity [%]	18.4180%
MAOP [bar]	11.5970%
OD [mm]	7.5817%

ANN_working_cap	
Summary	
Net Information	
Name	Net Trained on inventory_Thomas
Configurations Included in Search	GRNN, MLFN 2 to 6 nodes
Best Configuration	GRNN Numeric Predictor
Location	This Workbook
Independent Category Variables	1 (IN|OUT)
Independent Numeric Variables	4 (OD [mm], L [km], MAOP [bar], capacity [%])
Dependent Variable	Numeric Var. (Working Inventory [kt])
Training	
Number of Cases	214
Training Time	00:00:00
Number of Trials	81
Reason Stopped	Auto-Stopped
% Bad Predictions (30% Tolerance)	0.0000%
Root Mean Square Error	27.88
Mean Absolute Error	15.97
Std. Deviation of Abs. Error	22.86
Testing	
Number of Cases	38
% Bad Predictions (30% Tolerance)	0.0000%
Root Mean Square Error	66.55
Mean Absolute Error	40.89
Std. Deviation of Abs. Error	52.50
Data Set	
Name	inventory_Thomas
Number of Rows	252
Manual Case Tags	NO
Variable Impact Analysis	
OD [mm]	36.7258%
L [km]	31.9255%
MAOP [bar]	24.3702%
capacity [%]	5.1231%
IN|OUT	1.8555%

Best Net Search			
	RMS Error	Training Time	Reason Training Stopped
Linear Predictor	3.24	00:00:00	Auto-Stopped
GRNN	1.20	00:00:00	Auto-Stopped
MLFN 2 Nodes	0.76	04:00:00	Auto-Stopped
MLFN 3 Nodes	0.67	04:00:00	Auto-Stopped
MLFN 4 Nodes	0.69	04:00:00	Auto-Stopped
MLFN 5 Nodes	0.91	04:00:00	Auto-Stopped
MLFN 6 Nodes	0.90	04:00:00	Auto-Stopped

Best Net Search			
	RMS Error	Training Time	Reason Training Stopped
Linear Predictor	422.41	00:00:00	Auto-Stopped
GRNN	66.55	00:00:00	Auto-Stopped
MLFN 2 Nodes	150.30	04:00:00	Auto-Stopped
MLFN 3 Nodes	100.03	04:00:00	Auto-Stopped
MLFN 4 Nodes	99.07	04:00:00	Auto-Stopped
MLFN 5 Nodes	83.48	04:00:00	Auto-Stopped
MLFN 6 Nodes	184.37	04:00:00	Auto-Stopped

Figure B.3: Additional information about the generated neural networks ANNtime and ANNworking_cap as provided in the output report by NeuralTools (Palisade Corporation 2018).

Figure B.4-Figure B.7 display additional graphs illustrating the predictive capabilities of ANN_{time} and $ANN_{working\_cap}$. These were deployed in section 5.8.5 for calculating the sensitivities of line-depacking times and pipeline inventories to the examined key influential parameters. The graphs show how the discrepancies of the values predicted by the ANNs for line-depacking times and pipeline inventories are relatively evenly distributed around the actual values as determined by detailed hydraulic modelling, with no significant trend towards overprediction or underprediction.

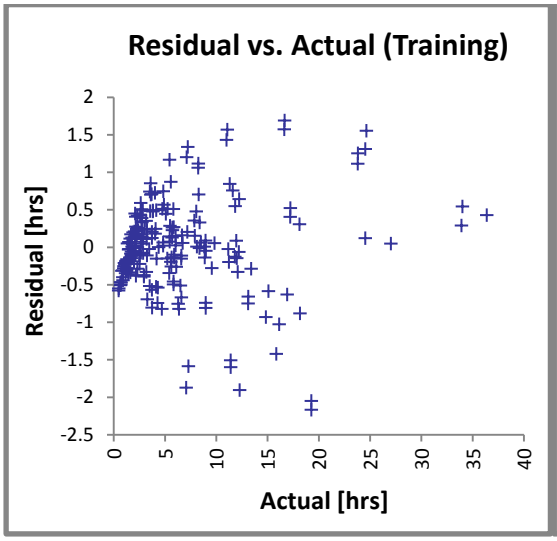

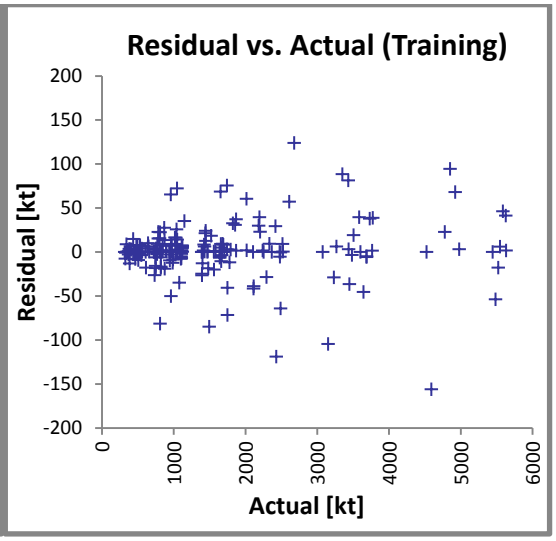

Figure B.4 (left): Discrepancy between line-depacking time ANN_{time} would predict and actual value within training dataset.

Figure B.5 (right): Discrepancy between inventory $ANN_{working\_cap}$ would predict and actual value within training dataset.

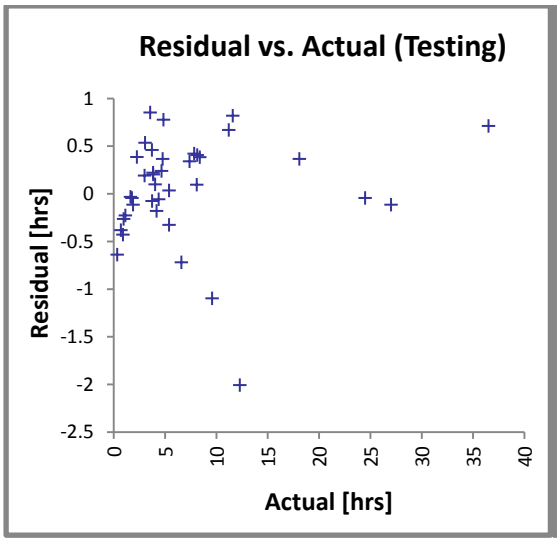

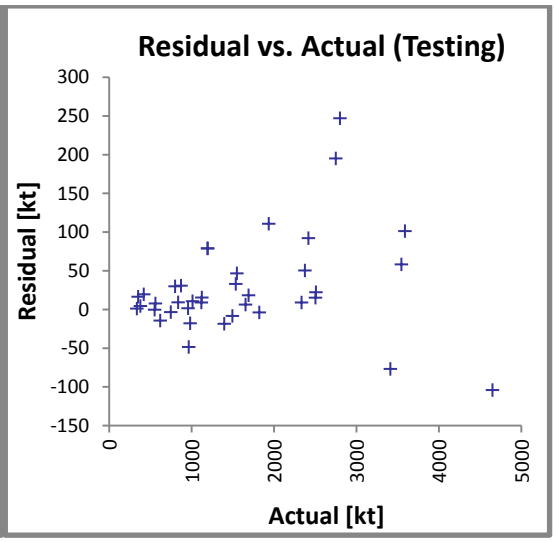

Figure B.6 (left): Discrepancy between line-depacking time ANN_{time} would predict and actual value within testing dataset.

Figure B.7 (right): Discrepancy between inventory $ANN_{working\_cap}$ would predict and actual value within testing dataset.

Appendix C

Table C.1: Other assumptions

Natural gas fuel composition [vol%]	
CH_4	87
C_2H_4	0.03
C_2H_6	8.46
H_2	0.36
N_2	3.65
O_2	0.07
CO_2	0.41
Fuel lower net heating value (LHV)[kJ/kg]	46280
Pump hydraulic efficiencies [%]	80%
Generator efficiency (mech./elec.)	99.4%/98.8%
Condenser cooling water flow [t/s]	10.57

Table C.2: Correlations for key performance parameters of the NGCC-CCS power station at various loads and operating conditions.

	Efficiency [%LHV] X = relative GT load in % $y = ax^3 + bx^2 + cx + d$ Applicable range: 100-40% GT load					**Power output [MWe] X = relative GT load in % $y = ax^3 + bx^2 + cx + d$ Applicable range: 100-40% GT load**					**CO_2 flow [kg/s] X = relative GT load in % $y = ax^3 + bx^2 + cx + d$ Applicable range: 100-40% GT load**				
	a	b	c	D	R	a	b	c	d	R	a	b	c	d	R
Bypass	1e-5	-0.0036	0.4262	41.077	1	0	-0.0049	8.4726	114.12	1	-	-	-	-	-
Solvent Storage	1e-5	-0.0035	0.4161	40.682	1	0	-0.0063	8.4178	111.95	1	-	-	-	-	-
Regular Operation	4e-6	-0.0019	0.3139	36.973	0.9999	0	-0.0060	7.7664	89.22	1	0	-5e-4	0.6660	17.480	1
Max. regen. – floating	2e-5	-0.0061	0.5901	29.742	0.9998	0	0	7.0748	95.876	1	-1e-4	0.0156	-0.2322	43.010	0.9996
Max. regen. - throttled	2e-5	-0.0069	0.8189	17.296	1	0	-0.0052	8.5231	5.9565	1	-6e-6	0.0012	-0.0699	79.619	0.9974

Table C.3: Power and steam cycle parameters at different operational load points of the NGCC-CCS power station.

Operating Mode	Bypass					Solvent Storage					Regular Operation					Max regen – floating				Max regen - throttled			
GT load	**100**	**80**	**70**	**50**	**40**	**100**	**80**	**70**	**50**	**40**	**100**	**80**	**70**	**50**	**40**	**80**	**70**	**50**	**40**	**80**	**70**	**50**	**40**
Fuel input [kg/s]	119.6	101.9	92.9	74.6	65.3	119.6	101.9	92.9	74.6	65.3	119.6	101.9	92.9	74.6	65.3	101.9	92.9	74.6	65.3	101.9	92.9	74.6	65.3
Air/fuel ratio [kg/kg]	39.0	40.2	41.2	43.7	45.5	39.0	40.2	41.2	43.7	45.5	39.0	40.2	41.2	43.7	45.5	40.2	41.2	43.7	45.5	40.2	41.2	43.7	45.5
GT power output [MWe]	594.7	478.0	419.1	300.6	240.9	594.7	478.0	419.1	300.6	240.9	594.7	478.0	419.1	300.6	240.9	478.0	419.1	300.6	240.9	478.0	419.1	300.6	240.9
Flue gas flow [kg/s]	4785	4202	3918	3336	3036	4785	4202	3918	3336	3036	4785	4202	3918	3336	3036	4202	3918	3336	3036	4202	3918	3336	3036
CO2 conc. [vol%]	4.20	4.08	3.99	3.77	3.63	4.20	4.08	3.99	3.77	3.63	4.20	4.08	3.99	3.77	3.63	4.08	3.99	3.77	3.63	4.08	3.99	3.77	3.63
HP turbine flow [kg/s]	177.2	158.4	148.2	127.3	116.7	177.2	158.4	148.2	127.3	116.7	177.1	158.3	148.2	127.3	116.7	158.3	148.2	127.4	116.7	158.3	148.2	127.4	116.8
IP turbine flow [kg/s]	199.8	177.8	166.2	142.5	130.1	199.8	177.8	166.2	142.5	130.1	197.3	176.1	164.7	141.6	129.5	176	164.7	141.5	129.4	176	164.5	141.1	129.0
LP turbine flow [kg/s]	219.6	194.4	181.4	154.9	141.2	219.6	194.4	181.4	154.9	141.2	116.6	106.2	100.9	89.9	83.9	93.4	84.6	73.6	68	90.6	77.2	50.6	36.9
HP turbine pressure [bar]	170.3	152.8	143.4	123.7	113.6	170.3	152.8	143.4	123.7	113.6	170	152.5	143.1	123.5	113.5	152.5	143.1	123.7	113.5	152.6	143.2	123.6	113.6
IP turbine pressure [bar]	41	36.5	34.2	29.2	26.7	41	36.5	34.2	29.2	26.7	40	35.8	33.5	28.7	26.3	35.7	33.4	28.7	26.2	35.8	33.5	28.7	26.3
LP turbine pressure [bar]	7.54	6.68	6.23	5.31	4.83	7.54	6.68	6.23	5.31	4.83	3.75	3.43	3.26	2.92	2.72	2.97	2.68	2.33	2.16	2.95	2.53	1.68	1.24
HP turb. inlet Temp. [°C]	601.4	601.7	601.7	601.7	601.5	601.4	601.7	601.7	601.7	601.5	601.7	601.7	601.7	601.7	601.6	601.7	601.7	601.7	601.6	601.7	601.7	601.7	601.6
IP turb. Inlet Temp. [°C]	594.5	594.9	593.7	590	587.4	594.5	594.9	593.7	590	587.4	595.3	594.7	594.2	590.3	587.6	594.7	594.2	590.3	587.7	594.7	594.3	590.6	588
LP turb. Inlet Temp. [°C]	339.5	338.8	337.5	333.9	331.4	339.5	338.8	337.5	333.9	331.4	263.7	266.1	267.8	270	270.8	250.7	246.7	246	245.6	274.9	281.9	296.3	304.9
Press. drop over LP throttle [bar]	-	-	-	-	-	-	-	-	-	-	-	-	-	-	-	-	-	-	-	0.80	1.21	2.06	2.51
Press. drop in extract. line [bar]	-	-	-	-	-	-	-	-	-	-	0.75	0.58	0.5	0.34	0.28	0.94	0.97	0.73	0.63	0.75	0.75	0.75	0.75
PCC Fan	-	-	-	-	-	16.5	11.4	9.3	5.7	4.4	16.5	11.4	9.3	5.7	4.4	11.4	9.3	5.7	4.4	11.4	9.3	5.7	4.4
Other PCC Auxiliaries	-	-	-	-	-	4.6	3.8	3.3	2.5	2.1	6.0	4.9	4.4	3.4	2.9	5.1	4.7	3.4	2.9	5.1	4.7	3.9	3.5
Power cycle auxiliaries	7.3	6.0	5.4	4.2	3.7	7.3	6.0	5.4	4.2	3.7	7.6	6.3	5.6	4.4	3.8	6.3	5.6	4.4	3.8	6.3	5.7	4.5	4.0
Compression power [MWe]	-	-	-	-	-	-	-	-	-	-	22.5	19.1	17.4	15.8	13.1	24.8	23.4	19.6	18.6	22.5	22.5	22.5	22.5
Compr. cooling aux. [MWe]	-	-	-	-	-	-	-	-	-	-	0.28	0.24	0.21	0.19	0.16	0.31	0.30	0.23	0.23	0.28	0.28	0.28	0.28